DOTTORATO DI RICERCA IN
INGEGNERIA IDRAULICA ED AMBIENTALE
XXI Ciclo

UNIVERSITÀ DEGLI STUDI DI PALERMO
Dipartimento di Ingegneria Idraulica ed Applicazioni Ambientali

Sedi consorziate:

UNIVERSITÀ DEGLI STUDI DI MESSINA
Dipartimento di Ingegneria Civile

A thesis presented to the graduate school of the University of Palermo in partial fulfilment of the requirements for the degree of Doctor of Philosophy

Tesi per il conseguimento del titolo di Dottore di Ricerca

ECOHYDROLOGICAL MODELLING IN MEDITERRANEAN AREAS AND WETLANDS

Dario PUMO

Coordinatore del dottorato:
Prof. Enrico NAPOLI
Department: DIIAA
Università degli Studi di Palermo

Tutors:
Dr. Leonardo Valerio NOTO
Department: DIIAA
Università degli Studi di Palermo

Prof. Ignacio RODRIGUEZ-ITURBE
Department: CEE
Princeton University - NJ – USA

Palermo, Febbraio 2010

ECOHYDROLOGICAL MODELLING IN MEDITERRANEAN AREAS AND WETLANDS

TESI PER IL CONSEGUIMENTO DEL TITOLO DI DOTTORE DI RICERCA

Dario PUMO

Acknowledgements

I would like to acknowledge and express my heartfelt gratitude to my tutor Dr. Leonardo Valerio Noto for providing me with the research opportunity and with a pleasant and productive graduate experience.

It is a great pleasure to thank my co-tutor Prof. Ignacio Rodriguez-Iturbe for his fundamental contribution to the development of part of this thesis and his hospitality at Princeton University.

I would like to express sincere gratitude to all the staff members of the University of Palermo, especially to Prof. Goffredo La Loggia, Dr. Giuseppe Ciraolo and Prof. Marcella Cannarozzo, for their support and guidance.

I am sincerely grateful to my colleagues and friends at the University of Palermo and Princeton University, that always supported me in the research work. I shared this triennial Ph.D. experience with Antonio Francipane, Pamela Fabio and Fulvio Capodici. I wish to thank them for their friendship and nice time spent together that I will never forget.

Finally, I dedicate this thesis to my family and, in particular, to my father, who always supported and encouraged me in my studies and in my life.

Table of Contents

List of Tables

CHAPTERS

TABLE *PAGE*

4 Ecohydrology in Groundwater Dependent Ecosystems

TABLE *PAGE*

List of Figures

CHAPTERS

1 Introduction

2 Literature Review

FIGURE *PAGE*

3 Ecohydrology in Mediterranean Water-Controlled Ecosystems

FIGURE *PAGE*

4 Ecohydrology in Groundwater Dependent Ecosystems

ECOHYDROLOGICAL MODELLING IN MEDITERRANEAN AREAS AND WETLANDS

by Dario PUMO

PALERMO, FEBRUARY 2010

A thesis presented to the graduate school of the University of Palermo in partial fulfillment of the requirements for the degree of Doctor of Philosophy

Tutors:
Dr. Leonardo Valerio NOTO
Prof. Ignacio RODRIGUEZ-ITURBE

Major department:
Dipartimento di Ingegneria Idraulica ed Applicazioni Ambientali (DIIAA)
Facoltà di Ingegneria - Università degli Studi di Palermo – Palermo - Italy
Dottorato in Ingegneria Idraulica ed Ambientale – Ciclo XXI

Abstract

The present dissertation focuses on the field of research known as *ecohydrology*. Although this science, studying the mutual interactions between hydrological cycle and natural ecosystems, has been deeply investigated in recent past, some of its numerous aspects are still relatively unexplored. The main purpose is to investigate the existing scientific literature in order to adapt concepts and models previously developed for some specific ecosystems to the peculiarities of other less explored environments such as those semi-arid within the Mediterranean zone and the wetlands. In particular this study explores an ecohydrological approach to the analysis of water-controlled ecosystems in Mediterranean areas and groundwater dependent ecosystems. Although both are strongly reliant on water availability, these two kinds of environments are deeply different with each other. The most important difference is certainly

played by the position of the water table. While on the one hand arid and semiarid ecosystems are usually characterized by a deep aquifer that does not exert any influence on soil water balance, on the other hand, in the case of groundwater dependent ecosystem, the water table position interacts directly with the root zone leading to important feedbacks between hydrological and ecological processes.

The existing ecohydrological literature on arid and semiarid ecosystems such as savannas, steppes, deserts and prairies is rather wide, complete and consolidated. In such ecosystems, the soil moisture plays a fundamental role in the mutual links between climatic variations and the pedological and vegetational dynamics. The most common ecohydrological models start from a stochastic differential equation describing the soil water balance, where the unknown quantity, the soil moisture, depends both on spaces and time. Most of the solutions existing in literature are obtained in a probabilistic framework and under steady-state condition; even if this last condition allows the analytical handling of the problem, it has considerably simplified the same problem by subtracting generalities from it.

The steady-state hypothesis, appears perfectly applicable in arid and semiarid climatic areas like those of African's or middle American's savannas, but it seems to be no more valid in areas with Mediterranean climate, where, notoriously, the wet season foregoes the growing season, recharging water into the soil. This soil moisture stored at the beginning of the growing season has a great importance, especially for deep-rooted vegetation, by enabling survival in absence of rainfalls during the growing season and, however, keeping the water stress low during the first period of the same season.

In this thesis, a numerical approach, developed during the triennial graduate school at the University of Palermo, is presented. In particular a non steady numerical ecohydrological model is here proposed to evaluate the soil moisture dynamics and the consequent vegetation response in terms of water stress in Mediterranean areas. Such model is able to reproduce soil moisture probability density function, obtained analytically in previous studies for different climates in steady-state conditions. A first application of this model to the Sicilian river basin of *Eleuterio at Lupo* (Italy) shows how the model allows to compute the soil moisture time-profile and the vegetation static water stress time-profile in non-steady conditions, resulting able to capture the effects of winter recharge on the soil moisture.

One of the possible applications of such model is to investigate the effects of potential climatic changes on vegetational stress in Mediterranean ecosystems. Many recent studies have demonstrated that CO_2 increase is driving the climate in Mediterranean areas towards important changes, mainly represented by a temperatures increase and a contemporaneous rainfall

reduction. Starting from this premise, the potential responses of vegetation, in terms of plants water stress, to different future scenarios are here investigated, throughout a second application of the model to the same river basin.

In recent years great attention has been paid to environments such as riparian zones, peatlands and unsubmerged wetlands, which are considered as fundamental “tanks” of biodiversity and where the water table plays a key role in major ecohydrological processes. Wetlands are groundwater dependent ecosystems, which require access to the water table to maintain their health and vigor. A new fascinating challenge for the scientific community is that to investigate such environments by an ecohydrological approach. The study of the dynamics of interactions between climate, soil and vegetation in groundwater dependent ecosystems requires to couple the water table dynamics with the dynamics of soil moisture in the unsaturated zone.

Only few recent frameworks have investigated a probabilistic approach also for the description of soil moisture and water table dynamics in the case of groundwater based ecosystems. In particular two models, the first for the analytical estimation of the water table position and the second for the analysis of the soil moisture dynamics, have been recently developed. Here, it is also presented a validation of the first model, which is the result of its application to three different sites within the Florida Everglades (USA).

Sommario

La seguente dissertazione verte sul campo di ricerca noto come *ecoidrologia*. Sebbene tale scienza, che studia le mutue interazioni fra ciclo idrologico e gli ecosistemi naturali, sia stata recentemente oggetto di svariati studi, alcuni dei suoi numerosi aspetti rimangono tuttavia ancora alquanto inesplorati. L'obiettivo principale di questa tesi è quello di rivisitare la letteratura scientifica esistente sull'argomento, cercando di adattare concetti e modelli sviluppati per certi ecosistemi anche alle peculiarità di altri ambienti meno studiati, come quelli aridi e semiaridi tipici della zona mediterranea o le cosiddette "*wetlands*", zone umide e paludose. In particolare, viene approfondito un approccio ecoidrologico allo studio di quegli ecosistemi controllati dalla risorsa idrica (*water-controlled ecosystems*) in aree mediterranee ed a quegli ecosistemi controllati dalla falda acquifera (*groundwater dependent ecosystems*). Questi due tipi di ambiente sono profondamente diversi fra loro, con la posizione della falda idrica a giocare un ruolo chiave. Se da un lato, infatti, gli ecosistemi aridi e semiaridi sono generalmente caratterizzati da un acquifero così profondo da non esercitare alcuna influenza sul bilancio idrico del suolo, dall'altro lato, nel caso di "*groundwater dependent ecosystems*", la posizione della falda idrica interagisce con la zona radicale della vegetazione, controllando i più importanti meccanismi d'interazione fra processi idrologi ed ecologici.

Nel campo dell'ecoidrologia, la letteratura scientifica esistente su ecosistemi aridi e semiaridi come savane, steppe e deserti risulta essere piuttosto ampia, completa e consolidata. In tali ecosistemi, l'umidità del suolo rappresenta certamente l'anello di congiunzione fra le variazioni climatiche e le dinamiche pedologiche e vegetative. I più comuni modelli ecoidrologici relativi a tali ambienti hanno alla base un'equazione stocastica differenziale che descrive il bilancio idrico del suolo, dove l'incognita, rappresentata dall'umidità del suolo, dipende sia dallo spazio che dal tempo. La maggior parte delle soluzioni a tale bilancio sono state ottenute in termini probabilistici e sotto l'ipotesi di stazionarietà. Tale ipotesi però, sebbene consenta la soluzione analitica del problema, semplifica considerevolmente l'analisi togliendo generalità da essa.

L'ipotesi di stazionarietà è, infatti, perfettamente applicabile in aree climatiche aride e semiaride come quelle africane o delle savane del Centro America, mentre sembra essere non più applicabile in quelle aree mediterranee dove, notoriamente, la stagione umida precede la stagione vegetativa, ricaricando di acqua il suolo. L'acqua immagazzinata all'interno del terreno all'inizio della stagione vegetativa ha un ruolo chiave per la vegetazione, specialmente per quella avente un apparato radicale più profondo, garantendone la sopravvivenza anche in assenza di pioggia durante la stagione vegetativa o comunque mantenendo bassi i valori di stress idrico durante la prima fase della stagione stessa.

Nella tesi viene presentato un approccio numerico sviluppato durante il corso triennale di Dottorato presso l'Università degli Studi di Palermo. In particolare, viene proposto un modello ecoidrologico numerico non stazionario per la studio delle dinamiche di umidità del suolo e la conseguente risposta della vegetazione in termini di stress idrico. Tale modello è in grado di riprodurre la funzione densità di probabilità di umidità del suolo, ottenuta analiticamente in precedenti studi relativamente a regimi climatici differenti e sotto l'ipotesi di stazionarietà. Attraverso una prima applicazione di tale modello al bacino siciliano dell'Eleuterio a Lupo, viene mostrato come lo stesso modello sia in grado di computare i profili temporali di umidità del suolo e di stress idrico statico per la vegetazione anche in condizioni non stazionarie, tenendo quindi in considerazione gli effetti dovuti alla ricarica invernale di umidità all'interno del terreno.

Una delle possibili applicazioni del modello è quella di studiare gli effetti di potenziali cambiamenti climatici sullo stress vegetativo di ecosistemi mediterranei. Recenti studi hanno infatti dimostrato che l'aumento di CO_2 sta gradualmente guidando il clima relativo alle aree mediterranee verso importanti cambiamenti, principalmente rappresentati da un aumento delle temperature e una contemporanea riduzione delle piogge. Partendo da tale premessa, attraverso una seconda applicazione del modello al bacino dell'Eleuterio a Lupo, vengono analizzati i possibili effetti che diversi scenari futuri potrebbero avere sulla vegetazione in termini di stress idrico.

Come precedentemente accennato, tantissimi sono i lavori che studiano le interazioni fra clima, suolo e vegetazione in ecosistemi aridi e semiaridi controllati dalla risorsa idrica. Svariati approcci analitici ci hanno consentito di ottenere una descrizione probabilistica delle dinamiche di umidità del suolo in tali ecosistemi, partendo dalla conoscenza delle precipitazioni e delle caratteristiche del suolo e della vegetazione. Recentemente grandissima attenzione è stata anche focalizzata sull'importanza di ambienti quali le zone riapariali, le paludi e le zone umide in generale, considerate come un serbatoio

di biodiversità fondamentale per la sostenibilità ambientale. Le *wetlands* sono classificate come *groundwater dependent ecosystems*, in quanto necessitano di un continuo apporto di acqua dalla falda idrica per mantenere il loro stato di salute e vigore. In tali aree quindi la posizione della falda idrica gioca un ruolo fondamentale nei maggiori processi ecologici ed idrologici. Una nuova e affascinante sfida per la comunità scientifica è costituita dallo studio di tali ecosistemi mediante un approccio ecoidrologico. Tale tipo di approccio richiede uno studio incrociato delle dinamiche della posizione della falda idrica e di umidità del suolo nella zona insatura sovrastante.

In tali tipi di ambienti, solo pochi lavori in letteratura hanno proposto un approccio probabilistico per lo studio le dinamiche di umidità del suolo e della falda idrica, analogo al caso degli ecosistemi controllati dalla risorsa idrica. Recentemente sono stati sviluppati due modelli ecoidrologici analitici per *groundwater dependent ecosystems*: il primo in grado di studiare la posizione della falda idrica e il secondo per lo studio delle dinamiche di umidità del suolo. In questa tesi, dopo aver presentato i due modelli, vengono anche mostrati i risultati di una validazione del primo modello, ottenuta mediante una sua applicazione a tre siti all'interno delle Everglades della Florida (USA), caratterizzati da una grande disponibilità di dati di pieno campo.

Chapter 1

Introduction

Ecohydrology is a relatively new science that seeks to study the mutual interaction between the hydrologic cycle and the ecosystems. Ecohydrology can be defined as that discipline that bridges the fields of hydrology and ecology and tries to propose unifying principles.

Natural ecosystems are complex structures that can be seen as three-components systems constituted by climate, soil and vegetation, all key factors interacting with each other. The first aim of ecohydrology is, thus, to understand the interplay among these three factors and, in general, the spatial and temporal linkages between hydrologic and ecological dynamics. A relevant point is that the interaction between the hydrological cycle and ecosystems results more intense when water is present intermittently, be it abundant, as in wetlands, or scarce, as in arid and semiarid regions.

The importance of a discipline such as ecohydrology is certainly related to the various and important thematic that it tries to study and analyze; desertification, species and biodiversity conservation, sustainable development and management of water resources are only some of the numerous topics dealt by ecohydrology.

The term “ecohydrology” was initially coined to describe interactions between water table and plant distributions in wetlands, and only in a second moment (*Baird and Wilby*, 1999), this concept was also extended to the plant-water interactions in all the terrestrial ecosystems such as drylands, forest, woodlands, etc. *Rodriguez-Iturbe* (2000) was the first that tried to give an exact and delimitated dimension and collocation to this discipline, fixing some fundamental concepts, later become milestones of ecohydrology. For this reason he may reasonably be considered the father of ecohydrology in a modern perspective.

In recent years, an increasing attention to the importance of natural ecosystems such as wetlands, peatlands, forests, drylands and savannas, led to a

rapid developing of ecohydrology, with a considerable increase also of modelling approaches and applications. However, despite the existing literature on ecohydrology is already rather wide, complete and consolidated [e.g., *Wassel et al.* (1996); *Baird et al.* (1999); *Eagleson* (2002); *Rodriguez-Iturbe et al.* (2004); *D'Odorico et al.* (2006); *Eamus et al.* (2006); *Wolansky* (2007); *Wood et al.* (2008); *Mitsch et al.* (2009)], there are still several aspects less explored that would need to be further investigated.

The main purpose of this thesis is to study, through an ecohydrological approach, two types of environments where water presence (or absence) has a key role in the dynamics of interaction between climate, soil and vegetation: water-controlled ecosystems within the Mediterranean zone and groundwater dependent ecosystems such as the wetlands.

Almost 40% of world's ecosystems is controlled by water availability (*Nemani et al.*, 2003) and can be classified as water controlled. In particular, *water-controlled* (or *water-stressed*) ecosystems are defined as all the ecosystems where water may be a limiting factor for life (because of its scarcity, as well as because of its intermittent and unpredictable appearance). In such ecosystems, water demand by plants is generally higher than water availability and the soil moisture represents the key variable controlling the dynamics of interaction between climate, soil and vegetation.

Also the vegetation has a crucial role in water controlled ecosystems, heavily conditioning the soil water balance by root uptake and, at the same time, being impacted by the arid conditions that the same plants contribute to produce. In water controlled ecosystems, water stress is frequently the most important stress factor for vegetation and its dependence on soil moisture and soil nutrient dynamics is fundamental for the growth, reproduction and competitive abilities of plants.

The impact of climate, soil and vegetation dynamics on plant response depends, on the one hand, by the soil moisture dynamics, controlling the intensity, duration and frequency of the periods of soil-water deficit, and, on the other hand, by the specific plant physiological activities. The modelling approach to water-controlled ecosystems is strictly related to the spatial and temporal scales chosen, and, in fact, the choice of certain scales suggests which hydrological (or ecological) processes needed to be taken into account and the ones that, on the contrary, can be neglected because unimportant at those modelling scales.

Numerous ecohydrological models for arid and semiarid ecosystems, such as savannas, steppes, deserts and prairies, have been deeply investigated in recent past and can be found within the existing ecohydrological literature (e.g., *Rodriguez-Iturbe et al.*, 1999a; *Laio et al.,* 2001b; *Caylor et al.*, 2005). In such ecosystems, the soil moisture plays a key role in the mutual links between climatic variations and the pedological and vegetational dynamics and for this

reason, the most common ecohydrological models start from a soil water balance equation where the unknown quantity is the same soil moisture. The soil water balance equation, in its simpler form, is a stochastic ordinary differential equation, describing at each point the behavior of soil moisture in time. It is constituted by a deterministic part given from the distribution of water fluxes within the soil (i.e. infiltration, evapotranspiration and leakage), and by a stochastic part given from the nature of the precipitation. It generally depends both on spaces and time. Most of the solutions existing in literature [e.g., *Rodriguez-Iturbe et al.* (1999a); *Laio et al.* (2001b)] are obtained in a probabilistic framework and under steady-state condition; this last condition, that makes the balance independent from the time, enables the analytical handling of the problem, allowing the models to obtain the probability density function of the soil moisture.

The steady-state condition can be hypothesized whenever the growing season for the plants is in phase with the wet season (i.e. period of more frequent precipitation and that of the higher temperatures are in phase), the transient effect in the soil moisture dynamics due to seasonality and related to a certain initial soil moisture condition is not significant and the fluctuations of the statistic features of rainfall during the growing season are negligible. Climatic conditions in arid and semi-arid environments, such as African's or Middle American's savannas, make the steady-state hypothesis reasonably satisfied. In the cases where transient soil moisture dynamics and climatic seasonality are important (e.g., Mediterranean climates, Patagonian steppe, temperate forests), the steady-state analysis is no more appropriate and would require further assumptions or different approaches.

In Chapter 2 a brief general introduction to ecohydrology will be provided. Some of the most important and consolidated notions and definitions about ecohydrology, together with the origins of such discipline will be initially discussed. The most important references texts and papers concerning ecohydrology will be revisited to show some of its potential fields of investigation. In this chapter, the peculiar aspects of environments such as water-controlled ecosystems will be also presented. A probabilistic steady-state model (*Rodriguez-Iturbe et al.*, 1999a), conceived for arid and semiarid water-controlled ecosystems different from Mediterranean ones, will be discussed in detail to show its basis concepts, whose understanding will be crucial for the comprehension of other models successively discussed.

As in the case of arid and semi-arid savannas, steppes and deserts, also in some Mediterranean ecosystems, the water can be the limiting factor for vegetation, since the scarcity of water could affect directly all the plants physiological activities and, at the same time, it could limit also the other biogeochemical cycles. Such ecosystems, strictly dependent on water resource, can then be classified as water-controlled ecosystems as well. In such

environments, deep and shallow rooted species cohabit and compete with each other for water.

Mediterranean ecosystems evolve under climatic conditions characterized by precipitation markedly out of phase with the growing period for the vegetation there established. Precipitations in Mediterranean semi-arid water-controlled ecosystems are mainly concentrated in the autumn–winter period, when the vegetation is almost inactive. For this reason, during the wet season the level of soil moisture tends to increase and it will be available for the vegetation at the beginning of the subsequent growing season (spring-summer period). The vegetation, adapting itself to these soil moisture dynamics, often develops an extensive water uptake strategy, by delving the roots into the soil in order to utilize the water stored in the deeper layers.

In scientific literature there are only few ecohydrological studies regarding climates with periods characterized by higher temperatures and more frequent rainfall, seasonally out of phase [e.g., *Kiang* (2002); *Baldocchi et al.* (2004); *Viola et al.* (2008)].

In Chapter 3 a numerical approach to the study of Mediterranean water-controlled ecosystems, that allows to overcome some limitations of an analytical approach in such climatic regimes preserving, at the same time, its simplicity, will be proposed. In particular, a non steady numerical ecohydrological model to evaluate the soil moisture dynamics and the consequent vegetation response in terms of water stress, will be presented. It will be shown how this model is able to reproduce soil moisture probability density function, obtained analytically in previous studies for different climates in steady-state conditions. It can be used to compute both the soil moisture time-profile and the vegetation static water stress time-profile in non-steady conditions, resulting able to capture the effects of winter recharge on the soil moisture. In the same chapter, two applications of this model on a Mediterranean river basin (*Eleuterio at Lupo*, Sicily, Italy) will be also shown.

The scope of the first application is that to assess the performances of the model and to show what results it is able to provide working on a single area, homogeneous in terms of climate, soil and vegetation. The influence of different annual climatic parameterizations on the soil moisture probability density function and on the vegetation water stress evaluation, will be also investigated through this application.

The aim of the second application is that to show the ability of this new approach to evaluate quantitatively the effects of predicted climate changes (*Christensen at al.*, 2007) in the Mediterranean areas on the vegetation water stress. The latest report of the *Intergovernmental Panel on Climate Change* (*IPCC*, 2007) affirms that the climate is changing in ways that cannot be accounted for by natural variability, since human activities have become a dominant force, and are responsible for most of the warming observed over the

past 50 years. Climate change resulting from the enhanced greenhouse effect is expected to have great implications for hydrological cycle and for existing surface and groundwater resources systems in great part of the world. The hydrological cycle will be intensified, with more evaporation and more precipitation, but the extra precipitation will be unequally distributed around the globe. Some parts of the world, such as southern Italy, may be affected by significant reductions in precipitation [e.g., *Giuffrida and Conte* (1989); *Piervitali et al.* (1997); *Cannarozzo et al.* (2006); *Christensen at al.* (2007)] or major alterations in the timing of wet and dry seasons [e.g., *Cislaghi et al.* (2005); *IPCC* (2007)]. The implications of climate change on water resources may be the most dramatic and certainly they affect the ecosystems health status. The second application is an attempt to provide and test an important new tool for the understanding and investigating of such implications in Mediterranean areas.

The last part of this thesis (Chapter 4) will focus on the study of groundwater dependent ecosystems, and in particular on the ecohydrological approach to the wetlands. Wetlands (or humid lands) are defined as those areas that are inundated or saturated at a frequency and duration sufficient to support a prevalence of vegetation typically adapted for life in saturated soil conditions. Wetlands are dynamical, complex habitats, supporting high levels of biological diversity (*Ramsar Convention Bureau*, 1996). They are considered the most biologically diverse of all ecosystems. These kinds of environments have aroused considerable attention only in recent years, as appreciation of their direct and indirect benefits has increased. The importance of wetlands is related, for example, to their role in protecting coastlines from hurricanes and tsunamis, mitigating flooding of streams and rivers. They provide an immense storage of carbon that, if released with climate shifts, could accelerate those changes. Furthermore, wetlands are very effective at filtering and cleaning water.

Wetlands are deeply different from arid and semi-arid water-controlled ecosystems, and the major role in identify such differences is certainly played by the position of the groundwater. On the one hand, arid and semiarid ecosystems are usually characterized by an aquifer so deep to exert no influence on soil water balance, on the other hand, in the case of the wetlands, the water table position interacts with the root zone leading to important feedbacks between hydrological and ecological processes. All those ecosystems whose current composition, structure and function are reliant on a supply of groundwater, and that require access to groundwater to maintain their health and vigor are defined as *groundwater dependent ecosystems*. Such ecosystems vary dramatically in how they depend on groundwater, from having occasional or no apparent dependence to being entirely dependent. Groundwater dependent ecosystems can be classified into two major groups: the first class relies on the surface availability of groundwater, while, the second class relies on the

availability of groundwater below the surface but within the rooting depth of the vegetation. Swamps, wetlands and rivers are typical examples of ecosystems that rely on the discharge of groundwater to the surface.

The ecohydrology of humid lands represents an extremely new frontier of scientific research (*Rodriguez-Iturbe et al.*, 2007). A relevant aspect is that the quantitative description of soil water dynamics in humid areas requires the coupled study of the stochastic fluctuations of the water table and soil moisture dynamics. Chapter 4 will focus on the peculiarities of these ecosystems, describing and discussing the state of the art related to the ecohydrological modelling for such environments. In particular, an ecohydrological analytical approach to the study of the coupled water table and soil moisture dynamics will be investigated, through the discussion of two new probabilistic models (*Laio et al*., 2009 and *Tamea et al.*, 2009). The former, for the investigation of the water table dynamics, is based on a soil water balance equation where the unknown quantity is the water table depth. The second, for the study of the soil moisture dynamics in the unsaturated zone, is based on a local, depth-dependent water balance equation where the unknown quantity is the soil moisture. Both the water balance equations are forced by stochastic precipitation, accounting for mechanisms such as rainfall infiltration and water table recharge, plant water uptake, capillary rise, groundwater lateral flow due to the presence of a nearby water body. The two models are able to provide the probability distribution functions of the water table depth (*Laio et al.*, 2009) and of soil water content at different depths (*Tamea et al.*, 2009).

In the last part of the chapter, an application of the first model, finalized to the study of the water table fluctuations, to three sites located within the Everglades (Florida, USA), will be presented. In particular, the water table depths predicted by the model will be compared to the historical series of water table depth observed at the three sites, testing the performances of the model.

Chapter 2

Literature Review

2.1 Introduction

This chapter provides a brief introduction to the vast scientific area known as *ecohydrology*. Such a discipline has seen a rapid development in the last decades, with a considerable increase of modeling approaches and applications to various research areas related to the intimate links between hydrology and the life sciences. Some of the most important and consolidated notions and definitions about ecohydrology, together with the origins of such discipline are initially discussed. Through the review of the most important references texts and papers concerning ecohydrology, some of its potential fields of investigation are shown, providing also the most important disciplinary basis behind such a discipline.

Since the aim of this dissertation is to study two less explored aspects of ecohydrology, that is an ecohydrological approach to Mediterranean areas and to groundwater dependent ecosystems, in this chapter are also presented the peculiar aspects of environments such as water-controlled ecosystems (WCEs) and wetlands. With regard to WCEs, a probabilistic steady-state model for the study of the temporal dynamics of soil moisture and the quantitative evaluation of vegetation response is discussed in detail. Although this model has been conceived for arid and semiarid ecosystems different from Mediterranean ecosystems, the understanding of its basis concepts is crucial for the comprehension of other models that will be successively shown.

In the last part of this chapter some of the most important peculiarities about wetlands are introduced, providing also different classifications for such kinds of environment.

2.2 Ecohydrology: notions, definitions and origin

Ecohydrology is the science that studies the mutual interaction between the hydrologic cycle and the ecosystems. The main purpose of ecohydrology, that is to joint together concepts and theories of two different disciplines, is, in part, contained in the etymological interpretation of its name, that derives from the crossing between the terms ecology (the science of the interrelationships between living organisms and their environment) and hydrology (the science of the hydrological cycle, dealing with the properties, distribution, and circulation of water in the environment).

Thus, ecohydrology bridges the fields of hydrology and ecology and proposes new unifying principles derived from the concept of natural selection (*Eagleson*, 2002). The interaction between water balance and plants is responsible for some of the fundamental differences among various biomes and for the developments of their space-time patterns (*Rodriguez-Iturbe and Porporato*, 2004).

Natural ecosystems are complex structures whose peculiarities and properties depend on three fundamental factors, interacting with each other: climate, soil and vegetation. The first aim of ecohydrology is thus to understand the various and numerous characteristics of these three factors. The interplay between climate, soil and vegetation is crucially influenced by the scale at which the phenomena are studied, and strongly depends on the physiological characteristics of the vegetation, the pedology of the soil, and the type of climate. Throughout the study of the spatial and temporal linkages between hydrologic and ecological dynamics, ecohydrology seeks to describe the hydrologic mechanisms that underlie ecological patterns and processes (*Rodriguez-Iturbe*, 2000). It is implied in this well-known definition, the need to understand how water cycles through the physical and biological environment, and the principle of continuity (or the balance equation) with regard to the water circulating within a certain system.

The interaction between the hydrological cycle and ecosystems is most intense when water is present intermittently, be it abundant, as in wetlands, or scarce, as in arid and semiarid regions. In either case, the fluctuating nature of the hydrological cycle, together with the network of dynamic links within the climate-soil-vegetation system, considerably complicates the analysis of the processes involved (*Porporato et al.*, 2002).

A considerable drift that encouraged the rapid developing of such a discipline during the last decades has been surely given by an increasing attention to the importance of natural ecosystems such as wetlands, peatlands or forests, drylands and savannas. Thematics such as desertification, species and biodiversity conservation, sustainable development and management of water resources are closely linked to the study of the mutual interaction between the

water cycle and the other elements within the context of the Earth's biological productivity.

Although it is not clear who coined first the word "ecohydrology" and when, since the late 1980s this term was already rather common among the scientific community. In *Kundzewicz* (2002) and *Nuttle* (2002), an excursus of various definitions and notions is provided, examining the state of art of such a discipline and the future perspectives.

A term similar to ecohydrology, "ecohydraulic", was coined in 1977 (*Hino*, 1977) to denote an ensemble of various topics such as the influence of aquatic plants on flow conditions, self-purification in streams, diffusion of radioactive waste and bioaccumulation. Probably this was the first attempt to go beyond the classic notion of hydraulic in order to delve into the complex interface with ecology.

In the early 1990s several academic meetings and publications in the Netherlands referred to the term "ecohydrology" or "hydro-ecology" to denote various activities concerning the management of the water resources in agricultural landscapes. *Garritsen* (1993) distinguished between ecohydrological modelling, defined as primarily hydrological modelling to supply data for ecological modelling, and hydro-ecological modelling, which try to link the abiotic characteristics of the site to the vegetation. In general, "hydro-ecology" seems to be used more in association with aquatic ecology and riparian systems, whereas "ecohydrology" seems to be used more in association with terrestrial ecology, particularly for drylands. Nowadays, although these two terms are used interchangeably, ecohydrology is used generally to refer to topics at their interface.

The term "ecohydrology" was initially coined by ecologists to describe interactions between water table and plant distributions in wetlands. However, in *Baird and Wilby* (1999), the concept of ecohydrology was extended to the plant-water interactions in all types of environment (drylands, freshwater wetlands, forest, woodlands, streams, rivers, lakes, etc.).

The concept of integration between hydrology and ecology (embracing also other socio-economics spheres) is probably attributable to *Zalewsky et al.* (1997), who believed that such integration can contribute to alleviation of all the three water problems: abundance, scarcity and pollution. However, the first notion of ecohydrology in a modern perspective is doubtless attributable to *Ignacio Rodriguez-Iturbe* (2000), who tried to give an exact and delimitated dimension and collocation to such discipline, fixing some fundamental concepts, later become milestones of ecohydrology. An extract of this paper, considered as an "ecohydrology manifesto" by some scientists, says:

> "*Rather than trying to describe a number of problems in different areas which are interesting and waiting to be tackled, I believe that the*

objective of this opinion will be better served by addressing a whole area which I feel does not occupy, yet, the central role it should have in hydrologic research. I am referring to what I will call ecohydrology, where I believe we will see major breakthroughs and intensive activity in the next decade".

The climate-soil-vegetation dynamics, as previously discussed in *Eagleson* (1978) and several further contributions, are seen as the core of ecohydrology itself. Focusing on ecosystem where water is a controlling factor and on those processes where soil moisture is the key link between climate fluctuations and vegetation dynamics in space and time, *Rodriguez-Iturbe* (2000) identified with the soil moisture balance equation, an essential tool for a quantitative analysis of the linkages between hydrologic dynamics and ecological patterns and processes. In this perspective, soil moisture and plants are undoubtedly the two main subjects of ecohydrology, being the heart of the hydrological cycle and the main component of terrestrial ecosystems respectively. The interaction between these two subjects is responsible for some of the fundamental differences among various biomes.

2.3 Major reference texts

A considerable contribute to the development of ecohydrology is given by the book "Ecohydrology of Water-Controlled Ecosystems", by *Rodriguez-Iturbe and Porporato* (2004), that represents one of the most important reference text in this dissertation. Using a probabilistic framework, this book presents a quantitative understanding of the impacts of soil moisture on ecosystem dynamics, with special emphasis on arid and semi-arid environments. In such kind of ecosystems, defined as "water-controlled", the soil moisture is seen as the crucial link between hydrologic and biogeochemical processes. This key role is delved and described throughout the entire book in all its aspects, especially with regard to its controlling influence on transpiration, runoff generation, carbon assimilation, and nutrient absorption by plants. The soil moisture is considered the central hydrologic variable synthesizing the interaction between climate, soil and vegetation, and consequently the study of its spatial/temporal dynamics represents the heart of the entire book and of the treated topics. The authors focused primarily on the non linear soil-plant-atmosphere continuum and on the propagation of stochastic rainfall pattern within such system. The stochasticity given by precipitations leads to a stochastic treatment of soil moisture, while the plant response is evaluated in terms of water stress. The book deals also with topics

such as coupled water and carbon uptake by plants, plant strategies and water use, the importance of opportune spatial and time scales, the connection between cycles of soil organic matter and nutrients, the influence of the spatio-temporal patterns of precipitation on vegetation structure.

A different approach to ecohydrology is provided by *Eagleson* (2002) in the book "Ecohydrology – Darwinian Expression of Vegetation Form and Function". The author focused on an idealized system, constituted by monocultures, where the influence of all kinds of animals (including man) and of diseases and fires is neglected and where the limiting resources for vegetation are water and light, assuming then infinite nutrient and carbon dioxide reservoirs. Following the Darwinian principle that biology is an expression of physical optimality and that the natural selection is responsible for both the form and function of vegetation, the evolution of an ecosystem can be considered crucially dependent on the need of its vegetation for light and water. These external inputs, that drive ecosystems productive mechanisms, are highly variable in time and space and their assimilation depends on the plant characteristics and on the ecosystems structure. Thus, vegetation is both cause and effect of the space-time dynamics of soil moisture and, similarly, vegetation characteristics result from and, at the same time, control the use and impact of the radiative energy. The book, using an analytical approach, presents a detailed description of the energy and water balances and the intimate links which these balances establish between soil, vegetation, and climate. Furthermore the author develops optimality principles for the form and function of natural forests, and criteria for optimal canopy structure. The evolutionary pressure, regulating all the mechanisms of interactions between climate, soil and vegetation, is seen as oriented towards a maximization of plant productivity, and, in turn, towards a maximum of canopy conductance of water vapor and carbon dioxide (Darwinian ecology). This bioclimatic optimal state is characterized by a maximum probability of reproductive success, assumed to correspond to maximum biomass productivity.

In "Dryland Ecohydrology", the authors (*D'Odorico and Porporato*, 2006) focused on drylands and studied the impact of different hydrologic regimes on soil properties and processes, landforms, and spatial patterns of soil moisture. Ecosystems such as drylands are very sensitive to daily, seasonal and decadal perturbations in water availability. This book provides an analysis of how arid ecosystems respond to such perturbations, with special emphasis on what is the effect of the hydrologic conditions on the biosphere and in particular on plant physiology, nutrient cycles, plant competition, fire regime, and spatial patterns of vegetation.

As mentioned above, research on wetlands has played a central role in the initial development of ecohydrology. Hydrologic and ecological processes are intimately connected in wetlands, and their interaction has consequences not

only for these ecosystems, but also for the functions they serve on larger scales. For example, water, ice, and permafrost constitute an important component of the organic soil formed in the extensive wetland regions found at high latitudes in the Northern Hemisphere (*Nuttle*, 2002).

In *Wassel et al.* (1996), ecohydrology is defined as an application-driven interdiscipline and aims at a better understanding of hydrological factors determining the natural development of wet ecosystems, especially in regard of their functional value for nature protection and restoration. Wetlands are analyzed in a landscape-ecological context, focusing on the chorological relations by water flow and the conditioning effect of water chemistry on site conditions. During its flow, not only flow direction and fluxes change but also water chemistry, depending on the mineral composition of parent material. Local nutrient, basis status and vegetation development are then affected by different water sources. The same perspective of ecohydrology, as that discipline seeking to describe such controlling effect of water on wetland vegetational patterns, is adopted in *Grootjans et al.* (1996).

The book "Ecohydrology: Plants and Water in Terrestrial and Aquatic Environments" (*Baird and Wilby*, 1999) represents the first attempt to joint together the already consolidated ecohydrology for wetlands and the rising ecohydrology for terrestrial environments such as forest and drylands. In the introduction, the authors stated:

> *" … it is undesirable and probably impossible to consider the links between plants and water solely in terms of how one affects the other…there is no intrinsic reason why eco-hydrology should be solely concerned with processes in wetlands. Eco-hydrological relations are important in many, indeed probably all, ecosystems. Although such linkages are very important in wetlands, they are arguably of equal importance in forest and drylands ecosystems, for example."*

The authors focus on plant-water mutual relations in both terrestrial and aquatic ecosystems, considering only five different environments: drylands, wetlands, forests, streams and rivers, and lakes. Other ecosystems, such as marine ones, or tundra and mid-latitude grasslands, are then neglected. Moreover, the animal component of the considered ecosystems is also neglected.

Another important contribute to the literature on ecohydrology is given by "Hydroecology and Ecohydrology: Past, Present and Future" by *Wood et al.*, (2008). The authors, in response to the growing volume of research on ecohydrology, provides an investigation on the state of the art, reviewing the evolution of such discipline, providing the last understanding on ecological/hydrological processes, interactions, dynamics and linkages, and

showing methodological approaches with detailed case studies. This book is significantly different from previous texts in providing coverage of a range of organisms (plants, invertebrates and fish), and of physical processes within terrestrial, riparian (aquatic-terrestrial ecotones) and aquatic habitats.

Other relevant reference texts for ecohydrology are "Ecohydrology: Vegetation Function, Water and Resource Management" by *Eamus et al.* (2006) and "Estuarine Ecohydrology" by *Wolansky* (2007).

Among the various scientific texts dealing with wetlands, two recent books overall are surely worth to be mentioned: "Wetlands" by *Mitsch et al.* (2007) and "Wetlands Ecosystems" by *Mitsch et al.* (2009).

2.4 Water-Controlled Ecosystems

2.4.1 Definition and levels of description

Climate has a fundamental role in determining ecosystem main characteristics. In particular water availability, temperature and radiation interact to impose complex and varying limitations on vegetation activity in different parts of the world. Whenever one of these three climatic constraints to vegetation becomes a limiting factor for an ecosystem, this ecosystem results to be controlled by that specific constrain. According to *Nemani et al.* (2003), almost 40% of globe ecosystems are controlled by water availability, 33% by temperature, while 27% of ecosystems are controlled by radiation (Figure 2.1). Then, the most part of ecosystems in the Earth can be classified as *water controlled*.

Water-controlled (or *water-stressed*) *ecosystems* are defined as all the ecosystems where water may be a limiting factor not only because of its scarcity but also because of its intermittent and unpredictable appearance (*Rodriguez-Iturbe et al.*, 2004). In WCEs, water demand by plants is generally higher than water availability. In such complex and evolving structures, soil moisture represents the key variable controlling the dynamics of interaction between climate, soil and vegetation, as well as the water balance and its dynamic impact on plants. The soil is the store and regulator in the water flow system of the ecosystems: it can be seen as a temporary store for the precipitation input and at the same time as a regulator controlling its use by vegetation and its partition between the major outflows (runoff, evapotranspiration, percolation). Also the vegetation has a crucial role in WCEs, heavily conditioning the soil water balance by root uptake and at the same time being impacted by the arid conditions that the same plants contribute to produce. Special adaptation to

water stress and intra/inter-species interactions are strictly linked to dynamics of the climate-soil-vegetation system, and affect the development of temporal and spatial vegetation patterns.

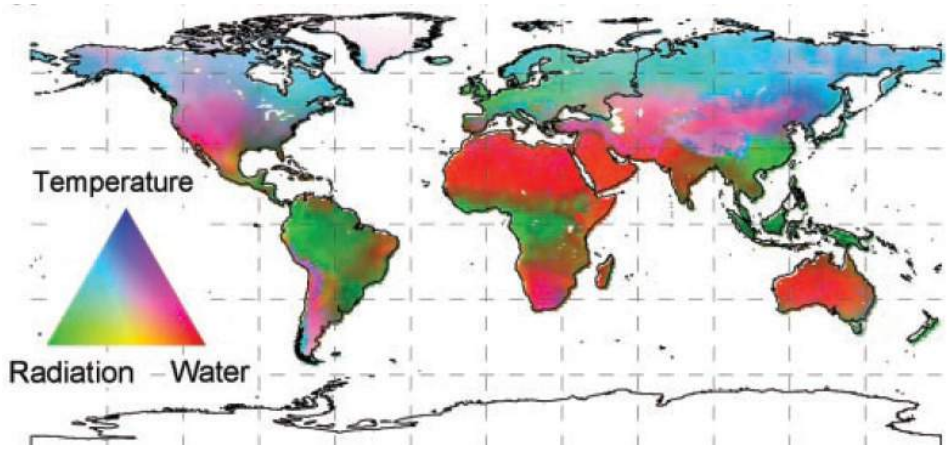

Figure 2.1: Geographic distribution of potential climatic constraints to plant grow derived from long-term climate statistics (from *Nemani et al.*, 2003)

Figures from 2.2 to 2.4 show some examples of typical WCEs. In particular some of the most studied environments (e.g. *Scholes et al.*, 1997; *Dowty et al.*, 2001; *Kiang*, 2002; *Baldocchi et al.*, 2004) are shown: Katambe Forest Reserve (Zambia), Kalahari Savanna (South Africa) and Blue Oak Savanna of California (USA).

The dynamics properties of WCEs depend on many interrelated links between climate, soil and vegetation: on the one hand, climate and soil control vegetation dynamics, on the other hand vegetation has an active role on the entire water balance and is responsible for many feedbacks to the atmosphere (*Rodriguez-Iturbe at al.*, 2004).

The study of a certain WCEs is strictly linked to the scale of interest chosen. The various hydrologic processes involved in the dynamics of the climate-soil-vegetation may have different importance whether one considers a daily, seasonal or interannual time-scale, or a point, regional or continental spatial-scale. Thus, the intended target, and then the intended level of analysis, has a fundamental importance in the choice of opportune spatio-temporal scales. At the same time, the choice of certain scales suggests which interactions deserve particular attention or the ones that could be neglected.

According to *Rodriguez-Iturbe et al.* (2004), three different levels of analysis can be identified, that are briefly described below.

(a)

(b)

Figure 2.2: (a) Woodland on Kalahari sand at Kataba Forest Reserve (Zambia) and (b) view inside the Kataba woodland, showing sparse grasses and various shrubs (from NASA web-site, SAFARI 2000 project)

Figure 2.3: Kalahari Savanna – South Africa (photo by Claire Spottiswoode)

Figure 2.4: Blue Oak Savanna, near White River, California – USA (Photo by Jim Shevock)

In this dissertation, a level of analysis that may be defined as basic (*first level* of analysis), is widely studied. This level considers a spatial scale of few meters (plot scale) and a temporal scale from seasonal to annual. Adopting such scales, the rainfall input, as well as the soil characteristics, may be considered as external forcing components, independent from the soil moisture conditions, while soil moisture dynamics pivots the mutual links between the vegetation and water stress (Figure 2.5). Another more complex level of analysis can be obtained considering the links between soil moisture, soil nutrient cycles and the related evolution of soil properties (*second level* of analysis). Finally, using continental spatial scales, the climatic component is no longer an external forcing, being influenced by the feedbacks induced by the soil-plant system. This level of analysis (*third level*), connects ecohydrology to the well known hydrometeorology.

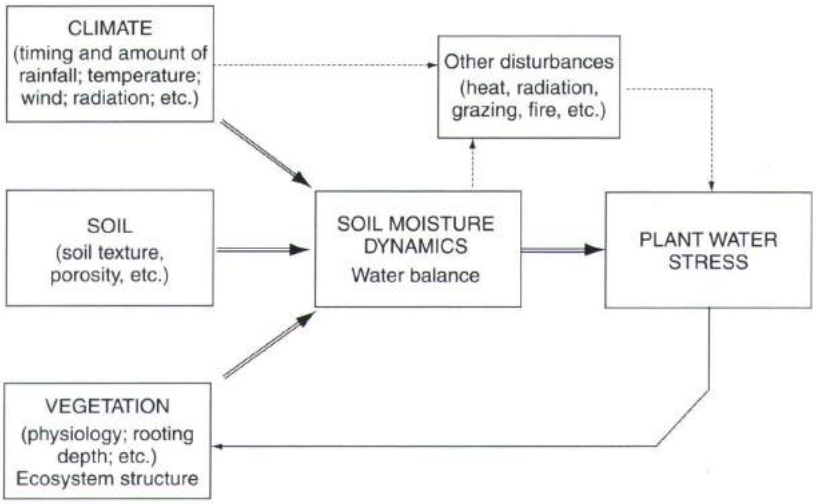

Figure 2.5: First and main level of description of the climate-soil-vegetation system [from *Rodriguez-Iturbe et al.* (2004), after *Rodriguez-Iturbe at al*. (2001), and *Porporato et al.* (2002)].

Soil moisture dynamics are also important in determining the duration of periods in which primary production and nutrient mineralization can occur. Water availability influences vegetation photosynthetic capacity, which, in turn, is directly related to vegetation productivity. At the same time, mineralization and uptake are strictly dependent from soil moisture. Water availability is a key factor regulating the hydrologic control on the soil nutrient cycles.

In WCEs, water stress is frequently the most important stress factor for vegetation and its dependence on soil moisture and soil nutrient dynamics is

fundamental for the growth, reproduction and competitive abilities of plants (Figure 2.6). In particular the formation and evolution of a certain vegetation pattern in a given area depend on the competition mechanisms among the different species present in that area, which, in turn, are strongly dependent from the hydrologic fluctuations and the correspondent specific response from a single species (as well as from each individual).

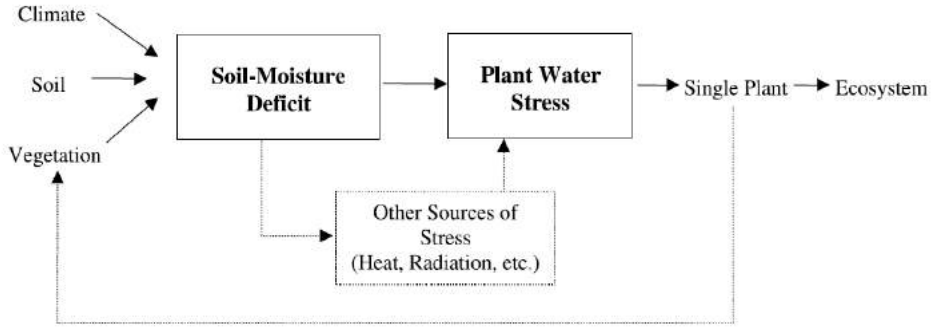

Figure 2.6: Schematic representation of the linkage between plant response and climate, soil and vegetation (from *Porporato et al.*, 2001)

The impact of climate, soil and vegetation dynamics on plant response depends, on the one hand, by the soil moisture dynamics, controlling the intensity, duration and frequency of the periods of soil-water deficit, and, on the other hand, by the specific plant physiological activities. Other important sources of ecological stress may be grazing and fire, or heat and radiation stress, but their impact on vegetation in WCEs, especially in arid and semi-arid climates, is often modulated by the soil-water dynamics and availability.

Plants require an adequate level of water in their tissues for the growth and survival and, at the same time, a continue flux of water to perform some vital processes such as photosynthesis and nutrient uptake. The occurrence of a soil-water deficit lowers plant water potential and leads to a decrease in transpiration, which, in turn, causes a reduction of turgor and relative water content of the plant's cell. Intensity, frequency and duration of such a water deficit may bring plants towards a sequence of increasing damages, from temporal to permanent up to the death.

The plants response, initially at the molecular level, determines successively the condition of the entire ecosystem through its control on growth, deaths, competition and reproduction mechanisms. Figure 2.7, extracted from *Porporato et al.* (2001), shows a simplified scheme of the various processes linking soil-moisture deficit to plant water stress.

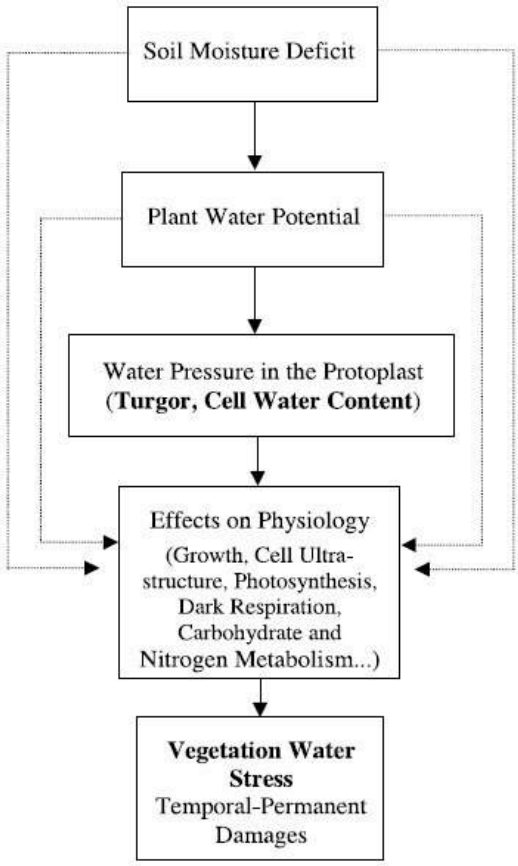

Figure 2.7: Schematic representation of the processes linking soil moisture deficit to plant water stress (from *Porporato et al.*, 2001)

2.4.2 Soil water balance

In this section one of the most known ecohydrological model is deeply analyzed: the probabilistic model for the study of the temporal dynamics of soil moisture, proposed by *Rodriguez-Iturbe et al.* (1999a) and improved by *Laio et al.* (2001b). It can be considered as a milestone in ecohydrological modelling, especially for the study of WCEs in arid and semi-arid areas at the first level of analysis; it is here presented because it is considered very important for the understanding of all the other models discussed through this dissertation. The model, working at the plot spatial-scale and at the time-scale of the growing season, provides a simplified realistic description, supported by an analytical

solution, of ecosystems response to soil moisture dynamics. It allows the study of some important feedbacks, such as the vegetation response to water stress and the hydrologic control on the cycles of nutrient, as well as the dynamics of plant competition for water.

The starting point of the model is the soil water balance, vertically averaged over the root zone; this balance is achieved using the equation of mass conservation of soil water as a function of time. The considered control volume is the upper portion of soil occupied by plants roots, and the lateral contributions of water to this volume are assumed negligible (i.e. under the simplifying assumption that the topographic effects over the area under consideration can be neglected). The system is assumed homogenous in terms of soil and vegetation characteristics.

The state variable of the water balance is the relative soil moisture *s*, that is defined as

$$s = \frac{V_w}{V_a + V_w} \tag{2.1}$$

where V_a and V_w are the volume of air and water components of the soil respectively, that summed to the volume of mineral component (V_m) give the total volume of the soil ($V_s = V_a + V_w + V_m$). The porosity n is equal to the ratio of the total pore volume ($V_a + V_w$) to V_s. Being the volumetric water content, θ, defined as the ratio of water volume to the total soil volume, the relative soil moisture can be equally expressed by the ratio of θ to n.

The soil water balance equation is a stochastic ordinary differential equation, describing at each point the behavior of soil moisture in time by linking climatic, pedological and vegetational features. It is constituted by a deterministic part given from the distribution of water fluxes within the soil (i.e. infiltration, evapotranspiration and leakage), and by a stochastic part given from the nature of the precipitation. With the above definitions and simplifying assumptions, the water balance equation may be expressed as

$$n \cdot Z_r \cdot \frac{ds(t)}{dt} = \varphi[s(t),t] - \chi[s(t)] \tag{2.2}$$

where Z_r is the rooting depth (that multiplied by the porosity n gives the active soil depth), $s(t)$ is the relative soil moisture content, $\varphi[s(t),t]$ is the rate of infiltration from rainfall (taking into account the amount of water lost through canopy interception $I(t)$ and runoff $Q[s(t),t]$), while $\chi[s(t),t]$ is the water losses from the soil (due to evapotranspiration $E[s(t)]$ and leakage $L[s(t)]$). The

equation does not have any particular time-scale. Figure 2.8 shows a scheme representing the various processes involved in the soil water balance.

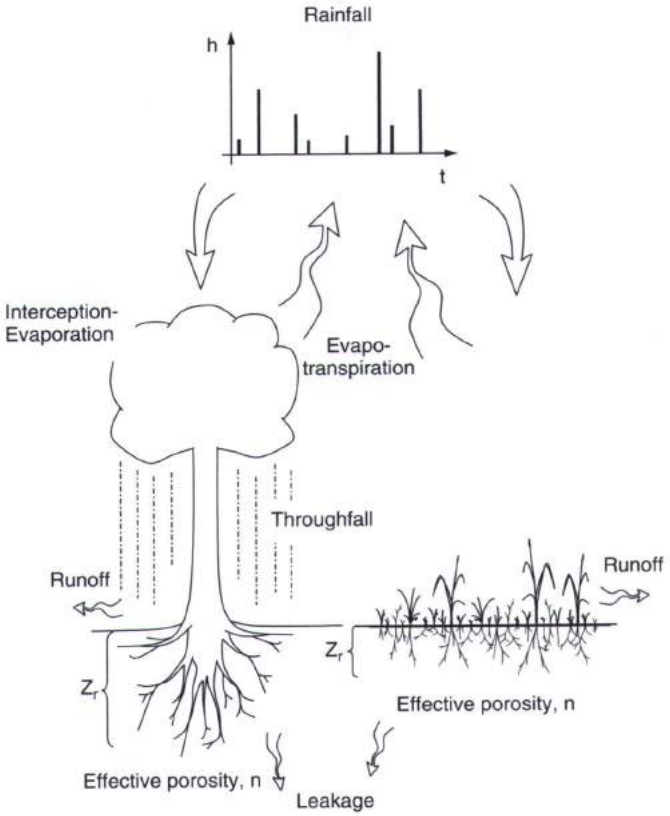

Figure 2.8: Scheme of the various mechanisms involved in the soil water balance for two different functional vegetation types (from *Laio et al.*, 2001b)

Working at the spatial scale of a few meters, the rainfall input may be considered as an external forcing, independent of soil moisture state. The stochastic process of rainfall is idealized as a series of point events, each one carrying a random amount of rainfall, and it results completely definite by two stochastic parameters: the occurrence and the amount of rainfall. In particular, the rainfall depth is idealized as an independent random variable exponential distributed with mean value α, while the occurrence of rainfall is assumed as a Poisson process with rate λ (*Rodriguez- Iturbe et al.*, 2004).

The temporal structure of each rainfall event is ignored and the rainfall process is physically interpreted at a daily time scale. The pulses of rainfall are assumed to be correspondent to daily precipitation concentrated at an instant in

time. Thus, the parameter α may be estimated as the mean daily rainfall in days when the precipitation occurs. Being the model at the time scale of the growing season, both the rainfall parameters are representative values of a typical growing season and are assumed to be time-invariant quantities.

Then, the distribution of the times τ between precipitation events can be written as

$$f_T(\tau) = \lambda \cdot \exp(-\lambda\tau) \qquad for \qquad \tau \geq 0 \tag{2.3}$$

where λ is the rate of the Poisson process and, then, $1/\lambda$ is the mean interarrival time.

The depth of rainfall events is assumed to be an independent random variable, *h*, described by an exponential probability density function with mean α, that is

$$f_H(h) = \frac{1}{\alpha} \cdot \exp\left(-\frac{1}{\alpha}h\right) \qquad for \qquad h \geq 0 \tag{2.4}$$

The vegetation intercepts part of the rainfall, which does not arrive to soil surface and is lost directly through evaporation. Following *Rodriguez-Iturbe et al.* (1999b), interception is incorporated in the stochastic model by fixing a constant threshold, Δ, for rainfall depth, below which no water reaches the ground, while for rainfall depth higher than this threshold, the water arriving to soil surface is equal to theirs difference. Such a threshold is assumed dependent on the kind of vegetation, neglecting the effect that fluctuations in wind and air temperature may have on interception losses. The scheme of such an interception model in Figure 2.9 also shows two typical values of Δ for trees and grasses in a typical savanna environment. The assumption of a vegetation interception threshold implies, from a mathematical viewpoint, the transformation of the rainfall process in a new marked-Poisson process (called *censored process*) with a different frequency of rainfall events, λ', equal to

$$\lambda' = \lambda \cdot \exp\left(-\frac{\Delta}{\alpha}\right) \tag{2.5}$$

When the net incoming water of the rainfall event after interception losses reaches the soil, only a limited part of water enters into the soil while the remaining part is lost by runoff. Infiltration is a complex mechanism that depends on both rainfall and soil moisture content. In particular the duration and the intensity of the rainfall and the capacity of the soil to receive this water have

a great importance in determining the amount of water infiltrating as well as the dynamic actions that rainfall events may have on the soil surface modifying the soil hydraulic conductivity (e.g. sealing or crusting due to the raindrop impact on the surface). Phenomena of hysteresis, shrinking and swelling typical for some soils, such as clayey soils, could also play an important role in the infiltration dynamics.

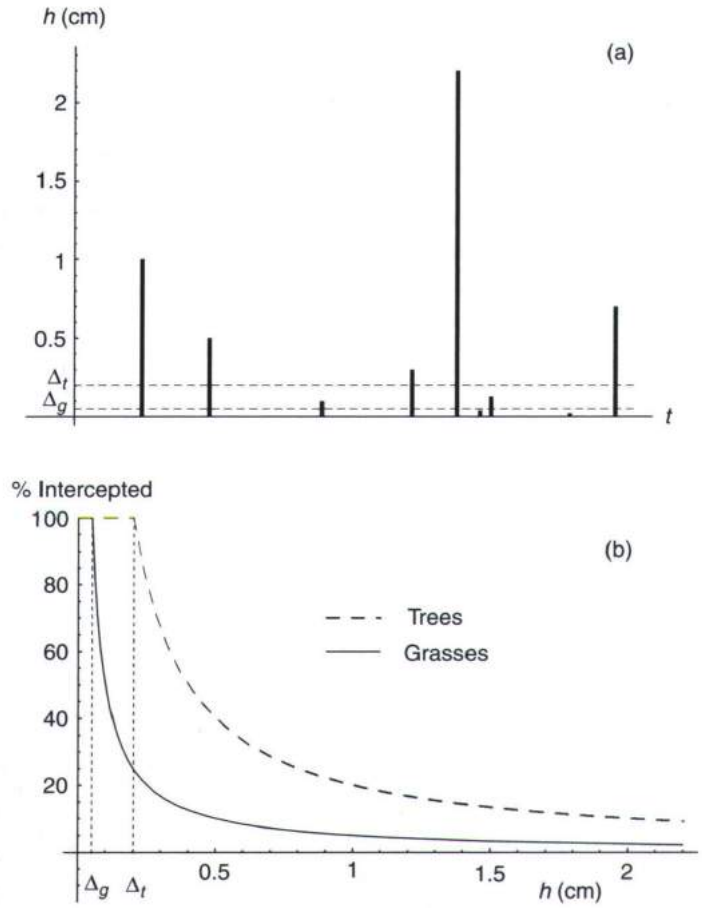

Figure 2.9: Representation of the model adopted for interception (from *Laio et al.*, 2001b). (a) Temporal sequence of rainfall events (*h* is the rainfall depth) and values of the typical interception threshold for trees (Δ_t= 0.2cm) and grasses (Δ_g= 0.05cm) in a typical savanna environment. (b) Percentage of rainfall intercepted by vegetation as a function of the total rainfall per event

In the hydrological modeling two different runoff generation mechanisms are usually considered: Hortonian and Dunnian (e.g., *Horton*, 1933; *Dunne*, 1978; *Beven*, 2004). The Dunnian mechanism, adopted by the model under consideration in this section, considers formation of runoff for saturation from below.

Infiltration from the rainfall is a stochastic, state dependent component, whose magnitude and temporal occurrence are controlled by the entire soil moisture dynamics. As mentioned above the model assumes a vertically lumped representation of such soil moisture dynamics, which are considered at the daily time scale. Thus the temporal propagation of the wetting front into the soil can be neglected and the simplifying model assumption of a Dunnian mechanism of runoff generation appears to be reasonable.

The soil is considered as a tank with a certain water storing capacity that depends on its initial soil moisture content and its porosity. Whenever the rainfall depth reaching the soil exceeds the available storage, all the excess is converted into surface runoff and is lost from the system while the other part enters into the soil (infiltration). Thus, two limit conditions can be identified: absence of runoff when the rainfall depth reaching the soil is less than the maximum capacity of storage for the soil and then all the incoming water is infiltrated into the soil; absence of infiltration when the soil is in condition of saturation and then all the incoming water is refused by the soil and is converted in runoff. The maximum volume of water, W_{max}, that a certain system can store at the time t per unit horizontal area, is given by

$$W_{\max} = (1 - s_0) \cdot n \cdot Z_r \tag{2.6}$$

where s_0 is the relative soil moisture at time t, n is the porosity and Z_r is the plant rooting depth.

It is worth to note the key role of the active soil depth (nZ_r). The values of porosity and soil depth are influenced by many factors. Porosity generally shows a strong dependence on soil texture but also plant roots and the action of small animals may have an important role in modifying the so-called *macro-porosity*, producing preferential directions for water movement inside the soil. The actual soil depth may show a large range of spatial variation, depending on soil pedology and vertical root distribution, and it is of course a difficult parameter to estimate in the soil water balance. Working with the time scale of the growing season, it is possible to consider the porosity dependent only on the soil texture and the soil depth dependent only on vegetation type, thus neglecting all the other factors that can be considered of secondary importance at this scale and that, on the contrary, should be taken into account for long-term analysis.

The water losses in Eq.(2.2) are due to the mechanisms of evapotranspiration and leakage. The former represent the sum of the water losses resulting from plant transpiration and evaporation from the soil. The latter represents the water losses assumed to happen by gravity at the lowest boundary of the soil layer, neglecting possible upward capillary fluxes.

The quantitative distinction of the portion of water lost by evaporation from that lost by transpiration is rather complex, and for sake of simplicity these two mechanism are usually considered together. The factors influencing the process of evapotranspiration are of different types: 1) *climatic factors* such as solar radiation, leaf area index, air temperature and humidity, wind speed, etc; 2) *physical factors* related to both the water and the soil such as the extension and shape of the evaporating surface, water availability and soil moisture, depth of the free water surface, color of the soil surface, etc; 3) *vegetational factors* such as vegetation type, age and dimension, depth and density of the root apparatus, physiological activity of the plant, etc. The estimation of the rate of evapotranspiration is related to the quantitative estimation of each of these factors and of the impacts that their interactions have on the system soil-climate-vegetation.

Being the contribution due to capillary rise from the water table or deeper layer of secondary importance in most of the WCEs, the leakage losses are assumed driven only by gravity, thus neglecting possible interaction with the underlying soil layers and the water table.

Figure 2.10 shows the scheme of the soil water losses as a function of relative soil moisture assumed in the model under consideration. It is possible to identify a critical value of relative soil moisture, s^*, which depends on both vegetation and soil characteristics, representing the condition of incipient stomatal closure.

When the relative soil moisture is higher than this critical value s^*, the soil moisture content is sufficient to permit the normal course of the plant physiological processes and the evapotranspiration is assumed to occur at its maximum rate. Thus, if the soil moisture content ranges from s^* up to the saturation condition, the evapotranspiration rate is assumed independent from s, constant and corresponding to the potential evapotranspiration E_{max}.

The leakage losses are modeled by adopting an exponential law (*Davidson et al.*, 1963; *Cowan*, 1965; *Sission et al.*, 1988), considering the loss rate at its maximum when soil is saturated while it is null when soil is at a field capacity s_{fc}. The hydraulic conductivity is assumed to decay exponentially from a value equal to the saturated hydraulic conductivity K_s at s=1, to a value of zero at s=s_{fc}. Thus, when the relative soil moisture is higher than s_{fc} the water losses from the soil are composed by both the losses for evapotranspiration (at maximum rate) and leakage, while for lower soil moisture contents the water losses are exclusively due to evapotranspiration.

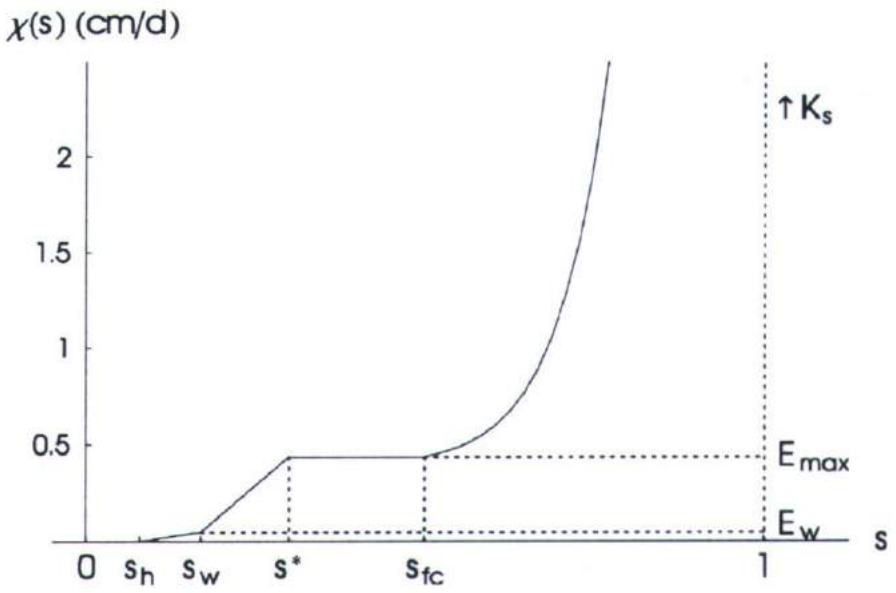

Figure 2.10: Soil water losses (evapotranspiration and leakage), $\chi(s)$, as a function of relative soil moisture for typical climate, soil and vegetation in semi-arid ecosystems (*Laio et al.*, 2001b)

When soil moisture content falls below the critical value s^*, plant transpiration is reduced by stomatal closure to prevent internal water losses. When soil moisture decreases, soil matrix potential decreases as well, and suction to extract water from the soil by plant increases. As the relative soil moisture reaches the so-called *wilting point* s_w, this suction is so high that wilting and irreversible plant damages begin to appear (e.g. *Lange et al.*, 1976, *Schulze*, 1986; *Nilsen and Orcutt*, 1998). At this level the stomatal closure is completed and there are only small water losses from the plant via cuticular transpiration (i.e., direct evaporation from the moist membranes into the atmosphere through the cuticle). The value of relative soil moisture at which transpiration starts being reduced and the wilting point, as well as their correspondent soil matrix potential values, depend on the type of vegetation and soil properties. Figure 2.11 shows a schematic representation of the three main critical soil moisture levels ($s = 1$, s_{fc} and s_w).

The model under consideration, supported by numerous studies and field experiments (e.g. *Schulze*, 1986, *Hale and Orcutt*, 1987), assumes a linear relationship between the transpiration and soil moisture content. Thus daily evapotranspiration losses decrease linearly from the potential value E_{max} at $s=s^*$ to a minimum value E_w at $s=s_w$. Below wilting point, soil water is further

depleted only by evaporation at a very low rate up to the so-called hygroscopic point, s_h. The model assumes a linear relationship also for these losses, and the loss rate is assumed to decrease from E_w at wilting point to zero at hygroscopic point. The value of E_{max} can be interpreted as the average daily potential evapotranspiration during the growing season and it could be estimated using physically based expressions, such as Penman-Monteith equation. As the water losses at low soil moisture levels are relatively small, a precise evaluation of E_w and s_h is not very important for the temporal evolution of the soil moisture process, and often conventional reference values are adopted.

It is worth to note that evapotranspiration is considerably reduced during precipitation events. Since the model assumes rainfall as a sequence of instantaneous pulses while evapotranspiration takes place continuously, this fact can be considered not relevant in the model under consideration. For this reason the model neglects the temporal interplay between rainfall and evapotranspiration, even if this might lead to a slight overestimation of the total water losses for evapotranspiration.

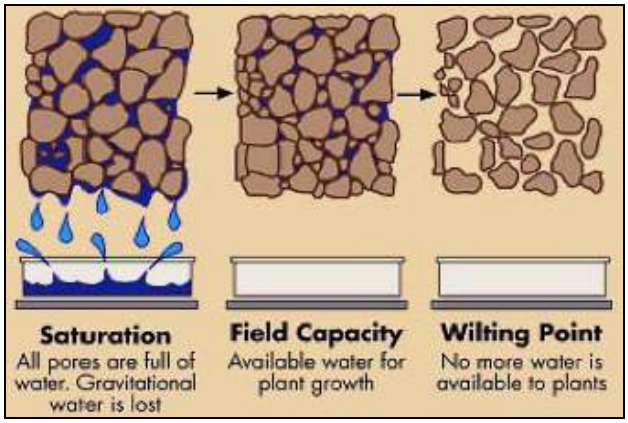

Figure 2.11: Schematic representation of some critical soil water levels (saturation, s= 1; field capacity, s= s_{fc}; wilting point, s= s_w)

2.4.3 Steady-state solution of soil water balance

Before studying the probabilistic structure of the soil moisture process, it is convenient to define some terms which will be useful hereafter. During interstorm periods the model Eq.(2.2) describes deterministic decay of soil moisture starting from initial values of relative soil moisture. The so-called

normalized loss function, $\rho(s)$, represents the water losses from the soil upon normalization with respect to the active soil depth, and it reads as follow

$$\rho(s) = \frac{E(s) + L(s)}{nZ_r} = \frac{\chi(s)}{nZ_r} \tag{2.7}$$

From this equation it is possible to derive the behavior of the system when undergoing a prolonged drought following a rainy period, obtaining the values of s as a function of the time and of the initial soil moisture condition. It is also possible to calculate the time to evolve, in the absence of rainfall, from a certain initial relative soil moisture value to the other characteristics values of soil moisture such as s_w, s^* or s_{fc} (*Rodriguez-Iturbe et al.*, 2004).

It is useful to define another term, that is the mean rainfall depth normalized by the active soil depth:

$$\frac{1}{\gamma} = \frac{\alpha}{n \cdot Z_r} \tag{2.8}$$

The stochastic nature of the soil water balance is given by the rainfall stochasticity, and it makes Eq.(2.2) solution possible in probabilistic terms. The probability density function of soil moisture, $p(s,t)$, can be derived from the Chapman-Kolmogorov forward equations for the evolution of the probability of s (*Cox et al.*, 1965; *Rodriguez-Iturbe et al.*, 1999a), here simply reported without further comments:

$$\begin{cases} \dfrac{\partial}{\partial t} p(s,t) = \dfrac{\partial}{\partial t}\left[p(s,t)\rho(s)\right] - \lambda' p(s,t) + \lambda' \displaystyle\int_{s_h}^{s} p(u,t) f_Y(s-u,u)\,du \\ \qquad\qquad + \lambda' p_0(t) f_Y(s - s_h, s_h) \\ \dfrac{d}{dt} p_0(t) = -\lambda' p_0(t) + \rho(s_h) p(s_h, t) \end{cases} \tag{2.9}$$

where $p_0(t)$ denotes the discrete atom of probability in the distribution of $s(t)$, appearing at time t for $s=s_h$, while the term $f_Y(y,s)$ is the probability distribution of the infiltration component (know as *jump distribution*), governing the normalized soil moisture increment, y (*Rodriguez-Iturbe et al.*, 2004).

The complete solution of the Chapman-Kolmogorov equations presents serious mathematical difficulties and only formal solution in terms of Laplace transforms have been obtained for simple cases (e.g. *Cox and Isham*, 1986). A

considerable simplification is given by removing the dependence on the time, that is the imposition of a steady state condition.

The steady-state condition can be hypothesized whenever: (i) the growing season for the plants is in phase with the wet season (i.e. rainfall and temperature in phase); (ii) the transient effect in the soil moisture dynamics due to seasonality and related to a certain initial soil moisture condition is not significant; (iii) the fluctuations of the statistic features of rainfall during the growing season are negligible. In the cases where transient soil moisture dynamics and climatic seasonality are important (e.g., Mediterranean climates, Patagonian steppe, temperate forests), the steady-state analysis is no more appropriate and would require further assumptions or different approaches such as that which will be shown in the next chapter.

The steady-state solution of the soil water balance equation has been obtained by *Rodriguez-Iturbe et al.* (1999a). Here, all the mathematical passages have been omitted and it is simply reported the general form of the solution relative to the unbounded case, that only differs from that relative to the bounded case (i.e., $s_h \le s \le 1$) by an arbitrary constant of integration C:

$$p(s) = \frac{C}{\rho(s)} \exp\left(-\gamma \cdot s + \lambda' \int \frac{du}{\rho(u)} \right) \tag{2.10}$$

where C is the normalization constant such that $\int_{s_h}^{1} p(s)ds = 1$.

This solution provides the steady-state probability distribution of soil moisture for s between the hygroscopic point (s_h) and saturation (s=1). Considering soil water losses approaching zero at s_h in a continuous manner (Figure 2.10), the steady-state solution is continuous with no atom of probability at s_h.

Considering the hypothesis and assumptions on the various terms of the soil water balance described before (see Sect. 2.4.2 and Figure 2.10), the soil water losses term could be expressed by means of a piecewise function, considering four components as a function of the relative soil moisture s (lower than s_w; between s_w and s^*; between s^* and s_{fc}; higher than s_{fc}). As a consequence, the term $\rho(s)$ [Eq.(2.5)] could be identically expressed by a system of four equations as a function of s. The approximate analytical solution of the water balance equation, given in *Laio et al.* (2001b), considers four different equations as well, and the limits of the integral in the exponential term of Eq.(2.10) are chosen so as to assure the continuity of $p(s)$ at the end points of the four different components of the loss function. *Rodriguez-Iturbe et al.* (2004) show some example of the pdf's of soil moisture derived from this analytical solution in order to emphasize the role of the various parameter of the

model (active soil depth, soil texture, type of vegetation, mean rainfall depth and frequency of storm event, etc.) in the soil moisture dynamics.

In Figure 2.12, from *Laio et al.* (2001b), some examples of pfd's of soil moisture for different types of soil, soil depths and mean rainfall rates are reported.

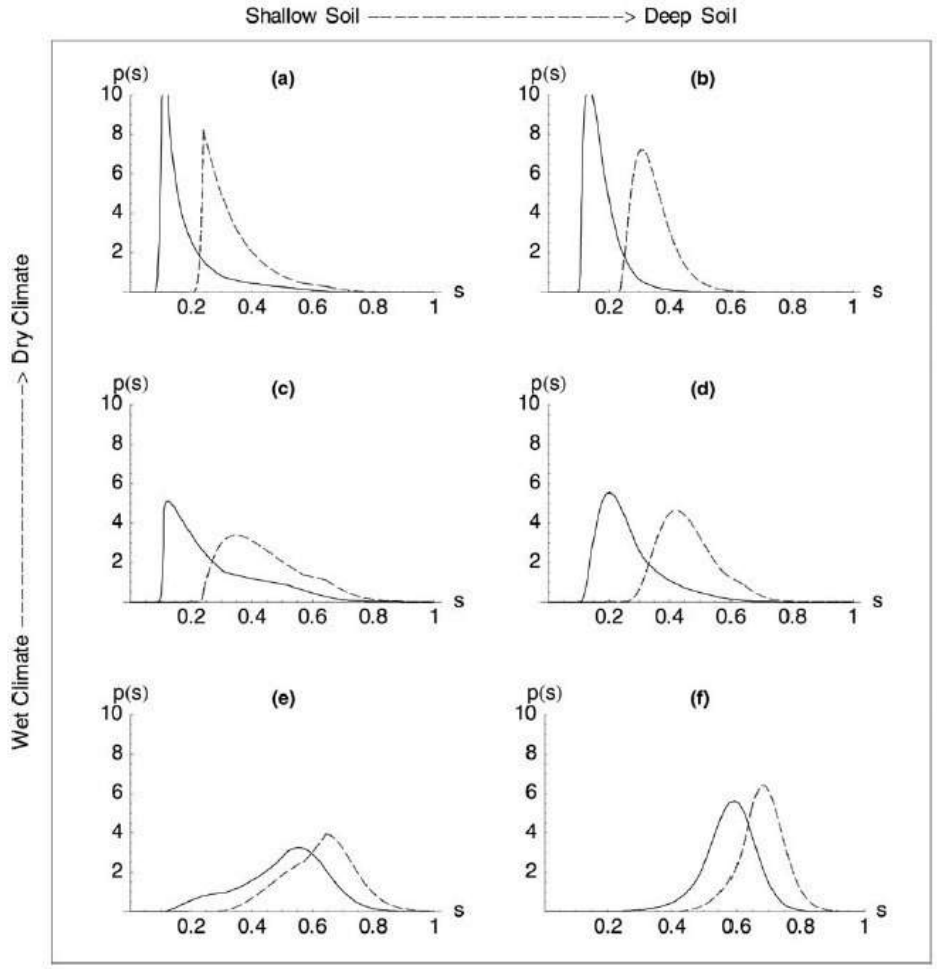

Figure 2.12: Examples of pdf's of soil moisture for different type of soil [loamy sand (continuous lines); loam (dashed line)], soil depth [Z_r= 30 cm (left panels); Z_r= 90 cm (right panels)] and mean rainfall rate [α= 1.5 cm; λ= 0.1 d^{-1} (top panels); λ= 0.2 d^{-1} (center panels); λ= 0.5 d^{-1} (bottom panels)] . Δ= 0 cm; E_w = 0.01 cm/d; E_{max}= 0.45 cm/d (from *Laio et al.*, 2001b)

2.4.4 Plant water stress

An ecological stress is a condition produced in an organism by potentially harmful levels of environmental factors (*Lauenroth et al.*, 1978). As mentioned in Sect. 2.4.1, in many WCEs, plant water stress represents the most important stress factor for vegetation with its effects on plant transpiration and photosynthesis and its direct and indirect control on the most important biogeochemical cycles (i.e. macronutrient cycles such as those of carbon, nitrogen, oxygen, phosphorous, sulfur and potassium). For example, microbial activities, responsible for ammonification and nitrification (that make nitrogen accessible for plant), are nonlinearly related to soil moisture (*Brady and Weil*, 1996).

A fundamental concept in ecohydrology for WCEs is that plant physiology is directly linked to water availability. Where there is ample water, as in rainforests, plant growth is more dependent on nutrient availability. However, in arid and semi-arid areas, vegetation type and distribution relate directly to the amount of water that plants can extract from the soil.

When insufficient soil water is available, a water-stressed condition occurs. It is important to point out that a drought condition for plants is not necessarily determined by precipitation scarcity but rather by insufficient soil moisture availability; thus plants could experience stress conditions even under favorable climatic conditions, due to poor soil characteristics. A large number of studies on physiological plant ecology have dealt with the problem of plant water stress (e.g., *Hsiao*, 1973; *Lange et al.*, 1976; *Levitt*, 1980; *Bradford and Hsiao*, 1982; *Smith and Griffith*, 1993; *Larcher*, 1995; *Ingram and Bartels*, 1996; *Nilsen and Orcutt*, 1998).

Different WCEs can be classified on the basis of the dominant vegetation present, identifying in this way different biomes. In Figure 2.13, a map describing the world distribution of the various biomes is shown. For example, in grasslands, average annual precipitation (that highly fluctuates from 500 to 900 mm/year) is great enough to support grasses (and in some areas a few trees); the soil of most grasslands is usually too thin and dry for trees to survive. Furthermore grasses can survive fires, which, on the opposite could prevent large forests from growing. Another important water-controlled biome is the savanna. Savannas vegetation is mainly constituted by grassland scattered with shrubs and trees. Savanna characteristics may be collocated between tropical rainforest and desert biome. Precipitation is usually limited to support a forest (often with wet-dry periods).

Water moves from the soil to the atmosphere by gradients of water potential (Figure 2.14). Soil water enters the roots because of the lower plant potential and moves along the xylem conduits up to the leaves driven by negative pressure gradients (Figure 2.15). The water flow along the soil-plant-

atmosphere system has to overcome a number of different resistances. When water reaches the leaf-atmosphere interface evaporates in the intercellular pores and diffuses out through the stomata (Figure 2.16). Plants have the possibility to change and control this last resistance varying the stomatal opening.

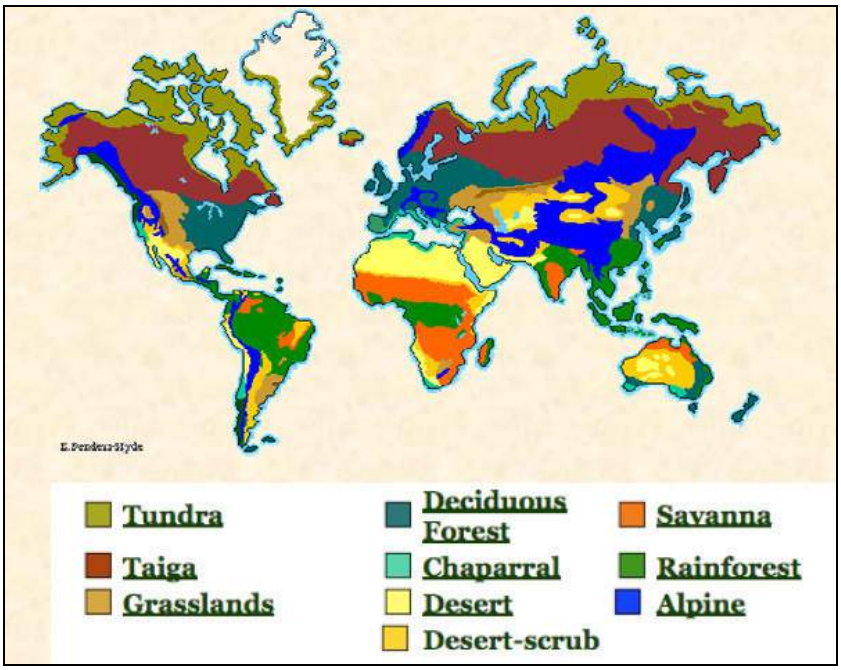

Figure 2.13: Map showing the world biomes (from *http://www.blueplanetbiomes.org/*)

Plant physiological response to water stress is quite complex and the effects of water stress differ from plant to plant and depend on the timing of drought during the growing season. Usually, the turgor pressure and the relative water content of the living tissue are the most important variables controlling plant water stress. These two variables are interdependent and are also related to the tissue water potential (*Rodriguez-Iturbe et al.*, 2004). Drought conditions cause a decrease in cell water potential which, in turn, produces a series of damages on plant physiology whose number and seriousness grow with the intensity and duration of water deficit: reduction of cell growth and wall cell synthesis; reduction of nitrogen uptake from soil; stomatal closure and reduction in CO_2 assimilation; flowering reduction and inhibition of seed and fruit production; potential insurgence of heat and radiation stress; wilting when the stomatal closure is complete (*Bradford and Hsiao*, 1982; *Nilsen and Orcutt*, 1998; *Rodriguez-Iturbe et al.*, 2004).

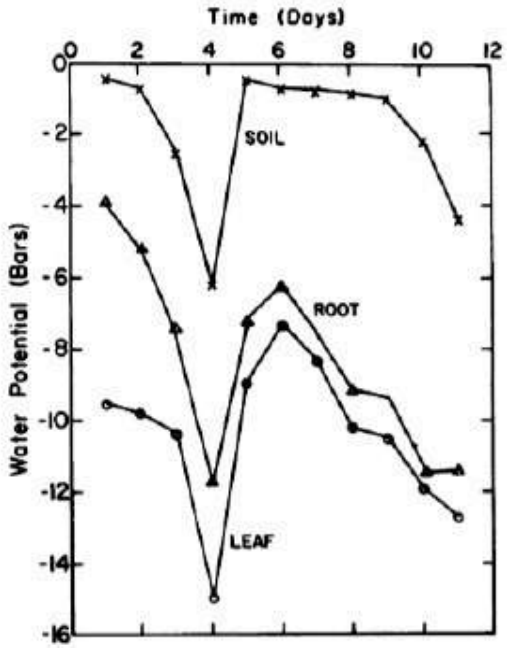

Figure 2.14: Soil, root and leaf water potentials of a moderately stressed plant (after *Adeoye et al.*, 1981)

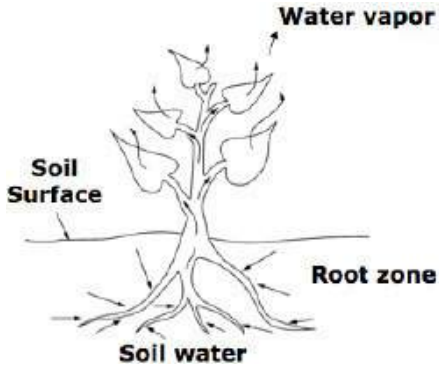

Figure 2.15: Schematic representation of water path along the plant during transpiration

Stomatal closure represents a key process for the description of the vegetation response to water deficit. Stomatal opening or closure is an osmoregulatory process controlled by guard cells surrounding the stomata; in particular high guard-cell turgor produces stomatal opening while low turgor induces stomatal closure (Figure 2.16). The diurnal cycle of stomatal opening

and closure is controlled by light presence while the degree of stomatal opening during daytime is mainly controlled by the soil moisture and secondarily by atmospheric humidity. The mechanism of stomatal closure can be seen as a preventive measure of plants to reduce internal water losses and risk of cavitation, before plant water potential is seriously lowered.

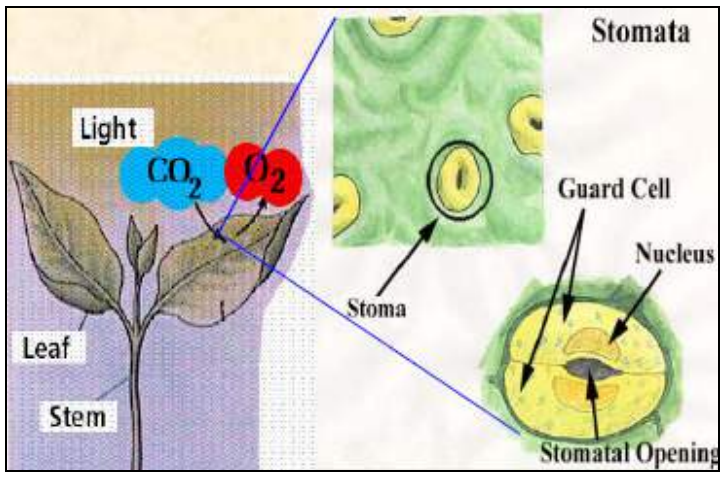

Figure 2.16: Schematic representation of plant stomata during transpiration process

The critical value of soil moisture s^*, introduced in Sect. 2.4.2, represents a threshold for the occurrence of water stress. Below this value, the plant begins to manifest a reduction of transpiration and the stomatal closure starts. The incipient stomatal closure is one of the first effects of water deficit on plants while, at the end of the sequence of the effects on physiology, the closure is complete and the plants starts wilting. This relation between stomatal closure and water stress suggests the stomatal closure as the ideal indicator of water stress.

In their attempt to model plant water stress as a function of the soil moisture, *Porporato et al.* (2001) assumed absence of water stress when the soil moisture is above the level of incipient stomatal closure, s^*, while when the complete closure is reached and then when the soil moisture is below s_w the water stress is assumed to be constant and at its maximum value.

With the aim to quantify plant water stress it is useful to define an index, *static water stress*, ζ, introduced by *Porporato et al.* (2001). This index ranges from 0 (absence of stress) to 1 (maximum stress), and defines plant water stress as a function of the soil moisture conditions at the time under consideration (for this reason it is referred as "static" water stress). The complete form of the equation defining ζ as a function of soil moisture is the following:

$$\begin{cases} \zeta(t)=1 & \longrightarrow s < s_w \\ \zeta(t)=\left[\dfrac{s^*-s(t)}{s^*-s_w}\right]^q & \longrightarrow s_w \le s \le s^* \\ \zeta(t)=0 & \longrightarrow s > s^* \end{cases} \tag{2.11}$$

where q is a measure of nonlinearity of the soil moisture deficit effects on plant conditions, which can vary with plant species and, to smaller extent, with the soil type.

This simple relation between soil moisture and water stress can be inverted in order to obtain a probabilistic description of static water stress. The inversion of Eq.(2.11) allows one to obtain the probability density function $f_z(\zeta)$ of $\zeta(s)$ as a derived distribution of the steady-state pdf of soil moisture $p(s)$, defined in the previous section by Eq.(2.10). The pdf of the static water stress presents two atoms of probability: the first one is equal to the probability of having no stress ($\zeta = 0$), that corresponds to the probability of soil moisture above the critical value s^*; the second atom is equal to the probability of having maximum stress ($\zeta = 1$), that corresponds to the probability of soil moisture below the wilting point s_w.

The continuous part of the pdf of ζ can be deduced from the pdf of s for $s_w < s \le s^*$, and it reads:

$$f_Z(\zeta)=\frac{C_\zeta}{\eta_w}\left[\left(1-\frac{\eta}{\eta_w}\right)\zeta^{\frac{1}{q}}+\frac{\eta}{\eta_w}\right]^{\frac{\lambda'(s^*-s_w)}{\eta-\eta_w}}\exp\left\{\gamma\left[\left(s^*-s_w\right)\zeta^{\frac{1}{q}}-s^*\right]\right\} \tag{2.12}$$

where:

$$\eta=\frac{E_{\max}}{nZ_r} \qquad \eta_w=\frac{E_w}{nZ_r} \tag{2.13}$$

and with λ' and γ defined by Eq.(2.5) and Eq.(2.8), respectively.

The constant of integration C_ξ can be deduced imposing the condition $\int_0^1 f_Z(\zeta)d\zeta = P(s^*) - P(s_w)$, where $P(s^*)$ and $P(s_w)$ are the values of the cumulative distribution of s calculated in $s = s^*$ and $s = s_w$ respectively.

The mean water stress during the growing season $\overline{\zeta}$ can be computed from Eq.(2.12) and considering the probability to have maximum stress $F_Z(1)$, that is equal to the probability of having soil moisture below the wilting point, $P(s_w)$. It takes into account also the periods when there is no stress and can be calculated analytically as

$$\overline{\zeta} = \int_0^1 \zeta \cdot f_Z(\zeta)d\zeta + F_Z(1) \tag{2.14}$$

Another water stress index, more meaningful in the valuation of the plant response to a certain soil moisture regime, is the mean water stress computed only during the periods when there is stress, then neglecting those periods when $\zeta = 0$. This term hereafter will be referred as *mean water stress modified*, $\overline{\zeta}'$, and can be obtained analytically dividing the mean water stress, $\overline{\zeta}$, by the value of cumulative distribution of soil moisture calculated in $s = s^*$. In this way, only the part of the pdf corresponding to ζ above zero is considered to obtain $\overline{\zeta}'$, i.e.,

$$\overline{\zeta}' = \frac{\overline{\zeta}}{P(s^*)} \tag{2.15}$$

This index gives the mean value of water stress provided that the plant is under stress and its definition is not restricted to steady-state condition but is also valid for transient conditions. In particular, the only quantity changing because of the transient condition is the probability of occurrence of a stress event. This is due to the Markovian nature (memory-less) of the dynamics provided by the Poisson process of rainfall. Thus, the presence of a transient condition could modify the value of the mean water stress and the value of $P(s^*)$, but their ratio, $\overline{\zeta}'$, keeps itself unchanged.

An interesting analysis of sensitivity of $\overline{\zeta}'$ to different rainfall conditions and different soil depths is presented in *Porporato et al.* (2001). The results of this study (shown in Figure 2.17) emphasize on the one hand a strongly non

linearity in the relationship between the average frequency of rainfall λ and the mean static water stress modified, with a rapid increase of $\overline{\zeta}'$ for dry climates (λ reduced and the average intensity α constant). On the other hand, considering moderate value of α and λ, the water stress $\overline{\zeta}'$ decreases with soil depth Z_r.

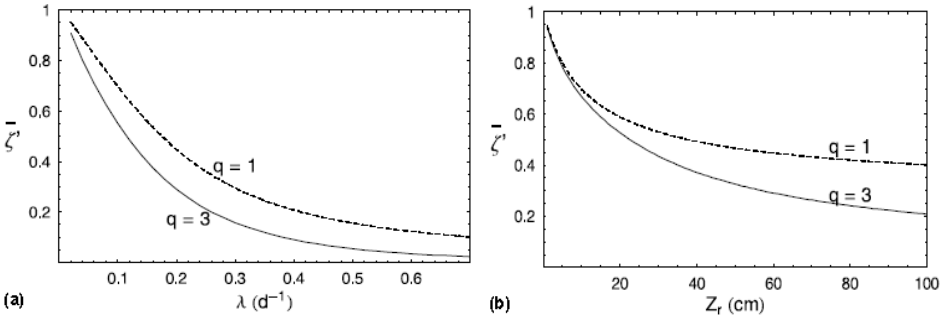

Figure 2.17: Sensitivity of the mean static stress, $\overline{\zeta}'$, with respect to: (a) rainfall frequency, λ; (b) active soil depth, Z_r. Common parameters are: α = 1.5cm; E_w= 0.01 cm/d; E_{max}= 0.45 cm/d; T_{seas}= 200 d. The active soil depth in (a) is Z_r= 60 cm, while the rainfall frequency in (b) is λ= 0.2 d^{-1}. The soil is a loam (b= 5.39; k_s= 20 cm/d; s_h= 0.19; s_w= 0.24; s*=0.57; s_{fc} = 0.65). From *Porporato et al.* (2001)

The response of plants to a certain soil moisture regime is not only linked to the soil moisture at that time, but it is strongly dependent also on the number and duration of the stress periods during the growing season. The static water stress described above is mostly related to the intensity of the soil moisture deficit, while the effects of other important features belonging to the time dimension such as duration and frequency of the water deficit periods are neglected.

It is clear that this static description of the physiological effects is not sufficient to fully describe the real sequence of damage that plants can suffer in relation to a certain soil moisture regime, especially for arid and semi-arid WCEs, where drought is often a prolonged and frequent phenomenon.

Duration and frequency of stress periods can be studied from the analysis of soil moisture *crossing properties*. According to definition of water stress given above, the period of stress occur whenever the soil moisture is below the value of incipient stomatal closure and persists until the soil water content raise above this value. The analytical expression of the mean length of the time intervals in which soil moisture is below a certain level during a growing season as well as the mean number of such intervals were obtained by *Rodriguez-Iturbe et al.* (2004). Here, for sake of simplicity, only the analytical expressions

are reported, omitting all the mathematical passages. In particular, considering as soil moisture threshold the value s^* and the function $\rho(s)$ and $p(s)$ defined by Eqs.(2.7) and (2.10), the mean number of upcrossing during a growing season of length T_{seas} and the mean duration of an excursion below the soil moisture level s^* are equal to

$$\begin{cases} \overline{n}_{s^*} = \rho(s^*) \cdot p(s^*) \cdot T_{seas} \\ \overline{T}_{s^*} = \dfrac{P(s^*)}{\rho(s^*) \cdot p(s^*)} \end{cases} \tag{2.16}$$

As mentioned before, the mean duration and frequency of water stress during the growing season are essential for understanding vegetation response to soil water deficits. *Porporato et al.* (2001) proposed a new index of water stress able to take into account also these two variables. This index, called *dynamic water stress* (or *mean total dynamic stress*) combines these two variables, defined by Eq.(2.16), with the previously defined mean static water stress [Eq.(2.15)]. The expression of the dynamic water stress $\overline{\theta}$ is the following:

$$\overline{\theta} = \begin{cases} \left(\dfrac{\overline{\zeta}' \cdot \overline{T}_{s^*}}{k \cdot T_{seas}} \right)^{\overline{n}_{s^*}^{-r}} & \rightarrow \quad if \quad \overline{\zeta}' \cdot \overline{T}_{s^*} < k \cdot T_{seas} \\ 1 & \rightarrow \quad otherwise \end{cases} \tag{2.17}$$

The parameter k represents an index of plant resistance to water stress and it is equal to the average static stress that a plant can experience without suffering permanent damage, when the duration of the stress period is coincident with the whole length of the growing season. The role of k is that to fix a threshold over which permanent damage appears, that is when $\overline{\zeta}' \cdot \overline{T}_{s^*} > k \cdot T_{seas}$. *Porporato et al.* (2001) found that one possible way to mathematically express the effect of $\overline{n}_{s^*}$ on the dynamic water stress is that to use a decreasing function of $\overline{n}_{s^*}$ as the exponent of $\left(\dfrac{\overline{\zeta}' \cdot \overline{T}_{s^*}}{k \cdot T_{seas}} \right)$; in particular, they

found the relation $\overline{n}_{s*}^{-1/2}$ as best function to interpreter the experimental evidences (*Levitt*, 1980; *Turner et al.*, 1985; *Larcher*, 1995). Thus, the parameter *r* in Eq.(2.17) is usually set equal to 0.5 (*Porporato et al.* 2001) and its role is that to link reasonably the mean number of periods of water stress to the actual plant water stress even in the case of very short, but frequent, stress periods, that otherwise would lead to an overestimated dynamic water stress.

Porporato et al. (2001) provide also an analysis on the impact of environmental conditions on dynamic water stress. Figures 2.18, 2.19 and 2.20 show respectively the behavior of the dynamic water stress as a function of the frequency of rainfall events, soil depth and total amount of rainfall during the growing season.

The first figure shows how the value of $\overline{\theta}$ decreases with an increase in the frequency of the storms, λ, considering constant both the mean depth of rainfall α and the soil depth Z_r. Thus, as rainfall becomes more frequent, soil water becomes more abundant and the water stress tends to disappear. The behavior of the different curves (characterized by different values of *k* and *q*) in Figure 2.18 shows a rapid decay of $\overline{\theta}$ for low values of λ and a slow decay to zero stress for high value of the frequency of storms. This is due to the fact that, for very arid climates, the duration of an excursion below *s** increases dramatically below a certain frequency of rainfall (there is a sort of threshold effect for a certain value of λ), strongly affecting the dynamic water stress, while, for very wet climates, all the components of the dynamic water stress (i.e., $\overline{\zeta}', \overline{T}_{s*}, \overline{n}_{s*}$) decrease with λ and then also the rate of decrease of the dynamic water stress becomes more marked. The figure shows also that the behavior of the dynamic water stress is rather robust to change of the parameters *k* and *q*.

Figure 2.19 shows the influence of the effective soil depth on the dynamic water stress. Three values of λ are considered with α constant, in order to analyze the behavior of $\overline{\theta}$ in dry, intermediate and wet conditions. When the climate is wet, the dynamic water stress decreases when the soil depth Z_r increases. In dry climates, the dynamic water stress manifests an opposite behavior, increasing with Z_r. This graph finds a strong correspondence in the reality. In dry climates, in fact, the shallower soil layers are the ones generally wetted by weak storm events, and, for this reason, it becomes fundamental for vegetation to have mostly superficial roots to be able to compete with the rapidly occurring evapotranspiration losses. On the opposite, in wet climates, the limit imposed by field capacity and the fact that the soil evaporation occurs mainly in shallower layers, lead to soil moisture conditions in the surface soil layers not too different from that occurring for drier climates, while a sizeable amount of water infiltrates to the deeper layers. Then, in wet climates, it is

important for a plant to have deep roots to be able to use the water stored into the deeper soil layers. One can note that this contrasting behavior can explain the fact that the curves in Figure 2.19, relative to an intermediate climate, develop a broad minimum for values of Z_r close to 30 cm.

Figure 2.20 shows the impact of timing and amount of rainfall on $\overline{\theta}$. The different curves are characterized by different values of the total amount of rainfall per season, Θ, while q, k and Z_r are kept fixed. The plot shows the dynamic water stress versus the frequency of rainfall events (for each curve, each value of λ corresponds to a value of α so that the total rainfall during the growing season, $\Theta = T_{seas}\alpha\lambda$, is constant). It is worth to note that, except for very wet conditions, there is a minimum in the curves that means an optimal condition for vegetation (minimum dynamic water stress). As a consequence it is possible to identify an optimal partition between the timing and amount of rainfall which minimizes the water stress. The position of such a minimum is decreasing and moving toward higher frequency (right-hand side of the diagram in Figure 2.20) for greater values of the total amount of rainfall Θ.

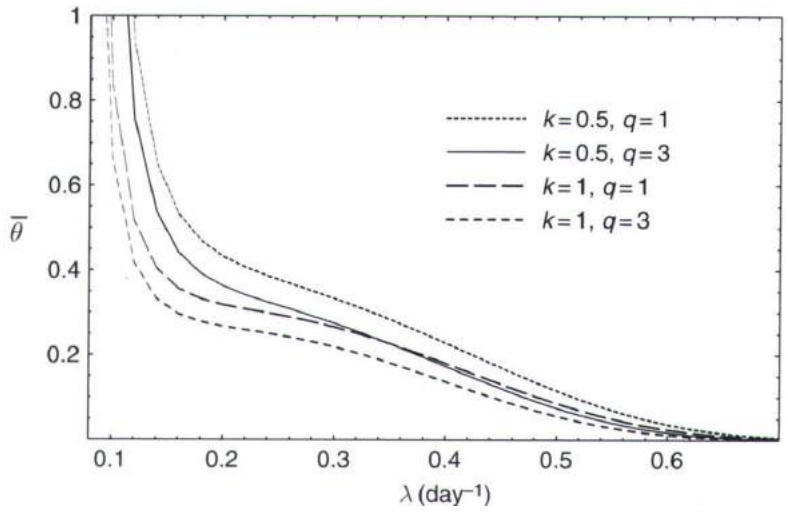

Figure 2.18: Mean dynamics water stress $\overline{\theta}$ as a function of the frequency of rainfall events λ for four different choices of the parameters k and q (T_{seas}= 200 days; α= 1.5 cm and Z_r= 60 cm). After *Porporato et al.* (2001).

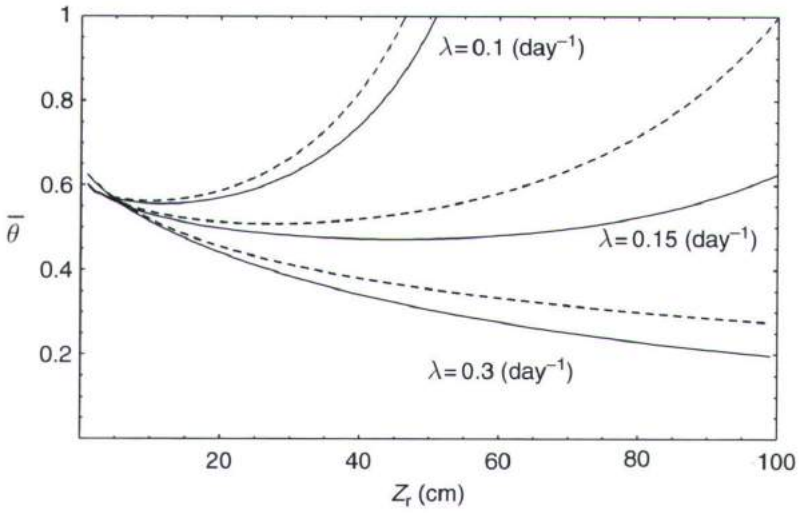

Figure 2.19: Mean dynamics water stress $\bar{\theta}$ as a function of the active soil depth Z_r for three different values of l two values of the parameters q (q=1 dashed lines, q= 3 continuous lines; T_{seas} = 200 days; k = 0.5 and α = 1.5 cm). After *Porporato et al.* (2001)

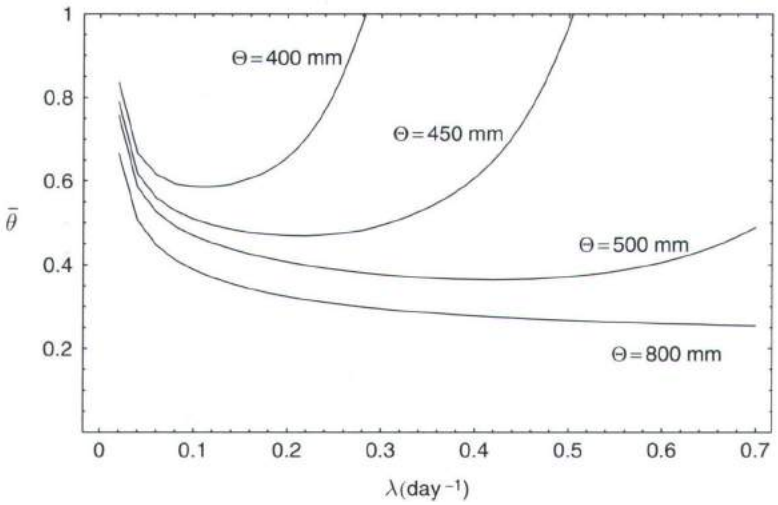

Figure 2.20: Impact of timing and amount of rainfall on dynamics water stress $\bar{\theta}$. Each curve corresponds to a constant total rainfall during the growing season, $\Theta = T_{seas}\alpha\lambda$. ($T_{seas}$ = 200 days; q= 2; k = 0.5 and Z_r= 60 cm). After *Porporato et al.* (2001)

2.5 Wetlands

2.5.1 Definition and characteristics

A wetland is an area of and whose soil is saturated either permanently or seasonally. Wetlands (or humid lands) are defined as those areas that are inundated or saturated by surface or groundwater at a frequency and duration sufficient to support a prevalence of vegetation typically adapted for life in saturated soil conditions. They have been categorized both as biomes (i.e., on the basis of the dominant vegetation present) and ecosystems, and are characterized as having a water table that stands frequently at or near the land surface. Wetlands have also been described as ecotones, providing a transition between drylands and water bodies. *Mitsch and Gosselink* (2009) stated that wetlands exist

> *"...at the interface between truly terrestrial ecosystems and aquatic systems, making them inherently different from each other, yet highly dependent on both."*

Wetlands have aroused considerable attention only in recent years as appreciation of the direct and indirect benefits of these ecosystems has increased. Due to their lack of potential financial benefits, wetlands have historically been the victim of large-scale draining efforts, but they are indeed far more important in the biosphere than their almost 7% of the landscape would suggest. Wetlands are very effective at filtering and cleaning water, so to represent a valid help with the ever increasing challenge of decreasing water pollution. The importance of wetlands is also linked to their role in protecting coastlines from hurricanes and tsunamis, mitigating flooding of streams and rivers. And overall they provide an immense storage of carbon that, if released with climate shifts, could accelerate those changes. Wetlands are dynamical, complex habitats, supporting high levels of biological diversity (*Ramsar Convention Bureau*, 1996). They are considered the most biologically diverse of all ecosystems, providing a bountiful habitat for a great diversity of plant and animal species. For all these reasons, in many locations, such as the United Kingdom, Iraq, South Africa and the United States, wetlands are the subject of many conservation efforts and biodiversity action plans.

Wetlands can take many forms; examples include: *marshes*, *estuaries*, *mudflats*, *mires*, *ponds*, *fens*, *pocosins*, *swamps*, *deltas*, *coral reefs*, *billabongs*, *lagoons*, *shallow seas*, *bogs*, *lakes and floodplain*. Figure 2.21 shows some photos of different wetlands. As it is shown in Figure 2.22, almost every country in the world possesses a wetland of some description. Some are seasonally aquatic, some seasonally terrestrial.

Figure 2.21: Examples of different wetland types. From left to right (clockwise): 1) Chitwan National Park, Nepal; 2) Kakadu National Park, Australia; 3) Gur River floodplain, Siberia; 4) Lochinvar National Park, Zambia; 5) and 6) Pantanal, Brazil. (photos from the WWF web-site: http://www.panda.org/)

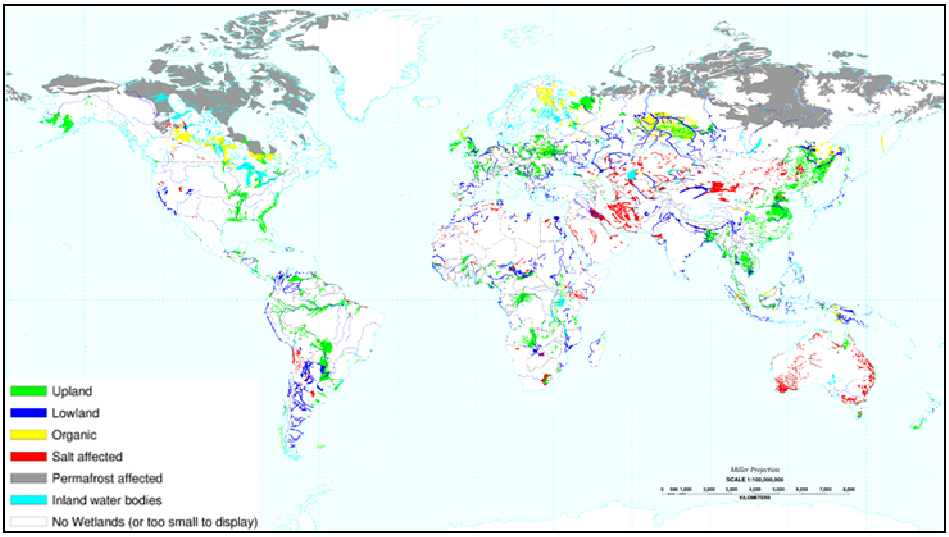

Figure 2.22: Distribution of the wetlands in the world (US Dept. of Agriculture, NRCS – from Wetland International Global Site)

In this paragraph, a brief description, from the WWF web site (http://www.panda.org/), of some of these different types of humid lands is provided to illustrate the huge variety of wetlands. *Mangrove swamps* are forested ecosystems found at sheltered tropical coastal areas (about 70% of tropical coastlines are mangrove-lined). The partly submerged roots of mangrove trees spread out beneath the water to trap sediment and prevent it being washed out to sea. *Floodplains* are areas of flat land seasonally flooded by rivers and lakes. *Inland floodplains* and *coastal deltas* are the natural overflow areas that slow the velocity of the floodwaters, allowing nutrients and sediments to settle. *Bogs* are waterlogged peatlands in old lake basins or depressions in the landscape. Almost all water in bogs comes from rainfall. *Pocosins* are evergreen shrub bogs found on the coastal plain of the southeastern United States. They are typically found on high areas of a flat water-logged landscape. Like bogs, *fens* were formed when glaciers retreated. Unlike bogs, some of the water in fens comes from small streams and groundwater. *Marshes* are one of the broadest categories of wetlands in the world and in general host the greatest biological diversity. Marshes form in depressions in the landscape, as fringes around lakes, and along slow-flowing streams and rivers. They slow down the rate of rainfall drainage and control its flow into rivers, lakes, and streams. Photos in Figure 2.23 show an example of a mangrove swamps and floodplains.

Figure 2.23: Examples of different wetland types. On the left, mangrove swamps in the Ndian River delta, Cameroon; on the right, floodplains of the Kafue river, Zambia (photos from the WWF web-site: http://www.panda.org/)

Wetlands can be considered as three-component ecosystems, where the basis components are geomorphology, hydrology and climate. The hydrology of landscapes influences and changes the physiochemical environment, which, in turn, along with hydrology, determinates the biotic communities that are found in the wetlands. Overall, climate is the most important component of the wetlands. Climate, which includes solar energy, temperature patterns, and precipitation, couples with the geomorphology of the landscapes to influence where and when water is present long enough to cause the presence of the wetlands.

In Figure 2.24 a sketch of the three fundamental and mutually connected components basis of wetlands is shown (*Mitsch et al.*, 2007).

As mentioned above, wetlands generally include swamps, marshes, bogs and similar areas. The water found in wetlands can be saltwater, freshwater, or brackish. There are several classification systems in literature to categorize wetland ecosystems. The core of the classification has three components: (a) geomorphic setting, (b) water source and its transport, and (c) hydrodynamics.

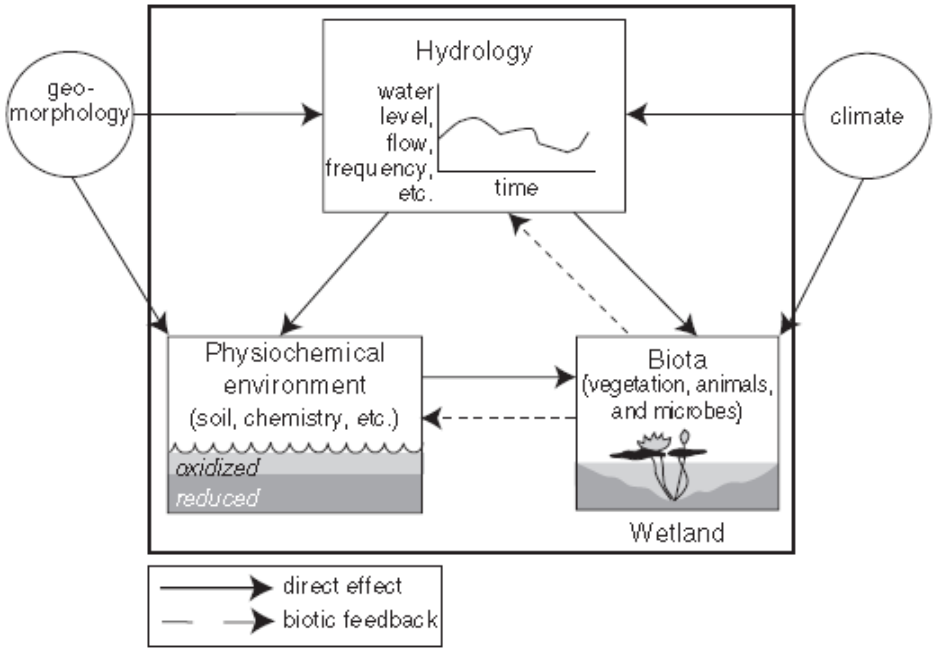

Figure 2.24: Conceptual model of a wetland ecosystems, showing the three-component basis of a wetland often used in wetlands definitions, and the principal cause of wetlands-climate and landscapes geomorphology (*Mitsch and Gosselink*, 2007)

Geomorphic setting is the topographic location of the wetland within the surrounding landscape. The types of water sources can be simplified to three: precipitation, surface or near-surface flow, and groundwater discharge. Obviously all the three water sources can coexist and the relative contribution of each one can determinate the type of wetland (Figure 2.25). Hydrodynamics refers to the direction of flow and strength of water movement within the wetland (Figure 2.26). While the three components are treated separately, it is apparent that they are subjected to a considerable interdependency.

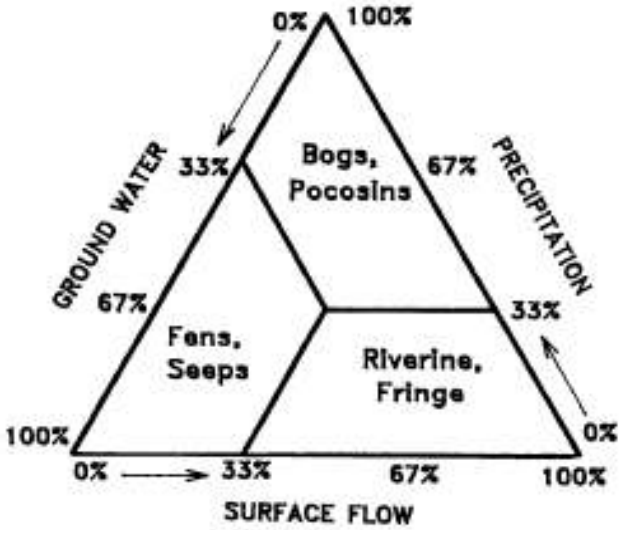

Figure 2.25: Relative contribution of the three water sources (precipitation, lateral surface flow and groundwater discharge) to a wetland: location of major wetland types (bog, riverine, etc.) within the triangle show the relative importance of water sources (*Brinson*, 1987)

The hydrologic characteristics of wetlands influence four ecosystems attributes: species composition of the plant community, primary productivity, organic deposition and flux, and nutrient cycling (*Brinson*, 1993).

Novitzki (1979) described the hydrologic characteristics of Wisconsin's wetlands with regard to water source and landform. In particular, the author recognized four hydrologic types of wetland: surface water depression, groundwater depression, surface water slope, and groundwater slope (Figure 2.27). Surface water depressions receive precipitation and overland flow. Losses are through evapotranspiration (ET) and downward seepage into a superficial aquifer. Groundwater depression wetlands, in contrast, intercept the water table, so they receive groundwater in addition to direct precipitation and overland flow. Groundwater slope wetlands differ from the groundwater

depressions by having an outlet and also tending to occur on slopes where groundwater has stronger flow than would normally be encountered in depressions. The size of these wetlands corresponds to the quantity of groundwater discharge. Surface water slope wetlands receive water from lake or river flooding, and the water can readily drain back into lake or river as the stages fall. They may be flooded infrequently, as in the cases of floodplains, or permanently, as in the case of lakeside wetlands.

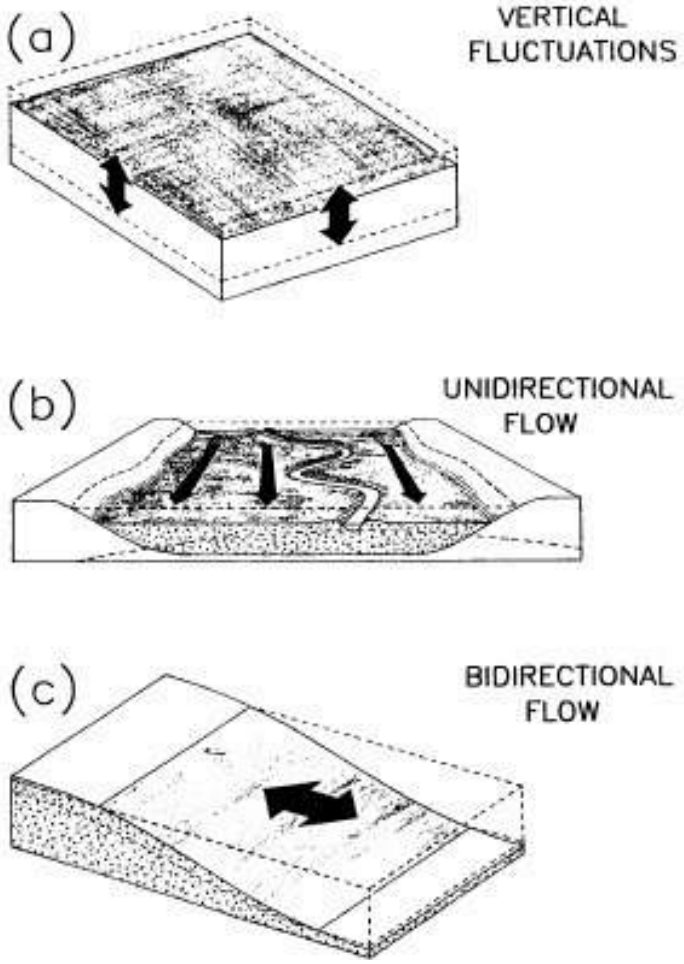

Figure 2.26: Categories of hydrodynamics based on dominant flow pattern: (a) vertical fluctuations (normally caused by evapotranspiration and precipitation); (b) unidirectional flows (horizontal surface and subsurface); (c) bidirectional flows (horizontal across the surface). From *Brinson* (1987)

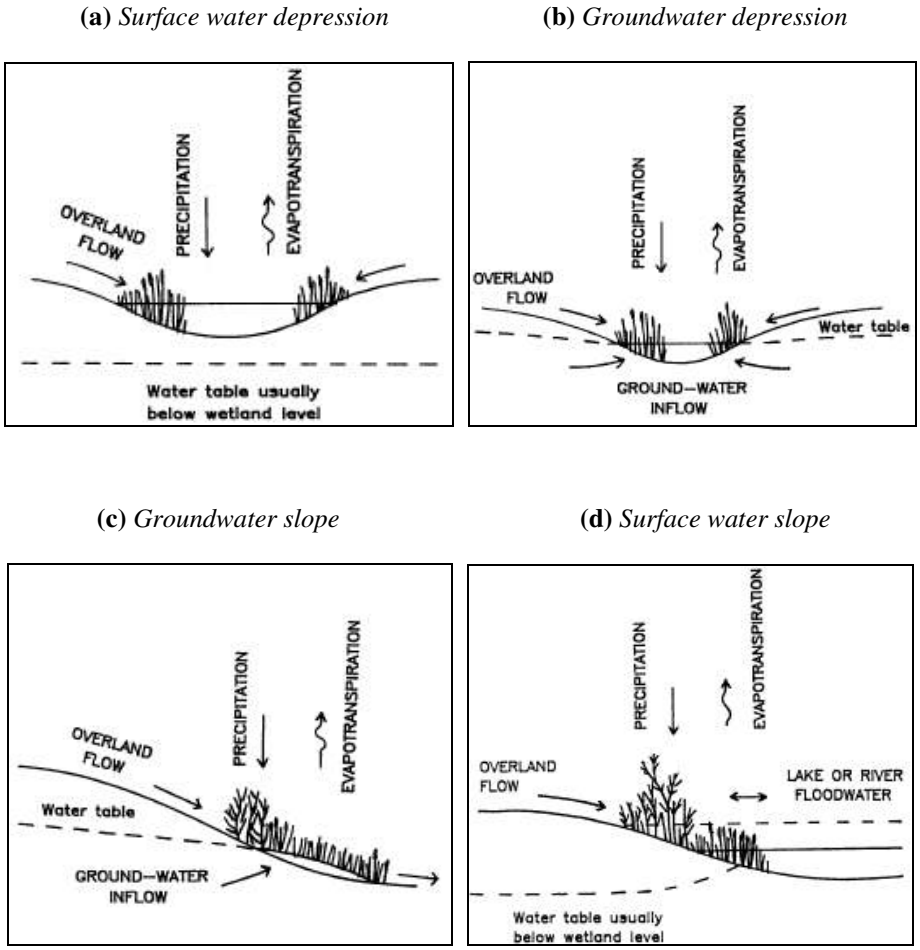

Figure 2.27: Four major hydrologic types of wetlands types in Wisconsin (after *Novitzki*, 1979 and *Brinson*, 1993)

The dependence of many types of wetlands on the groundwater makes them classifiable as groundwater dependent ecosystems. In Chapter 4, these kinds of ecosystems will be deeply discussed together with the ecohydrological modelling for the study of the dynamics of interaction between climate, soil and vegetation and for the study of the interdependence between soil moisture and groundwater fluctuations in such environments.

2.5.2 Wetlands classification

There are several possible classifications of the wetlands. The most used and known of these is certainly that dividing wetlands into two major groups (*Brinson et al.,* 1993):

- *Coastal wetlands*
- *Inland wetlands*

The first group regards those tidal areas located in coastal regions, while the second one is constituted by non tidal wetlands and can be divided into two further subclasses: *freshwater swamps* and *marshes*; and *peatlands*.

Several types of *coastal wetlands* are influenced by alternate floods and ebbs of oceanic tides. Near coastlines, the salinity of the water approaches that of the ocean, whereas further inland, the tidal effect can remain significant even when the salinity approaches that of freshwater. Coastal wetlands include tidal salt marshes, tidal freshwater wetlands, and mangroves swamps.

Salt marshes are found throughout the world along protected coastlines in the middle and high latitudes. They are primarily detrital-based, with abundant fauna dependent directly (e.g., crabs) or indirectly (e.g., birds, estuarine fish) on this detrital production. A modest amount of the marsh grass productivity is consumed by grazing. Plants and animals in these systems have adapted to the stresses of salinity, periodic inundation, and extremes in temperature.

Tidal freshwater marshes and swamps are found inland from the tidal salt marshes or mangroves but still close enough to the coast to experience tidal effects. These wetlands are usually dominated by a variety of grasses and by annual and perennial broad-leaved aquatic plants but sometimes by trees. Tidal freshwater marshes can be described as intermediate in the continuum from coastal salt marshes to freshwater marshes. Because they are tidally influenced but lack the salinity stress of salt marshes, tidal freshwater marshes have often been reported to be very productive ecosystems, although a considerable range in their productivity has been measured. Tidal freshwater swamps are similar to upland riverine swamps, except that the water levels are variable on a daily schedule and are less prone to excessive changes.

Tidal salt marshes are replaced by mangrove swamps in subtropical and tropical regions of the world. The word *mangrove* refers to both the wetland itself and to the salt-tolerant trees that dominate those wetlands. Mangrove swamps are found all over the world in tropical and subtropical regions, generally between 25°N and 25°S, and are estimated to cover 24 million ha worldwide. In the United States, they are limited primarily to the southern tip of Florida where 300,000 to 500,000 ha are found. In Florida, mangrove wetlands are generally dominated by the red mangrove tree *(Rhizophora)* and the black

mangrove tree *(Avicennia)* and export organic matter to the adjacent estuaries, as do salt marshes. Like salt marshes, the mangrove swamps require protection from the open ocean and occur in a wide range of salinity and tidal influence.

On a real basis most of the wetlands of the world are not located along coastlines but are found inland. These wetlands are sometimes referred to as ''non-tidal'' in coastal regions to distinguish them from the coastal wetlands described previously. As mentioned above, according to *Brinson* (1993) it is possible to divide these inland wetlands into two different categories: the first is constituted by *freshwater marshes* and *freshwater forested swamps*; the second is constituted by *peatlands*.

Freshwater marshes includes a diverse group of wetlands characterized by emergent soft-stemmed aquatic plants such as cattail, bulrush, arrowhead, pickerel-weed, reed, and several other species of grasses and sedges, a shallow, seasonally changing water regime, and shallow organic soil deposits. Major regions where marshes dominate include the Okavango Delta in Botswana, the prairie pothole region of the Dakotas, and the Everglades of Florida. They occur in isolated basins, as fringes around lakes, and along sluggish streams and rivers. *Freshwater forested swamps* range from wetlands that have standing water for most, if not all, of the growing season to riparian bottomland forests that are less frequently flooded but found all around the world across many climates. Riparian wetlands also occur in arid and semi-arid regions, where they are often a conspicuous feature of the landscape in contrast with the surrounding arid grasslands and desert. Riparian ecosystems are generally considered to be more productive than the adjacent uplands because of the periodic inflow of nutrients, especially when flooding is seasonal rather than continuous.

Finally, *peatlands* include the deep peat deposits of the boreal regions of the world. They are the most ubiquitous wetland in the world. *Bogs* and *fens*, the two major types of peatlands, occur as thick peat deposits in old lake basins or as blankets across the landscape. Many of these lake basins were formed by the last glaciation, and the peatlands are considered to be a late stage of a ''filling-in'' process. Bogs are noted for their nutrient deficiency and waterlogged conditions and for the biological adaptations to these conditions such as carnivorous plants and nutrient conservation.

Another more complex classification of the wetlands is based on the relative contribution of water sources (see also Figure 2.25). The system described in Figure 2.28, has been developed for the East Anglian fens (*Gilvear et al.*, 1989) and distinguishes between seven different classes:

- surface water runoff and riverine flooding (two subclasses);
- leaky aquifer with some surface water inputs;

- superficial aquifer sequences with some surface inflow;
- both superficial and aquifer sources;
- leaky main aquifer although some surface water input;
- groundwater inputs from an unconfined main aquifer;
- sources totally from the superficial aquifer.

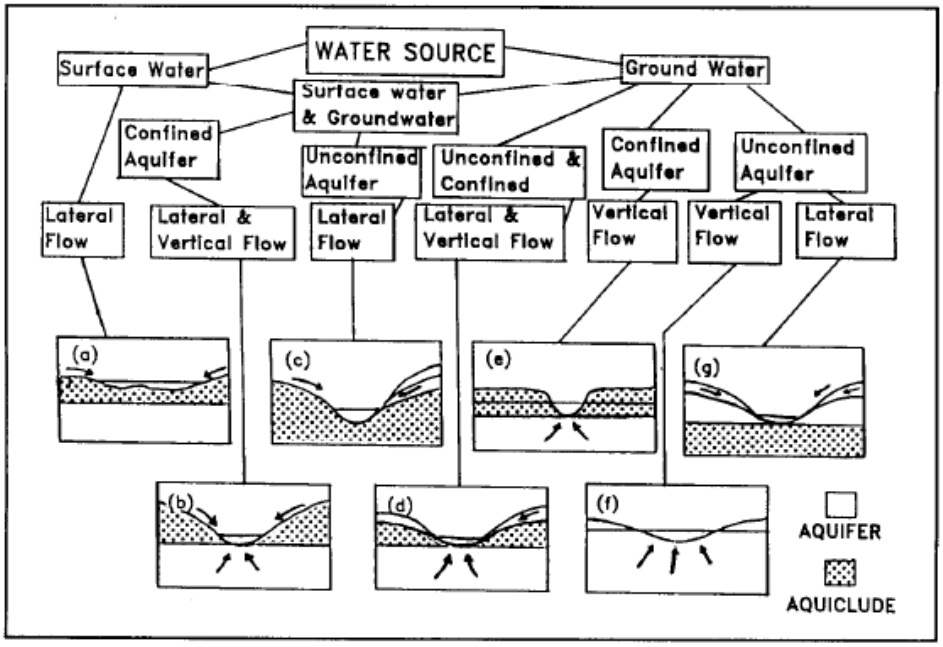

Figure 2.28: Hydrogeologic classification of *Gilvear et al.* (1989) for East Anglian fens. Description of wetland classes are as follows: (a) those fed by surface water runoff and wetlands that receive river flooding, (b) those receiving aquifer discharge in addition to some surface water, (c) those fed by superficial groundwater in addition to some surface water, (d) those receiving both superficial groundwater and aquifer discharge, (e) those fed predominately by aquifer discharge with minor surface water input, (f) those fed by unconfined main aquifer, and (g) those receiving total superficial groundwater. Precipitation inputs are assumed similar in all examples (after *Brinson*, 1993)

Chapter 3

Ecohydrology in Mediterranean Water-Controlled Ecosystems

3.1 Introduction

In this chapter an ecohydrological approach to the study of the soil moisture dynamics and the consequent response of vegetation in Mediterranean water-controlled ecosystems is discussed. In particular, in the first part of this chapter a non-steady ecohydrological model developed by the candidate is presented. This work, presented at the *European Geosciences Union Assembly 2007*, was published in 2008 (*Pumo et al.*, 2008). The innovative model here described is able to reproduce soil moisture probability density function, obtained analytically in previous studies for different climates and soils in steady-state conditions; consequently it can be used to compute both the soil moisture time-profile and the vegetation static water stress time-profile in non-steady conditions.

In the second part of this chapter two possible applications of such a model are discussed. Initially the model has been applied at the forested *Eleuterio at Lupo* river basin in Sicily (Italy) with the purpose to show this different kind of approach to ecohydrological models in Mediterranean areas, investigating also the influence of different annual climatic parameterizations on the soil moisture probability density function and on the vegetation water stress evaluation.

The second application of the ecohydrological model shows the ability of this new approach to evaluate quantitatively the effects of climatic forcing changes on the vegetation water stress. In particular the model is again applied to the *Eleuterio at Lupo* river basin, considering the possible climate changes recently predicted in Mediterranean areas.

3.2 An ecohydrological model for Mediterranean water controlled ecosystems

3.2.1 Mediterranean water controlled ecosystems

Water-controlled ecosystems in arid and semi-arid environments such as African's or middle American's savannas were optimal systems in the development of the first ecohydrological models because of the relative simplicity of the mechanisms related to all the hydrologic processes involved in the soil moisture dynamics. In particular the absence of transient conditions allowed a simplified analytical approach to the models for the description of the soil moisture dynamics in such ecosystems.

Starting from the model proposed by *Rodriguez-Iturbe et al.* (1999a) and described in the previous chapter (see Sect. 2.4), several ecohydrological models have been developed and improved, different each other and characterized by different goals. Most of the existing ecohydrological models are based on a soil water balance, even if some differences are present in the model components and in the solving approaches. The most common ecohydrological models, such as that proposed by *Rodriguez-Iturbe et al.* (1999a), start from a stochastic differential equation describing the soil water balance, where the unknown quantity, the soil moisture, depends both on spaces and time. Most of the solutions existing in literature are obtained in a probabilistic framework and under steady-state condition; even if this last condition allows the analytical handling of the problem, it has considerably simplified the same problem by subtracting generalities from it. For example, *Laio et al.* (2001b) obtained the analytical expression for the soil moisture pdf in steady state conditions (see Sect. 2.4.3). This model has been applied in regions where the growing season is usually in phase with the wet one (*Laio et al.*, 2001a). These climatic conditions make the steady-state hypothesis reasonably satisfied, since the effects of the transient condition, due to an initial soil moisture condition (at the beginning of the growing season), are limited to a short time-period.

The steady-state hypothesis, whose characteristics were described in Sect. 2.4.3, appears perfectly applicable in such kinds of WCEs, but it seems to be no more valid in areas with Mediterranean climate.

In many arid and semi-arid Mediterranean ecosystems the water is the limiting factor for vegetation: the scarcity of water affects directly all the plants physiological activities and at the same time limits also the other biogeochemical cycles. Such ecosystems are strictly dependent on water resource and then on the soil moisture dynamics and for this reason they can be

defined as WCEs. In such environments, deep and shallow rooted species cohabit and compete with each other for the same resource, that is the water.

The climate, especially with regard to the precipitation and the evapotranspiration processes, plays then a fundamental role in the vegetational patterns formation (*Hubbell*, 2001). Mediterranean ecosystems evolve under climatic conditions characterized by precipitation markedly out of phase with the growing period for the vegetation there established (*Bolle*, 2003). Precipitations in Mediterranean semi-arid WCEs are mainly concentrated in the autumn–winter period, when the vegetation is almost inactive. For this reason, during the wet season the level of soil moisture tends to increase and it will be available for the vegetation at the beginning of the subsequent growing season (spring-summer period). The vegetation, adapting itself to these soil moisture dynamics, often develops an extensive water uptake strategy, by delving the roots into the soil in order to utilize the water stored in the deeper layers.

During the wet season there is then a recharge of soil moisture into the root zone that is important in the following drier and hotter season especially for deep rooted species, while shallow rooted plants are mainly dependent to the intermittent seasonal precipitation (*Rodriguez-Iturbe et al.*, 2001a).

In scientific literature there are only few studies regarding climates with periods characterized by higher temperatures and more frequent rainfall, seasonally out of phase. *Kiang* (2002) and *Baldocchi et al.* (2004) analyzed the stochastic soil moisture dynamics and the related water stress for a Californian savanna, where the climate is semi-arid and similar to Mediterranean one. Using soil moisture data recorded in situ, *Kiang* (2002) compared these data with the predictions of the stochastic model proposed by *Laio et al.* (2001b), finding a general good agreement but with some differences due to the role of the initial soil moisture transient, not included by the analytic model. Although other attempts to face transient problems analytically have been made (e.g. *Viola et al.*, 2008, described analytically the transient soil moisture dynamics as a function of the initial conditions at the beginning of the growing season), this kind of approach has been recently abandoned and does not seem to be the best way to investigate soil-climate-vegetation interactions in Mediterranean area.

In the following sections a non-steady ecohydrological model is presented and discussed, showing how this innovative model is able to describe soil moisture dynamics and the vegetation water stress also in non-steady conditions.

The differences between the steady-analytical and the non-steady numerical probability density functions are analyzed, showing how the proposed model is able to capture the effects of winter recharge on the soil moisture. The new approach in fact uses a model which implicitly takes into account the transient effects of the initial soil moisture condition at the beginning of the growing season and works using an opportune time-scale

(lower than daily), through a finite differences method, computing the soil moisture temporal evolution. The soil moisture dynamics, reproduced through this numerical model, summarize the interrelationships among climate, soil and vegetation and furthermore are strongly correlated with the vegetation stress, defined by *Porporato et al.* (2001). In particular, the mean static water stress modified (see Sect. 2.4.4) is numerically computed from the soil moisture time-profile. Starting from the same profile it is also possible to calculate the mean duration and frequency of water stress periods and hence a dynamic water stress index conceptually similar to that described in Sect. 2.4.4.

The application to a case study characteristic of Mediterranean climate is functional to the understanding of the model and shows the sensitivity of the same model to different annual parameterization of the climatic forcings.

3.2.2 Soil water balance at a point and analytical solution

The model here discussed is conceptually similar to the one proposed by *Rodriguez-Iturbe et al.* (1999a), improved by *Laio et al.* (2001b) and partially described in the previous chapter.

In the analysis of the dynamic relationships among climate, soil and vegetation, soil moisture constitutes the main link, in space and in time, between the climatic variations on the one hand and the vegetational dynamics on the other hand. If a seasonal time-scale, i.e. the growing season, and a space-scale of few meters are considered, climate can be assumed as external forcing for the considered system, being not dependent on the soil moisture.

The soil-vegetation system is hypothesized homogeneous with regard to the soil type and the plant there present, with depth coincident with the root zone, Z_r; moreover, both the soil and vegetation features are considered time invariant. No interactions with the water table and no dynamic effects due to the impact of the rainfall drops arriving onto the soil surface are considered.

As for the model presented in Sect. 2.4, the water balance is considered vertically averaged over the root zone, under the simplifying assumption that the lateral water contributions, mainly due to topographic effects, can be neglected. The assumption of vertically averaged conditions over Z_r is realistic if the propagation of the wetting front and the soil-moisture redistribution over the rooting zone may be assumed to take place within the daily timescale. *Guswa et al*. (2002) demonstrated that such assumption is reasonable also for deeper rooted plants concluding that the plant has the ability to compensate for spatial variation in saturation.

The soil water balance equation can be written in the same form of Eq.(2.2), and it is a stochastic ordinary differential equation describing at each point the behavior of soil moisture in time.

The net rainfall, equal to the difference between the rainfall and the water losses due to interception and runoff, is generated through a Dunnian saturation mechanism (i.e. the runoff is produced when the rainfall exceeds the maximum storage capacity of the soil at a certain time). Rainfall depth is again considered as an independent random variable exponential distributed with mean α, while the occurrence is considered to be a stationary Poissonian process with frequency λ (*Rodriguez-Iturbe et al.,* 2004).

Vegetation intercepts part of the rainfall, which never arrives to soil surface and is lost directly through evaporation. The interception, due to the leaf apparatus of vegetation, is modeled by means of a fixed threshold model, in which the threshold value Δ depends on vegetation type.

For the evapotranspiration losses a piecewise function is considered, adopting the same assumption introduced in Sect. 2.4.2. The dependence of evapotranspiration losses on soil moisture is thus summarized in the following expression

$$E(s)=\begin{cases} 0 & \longrightarrow 0 < s \le s_h \\ E_w \dfrac{s-s_h}{s_w-s_h} & \longrightarrow s_h < s \le s_w \\ E_w + \left(E_{\max}-E_w\right)\dfrac{s-s_h}{s_w-s_h} & \longrightarrow s_w < s \le s^* \\ E_{\max} & \longrightarrow s^* < s \le 1 \end{cases} \tag{3.1}$$

where the evaporation losses rate E_w at wilting point, s_w, is fixed equal to a conventional value 0.01 cm/day (*Rodriguez-Iturbe et al.*, 1999c). The relation linking soil moisture to evapotranspiration is not unique and may be nonlinear, depending on the vertical distribution of soil moisture (*Guswa*, 2005). Thus, the same average root zone saturation level might lead to different transpiration rate. However this non uniqueness is attenuated by the ability of the root system to compensate for spatial variations in soil moisture (e.g., hydraulic lift and other plant active mechanisms).

Leakage losses intervene when the value of soil moisture is higher than the field capacity. When the relative soil water content is higher than field capacity

s_{fc}, the active soil depth tends to lose water excess by gravity. The loss rate is assumed to be at the maximum (K_s, saturated hydraulic conductivity) when the soil is saturated and then rapidly decays as the soil dries following the decrease of hydraulic conductivity $K(s)$. For soil moisture equal to field capacity, hydraulic conductivity can be assumed equal to zero. The decay of the hydraulic conductivity is usually modelled using empirical relationships. Here, the exponential form (*Rodriguez-Iturbe et al.*, 2004) is considered, using a coefficient $\beta = 2b+4$, where b is an index related to the type of soil and pore size. The assumed behavior of leakage losses is thus expressed as

$$L(s) = \frac{K_s}{e^{\beta(1-s_{fc})}-1}\left[e^{\beta(s-s_{fc})}-1\right] \qquad \longrightarrow s_{fc} < s \le 1 \tag{3.2}$$

where the coefficient β is used to fit the above expression to the well-known power law by *Clapp and Hornberger* (1978).

Figure 3.1 shows the assumed scheme for the soil water losses and, in particular, the dependence of $\chi[s(t),t]$ by the relative soil moisture content, considering two different values for E_{max}; the former is a mean value of potential evapotranspiration during the growing season for a typical Mediterranean climate, while the latter is a mean value during the dormant season for the same climate. The water losses scheme in Figure 3.1 does not differ conceptually from the one discussed in Sect. 2.4.2 and represented in Figure 2.10.

In relation to the soil moisture conditions it is then possible to identify five different regimes of water losses from the soil. Considering the definition of η and η_w provided by Eq.(2.13) and defining m as

$$m = \frac{K_s}{nZ_r\left(e^{\beta(1-s_{fc})}-1\right)} \tag{3.3}$$

the complete form of Eq.(2.10), that gives the normalized loss function, can be rewritten as

$$\rho(s)=\begin{cases} 0 & \longrightarrow 0 < s \le s_h \\ \eta_w \dfrac{s-s_h}{s_w-s_h} & \longrightarrow s_h < s \le s_w \\ \eta_w + (\eta-\eta_w)\dfrac{s-s_h}{s_w-s_h} & \longrightarrow s_w < s \le s* \\ \eta & \longrightarrow s^* < s \le s_{fc} \\ \eta + m\left[e^{\beta(s-s_{fc})}-1\right] & \longrightarrow s_{fc} < s \le 1 \end{cases} \tag{3.4}$$

The analytical solution of Eq.(2.2) consists in the determination of the soil moisture pdf that, in general, depends on time.

Assuming that the soil moisture pdf is not time dependent (steady-state condition), it is possible to utilize the approximate analytical solution of water balance equation given by *Laio et al.* (2001b) in piecewise form, that reads

$$p(s)=\begin{cases} \dfrac{C}{\eta_w}\cdot\left(\dfrac{s-s_h}{s_w-s_h}\right)^{\frac{\lambda'\cdot(s_w-s_h)}{\eta_w}-1}\cdot e^{-\gamma s} & \longrightarrow s_h < s \le s_w \\ \dfrac{C}{\eta_w}\cdot\left[1+\left(\dfrac{\eta}{\eta_w}-1\right)\cdot\left(\dfrac{s-s_w}{s^*-s_w}\right)\right]^{\frac{\lambda'\cdot(s^*-s_w)}{\eta-n_w}-1}\cdot e^{-\gamma s} & \longrightarrow s_w < s \le s* \\ \dfrac{C}{\eta}\cdot e^{-\gamma s+\frac{\lambda'\cdot(s-s^*)}{\eta}}\cdot\left(\dfrac{\eta}{\eta_w}\right)^{\frac{\lambda'\cdot(s^*-s_w)}{\eta-n_w}} & \longrightarrow s^* < s \le s_{fc} \\ \dfrac{C}{\eta}\cdot e^{-(\beta+\gamma)\cdot s+\beta\cdot s_{fc}}\left(\dfrac{\eta\cdot e^{\beta\cdot s}}{(\eta-m)\cdot e^{\beta\cdot s_{fc}}+m\cdot e^{\beta\cdot s}}\right)^{\frac{\lambda'}{\beta(\eta-m)}+1}\left(\dfrac{\eta}{\eta_w}\right)^{\frac{\lambda'\cdot(s^*-s_w)}{\eta-n_w}} e^{\frac{\lambda'\cdot(s_{fc}-s^*)}{\eta}} & \longrightarrow s_{fc} < s \le 1 \end{cases} \tag{3.5}$$

with γ given by Eq.(2.8) and C is equal to the normalization constant.

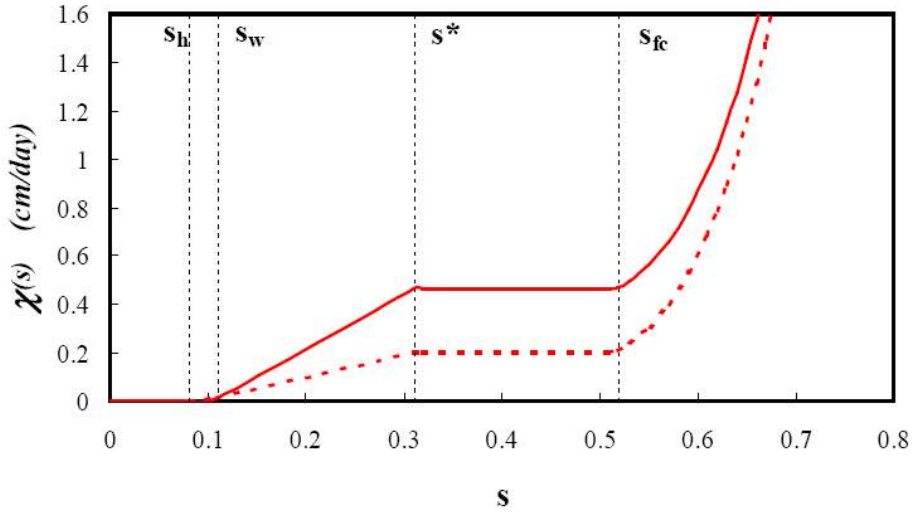

Figure 3.1: Soil water losses $\chi(s)$ as a function of relative soil moisture in a loamy sand soil (with features in Tab.3.2, Sect. 3.3). The solid line is referred to a value of E_{max}= 0.464 *cm/day* while the dashed line considers E_{max}= 0.203 *cm/day* (see Tab.3.5, Sect. 3.4.1). E_w =0.01 cm/day

3.2.3 Numerical solution of soil water balance

In the above section, the analytical solution in steady state condition has been shortly discussed. As mentioned before, it is difficult to find steady-state condition in Mediterranean areas since the soil moisture at the beginning of the growing season is higher than the average of the same period, generating a transient dynamic. In order to overcome the limitation implicitly related to the analytical formulation, the soil moisture pdf during the growing season can be evaluated solving the soil water balance, through a finite differences method. It is possible to estimate the relative soil moisture content s_{i+1} at the time t_{i+1}, starting from its value s_i at the time t_i using the following balance equation [derived from Eq.(2.2)]:

$$\Delta s = s_{i+1} - s_i = \left(\frac{\varphi_i}{n \cdot Z_r} - \frac{\chi_i}{n \cdot Z_r} \right) \cdot \Delta t \tag{3.6}$$

where Δt is the temporal step, while φ_i and χ_i are the infiltration and the losses, both referred to the time t_i.

The seasonal climate variability is represented through a partitioning of the hydrologic year (annual discretization) in several periods with fixed climatic forcing (precipitation and evapotranspiration). The proposed approach could be applied using a simple distinction between the growing (dry) and the dormant (wet) seasons, for which only two sets of parameters, for the rainfall and the evapotranspiration description, are needed. Otherwise, it could be applied using a monthly discretization: this kind of representation requires the estimation of twelve mean values of rainfall intensity, rainfall frequency and maximum evapotranspiration rate.

Another crucial point for the proposed numerical approach concerns the choice of the temporal discretization Δt; the importance of this aspect in the numerical estimate of the soil moisture pdf has been tested, evaluating, with different Δt, the ability of the proposed numerical model in reproducing the analytic soil moisture pdf in steady conditions proposed by *Laio et al.* (2001b). The agreement between the pdf arising from the two different approaches has been verified using the Pearson's chi-square test.

In particular, through an iterative procedure, the minimum Δt required for a good fit between the analytical and the numerical pdf has been calculated. Figure 3.2 shows as different soils (having different proprieties such as n, K_s, β, etc.) and rainfall conditions (schematized with a change in the frequency of the rainfall events, λ, while mean depth, α, is constant) require different temporal discretizations, while different tests have pointed out that the influence of the rooting depth, Z_r, is negligible. The key point explaining the behavior of Figure 3.2 is the relation between the rainfall and the leakage losses. The leakage losses functions [Eq.(3.2)] have been considered with a non linear behavior (as it is shown in Fig.3.1 for $s \geq s_{fc}$) and they are characterized by K_s, β and s_{fc} relative to each soil type.

High rates of rainfall imply a higher probability of wet soil conditions and thus the activation of leakage mechanism. The numerical estimation of these leakage losses is very sensitive to the temporal discretization. Particularly, a wide time-step Δt leads to an overestimation of leakage contributions; this may be due to the non linear behavior of the used leakage loss equation (*Manfreda et al.*, 2005). Consequently, for assigned soil type, as the rainfall input increases the time-step should be shorter. Keeping constant the rainfall, it is instead possible to observe a relation between the soil parameters (the saturated hydraulic conductivity K_s and the exponent of leakage losses equation β) and the values of Δt: highly permeable soils with low values of β (i.e. loamy sand, K_s=100 cm/d, β=12.7) require lower Δt.

As shown in Figure 3.2, it is possible to reach a satisfactory reproduction of steady state analytical solution in semi-arid or dry climate (less than 300mm of rainfall in the considered season) with Δt =12 h (two steps for day) for all the

soil types, while for wet seasons (more than 500 mm) Δt should be lower for the loamy sand soil (4 h) and higher for the clay (8 h). On the other hand, a lower time-step implies a higher computational effort, often not negligible. Obliviously, after that Δt has been chosen, it is necessary to reduce all the input data at the same time-scale.

Once the soil water balance equation has been solved using the finite differences method, the soil moisture time profile is obtained and it is possible to estimate the vegetation water stress following the methodology below described.

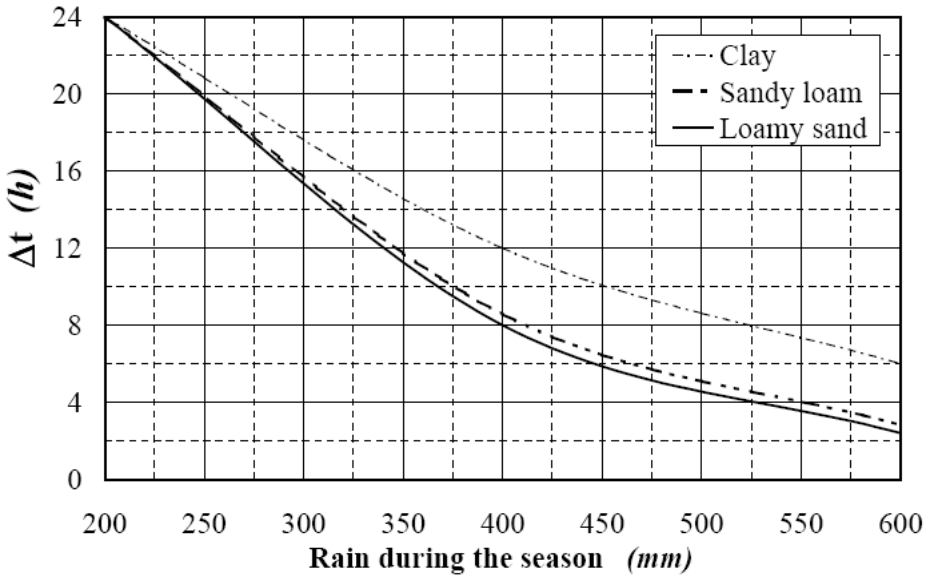

Figure 3.2: Minimum temporal discretization needed for a satisfactory reproduction of the analytic soil moisture pdf (α= 1.5 *cm* ; Z_r= 90 *cm*; E_{max}= 4.6 *mm/day*; T_{seas}=214 *days*; the soil parameters from Table 3.2, Sect. 3.3)

3.2.4 Numerical approach to the vegetation water stress

Moisture reduction into the active soil layer leads to a decrease of plant water potential and consequently of transpiration, potentially dangerous for plant physiological functions. As discussed in Chapter 2 (Sect. 2.4.4), under

steady-state hypothesis, it is possible to study the vegetation response to a certain soil moisture regime following an analytical approach and using the vegetation water stress proposed by *Porporato et al.* (2001). In particular it is possible to calculate three water stress indexes: the static water stress, ζ; the static water stress modified, $\overline{\zeta}'$; and the dynamic water stress.

The static water stress, ζ, can be analytically obtained by Eq.(2.11). It is also possible to obtain the pdf of the static stress, $f_z(\zeta)$, from the soil moisture pdf [see Eq.(2.12)]. Finally, Eq.(2.14) provides the analytically formulation for the mean value of the static water stress $\overline{\zeta}$.

Actually, as mentioned in Sect. 2.4.4., it is more helpful to estimate another index, that is the static water stress modified, $\overline{\zeta}'$, that can be obtained by Eq.(2.15). Since the static water stress modified, $\overline{\zeta}'$, takes only into account the mean intensity of water deficits and does not contain information on their duration and frequency (crossing properties), *Porporato et al.* (2001) suggest to use another index for the evaluation of plant water stress, that is the dynamic water stress, $\overline{\theta}$. It can be determined by means of Eq.(2.17). The plant response in terms of dynamic water stress, strongly depends on the active soil depth Z_r. In fact, deep-rooted species (e.g. trees) rely on the winter water recharge into the soil, as opposed to shallow-rooted species (e.g. grasses) that quickly respond to the intermittent rainfall (*Rodriguez-Iturbe et al.*, 2001b).

As the other two water stress indexes, also the dynamic water stress definition is referred to steady-state conditions. Thus, such indexes obtained analytically are specific for those areas where it is possible to assume a steady-state hypothesis and, whenever a not negligible transient period is present, this definition is not valid. For example, the Mediterranean climate, where the presence of a winter recharge creates a transient in the soil moisture dynamics (whose duration depends mainly on the active soil depth Z_r), is a typical case of not applicability of this kind of approach since it would lead to overestimation of the water stress.

Moreover, using an analytical approach, some of the terms involved in the dynamic water stress formulation may assume physically unrealistic values; e.g. the value of $\overline{T}_{s*}$ is not bounded to the duration of the season, T_{seas}, and using its analytical formulation [Eq.(2.16)], it is possible to obtain a mean duration of stress periods during the growing season higher than the same duration of the growing season.

In order to overcome these limitations, a numerically estimation of the dynamic water stress is here proposed and explained.

Once the soil water balance equation has been solved by finite differences method [Eq.(3.6)] obtaining the soil moisture time-profile, it is possible to evaluate the vegetation response in terms of water stress.

Through Eq.(2.11) the static water stress time-profile can be obtained. It is also possible to calculate, during the growing season, the mean static water stress modified. The seasonal values of the number of periods with stress and theirs mean duration can be assessed year-by-year.

Averaging the seasonal data on the whole number of simulated years, it is possible to evaluate the mean values for soil moisture, $\bar{s}$, for static water stress, $\bar{\zeta}$, and static water stress modified, $\bar{\zeta}'$, and finally for the crossing properties $\bar{T}_{s*}$ and $\bar{n}_{s*}$; the evaluation of these variables allows the estimation of the mean dynamic water stress using the same Eq.(2.17). It is important to point out that the main differences between the proposed approach and the analytical one are that, in the former, the variables $\bar{T}_{s*}$ and $\bar{n}_{s*}$ are numerically computed and for this reason they are bounded, that so it is impossible to have values of $\bar{T}_{s*}$ higher than T_{seas}.

Also the evaluation of the mean static water stress is different, since it is not obtained from the static stress pdf but it is evaluated starting from the soil moisture time-profile, step-by-step evaluating the static water stress by the Eq.(2.11) and averaging all the results. Similarly the mean static water stress modified is not obtained by the Eq.(2.15) but simply averaging year by year the static water stress only on the periods in which ζ is different from zero and then evaluating the mean value using the entire simulated series.

Even if the three indexes given by *Porporato et al.* (2001) are defined for steady-state conditions, their numerical estimation allows the proposed approach to provide a complete description of the plants water stress also in presence of a not negligible transient period.

3.3 Case Study: Eleuterio at Lupo river basin

The following two applications are referred to climatic and vegetational conditions present at the watershed of *Eleuterio at Lupo*, located near Palermo (Sicily, Italy), at latitude 37.53°N (Figure 3.3). In ancient time this area, near the town of Ficuzza, was a royal hunting reserve, and also for this reason, is nowadays well conserved, with few anthropic actions. The watershed of Eleuterio at Lupo has an extent of almost 9.5 km^2 and its elevation ranges from

517.5 *m a.s.l* (at the outlet to the *Scanzano Lake*, Figure 3.4) to 1635.5 *m a.s.l.* (at mountain peak of *Rocca Busambra*, Figure 3.5) with a mean elevation of 792.2 *m. a.s.l.* and standard deviation of 194.6 *m*.

The watershed is located within the "Bosco della Ficuzza" wood. The natural reserve of "Bosco della Ficuzza" with an extent of about 7000 *ha* represents one of the widest natural reserves in Sicily. The reserve is mainly constituted by woody species (*Quercus Ilex*, *Q. pubescens*, *Q. suber*, *Q. Gussonei*, *Castanea sativa*, *Acer campestre, Populus nigra, P. alba, P. canascens, Salix pelicellata, S. alba, Ficus carica, Fraxinus ornus, F. angustifolia*) with also a lower presence of shrubs (*Solanum dulcamara*, *Tamus communis*, *Rubia peregrine*, *Rubus ulmifolius*) and grasses (*Hypericum hircinum*, *Arum italicum*, *Acanthus mollis*, *Mentha longifolia*, *Equisetum telmateja*, *Carex pendula*, *Agrimonia eupatoria*). Figure 3.6 shows some example of vegetation present within the Eleuterio at Lupo river basin, relative to the winter period.

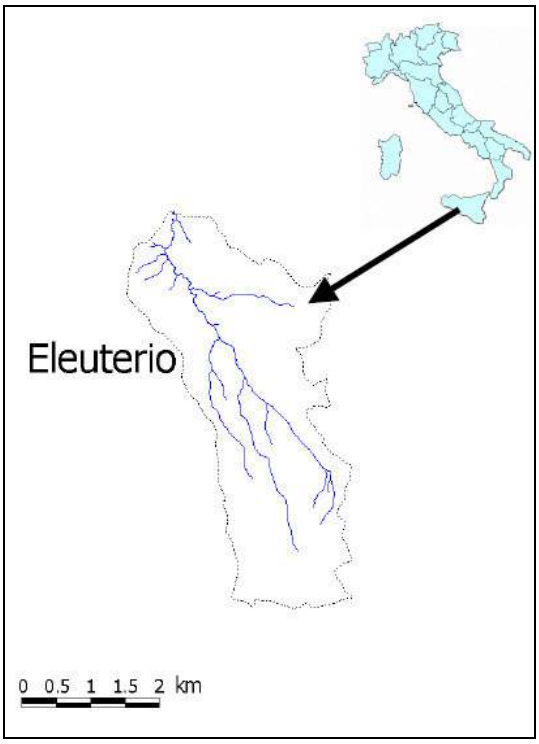

Figure 3.3: Location of the Eleuterio at Lupo river basin (Sicily-Italy). In blue are highlighted the main river channels

Figure 3.4: Eleuterio at Lupo river basin (Sicily-Italy). View of the Scanzano Lake

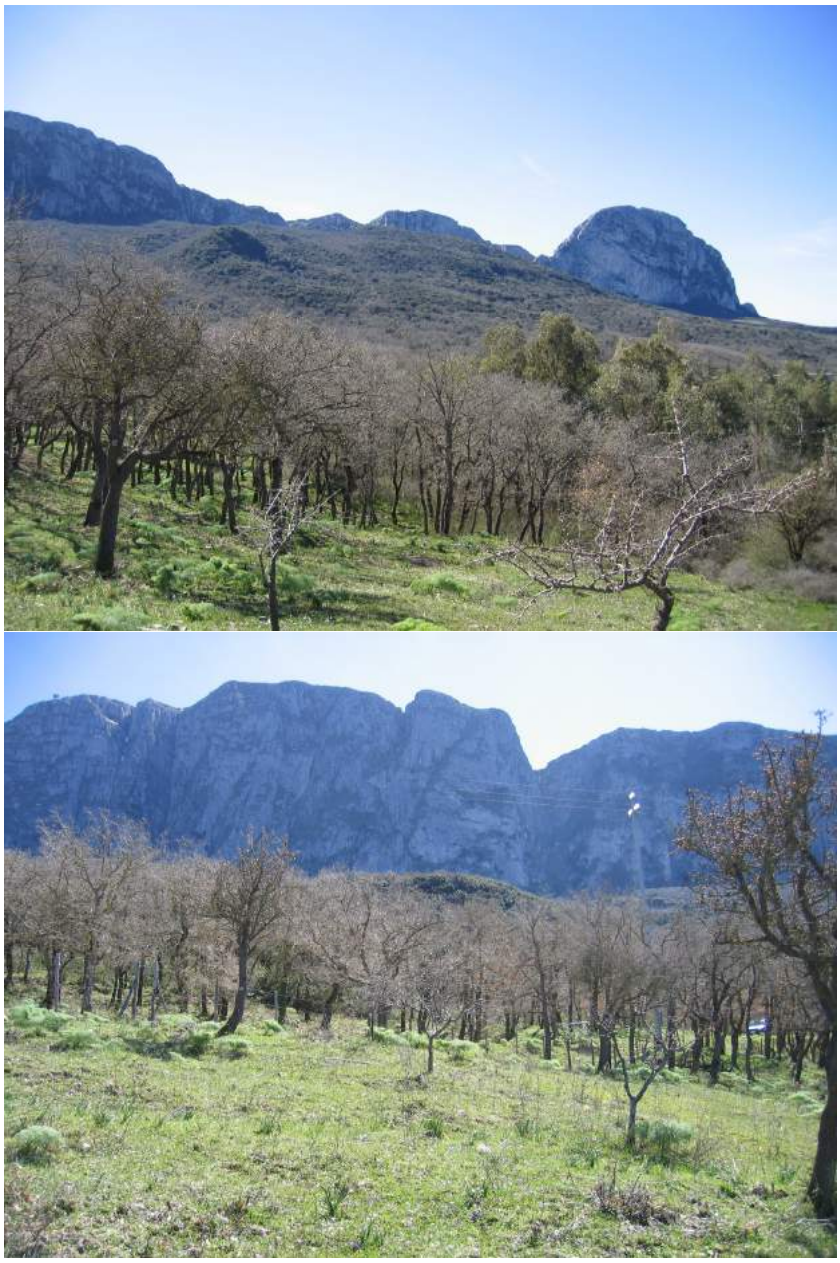

Figure 3.5: Eleuterio at Lupo river basin (Sicily-Italy). View of the Rocca Busambra mountain

Figure 3.6: Eleuterio at Lupo river basin (Sicily-Italy). Example of vegetation present within the basin (winter season)

The area presents a typical Mediterranean climate, with hot and dry summer while the winter period is cooler and rainy. The mean annual temperature is 16.2°*C* while the mean annual precipitation is about 750 *mm*, whose about 70% is concentrated during the autumn-winter period.

The watershed presents a low variability of total annual precipitation and being an ecosystem in an ecological state of maturity, it is also characterized by a low variability in time from pedological and vegetational point of view. Moreover, no interaction between soil and water table is taken into account, since of the deep groundwater observed in the area.

The Eleuterio river basin is constituted by several river channels merging into the Scanzano reservoir (Figure 3.3).

Three maps of the Eleuterio area (*Agricultural Map, Hydrogeological Map, Geological Map*), produced in a previous study (*Liguori et al.*, 1983), have been taken into account in determining spatial patterns of soil texture and vegetation.

The *Agricultural Map* shows that there is an overriding presence of woody vegetation, even if vineyard, olive tree grove and pastureland with shrub vegetation are also present as well as a low percentage of dry seminative land and bare soils. From this map it has been derived a vegetational pattern that considers three types of vegetation: trees (areas classified as woody, degraded woody, reforestation zone); shrubs (vineyard, olive tree grove and pastureland); and finally grasses (seminative and sterile). This classification differs from the classical definition of tree, shrub or grass species, because it is based on the deepness of vegetational root-apparatus. The vegetational ecohydrological model parameters related to trees and grasses are shown in Table 3.1.

		Vegetation Type	
		Tree	*Grass*
rooting depth *(cm)*	$\mathbf{Z_r}$	150	30
threshold of canopy interception *(cm)*	$\mathbf{h_\Delta}$	0.20	0.10
water stress resistance index	**k**	0.7	0.5
vegetation height *(m)*	**H**	4.0	0.5
shortwave albedo	$\boldsymbol{\alpha_s}$	0.10	0.12
leaf area index *(m^2/m^2)*	**LAI**	1.50	0.25
maximum stomatal conductance *(m/s)*	$\mathbf{g_{s,max}}$	0.0100	0.0167

Table 3.1: Parameters describing the vegetation characteristics used in the model applications. After *Caylor et al.* (2005)

The *Hydrogeological Map* and the *Geological Map* show that the zone of interest is mainly constituted by lithological-technical complexes classifiable as incoherent soil materials in the southern part, pseudo-coherent soil materials in the middle part of the basin and coherent soil materials with pseudo-coherent levels in the northern part and in the eastern one.

The information arising from these maps has allowed to recognize three soil types (according to USDA classification) within the basin: sandy loam, loamy sand, and clay. The soils features are summarized in the Table 3.2.

The Figure 3.7 shows the vegetational and soil information on the Eleuterio river basin, used in order to obtain the spatial patterns of vegetation and soil; finally the spatial overlay between these layers points out that eight of the nine possible different combinations of soil-vegetation are present within the basin. However in the two following applications of the model not all the possible combinations will be considered, in agreement with the purposes of each: in the first application only the woody vegetation will be considered while the second one will investigate also the grass component.

	coefficient of the hydraulic conductivity power law	*saturated hydraulic conductivity*	*porosity*	*characteristic values of relative soil moisture*			
Soil type	β	K_s *cm/d*	*n*	s_h	s_w	s^*	s_{fc}
Loamy sand	12.7	100	0.42	0.08	0.11	0.31	0.52
Sandy loam	13.8	80	0.43	0.14	0.18	0.46	0.56
Clay	26.8	2.5	0.50	0.47	0.52	0.78	0.91

Table 3.2: Parameters describing the soil characteristics used in the model applications. After *Laio et al.* (2001)

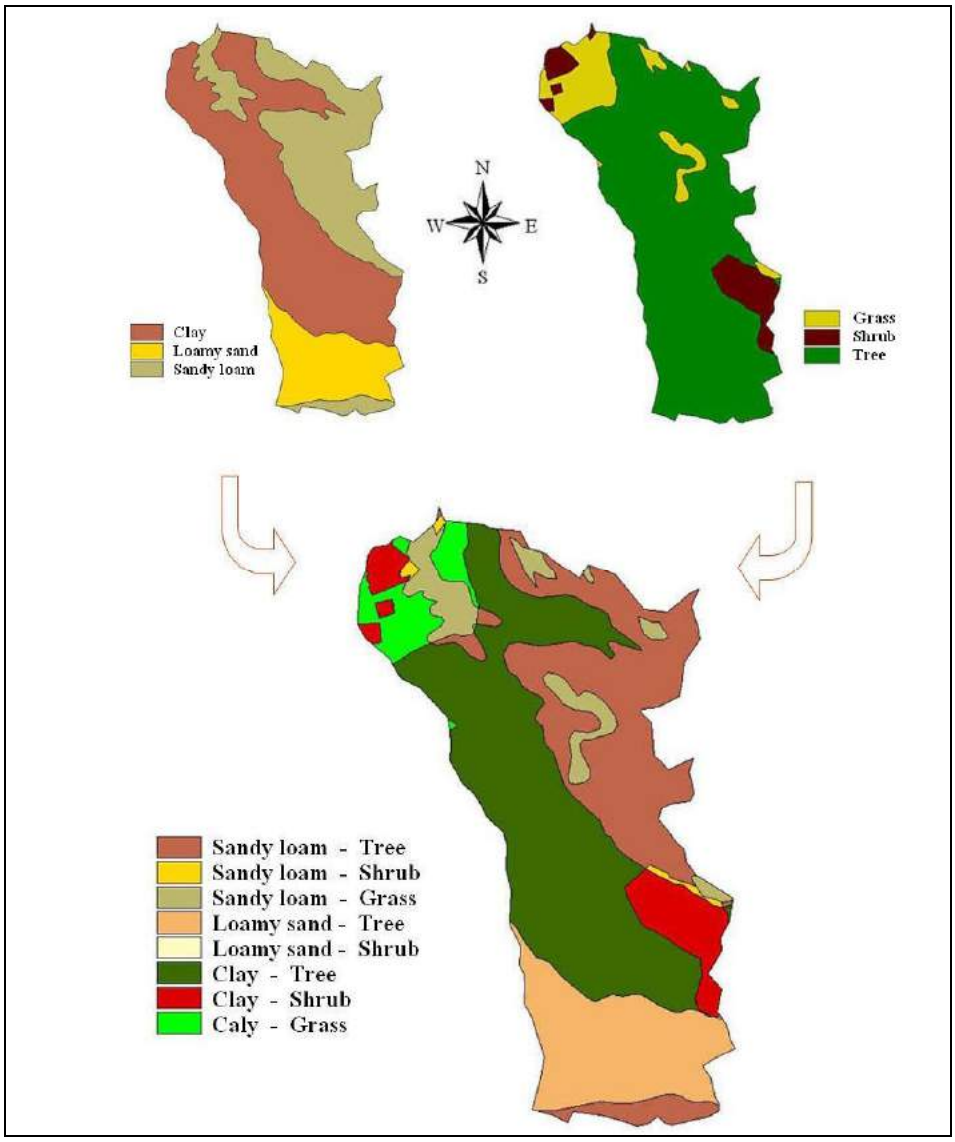

Figure 3.7: Spatial pattern of soil texture (top left) and vegetation (top right) for the Eleuterio at Lupo river basin and theirs spatial overlay (at bottom)

3.4 First Application

The aim of the first application is to assess the performances of the model and to show what results it is able to provide working on a single area, homogeneous in terms of climate, soil and vegetation. The application is also an attempt to investigate on the importance of the annual discretization of the rainfall parameters and the values of the potential evapotranspiration.

Since the primary aim of this application is to investigate on the possibility to overcome the problems connected to the transient effect due to a not negligible soil moisture initial condition in Mediterranean areas, for this first application, the model has been only applied to the areas covered by trees, that is the most critical vegetation cover in relation to the transient effect (*Laio et al.*, 2001c; *Caylor et al.*, 2005). Particularly, the presence of a deep active soil layer causes the increasing of water that can be stored into the soil during the dormancy season, and the drying processes for these deep soils are slower; as consequence of these aspects, more time is required to reach a stationary condition during the growing season. For this reason the application has been limited to a unique vegetation type (that is also the most present within the basin), investigating also on the importance of different soil types (sandy loam, loamy sand and clay).

3.4.1 Evapotranspiration and schematization of climatic variability

It is assumed that the growing season, in the study area and for the considered vegetation, starts at the beginning of April and finishes at the end of October, with duration of 214 days.

The evapotranspiration at minimum rate E_w, in correspondence to the wilting point s_w, can be fixed at value 0.1 *mm/day* (*Rodriguez-Iturbe et al.*, 1999b). In order to estimate potential evaporation, monthly time series of air relative humidity, heliophany and wind speed have been used because of the difficulty to find daily data series.

Such time series have been extracted from records of the Ficuzza gauge station (*Atlante Climatografico della Sicilia*, Regione Siciliana; *Augi*, 2003). Table 3.3 shows some meteo-climatic features within the basin; it points out the monthly mean values of the daily maximum and minimum air temperatures and of the daily air humidity, which have been obtained from the observations.

Potential evapotranspiration has been estimated by Penman-Monteith method at the monthly time scale, following a procedure similar to that used by *Caylor et al.* (2005). Some of the parameters useful for the evaluation of the potential evapotranspiration are reported in Table 3.1 and Table 3.3.

Latitude =	37° 53' N	
Mean Elevation =	792.2	*m a.s.l.*
ρ =	1.1	kg/m^3
C_p =	0.001013	*J/°C*

	Temperature (°C)		**Average Air Humidity (%)**
Month	**T_{max}**	**T_{min}**	**RH_{mean}**
January	11.7	3.8	69
February	12.3	3.9	68
March	15.0	5.2	73
April	18.3	7.1	74
May	22.9	10.6	73
June	28.5	13.7	72
July	31.8	16.6	73
August	32.6	17.3	74
September	28.2	14.9	76
October	22.6	12.0	75
November	17.2	8.2	74
December	13.3	5.1	71

Table 3.3: Meteo-climatic data for the Eleuterio at Lupo river basin. ρ and C_p are the density and the specific heat capacity of air, respectively; T_{max} and T_{min} are the mean daily values of maximum and minimum temperatures respectively; RH_{mean} is the average daily air humidity

Figure 3.8a and Figure 3.8b represent the recorded precipitation in the Eleuterio river basin. The former shows the annual precipitations during the observation period, divided into precipitation during growing season (green) and that during dormant season (yellow), while the latter shows the mean monthly precipitations. The mean annual precipitation observed is 773 *mm*, (526 *mm* during the dormant season). A strong seasonality is evident in monthly precipitation, with higher and more frequent rainfall events during the winter months (in December, January and February over 100 *mm* of monthly precipitation) and only 5 *mm* of mean monthly rainfall in July.

In order to analyze the effects of a different schematization of the year, two different computational schemes (SCHEME A and SCHEME B) have been here used. In SCHEME A, the year is divided into two seasons, growing season (GS) and dormant season (DS), each one with its own values of α and λ for the precipitations and E_{max} for the evapotranspiration, time-invariant (during the season and also year by year), quantities representative of the two seasons. In SCHEME B, the sets of parameters α, λ and E_{max} are assumed to be time-invariant quantities at monthly time-scale, so twelve sets of these parameters are present.

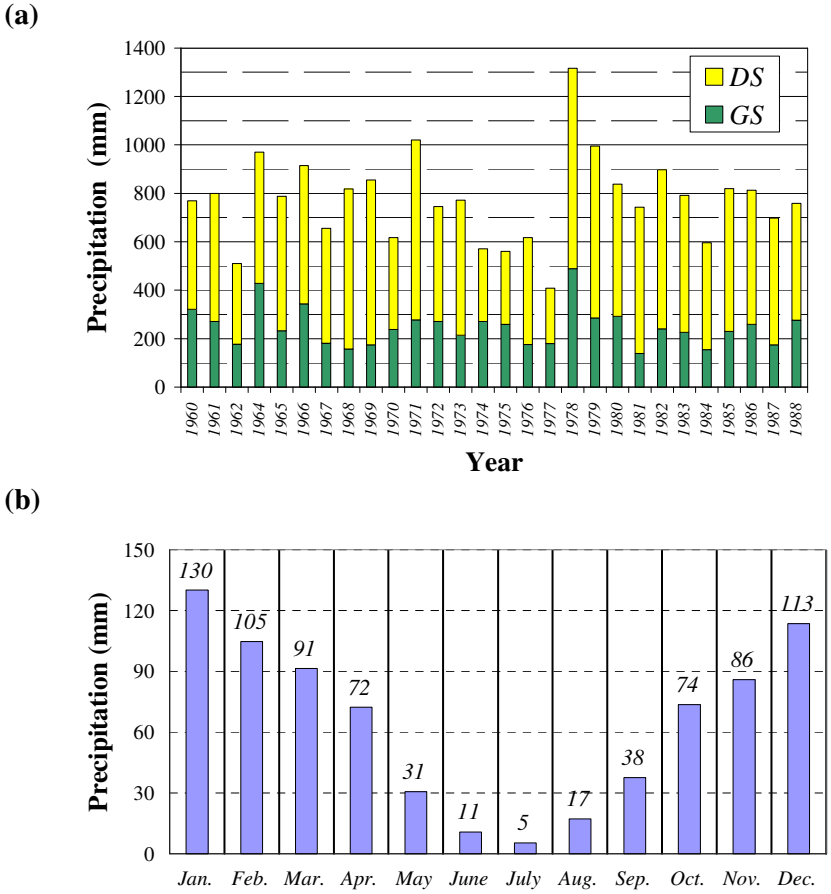

Figure 3.8: Eleuterio at Lupo river basin. **(a)**: Historical rainfall series (from Ficuzza raingauge, 1960-1988). In yellow the precipitation during the dormant season (DS) while in green that during the growing season (GS). **(b)**: Mean monthly precipitations

Starting from the historical data series, the seasonal values of α and λ (useful for SCHEME A) and the monthly values (useful for SCHEME B) have been derived by considering the mean values of the depth of the rainfall events (α) and of the interarrival time between two consecutive rainfall events (λ), during each season (Table 3.4a) or each month (Table 3.4b), respectively.

(a)

		α mean rainfall depth		λ mean time between two events		Monthly Precipitation	
	T	Mean	S.D.	Mean	S.D.	Mean	S.D.
Season	*days*	*mm*	*mm*	*1/day*	*1/day*	*mm*	*mm*
GS	*214*	5.95	*4.34*	0.195	*0.144*	248	*139*
DS	*154*	7.01	*2.91*	0.493	*0.145*	526	*80*
Annual	*365*	6.63	*3.84*	0.319	*0.204*	773	*181*

(b)

	α mean rainfall depth		λ mean time between two events		Monthly Precipitation	
	Mean	S.D.	Mean	S.D.	Mean	S.D.
Month	*mm*	*mm*	*1/day*	*1/day*	*mm*	*mm*
January	7.52	*2.25*	0.526	*0.109*	130	*58*
February	7.20	*1.90*	0.502	*0.128*	105	*41*
March	6.45	*2.34*	0.450	*0.123*	91	*42*
April	6.32	*3.17*	0.354	*0.100*	72	*48*
May	4.71	*2.75*	0.191	*0.076*	31	*23*
June	2.97	*2.37*	0.120	*0.056*	11	*10*
July	3.35	*2.40*	0.051	*0.053*	5	*7*
August	6.07	*4.52*	0.086	*0.053*	17	*18*
September	6.14	*2.94*	0.213	*0.081*	38	*20*
October	7.80	*2.49*	0.313	*0.101*	74	*29*
November	6.74	*2.53*	0.413	*0.107*	86	*40*
December	7.00	*2.32*	0.512	*0.108*	113	*48*

Table 3.4: Eleuterio at Lupo river basin. In the upper part (**a**) seasonal and annual values of α, λ and the total amount of rainfall, with standard deviations. At bottom (**b**), mean monthly values and standard deviation (S.D.); GS = growing season; DS = dormant season

In SCHEME A, α and λ are constant during each season and are equal to 5.95 *mm* and 0.195 *1/day* respectively during the growing season, and 7.01 *mm* and 0.493 *1/day* during the dormant season. In SCHEME B α ranges from 2.97 *mm* (June) to 7.80 *mm* (October), while λ ranges from 0.051 *1/day* (July) to 0.128 *1/day* (February).

Similarly, starting from the data shown in Table 3.1 and Table 3.3, the seasonal and monthly values of E_{max} for the woody component of vegetation have been obtained and reported in Table 3.5. Here it is possible to point out high values of evapotranspiration during the entire summer period with a maximum in July (5.84 *mm/day*).

The different annual fluctuations of the three parameters α, λ and E_{max} used in the two schemes are emphasized in Figure 3.9.

(**a**)

Season	E_{max} *mm/day*
GS	4.64
DS	2.03

(**b**)

Month	E_{max} *mm/day*
January	1.67
February	1.91
March	2.23
April	3.06
May	4.13
June	5.19
July	5.84
August	5.79
September	4.82
October	3.59
November	2.50
December	1.86

Table 3.5: Seasonal (**a**) and monthly (**b**) values of E_{max} for woody vegetation within the Eleuterio at Lupo river basin. GS = growing season; DS = dormant season

(a)

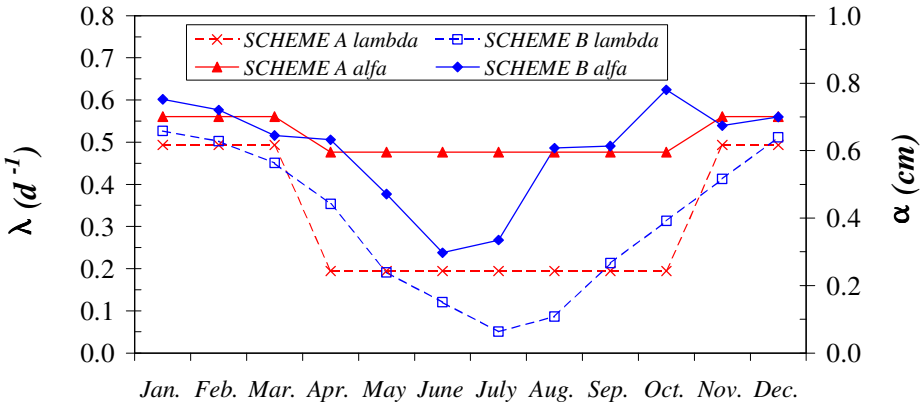

(b)

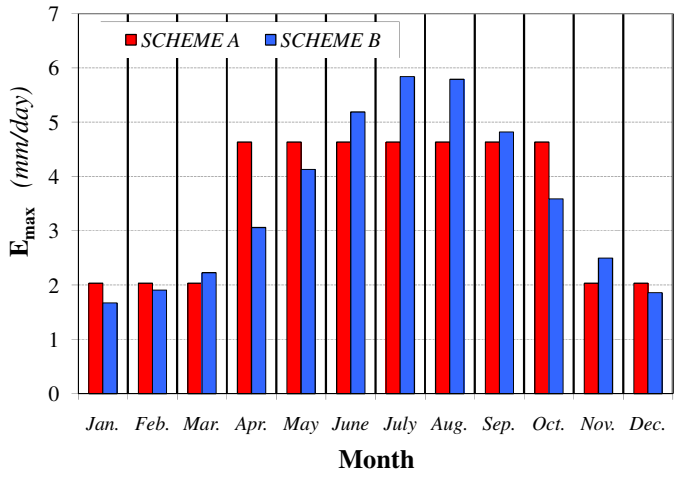

Figure 3.9: Eleuterio at Lupo river basin. **(a)**: Annual fluctuation of the mean seasonal (SCHEME A) and monthly (SCHEME B) values of $\alpha\,(cm)$ and $\lambda\,(1/day)$. **(b)**: Annual fluctuations of the mean monthly E_{max} (mm/day) used in SCHEME A and SCHEME B

The numerical model requires as input a synthetic rainfall series, long enough to allow long-term evaluations for the response of vegetation in a river basin. For this purpose, two synthetic series of 100 years have been generated, one for each considered scheme (A and B), following the procedure described in Sect. 3.2.2 and using α and λ parameters shown in Table 3.4.

It is important to point out that, even if the two different generated rainfall series present the same mean value with regard to the seasonal rainfall relative to the growing and the dormant seasons, this fact does not warrant also a correspondence year by year of the seasonal rainfall.

3.4.2 Results and analysis

For the Eleuterio at Lupo river basin, a time step, Δt, equal to four hours has been chosen, according to the concepts expressed in Sect. 3.2.3 (see Figure 3.2).

Starting from an initial condition of soil moisture equal to the field capacity and solving the Eq.(3.6), the soil moisture time-profile can be calculated for all the three considered soil-types.

For the computation step by step of the static water stress, Eq.(2.11) has been used with the exponent q equal to 3, assuming a strongly non-linear relationship between water stress and soil moisture. In this way six static water stress time profiles (one for each of the three soil types and for each of the two considered schemes), have been obtained.

Some of the results of simulations carried out using the two schemes are summarized in Fig. 3.10a and Fig. 3.10b. Both this plots show the soil moisture time-profile (middle panel) and the static water stress (bottom panel), in response to the synthetic rainfall series (top panel). These figures represent the results relative to two different representative years (one year for each scheme) extracted from the two 100 years series generated using SCHEME A and SCHEME B. These years have been chosen by ensuring that they have the same total values of precipitation during the growing season and during the dormant season in both the two schemes (equal to 242 *mm* and 560 *mm* respectively). The aim of the comparison between the two figures is to emphasize, in a qualitative manner, the different behaviors of the soil moisture and the consequent trees response, arising from two different climate variability assumed. Analyzing Fig. 3.10, it is possible to extrapolate some of the peculiarities of the two proposed schemes. In the SCHEME B, because of its higher discretization, the rainfall input, the soil moisture and the water stress time profiles are more regular, with less abrupt variations in the temporal evolution (mainly with regard to the passage from a season to the other).

(a)

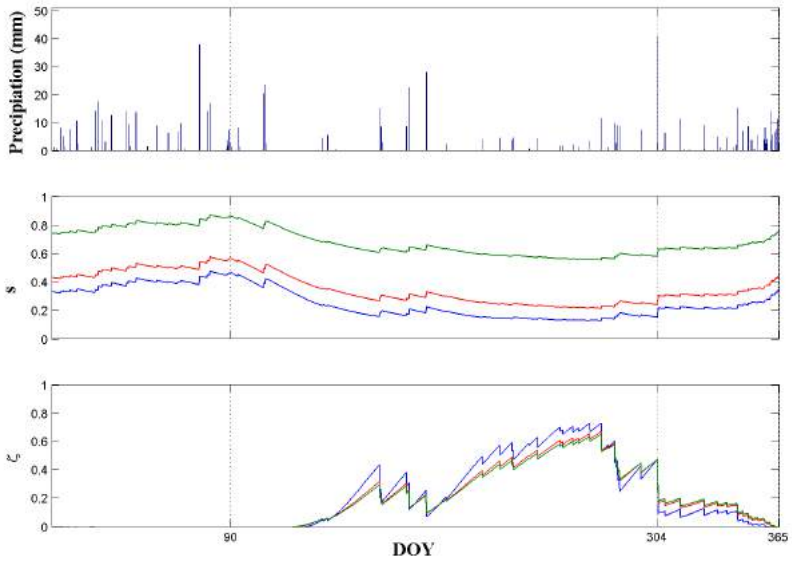

(b)

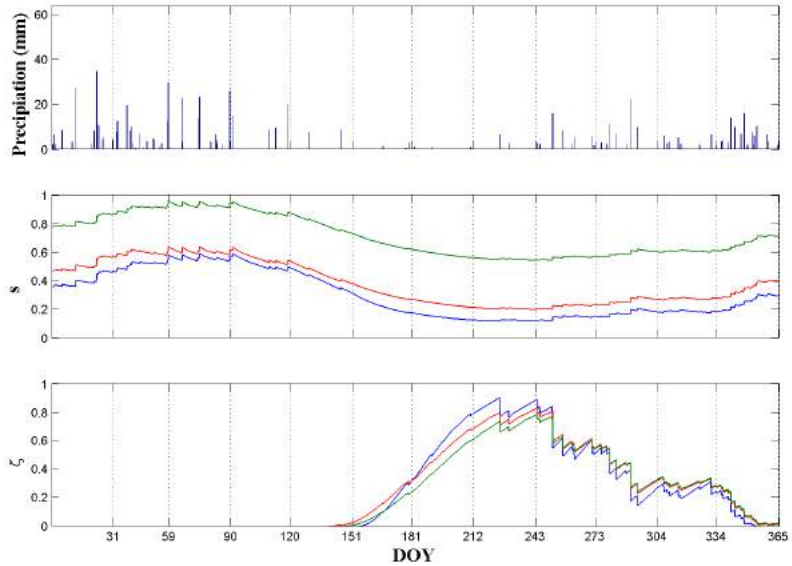

Figure 3.10: Time-profiles for one generic representative year. The years relative to SCHEME A **(a)** and SCHEME B **(b)** are different but present the same total precipitation during the G.S. (242 *mm*) and during the D.S. (560 *mm*). Vegetation type: tree. Soil type: loamy sand (blue), sandy loam (red) and clay (green). On the top the precipitation series, in the middle the soil moisture time-profile and at bottom the static water stress time-profile. DOY = day of year. Initial day for the GS is DOY=90, while the last day of the GS is DOY=304

With a two seasons discretization (SCHEME A) the static water stress appears early in the growing season and continue increasing until the end of the season. Using the twelve months discretization (SCHEME B), the static water stress arrives later and increases more rapidly than the previous scheme, reaching a maximum in August and then decreases because of the high rain contributions during September and October. The comparison between the maximum values of static water stress reached with the two schemes shows that the SCHEME B gives the highest values. In conclusion the SCHEME A leads to less intensive but more protracted periods of water stress during the growing season.

Afterwards, the analysis has been only focused on the growing season for both the considered schemes. The final results, concerning the 100 years time series, show that SCHEME B gives values of the mean soil moisture during the growing season higher than SCHEME A (about 10% for loamy sand, 3% for sandy loam and 2% for clay, see Table 3.6). In fact, using SCHEME B, two different periods are observable during each simulated year. During the first, at the beginning of the growing season, this scheme simulates lower water losses (evapotranspiration lower than SCHEME A, see Fig. 3.9b) and, at the same time, the rainfall events, which are more frequent, keep the soil moisture higher than that coming from SCHEME A. The second period presents two different behaviors: during the first driest months (from June to August), the evapotranspiration losses are much higher than the ones calculated by SCHEME A, but they are concentrated and bounded in a shorter period, while during the last months, the soil moisture tends to grow again until the end of the season, because of the rainfall contribution increase (see Fig. 3.9a) as well as the contemporaneous reduction of evapotranspiration rate in October (see Fig. 3.9b). All that, in conclusion, leads to a higher mean soil moisture during the entire growing season using SCHEME B than the same value calculated by SCHEME A.

Using a numerical approach, the mean number of periods with water stress during the growing season, and theirs mean durations can be assessed for each simulated growing season. Averaging on the whole considered period (100 years), it is possible to obtain the long-term seasonal values of the mean number of downcrossing n_{s*} and theirs mean duration T_{s*}. Finally, using Eq.(2.17), with $r = 0.5$ and $k = 0.7$ for the woody vegetation (*Caylor et al.*, 2005), the dynamic water stress, $< \theta >$, representative of long-term plants condition within the Eleuterio at Lupo basin can be obtained for both the proposed schemes.

Even if for SCHEME B the mean soil moisture during the growing season is higher than the one obtained by SCHEME A, also the mean static water stress calculated with the former results higher than the one provided by the latter (19% for loamy sand, 24% for sandy loam and 23% for clay). This fact, apparently contradictory, is mainly due to the short stress periods with very high

values of plant stress in SCHEME B. The same considerations are also valid for the mean static water stress modified, which is more sensitive to the prolonged and intense stress periods. In fact, the differences between the results arising from the two schemes are on the order of 36 % for loamy sand, 38 % for sandy loam and 39 % for clay. As direct consequence, also the dynamic water stress index for SCHEME B is slightly higher than that obtained using SCHEME A (22 % for loamy sand, 17 % for sandy loam and 21 % for clay).

Comparing the results of the three different soils it is possible to point out that the woody vegetation suffers less water stress in a clayey soil than that in the other considered soil types, because clayey soil has higher water storage capacity and moreover retains for a longer period the initial moisture during the growing season (Table 3.6).

Soil Type:	**Loamy sand (s^*=0.31)**		**Sandy loam (s^*=0.46)**		**Clay (s^*=0.78)**	
SCHEME:	**A**	**B**	**A**	**B**	**A**	**B**
$< s >$ =	0.22	0.24	0.31	0.32	0.65	0.66
$<n_{s^*}>$=	1.31	1.19	1.29	1.39	1.36	1.30
$<T_{s^*}>$ =	136.2	130.8	149.6	124.2	139.6	129.1
$<\zeta>$=	0.29	0.35	0.27	0.34	0.25	0.31
$<\zeta'>$ =	0.35	0.48	0.30	0.42	0.29	0.40
$<\theta>$ =	0.37	0.45	0.35	0.41	0.32	0.39

Table 3.6: Eleuterio at Lupo river basin. Mean values during the growing season of soil moisture $<s>$, seasonal number of stress periods n_{s^*} and its duration T_{s^*} (days), static water stress $<\zeta>$ and static water stress modified $<\zeta'>$, and dynamic water stress $<\theta>$. The symbol <..> denotes that the values are averages on 100 years. Woody vegetation. s^* is the soil moisture relative to the incipient stomatal closure (for each considered soil type)

In conclusion, even if the differences between the results obtained with the two proposed schemes are minimal with regard to the evaluation of the mean values of soil moisture during the growing season, these differences seems to be more relevant with regard to the evaluation of vegetation response.

In order to give a comparison between the results provided from the analytical solution in stationary condition and from the proposed numerical

models, the soil moisture pdf's during the growing season have been compared for different soil characteristics. Figures 3.11 (relative to loamy sand), 3.12 (relative to sandy loam) and 3.13 (relative to clay) show that, for all the soil types, the analytical pdf is unimodal with low symmetry and low variance, whereas the numerical pdf's show a greater dispersion of the values around the mode and an asymmetric behavior; this is due to the fact that the proposed model takes into account the transient effects of soil moisture at the beginning of the growing season. For this reason, the resulting mean values during the growing season for both the numerical soil moisture pdf's are consistently higher than that relative to analytical pdf.

The transient effect manifests itself in two different ways for the two annual discretization considered. SCHEME B leads to a bimodal pdf. The right-mode accounts for the transient period and is justified by the high value of soil moisture at the beginning of the growing season but also from the rainfall input assumed in the April - May period, that are higher than the mean seasonal value used in SCHEME A. The left-mode instead takes into account the soil moisture dynamics after the end of the transient period, when a stationary condition could be reached; actually it is very close to the analytical mode, even if it obviously presents a lower probability. In SCHEME A, the winter soil water recharge is the same as the previous scheme (SCHEME B) but, because of the lower contribution of the rainfall during the first months of the season, the resulting pdf has lower probability in correspondence of high values of soil moisture. Conversely, because of the higher rain input in the July - August period, the unique mode of the pdf resulting from SCHEME A is higher than the left-mode obtained by SCHEME B, and it also presents a higher probability for all the three soil types. SCHEME A works with the same climatic input data used in the analytical formulation (namely with the mean seasonal values of α, λ and E_{max} during the growing season) and then the differences between the pdf's derived using these two different approaches, are exclusively due to the effects of the winter recharge of moisture into the soil before the growing season.

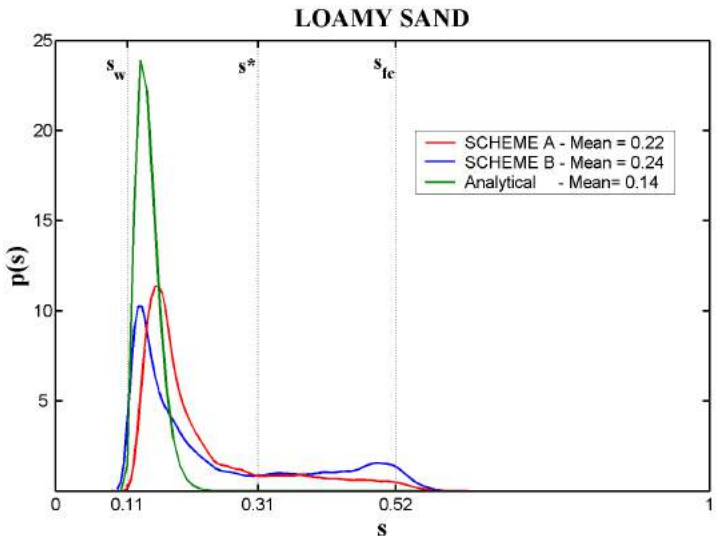

Figure 3.11: Eleuterio at Lupo river basin. Probability density functions of soil moisture and mean soil moisture during the growing season relative to the analytical solution (green), and to the numerical solutions for SCHEME A (red) and SCHEME B (blue). Vegetation type: tree; Soil-type: loamy sand

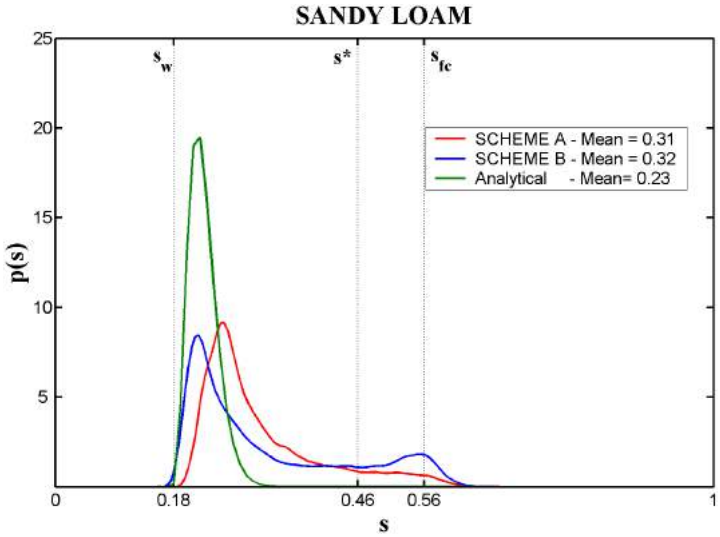

Figure 3.12: Eleuterio at Lupo river basin. Probability density functions of soil moisture and mean soil moisture during the growing season relative to the analytical solution (green), and to the numerical solutions for SCHEME A (red) and SCHEME B (blue). Vegetation type: tree; Soil-type: sandy loam

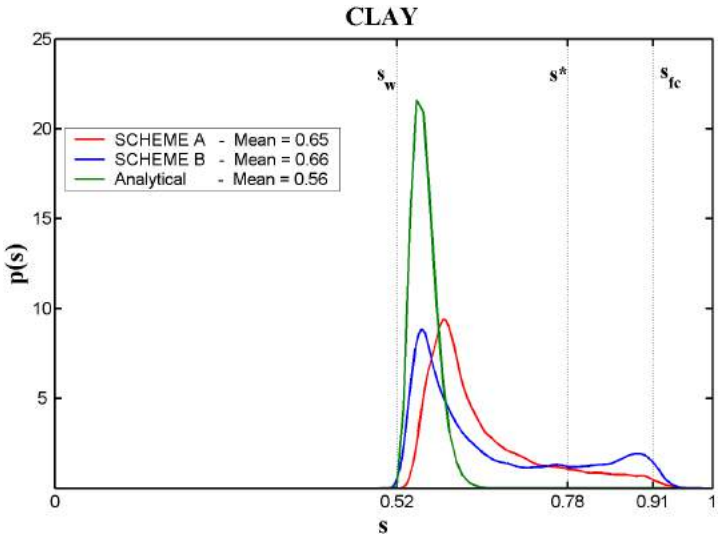

Figure 3.13: Eleuterio at Lupo river basin. Probability density functions of soil moisture and mean soil moisture during the growing season relative to the analytical solution (green), and to the numerical solutions for SCHEME A (red) and SCHEME B (blue). Vegetation type: tree; Soil-type: clay

3.5 Second Application

Many recent studies have demonstrated that CO_2 increase is driving the climate in Mediterranean areas towards important changes, mainly represented by a temperatures increase and a contemporaneous rainfall reduction. Starting from this premise, the primary aim of this second application is to investigate the effects of potential climatic changes on vegetation in Mediterranean WCEs and to demonstrate how the approach here proposed allows a quantitative evaluation of such effects in terms of vegetation water stress. In particular, different future climatic scenarios, arising from recent predictions in Mediterranean areas, and their effects on woody and grassy vegetation in the Eleuterio at Lupo river basin are analyzed. Great attention is paid to the effects that rainfall decrease may have on vegetation water stress, by itself or coupled with the temperature increase, neglecting the influence that the increase in atmospheric CO_2 concentration may have on the efficiency of plants transpiration processes (*Chartzoulakis and Psarras*, 2005).

Different works, focused on the qualitative analysis of the coupled effect of rainfall reduction and temperatures increase, have concluded that the main effect of the simultaneous presence of these two trends is a reduction in soil moisture, leading to an increase of the water stress (*Palutikof et al*., 1994; *Porporato et al*., 2004b). This application differs from the above mentioned ones not only for the quantitative approach to the problem, but also for the presence of a detailed investigation on the influence of the variations in rainfall frequency and intensity characterizing some possible future scenarios, on the vegetation state. The application has been done considering two different vegetation covers and three types of soil with the purpose to estimate the vegetations response, in terms of water stress, to the different future climate scenarios as function of vegetation and soil characteristics.

3.5.1 Hypotheses and assumptions

In this application many of the hypotheses and assumptions adopted for the previous application have been considered again:

- seasonal time-scale (i.e. growing season), and space-scale of few meters;
- the soil-vegetation system has been hypothesized homogeneous with regard to the soil type and the plant there present, with depth coincident with the root zone;
- both the soil and vegetation features are considered time invariant;
- no interactions with the water table and no dynamic effects due to the impact of the rainfall drops arriving onto the soil surface are considered;
- the relative soil water content is vertically and horizontally averaged.

The model is applied following the same procedure discussed in Sect. 3.2 with the soil moisture evaluated numerically solving Eq.(3.6) and the response of vegetation, in terms of dynamic water stress, evaluated as function of soil moisture dynamics during the growing season.

Mediterranean climate is characterized by a strong seasonality in rainfall, which is mainly concentrated during the autumn and the winter. Even for solar radiations and temperatures, there is a clear difference between spring-summer period and the remaining periods of the year. In order to take into account this climatic forcings seasonality, as shown before, the model considers two different seasons corresponding to the two vegetational phases typical of

Mediterranean environments: dormant and growing season (the growing season has again a duration of 214 days starting from April the 1st so that the scheme here used can be considered exactly the same of the SCHEME A of the previous application). All the model parameters are considered time-invariant during each season and also year by year.

The time step Δt chosen is again equal to 4 hours. The only modeling difference in respect to the previous application regards the interception model, that in this case considers a fixed threshold Δ that depends also on the season considered and in particular the dormant season values are set two times the values relative to the growing season.

All the parameters required by the model and describing the vegetation and the soil characteristics are those reported in Table 3.1 and Table 3.2.

Also the procedure used for the vegetation water stress evaluation is the same of the previous application with the exponent q of Eq.(2.11) considered initially equal to 3 for both the vegetation types investigated, while successively an analysis on the importance of such a parameter in the valuation of the vegetation response is presented, showing a comparison between the results, in terms of dynamic water stress, obtained by fixing q= 2 and q= 3 only for woody vegetation.

3.5.2 Climatic data and generation of climatic scenarios

In Mediterranean area, the most evident consequences of climate changes generated by CO_2 increase are certainly represented by the temperatures increase and the contemporaneous rainfall reduction (*Christensen et al.*, 2007). Many studies, carried out using historical precipitation series, agree on a rainfall decrease in this area (*Giuffrida and Conte,* 1989; *Amanatidis et al.*, 1993; *Kutiel et al.*, 1996; *Piervitali et al.*, 1997; *Esteban-Parra et al.*, 1998; *De Luis et al.*, 2000; *Cannarozzo et al.*, 2006). Even if probably, this reduction could be accompanied by an increase in events intensity and, at the same time, by a decrease in the number of annual events (*Cislaghi et al.,* 2005; *IPCC*, 2007), there is no certainty about possible changes in the distribution of the rainfall events over the year. However, according to the analysis of the recorded trend by *Cannarozzo et al.* (2006) in Sicily (Italy), it is possible to assume that the rainfall reduction will be mainly concentrated during the autumn and the winter.

Figure 3.14, from *Christensen et al.* (2007), shows some of the projected climate changes relative to Europe and the Mediterranean. In particular the annual and three-months (DJF= December, January and February; JJA= June, July and August) changes in temperature and precipitation over 100 years are shown. Other works (*Liuzzo et al*., 2008; *Noto et al*., 2007), carried out on temperature series recorded in Sicily during the last century, confirm this trend.

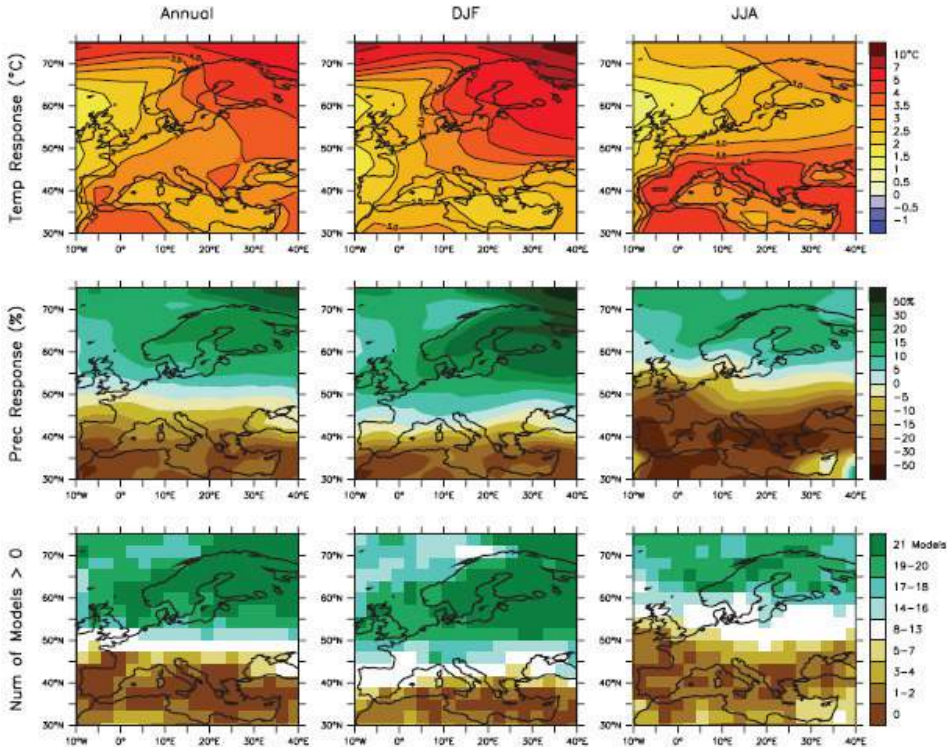

Figure 3.14: Temperature and precipitation changes over Europe Top row: Annual mean, December-January-February (DJF) and June-July-August (JJA) temperature change between 1980 to 1999 and 2080 to 2099, averaged over 21 models. Middle row: same as top, but for fractional change in precipitation. Bottom row: number of models out of 21 that project increases in precipitation (from *Christensen et al.*, 2007)

As mentioned previously, the Eleuterio river basin presents a typical Mediterranean climate, with hot and dry summer while the winter period is cooler and rainy.

The analysis of daily precipitation series chosen for this application and recorded at the Ficuzza raingauge station by *OA-ARRA* (*Osservatorio delle Acque dell'Agenzia Regionale per i Rifiuti e le Acque*) from 1977 to 1994, has allowed to evaluate the mean values interarrival time and intensity for rainfall during the growing (α_g, λ_g) and of the dormant season (α_d, λ_d). Figure 3.15 shows the behavior of the 4 years-moving averages relative to the annual and dormant season precipitation. It is possible to identify a clear trend for both these variables while no trend can be found out for the growing season rainfall

data. This fact confirms the above mentioned prevision for Sicilian areas by *Cannarozzo et al.* (2006).

Other input data as the values of mean temperature, relative air humidity and wind speed, have enabled the assessment of the potential evapotranspiration during both the seasons ($E_{max,g}$ for the growing and $E_{max,d}$ for the dormant season) using Penman-Monteith method. The mean annual temperature is 16.2°*C* while the mean annual precipitation is about 750 *mm*, whose about 70% is concentrated during the autumn-winter period.

In this application information about climate changes arising from *Christensen et al.* (2007) have been used in the determination of three different future scenarios; these have been created considering linear variations in temperatures and precipitation in order to evaluate the vegetation response at 25, 50 and 100 years.

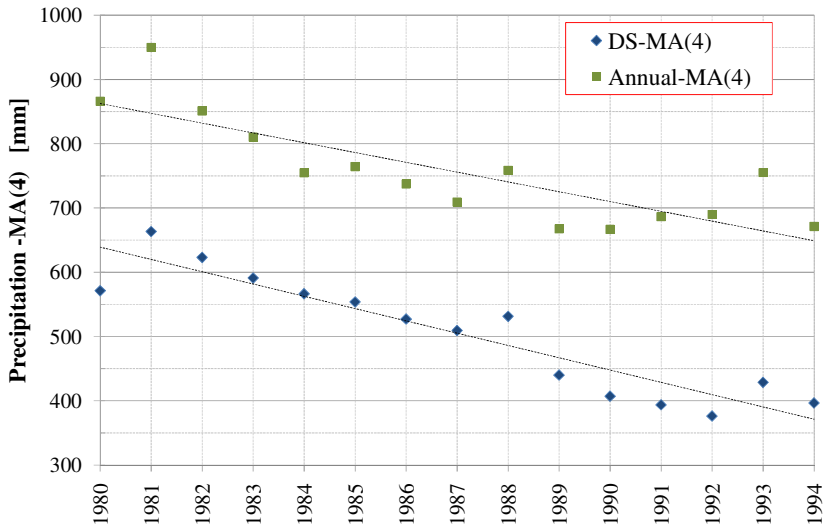

Figure 3.15: Historical rainfall data from Ficuzza raingauge (1977-1994); moving average with lag 4 for the series of annual data (Annual-MA) and of the dormant season precipitation (DS-MA)

3.5.2.1 Rainfall trends

The three scenarios have been generated starting from the prevision of *Christensen et al*. (2007) at 100 years and hypothesizing a linear trend in the rainfall. In particular, since the reduction at 100 years is estimated equal to 40% (reduction coefficient r_{100}=0.6), the reduction in rainfall at 50 and 25 years is equal to 20% and 10% (r_{50}=0.8, r_{25}=0.9). The total annual precipitation $\Theta_{y,tot}$ after the application of the trend at the generic year y (y= 25, 50 or 100 years) is equal to the product of r_y by the current value of the annual precipitation $\Theta_{0,tot}$. While on the one hand the reduction in annual precipitation appears likely on the basis of several studies on rainfall trend, on the other hand it is not clear how this reduction will take place over the year. In order to overcome this lack of knowledge two cases have been hypothesized.

In the first case (Case *A*), despite the reduction in time, the ratio K_Θ between precipitation during the growing and the dormant season Θ_d/Θ_g, keeps itself constant; currently the precipitation during the growing season represents about the 35% of the annual precipitation ($K_\Theta \cong 1.95$).

Another different situation, which represents an extreme condition, has been deepened. This scheme (Case *B*), considers the reduction of the precipitation concentrated only during the dormant season and for this reason the ratio K_Θ is not constant, but decreasing in time.

The Case *A* is very easy to handle, while the Case *B* appears more likely because is supported by historical rainfall data analysis carried out in Sicily (*Cannarozzo et al*., 2006).

For the generic scenario y (25, 50 or 100 years), the annual precipitation, $\Theta_{y,tot}$ can be easily calculated as mentioned above; consequently both the quantities of precipitation during the growing, $\Theta_{y,g}$, and the dormant season, $\Theta_{y,d}$, can be obtained for the Case *A* or *B*, using the following expression

$$\begin{cases} \Theta_{tot} = \Theta_g + \Theta_d \\ \alpha_g \lambda_g T_g = \Theta_g \\ \alpha_d \lambda_d T_d = \Theta_d \end{cases} \tag{3.7}$$

where T_j, λ_j and α_j (with j= g or d) are respectively the duration of each season, the seasonal rainfall frequency and the mean seasonal rainfall depth.

However, there are still infinite possible combinations of α_g, λ_g, α_d and λ_d that respect the Eq.(3.7) and it is not well clear how the mean intensity and interarrive time of rainfall events will change over the years. Then, being not possible to give a unique answer about the future values of λ_j and α_j (with j= g or d), it is here proposed an analysis with parameter λ_g, as below shown, adding

a further hypothesis that is the invariance of the ratio λ_g / λ_d. This parametric analysis has been carried out in the following way:

1) fix the parameter λ_g among a wide range;

2) use the hypothesis of the invariance of the ratio λ_g / λ_d to obtain λ_d;

3) calculate the seasonal rainfall using the formulas

$$\left.\begin{aligned} \Theta_{y,g} &= \frac{\Theta_{y,tot}}{1+K_\Theta} = r_y \frac{\Theta_{0,tot}}{1+K_\Theta} \\ \Theta_{y,d} &= K_\Theta \Theta_{y,g} \end{aligned}\right\} \quad Case\ A$$

$$\left.\begin{aligned} \Theta_{y,g} &= \Theta_{0,g} \\ \Theta_{y,d} &= \left(r_y - \frac{1}{1+K_\Theta} \right) \Theta_{0,tot} \end{aligned}\right\} \quad Case\ B \tag{3.8}$$

4) determine α_g, and α_d satisfying the Eq.(3.7).

For each simulated scenario *y* (25, 50 and 100 years), eight different values of λ_g have been considered (and consequently also eight values of α_g, α_d and λ_d), chosen in a range whose size depends on the percentage reduction in the annual precipitation in respect to the current value. In particular, the higher is the reduction in the annual precipitation, the larger is the range of variation of λ_g considered.

The Figure 3.16 and 3.17 show the eight different combinations of α_g, λ_g and the correspondent α_d, λ_d for each scenario and for both the Case *A* and *B*. With reference to the Case *A* (Figure 3.16) the rainfall reduction, which is equally divided among the growing (upper panel) and the dormant (bottom panel) season, produces a lowering of the curves relating the mean rainfall depth α and the mean frequency λ. The seasonal precipitation could occur through a decrement of α and an increment in frequency λ (points of type 1, 2 and 3). The opposite situation, with rare and intense precipitation is depicted through a decrement in λ and an increment in α (points 7 and 8). In the Case *A*, the points 6 of each scenario (25, 50 and 100 years) are obtained keeping α_g and α_d constant and equal to the current values. For both the Case *A* and *B*, the points 4 are characterized by λ_g and λ_d constant among the different temporal horizon (25, 50 and 100 years) and equal to the current values. In the Case *B*

(Figure 3.17) the growing season rainfall is kept constant, thus the combination of α_g and λ_g for all the scenarios lies in the same line. The rainfall reduction in this case is concentrated in the dormant season: as a consequence, for each future scenario (25, 50 and 100 years) the curves relating the mean rainfall depth α and the frequency λ appears to be shifted more downward than in the Case *A*.

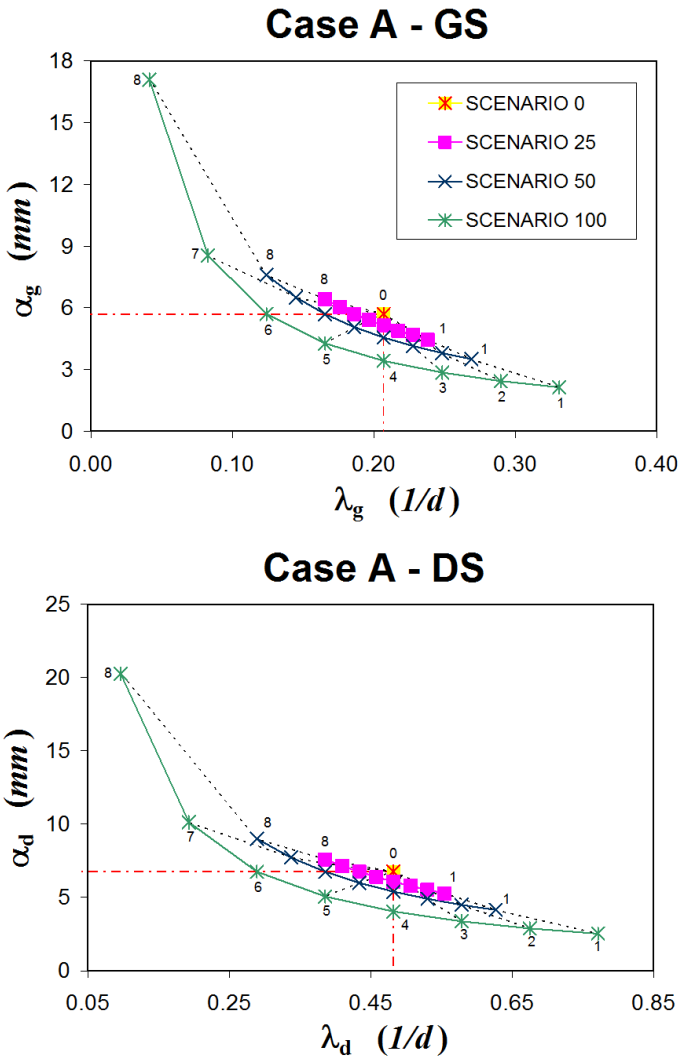

Figure 3.16: Case *A* (rainfall reduction over the whole year). Analyzed combinations of α_g and λ_g (upper panel) and the correspondent combinations of α_d and λ_d (bottom panel) for 25, 50 and 100 years scenario. The current scenario is marked as a point zero

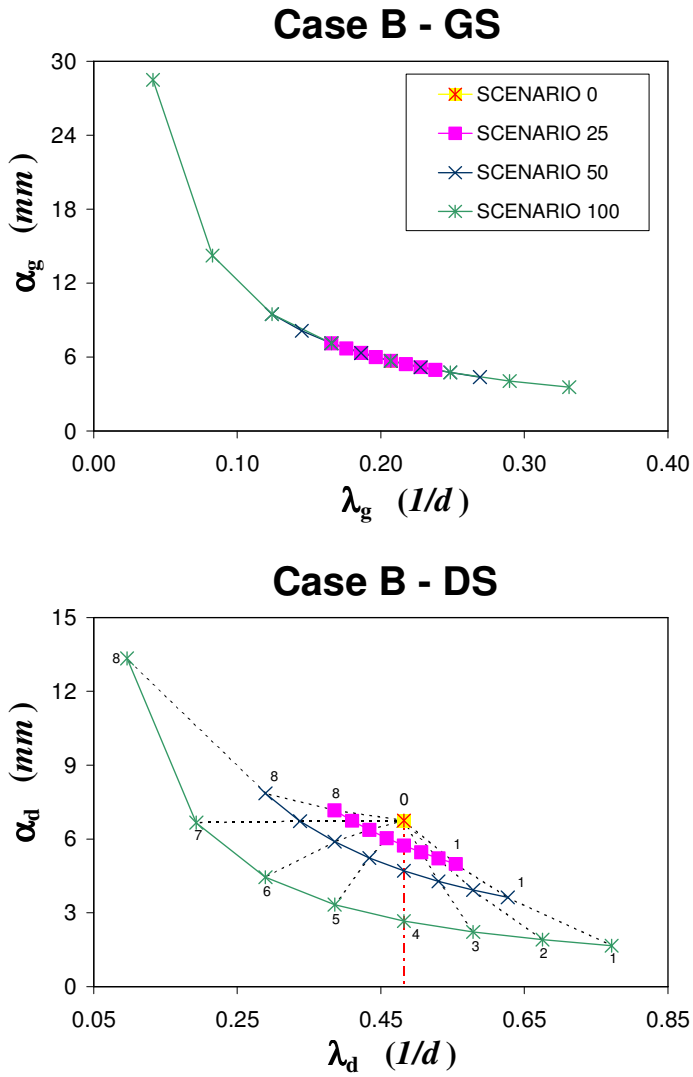

Figure 3.17: Case *B* (rainfall reduction concentrated in the dormant season). Analyzed combinations of α_g and λ_g (upper panel) and the correspondent combinations of α_d and λ_d (bottom panel) for 25, 50 and 100 years scenario. The current scenario is marked as a point zero

3.5.2.2 Temperature trends

Following *Christensen et al.* (2007), the projection at 100 years of climatic changes in Sicily (Italy), estimated an increment in temperature values equal to 2.9 °C. Hypothesizing a linear variation in time, this increment has been

rescaled at 25 and 50 years scenarios, using then the same approach considered for the precipitation.

Assuming that all the other climatic variables (i.e., wind velocity, relative humidity, net radiation) are not affected by climate changes and remain stationary, the temperatures increase leads to a growth also in the potential evapotranspiration rates during both the seasons ($E_{max,g}$ and $E_{max,d}$). In this application, Thornthwaite method (*Thornthwaite*, 1948) has been used in order to convert temperatures increase into evapotranspiration increase, at the monthly time scale. In Table 3.7, all the maximum evapotranspiration rates considered for the growing season ($E_{max,g}$) and for the dormant season ($E_{max,d}$) for both the vegetation covers considered and in relation to the three temporal horizons investigated, are shown.

SIMULATIONS		Temp. Var.	Vegetation Type				Rainfall			
			Tree cover		Grass cover					
SCENARIO	Temporal horizon	ΔT	$E_{max,d}$	$E_{max,g}$	$E_{max,d}$	$E_{max,g}$	ANN Θ	Precipitation distribution during the year	DS Θ_d	GS Θ_g
	(years)	*(°C)*	*(mm/day)*		*(mm/day)*		*(mm)*		*(mm)*	*(mm)*
0	0	0	2.03	*4.64*	1.11	*3.22*	744	*Current*	492	252
T25	25	0.73	2.11	*4.78*	1.15	*3.32*	744	*Current*	492	252
T50	50	1.45	2.19	*4.93*	1.20	*3.42*				
T100	100	2.90	2.34	*5.23*	1.28	*3.63*				
R25A	25	0	2.03	*4.64*	1.11	*3.22*	670	*Case A*	443	227
R50A	50						595		394	202
R100A	100						447		295	151
RT25A	25	0.73	2.11	*4.78*	1.15	*3.32*	670	*CaseA*	443	227
RT25B								*Case B*	418	252
RT50A	50	1.45	2.19	*4.93*	1.20	*3.42*	595	*Case A*	394	202
RT50B								*Case B*	343	252
RT100A	100	2.90	2.34	*5.23*	1.28	*3.63*	447	*Case A*	295	151
RT100B								*Case B*	194	252

Table 3.7: Rainfall, temperature and evapotranspiration for the different scenarios. ΔT= temperature variation in Celsius degree; E_{max}= potential evapotranspiration; ANN= annual precipitation; DS = dormant season precipitation; GS = growing season precipitation

The response of vegetation in terms of dynamic water stress has been evaluated firstly under an increment of temperature, secondly under a decrement in rainfall and, finally considering the coupled effects.

In Table 3.7 all these scenarios are described labeling them with an alphanumeric string. The first part denotes the kind of modification considered (*T* for temperatures increase; *R* for rainfall decrease; *RT* for simultaneous temperatures and rainfall variations). This first part is followed by a number denoting the temporal horizon (25, 50 or 100 years) related to the climatic projection; in the case *RT*, a letter denoting the rainfall reduction scheme (*A* or

B) is located at the end of the code. For example, the code *RT50B* identifies the simulation relative to a simultaneous variation of rainfall and temperatures, considering a reduction in precipitation driven by the hypothesis relative to the Case *B* and for a temporal horizon equal to 50 years. The scenario named *0* simulates the current climatic conditions.

3.5.3 Results and analysis

3.5.3.1 Effects of climate changes

The first simulations carried out, whose results are shown in Figure 3.18 and Table 3.8, regard the application of the only temperatures trends. Grass vegetation seems to be less influenced by the increase in temperature than trees.

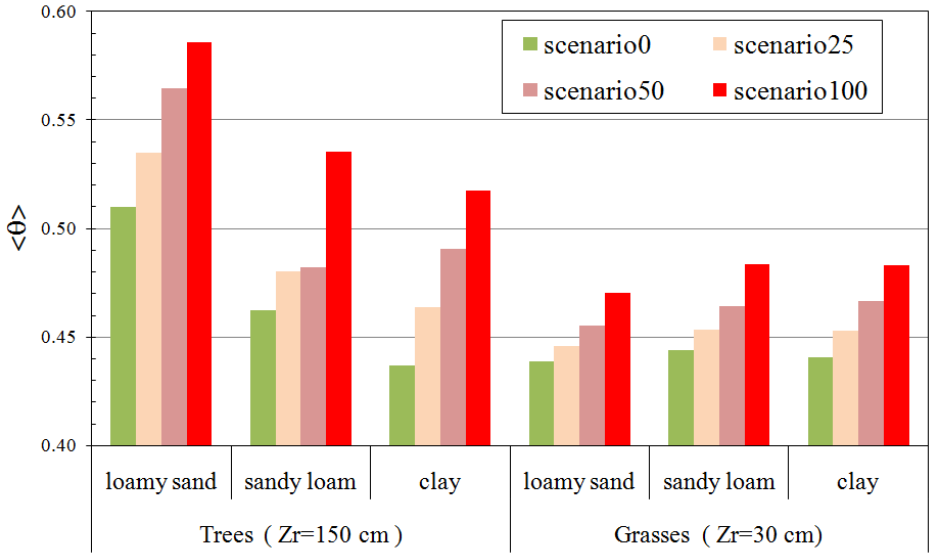

Figure 3.18: Temperatures trend effects on vegetation water stress <θ>

In particular Table 3.8, showing the variations of water stress in respect to the current values due to the application of the only temperatures trends, points out that grass water stress increases of just 7% on a loamy sand, up to 10% on a clayey soil over 100 years. Conversely, for the woody vegetation the model predicts an increment of the dynamic water stress in the order of almost 19% on a clayey soil and of 15% on a loamy sand over 100 years. For all the considered scenarios and soil types, the water stress variation is consistently higher in trees

than in grasses. In fact, except for the case of sandy loam, percentage increments in trees are about two times (three times for loamy sand) those relative to grasses; moreover, one can note that these differences between the percentage variations of the dynamic water stress in trees and in grasses are less marked passing from the projection at 25 years to those at 100 years. This general behavior is due to the higher evapotranspiration rates and to the higher interception relative to woody vegetation.

			$(\Delta\theta/\theta_0)$ [%]					
	ΔP	ΔT	TREE			GRASS		
Scenario	%	°C	loamy sand	sandy loam	clay	loamy sand	sandy loam	clay
T25	-	0.73	4.9	3.8	6.2	1.7	2.1	2.7
T50	-	1.45	10.6	4.3	12.2	3.8	4.5	5.9
T100	-	2.90	14.8	15.7	18.5	7.2	8.9	9.6

Table 3.8: Percentage variations of water stress due to the application of the only temperatures trend for each considered scenarios (25, 50 and 100 years)

Figure 3.19 reports a comparison between the results relative to only the precipitation trend (*R*, dashed lines) and those relative to the coupled effect of temperatures increase and precipitation decrease (*RT*, continuum lines); all simulations have been carried out using the Case *A* hypothesis. Each subplot shows the dynamic water stress $< \theta >$ as a function of λ_g. As expected, the rainfall decrease, coupled or not with the temperature increase, leads to an increment of the water stress. The water stress increases also with the rainfall frequency and this behavior is more evident for the grasses. For both the vegetation covers, for every considered soil type and for all the three temporal scenarios, the dynamic water stress is minimum at the lowest values of λ_g (points 8) and maximum for the highest ones (points 1). This means that vegetation suffers less water stress in the case of rarer and more intense events. The reason of this behavior could be ascribed to the model structure: more intense and rare precipitations are subjected to less interception because of the fixed threshold and so they are more water conservative than frequent events.

The rainfall distribution over the year and its likely future variation are crucial in determining the water stress conditions. With this regard, a comparison between the dynamic water stress values arising from the two different cases analyzed (*A* and *B*) has been represented in Figure 3.20. The grasses seem to be much more dependent by rainfall distribution than trees. Keeping the rainfall constant over the growing season (Case *B*), the water stress remains almost the same notwithstanding the winter reduction. Comparing the water stress value in the scenarios *0* and *RT100B*, only a slight increment can be observed. This result confirms how the grasses rely only on the growing season

rainfall, since their water stress does not depend on the winter soil recharge. Conversely, if the rainfall is reduced in both dormant and growing season (Case *A*), the water stress increases up to unbearable conditions ($<\theta>=1$) obtained for frequent events.

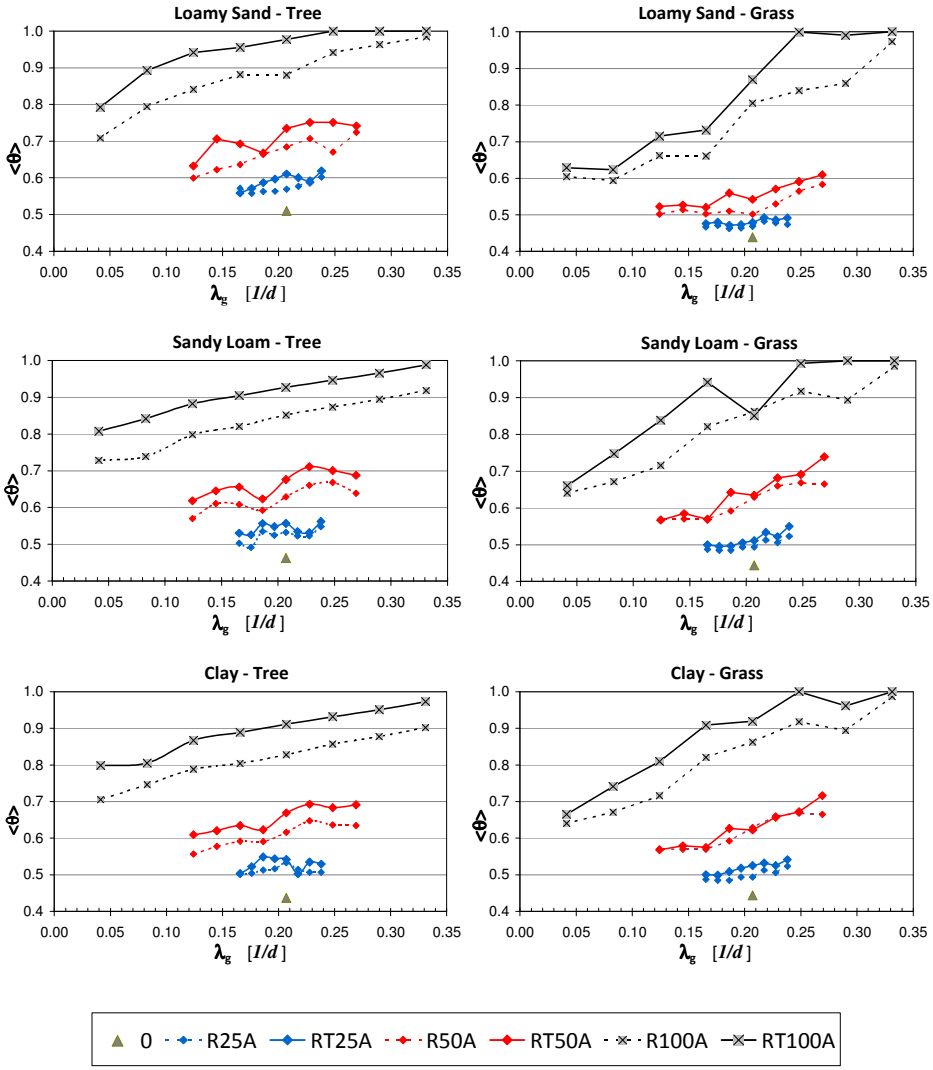

Figure 3.19: Effects on vegetation water stress <θ> of the precipitation decreasing trend (dashed lines) and of the coupled temperatures increase and precipitation decrease (continuous lines): Case *A*

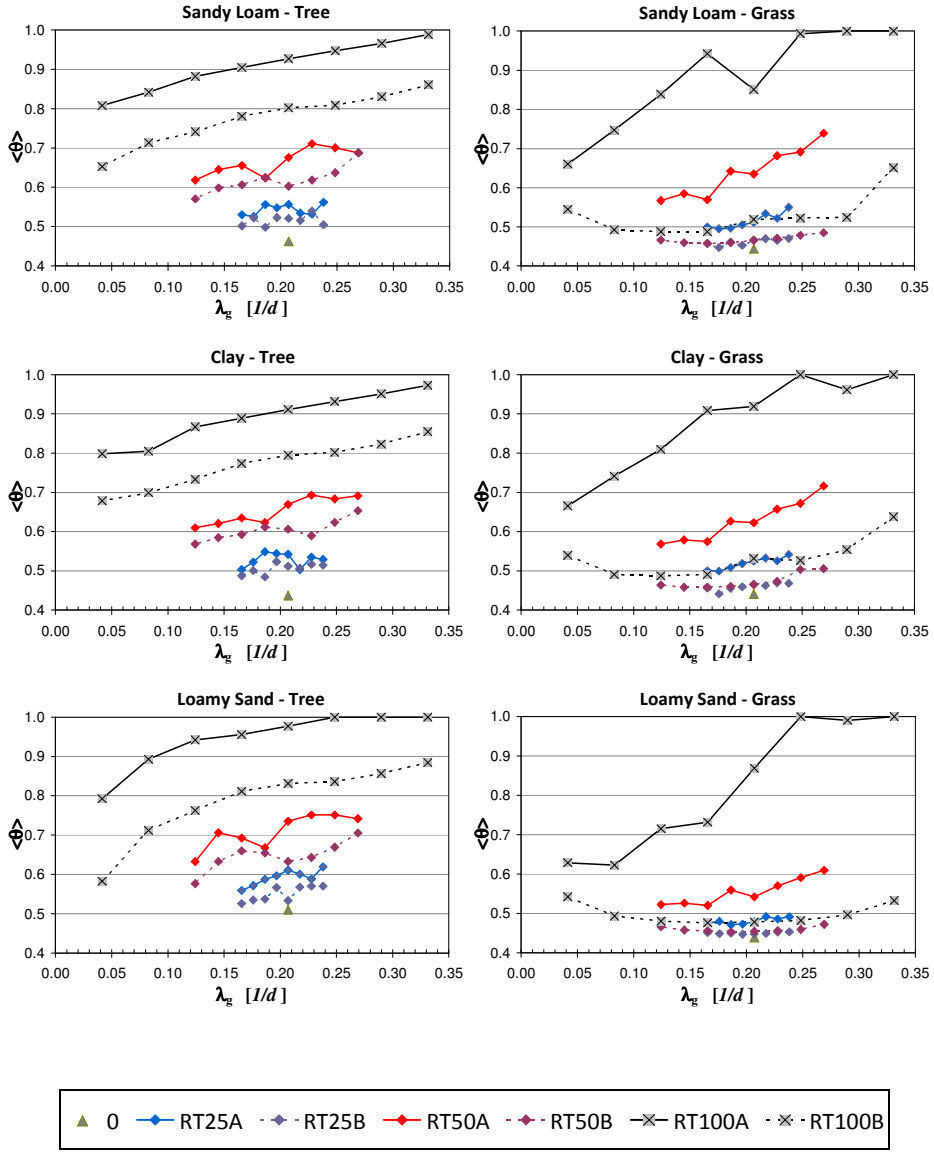

Figure 3.20: Vegetation water stress <θ> in different soil types and climate change scenarios. The future scenarios are characterized by the coupled effect of temperatures increase and precipitation decrease. With continuous lines the results arising from the Case *A*, while with dashed lines the ones coming from the Case *B*

Trees response is also dependent on the rainfall reduction scheme. In both the considered cases, the water stress significantly increases going from the scenario *0* to the *RT100A* or *RT100B*. This increment is due to a decrement of the water stored during the dormant season, and then of the initial relative water content condition at the beginning of the growing season. In addition it can be observed that if the rainfall is reduced along the whole year (Case *A*) trees suffer more than the case in which the reduction is concentrated in the dormant season (Case *B*). Even in this case frequent rainfall events generate higher water stress condition because of the interception model with a fixed threshold.

Table 3.9 shows the maximum and minimum percentage variation of water stress observed among the eight possible combinations of α_g, λ_g, α_d, λ_d which constitute each considered scenarios (25, 50 and 100 years) for the cases *R* and *RT*. It is clear from the comparison of Tables 3.8 and 3.9 how the major cause of water stress increase is the rainfall decrease, while the temperature increase emphasizes slightly the water stress. This result is also explained by the model structure: here the rainfall has a direct influence on the water balance equation while the temperature affects the soil moisture only indirectly through the evapotranspiration term.

Considering the case of rainfall reduction along the whole year (Case *A*), for both the scenarios of application of only rainfall trend (scenarios R) and contemporaneous application of rainfall and temperatures trends (scenarios RT), one can note that, in the projection at 25 years, the maximum percentage variations of dynamic water stress are slightly higher for trees than for grasses, while, in the projection at 50 years, they are comparable. Conversely, in the projection at 100 years, the maximum percentage variations of water stress in the case of grasses are higher than those for trees.

From the observation of the minimum values found among the eight possible combinations of rainfall parameters, it is possible to note that, except for the case of sandy loam, the behavior is similar to that relative to the case of application of the only temperature trend (see Table 3.8), with percentage increments for trees higher than those for grasses, even if their ratio is generally lower than that previously found for the scenarios of type T (about 2). Furthermore, in the scenarios of type RT it is possible to note that such differences in the percentage increments between trees and grasses tend to be more marked passing from the projection at 25 years to those at 100 years, while no trend over the years is possible to identify in the case of scenarios of type R.

On the contrary, in the case of rainfall reduction concentrated only in the dormant season (Case *B*), both the maximum and minimum values of the dynamic water stress percentage increments in the case of trees are always much more higher than those relative to grasses. This fact highlights how woody vegetation in a Mediterranean area, such as that of the Eleuterio at Lupo,

is very reliant on winter water recharge, and for this reason a rainfall reduction concentrated during this season, coupled with the temperatures increase, would lead to relevant changes in vegetation status for trees. From the comparison between the results shown in Table 3.8 and in Table 3.9, it is evident that the relative contribution to the dynamic water stress increments given by the rainfall reduction for the Case *B* is very high in trees, while it seems to be comparable to that given by the temperatures increase in the case of grasses.

			$(\Delta\theta/\theta_0)$ [%]											
			TREE						GRASS					
	ΔP	ΔT	loamy sand		sandy loam		clay		loamy sand		sandy loam		clay	
Scenario	%	°C	max	*min*	max	*min*	max	*min*	max	*min*	max	*min*	max	*min*
R25A	-10	-	18	*9*	18	*6*	22	*15*	10	*5*	18	*9*	21	*10*
R50A	-20	-	42	*18*	44	*23*	48	*27*	33	*14*	50	*28*	51	*26*
R100A	-40	-	93	*39*	99	*57*	106	*61*	122	*35*	122	*44*	121	*46*
RT25A	-10	0.73	21	*10*	22	*14*	26	*15*	12	*8*	24	*12*	23	*13*
RT50A	-20	1.45	47	*24*	54	*34*	59	*39*	39	*19*	66	*28*	62	*29*
RT100A	-40	2.90	96	*55*	114	*75*	123	*83*	128	*42*	125	*49*	127	*51*
RT25B	-10	0.73	12	*3*	17	*8*	20	*11*	3	*2*	6	*1*	6	*0*
RT50B	-20	1.45	38	*13*	49	*23*	49	*30*	8	*3*	9	*3*	15	*4*
RT100B	-40	2.90	73	*14*	86	*41*	96	*55*	24	*9*	46	*10*	45	*11*

Table 3.9: Maximum and minimum percentage variations of water stress observed among the eight points (eight possible combinations α_g, λ_g, α_d, λ_d) of each considered scenarios (25, 50 and 100 years) for the cases R and RT (Case *A* and *B*)

3.5.3.2 Uncertainty in the vegetation response: role of the exponent *q*

The evaluation of the vegetation response to the predicted climate changes is subjected to uncertainty in the estimation of some parameters, such as the exponent *q* of the Eq.(2.11), which plays an important role in the assessment of the dynamic water stress. This exponent is a measure of the nonlinearity of the effects of soil-moisture deficit on plant conditions.

The value of *q* varies usually with plant species and, in a narrower range, with the soil type, from 1 to 3. Even if it is common to use the value 2 (*Rodriguez-Iturbe et al.*, 1999b), it seems to be reasonable to consider the highest values (q= 2 or 3) for woody vegetation. In fact, these plants have the possibility to store a higher water amount within their apparatus and then are more able to face longer water deficit periods, while the grasses manifest a linear response.

A value of *q* equal to 3 has been considered in this work, and obviously all the conclusions made are strictly dependent on this assumption. For this reason a parametric survey on the role of the exponent *q* has been here carried out.

A comparison between the results obtained by fixing q= 2 and q= 3 only for woody vegetation is shown in Figure 3.21. As expected, the highest values of the dynamic water stress are those relative to the lower values of *q*, while, and that is less obvious, the dynamic water stress as a function of λ_g and for fixed seasonal precipitation presents a similar behavior in both the cases. The two compared values of *q* represents, for woody vegetation, two extreme conditions, and it is more likely that the actual relation between the soil moisture and the vegetation water stress could be better modeled by a value of *q* between 2 and 3. As a consequence, the water stress found in this work using *q* equal to 3 represents probably the best situation that could happen in the next years if the hypothesized rainfall and temperatures trends were confirmed. Analogous considerations may be valid also in the case of grass vegetation, where the extreme condition is represented by *q* equal to 1.

The occurrence of a linear, or almost linear, relation between the soil moisture condition and the consequent plant response, could further exacerbate the future water stress values in respect to the here predicted results. However, it is known that plants apply several kinds of long-term strategy to face prolonged stress periods, tending to adapt themselves to new external conditions. For these reasons it is reasonable to think that, in the case of future scenarios similar to those predicted by *Christensen et al*. (2007), the relation between the soil moisture and the water stress value may be characterized by an increasing value of *q*.

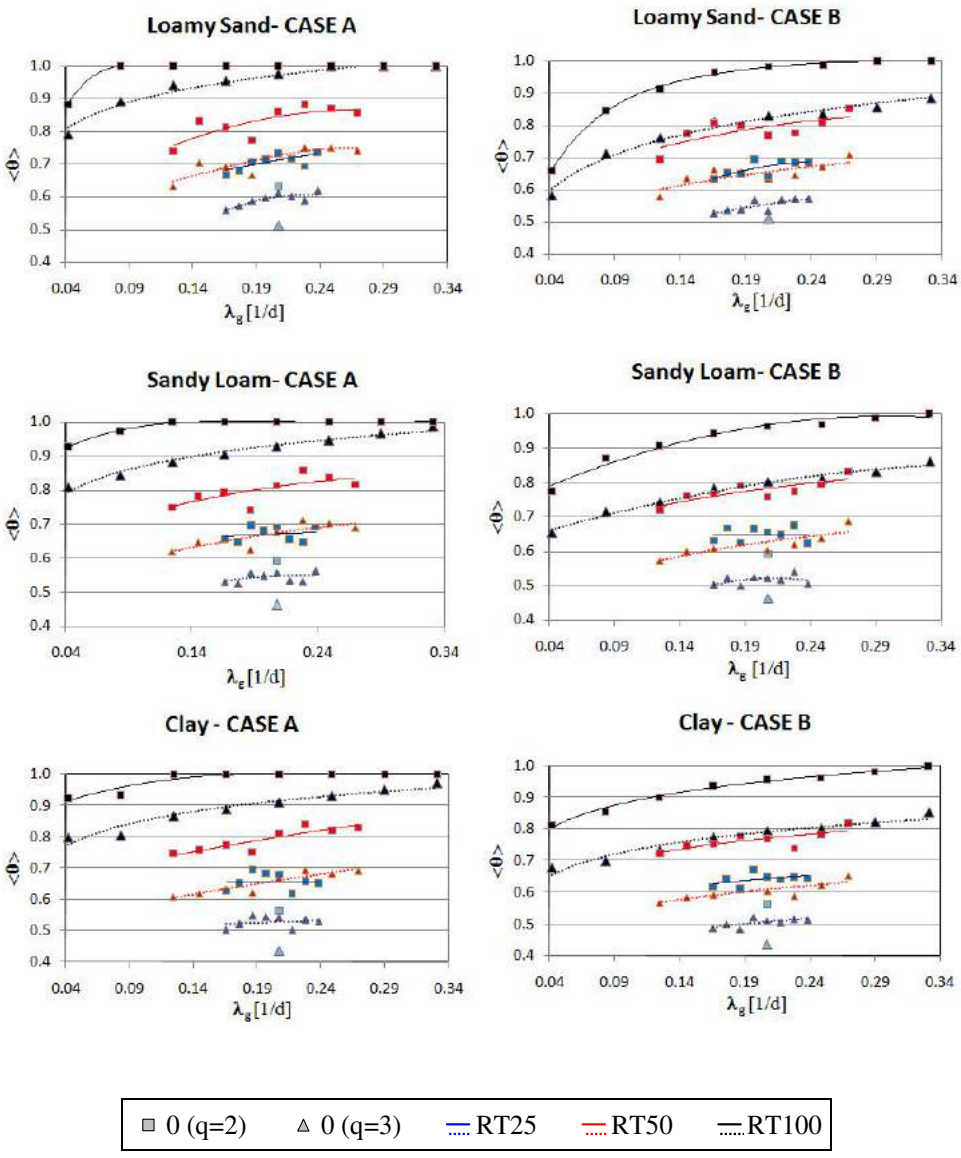

Figure 3.21: The role of the exponent q in trees water stress estimation. Comparison between the results arising from q=2 (squares interpolated by the continuous lines) and from q=3 (triangle interpolated by the dashed lines). In the left panels the results arising from the Case *A*, while in the right panels the results coming from the Case *B*

3.6 Concluding Remarks

The soil moisture dynamics and the vegetation water stress in Mediterranean climate, where the wet and the growing season are out of phase, have been here investigated proposing a numerical ecohydrological model which takes into account the seasonality of the rainfall and of the evapotranspiration demand. Working on the entire year, the proposed model is able to reproduce the winter process of water recharge into the soil, which gives the soil moisture condition at the beginning of the growing season, leading to transient effects during the same season.

In the first application, discussed in Sect. 3.4, particular attention has been focused on woody vegetation cover (deep soil) because it is the most critical with regard to the effects on soil moisture dynamics due to a transient period. The proposed model solves the soil water balance, through a finite difference method, working with a temporal step short enough to give a satisfactory approximation of the water losses. Once the soil moisture values in the growing season are assessed, it is possible to estimate the soil moisture pdf, which implicitly considers the transient effects. Through the application to the watershed of Eleuterio at Lupo (whose characteristics are described in Sect. 3.3) and for three different soil types, the numerical pdf's have been compared with those analytically obtained, showing important differences. The numerical pdf's are not symmetric and spread over a wide range, from the field capacity, which is a likely value at the beginning of the growing season, to the stomata closure point, which is the most likely value during the growing season (when a steady state condition can be considered reached). The numerical approach allows to take into account the transient effects and consequently gives values of the mean soil moisture during the growing season higher than the values obtained using the analytical approach; in particular this is evident from the comparison between the pdf's arising from the analytical model and the numerical model with a bi-seasonal annual discretization (SCHEME A). This high value of the mean soil moisture during the growing season, often warrants the survival of woody species and theirs presence in Mediterranean areas, otherwise impossible to explain by the analytical approach, that would lead to a too high water stress.

The higher is the annual discretization considered for rainfall and evapotranspiration parameters, the more physically consistent is supposed to be the annual soil moisture behavior and then the resulting pdf. For this reason, the influence of the description of the annual climate variability on the soil moisture pdf has been also analyzed. Considering a monthly climate variability (SCHEME B), the numerical approach leads to a bimodal soil moisture pdf. The behavior of the pdf arising from this type of schematization shows as in a Mediterranean area, two different periods during the growing season can be identified: the former is characterized by high values of soil moisture due to

both the winter water recharge into the soil and the persistence of high precipitations and low water losses from the soil, while the second one, characterized by lower values of precipitations and higher water losses, is not dependent on soil moisture state at the beginning of the growing season and it could be considered as a steady period. The shape of the soil moisture pdf relative to SCHEME B appears hence as the result of an overlap of a typical analytical pdf in a steady state condition and a more disperse non-steady pdf relative to the transient period.

In order to evaluate the plant response to the soil moisture dynamics, a new approach has been proposed. Following the proposed procedure, the mean static and the dynamic water stress indexes can be numerically computed since the soil water balance equation has been solved and the soil moisture time-profile has been obtained. Also the water stress evaluation is influenced by the description of the annual climate variability. The results arising from the first application to the Eleuterio at Lupo watershed, show that the higher is the annual discretization, the higher are all the indexes of the vegetation water stress, and in particular with regard to the static water stress modified. The substantial difference between the two considered schematizations is that the SCHEME B simulates shorter stress periods with more intensive static water stress.

The numerical evaluation of the dynamic water stress is a new definition of water stress and leads to different results from the analytical estimate, allowing to consider a non-steady condition for the soil moisture dynamics, and thus to calculate the vegetation water stress in Mediterranean climate, where the presence of a transient period is crucial especially for deep root vegetation.

The second application of the model to the Eleuterio at Lupo river basin has analyzed the effects of possible climatic change on vegetation in terms of water stress. Mediterranean ecosystems will probably face, in the next future, a radical modification of the climatic conditions, summarizable in a rainfall reduction and a temperature increase, already widely recognized in historical climate series.

Temperature increase consequently leads to an increase in the evapotranspiration rates, hypothesizing a constant efficiency of the plants transpiration processes. Thus, the resultant effect is an increase of the vegetation water stress. Following the evapotranspiration demand, one can observe that the higher the rooting depth, the higher the increase of water stress.

The effects of rainfall decrease are less obvious to understand because there is large uncertainty about seasonal variations, frequency and intensity of future rainfall. In order to overcome these uncertainties, a parametric study on rainfall frequency has been carried out, modeling the future rainfall distribution over the year with two different schemes.

Rainfall reduction increases the vegetation water stress much more than temperature increase does. Intense and rare rainfall events, as they are expected to be in the future, could attenuate the effects of rainfall reduction because of the less interception correlated to them.

The future rainfall distribution over the year is also crucial for vegetation water stress. The contemporaneous application of the temperatures and rainfall trends have shown that the highest increments of dynamic water stress are those relative to the Case *A*, with rainfall reduction distributed over the whole year, and this is particularly true in the case of grasses. If the current ratio between the growing season and the dormant season rainfall will be maintained (i.e., Case *A*), trees and grasses could be subjected to an increase of water stress almost in the same manner. Otherwise, if the rainfall reduction could be concentrated during the dormant season (i.e., Case *B*), as emerges from literature, grasses will have some advantages over the trees species. In this conditions grasses will keep the water stress similar to the nowadays value, while trees will suffer for the lack of the winter recharge, increasing their water stress. All this could cause a significant modification of vegetation patterns characteristic of Mediterranean areas in the coming years.

Chapter 4

Ecohydrology in Groundwater Dependent Ecosystems

4.1 Introduction

The main aim of this chapter is the study of groundwater dependent ecosystems through an ecohydrological approach. After a first part devoted to the description of the peculiarities of groundwater dependent ecosystems, in the second part of the chapter the state of the art related to the ecohydrological modelling in this type of environment is discussed.

In particular, an ecohydrological analytical approach to the study of the coupled water table and soil moisture dynamics is delved. *Rodriguez-Iturbe et al.* (2007) have highlighted the lack of quantitative methods for the study of the stochastic water balance in humid lands. As a consequence, a very recent school of thought (e.g., *Ridolfi et al.*, 2008), is providing innovative tools for the study of groundwater dependent ecosystems. In this chapter two process-based probabilistic models for the study of water table depth (*Laio et al.*, 2009) and soil moisture dynamics (*Tamea et al.*, 2009) are discussed in detail. These two models were conceived for groundwater dependent ecosystems with below-ground water table fluctuations. The former is based on a soil water balance equation where the unknown quantity is the water table depth, while the latter is based on a local, depth-dependent water balance equation where the unknown quantity is the soil moisture. Both the water balance equations are forced by stochastic precipitation, accounting for mechanisms such as rainfall infiltration and water table recharge, plant water uptake, capillary rise, groundwater lateral flow due to the presence of a nearby water body.

The two models provide a semi-analytical formulation of the probability distribution function of the water table depth (the first model by *Laio et al.*,

2009) and of soil water content at different depths (the second model by *Tamea et al.*, 2009).

In the last part of this chapter, an application of the first model (i.e., for the study of the water table fluctuations) to three sites, located within the Everglades (Florida – USA), is presented. In particular a comparison between the water table depths predicted by the model and the historical series of water table depth observed at the three sites is shown.

4.2 Groundwater Dependent Ecosystems

Starting with the premise that all vegetation, even desert cacti, requires water to grow, it is possible to distinguish different mechanisms by which ecosystems rely on water.

In several areas, rainfall is the dominant and often the only source of water available for the plant. As mentioned before, water is required by plants to keep leaves turgid, to drive growth and to provide a medium for all the biochemical reactions that take place in cells. In addition, a large amount of water is lost from leaves as transpiration when stomata open to allow carbon dioxide to enter for photosynthesis.

Although rain is the most common source of water for plants, there is a class of vegetation that routinely uses groundwater to support growth and photosynthesis. This class is said to be *groundwater dependent* because the absence of groundwater has a negative impact on the growth and health of the vegetation. Prolonged absence of groundwater from sites that formerly had groundwater available leads to plant death and a change in ecosystem composition and hence ecosystem structure and function (*Eamus*, 2009).

It is therefore possible to define as *groundwater dependent ecosystems* (GDEs) all those ecosystems whose current composition, structure and function are reliant on a supply of groundwater, and that require access to groundwater to maintain their health and vigor. Thus, GDEs are communities of plants, animals and other organisms whose extent and life processes are dependent on groundwater and that would be significantly altered by a change in the chemistry, volume or timing of groundwater supply.

Such ecosystems vary dramatically in how they depend on groundwater, from having occasional or no apparent dependence through to being entirely dependent. There are many types of GDEs (e.g. possible examples include riparian zones, peatlands, and unsubmerged wetlands). According to *Eamus* (2009), they can all be classed into one of two major groups: the first class of GDE relies on the surface availability of groundwater; while, the second class

relies on the availability of groundwater below the surface but within the rooting depth of the vegetation. Swamps, wetlands and rivers are typical example of ecosystems that rely on the discharge of groundwater to the surface, either into a river or into a swamp or wetland. Rivers and streams that flow all year (perennially flowing) are generally groundwater dependent because a significant proportion of their daily flow is derived from groundwater discharging into the river course. When groundwater availability declines, river flow is reduced and swamps and wetlands may become dry, temporarily or permanently. The second class is constituted by terrestrial ecosystems and includes riparian forests, vegetation on coastal sand dunes and other terrestrial vegetation.

The response of vegetation to reduced availability of groundwater is incremental. Initially, following a decline in groundwater availability, plants show short-term adaptive responses, the most important of which is a reduced opening of the stomata on leaves. This occurs to reduce the amount of water required by the plant canopy, but it also reduces the rate of carbon fixation and hence growth is also reduced. If the decrease in availability persists, the leaf area index of the site reduces itself as trees lose their leaves in an effort to further reduce their water use. Growth at this stage is very much reduced as well as recruitment of seedlings of the current suite of species and, over time, seedlings of new species could be observed.

The importance of GDEs is strictly linked to their conservation, biodiversity, ecological, social and economic value. Such ecosystems are of particular interest for several reasons. Some have obvious and immediate commercial value (for example, plantations), some have tourism value (for example to keep rivers flowing and healthy). The importance of these areas is also related to their relatively high richness both in animal and plant species, and their ability to sequester and store carbon (*Mitsch and Gosselink*, 2007). Riparian forests provide pathways for the movement of animals across fragmented landscapes. The dewatering of landscapes by trees can stop the development of dryland salinity, while their ability to hold onto soil and capture runoff is important in maintaining land and water quality.

The presence of a GDE can be logically inferred from a set of observations or experimentally shown using a range of techniques (*Eamus*, 2009). A simple way to recognize if a certain ecosystem is GDE or not can be to observe the position of the water table and its daily fluctuations: if groundwater is found to be within the rooting depth of the vegetation we may reasonably conclude that the vegetation is using that groundwater; moreover, if diurnal changes in groundwater depth are observed, this is strong evidence of groundwater uptake by vegetation.

In ecohydrological key, groundwater-dependent environments are areas where the groundwater plays a key role both on vegetation dynamics and on the

soil water balance. The dynamics of these ecosystems are controlled by the soil water balance and are affected by water table depth and soil water content. Water table fluctuations and soil moisture profiles, in fact, play a fundamental role in major ecohydrologic processes, including infiltration, surface runoff, groundwater flow, land-atmosphere feedbacks, vegetation dynamics, nutrient cycling, and pollutant transport. Understanding and modeling the soil water balance and its relationships with climate, soil and vegetation is therefore a crucial aspect for geosciences such as hydrology and ecology. The ecohydrology of humid lands represents a new frontier of scientific research and the quantitative description of soil water dynamics in humid areas presents particularly challenging features since it needs to be linked to the intertwined stochastic fluctuations of the water table and the soil moisture of the unsaturated zone (*Rodriguez-Iturbe et al.*, 2007).

4.3 Ecohydrological modelling of GDEs

The soil water balance exerts the main hydrologic control on the structure and function of terrestrial ecosystems, mediating the impact of hydrologic processes on the dynamics of plant and soil microbial communities (*Linn and Doran*, 1984). On the one hand, low values of soil moisture may cause water stress conditions both in vegetation and in soil microorganisms, limiting the rates of photosynthesis, transpiration, microbial respiration, and soil organic matter decomposition. Also the transport of water through the soil-plant-atmosphere continuum as well as of substrate in the soil solution, are limited by low soil water contents (*Meixner and Eugster*, 1999). On the other hand, the anoxic conditions associated with an increase of the water table may limit plant productivity (*Wilde et al.*, 1953; *Roy et al.*, 2000), microbial decomposition (*Skopp et al.*, 1990), and mineralization (e.g., *Brady and Weil*, 1996), while provide favorable conditions for the biogenic emissions of nitrogen oxides (denitrification) and methane (e.g., *Meixner and Eugster*, 1999).

Thus a complete analysis of plant and microbial response to changes in hydrologic conditions for humid lands requires the analysis of fluctuations both in root zone soil moisture and in water table depth. Because of the intermittency and uncertainty inherent to the rainfall regime, both soil moisture and water table depth undergo coupled stochastic dynamics (*Rodriguez-Iturbe et al.*, 2007).

In the recent past, these dynamics were mostly investigated either in terms of mean seasonal water fluxes (mean precipitation, evapotranspiration, drainage), or through more detailed numerical simulations of the soil water

balance (e.g., *Feddes et al.*, 1988; *Berendrecht et al.*, 2004; *Yeh and Eltahir*, 2005). While coarse-scale evaluations of the mean soil moisture are not capable of resolving pulses and high-frequency (stochastic) fluctuations, numerical calculations of soil moisture dynamics and their impact on vegetation are not well suited for an effective and exhaustive analysis of the interdependence of soil, vegetation, and climate drivers, especially when it is necessary to account for the stochastic nature of the involved phenomena (*Rodriguez-Iturbe et al.*, 2007).

In recent years a different approach has been proposed: *Rodriguez-Iturbe et al.* (2007) highlighted the lack of an analytical framework for the study of the stochastic soil water balance in humid lands. The finding of analytical solutions (e.g., *Rodriguez-Iturbe et al.*, 1999a; *Laio et al.*, 2001b) of the stochastic soil water balance equation at timescales crucial for the description of its interaction with vegetation suggest the use of minimalist models of soil moisture dynamics that are able to account for the random character of precipitation along with the pulsing character of soil moisture. As mentioned in the previous chapter, most of the early analytical researches in ecohydrology were concentrated on water-controlled ecosystems, where productivity strongly depends on soil water availability, while the effect of water table dynamics on vegetation can be neglected; in such ecosystems, in fact, the water table, because of its deepness, can be assumed mostly inaccessible for the same vegetation (*D'Odorico and Porporato*, 2006).

As mentioned in Chapter 2, wetlands are humid GDEs which exhibit either shallow water tables or standing water over certain periods of time. Despite the lack of general consensus on the distinctive features defining wetland environments (e.g., *Mitsch and Gosselink*, 2007), the presence of saturated soils/shallow water tables or the recurrence of flooding conditions remain key elements of humid land and wetland hydrology. There are other commonly recognized attributes of wetland ecosystems derived from these two key elements, such as the presence of undrained hydric soils and of species adapted to water logging conditions (i.e., *hydrophytes*, plants that obtain a significant portion of the water that they need from the zone of saturation or the capillary fringe above the zone of saturation; *phreatophytes*, aquatic plants that can only grow in water or permanently saturated soils). Thus the definition of such ecosystems would require that shallow water tables persist for sufficiently long periods of time to determine the dominance of phreatophytic or hydrophytic plant communities.

Thus, the quantitative understanding of the hydrologic regime determining the persistence of hydrophyte/phreatophyte vegetation, and the development of quantitative frameworks capable of relating climate, soil, and vegetation to water table fluctuations or the occurrence of flooding assume a crucial importance to the study of wetlands.

Humid lands can be considered water-controlled environments as well, even if their dynamics are substantially different from those of arid and semiarid ecosystems (*Naiman et al*., 2005; *Mitsch and Gosselink*, 2007). In the case of wetlands, the hydrologic controls on vegetation and microbial stress do not arise from water limitation but rather arise most frequently from waterlogging conditions and the consequent limitation on soil oxygen availability (e.g., *Kozlowski*, 1984; *Roy et al.*, 2000; *Brolsma and Bierkens*, 2007). At the same time plants may, in turn, affect the water table depth, as observed in several kinds of wetland (*Dacey and Howes*, 1984; *Dube´ et al.*, 1995; *Roy et al.*, 2000*; Wright and Chambers*, 2002).

The study of terrestrial vegetation in GDEs cannot hence prescind from a coupled analysis of soil moisture and water table dynamics, with important complications for the analytical treatment of the water balance equation.

The interactions between vegetation and water-table dynamics leads to important feedbacks: the most important are listed below following *Rodriguez-Iturbe et al.* (2007).

Vegetation–water table interactions may induce the emergence of bistable vegetation dynamics. *Ridolfi et al.* (2006) showed that, by increasing the water table depth, riparian plant communities may modify the physical environment creating conditions favorable to their own survival. This positive feedback may lead to the emergence of two alternative stable states with the system dominated either by water intolerant species on deep water tables, or water tolerant species on shallow water tables (*Chambers and Linnerooth*, 2001; *Wright and Chambers*, 2002).

The decrease in water table depth (watering-up process) subsequent to the disturbance/clearcut of wetland forests could prevent or delay seedling establishment, thereby favoring the invasion of grasses, shrubs, or mosses. By lowering the water table elevation, these invasive species could facilitate the reestablishment of tree seedlings, thereby leading to interesting hydrologically controlled successional dynamics [e.g., *Dube´ et al.*, 1995, *Ridolfi et al.*, 2007].

Another characteristic of the interactions vegetation-water table dynamics is that species richness is observed to decrease with decreasing values of water table depth (e.g., *McKnight et al.*, 1981). Most vascular plants (i.e., plants that have lignified tissues for conducting water, minerals, and photosynthetic products) suffer under conditions of frequent waterlogged soils, and then species diversity result limited under shallow water table conditions.

The activity (anaerobic versus aerobic) of microbial biomass is strongly affected by changes in soil water content and in soil aeration. This fact has important implications for the processes of decomposition, mineralization, nitrification and denitrification. Moreover, the low decomposition rates existing in waterlogged soils favor the accumulation and burial of soil organic matter,

with important impacts on soil physical properties and ecohydrological processes.

Capillary rise, a process of water transport from the water table to the surface (where water is lost by evaporation), is associated with the accumulation of salts at the surface. In the case of shallow water table this process becomes very important, controlling ecosystems response to soil salinization. An excessive presence of salt at the soil surface may induce mortality of riparian vegetation, thus affecting the composition and structure of wetland plant communities. In particular, a decrease in water table depth, which could further enhance capillary rise and soil evaporation, leads to an increase in the accumulation of salt at the soil surface.

All this important implications and feedbacks arising from the mutual interactions between vegetation and water table dynamics highlight how important is a coupled study of water-table and soil moisture dynamics for GDEs. The understanding of the dynamics of such ecosystems requires the development of a process-based quantitative framework relating water table and soil moisture dynamics to the random character of the rainfall regime, the vegetation type (e.g., root profile, water tolerance, root uptake strategies, plant-water relations), and the soil physical properties (e.g., storage capacity, hydraulic properties).

In the case of GDEs, the presence of the water table interacting with the rainfall regime, vegetation, and regional water bodies, makes the problem much more challenging than in the case of WCEs. *Rodriguez-Iturbe et al.* (2007) highlighted how the relatively new field of humid land ecohydrology would need to develop new theoretical frameworks for the study of the water balance in the presence of a shallow water table, with explicit consideration of the stochasticity of the involved processes.

Quantitative methods for the study of the stochastic water balance in humid land ecosystems could enable new and important research avenues in ecohydrology, for example providing a framework to understand the role of wetlands as filters for contaminated streams and aquifers and to investigate how hydrologic processes affect ecosystem productivity, the emergence of plant water stress, interspecies competition, the stability and resilience of wetland plant communities, and the complexity and nonlinearity of vegetation successional dynamics.

The probability distributions of the position of the water table and the soil moisture content for soil layers at different depths in the unsaturated zone are crucially important for the understanding of the ecohydrology of regions with shallow water table and humid lands.

Interactions between precipitation, soil water content and vegetation in water-controlled ecosystems have been studied in the recent past within the ecohydrology framework proposed by *Rodriguez-Iturbe et al.* (1999a). This

process-based approach that has been partially discussed in the previous chapter, accounts for the random character of precipitation within simple models of soil moisture dynamics (see, e.g., *Laio et al.*, 2001b; *Porporato et al.*, 2001; *Laio*, 2006). This theoretical approach for the study of probabilistic dynamics of soil moisture have been applied to a variety of arid and semiarid ecosystems (e.g., *Rodriguez-Iturbe and Porporato*, 2004) characterized by scarce rainfall, relatively low average soil water content, recurrent water stress, and absence of a shallow water table, where groundwater does not exert any influence on the soil water balance.

In the case of GDEs, the water table is fundamental in supplying water to plants, and it interacts directly with the root zone. Then it is fundamental to consider the strong coupling between rainfall, vegetation, water table position and soil water content and all the important feedbacks between hydrological and ecosystem processes (see *Ridolfi et al.,* 2006; *Rodriguez-Iturbe et al.*, 2007). In particular, water table and capillary rise play an active role in the subsurface water balance.

Before the challenging approach proposed by *Rodriguez-Iturbe et al.* (2007), a large number of researches dealt with the study of the interactions between plants and the stochastic dynamics of soil moisture. *Salvucci and Entekhabi* (1994) studied numerically the fluxes and moisture states at different timescales and for different water table positions, testing the reliability of an equivalent steady profile of soil moisture. In a different work, the same authors (*Salvucci and Entekhabi*, 1995) investigated the coupled unsaturated-saturated flows throughout a hillslope. *Bierkens* (1998) investigated the water table dynamics introducing also an additive Gaussian noise term to consider the environmental randomness, while *Kim et al.* (1999) used a mixed analytical-numerical approach to investigate soil moisture patterns along a hillslope.

The first attempt to study these interactions by means of an analytical approach for the calculation of the probability distributions of soil moisture and water table depth is probably attributable to *Ridolfi et al.* (2008) that have recently developed a probabilistic framework to investigate the coupled soil moisture–water table dynamics in the case of bare soil conditions.

In two very recent works, *Laio et al.* (2009) and *Tamea et al.* (2009) proposed a process-based probabilistic model for the study of water table depth and soil moisture dynamics, respectively, in the case of presence of vegetation having root apparatus interacting with saturated and unsaturated zones.

4.4 A model for the study of stochastic water table and soil moisture dynamics in groundwater dependent ecosystems

4.4.1 Modelling below-ground water table dynamics

In this section the model proposed by *Laio et al.* (2009) is discussed recalling all the basic concepts and assumptions of the original papers. This framework is based on the soil water balance equation forced by stochastic precipitation.

This new process-based ecohydrological framework accounts for water table fluctuations, capillary rise, vertical distribution of soil moisture, and the complex mechanisms of plant water uptake. The water balance equation is explicitly solved at each infinitesimal horizontal soil layer by accounting for rainfall infiltration, water table recharge, plant water uptake, capillary rise, groundwater flow, and the coupling between water table fluctuations and soil moisture dynamics in the unsaturated portion of the soil column.

It is important to point out that this model does not allow to investigate all the potential positions that the water table can reach but only those below the soil surface. A more detailed model that accounts also for above ground water table positions is currently under development by the same authors.

The model for below ground water table fluctuations was also object of an application in the Florida Everglades to test its potentialities. At the end of this chapter this application will be deeply discussed.

4.4.1.1 Water balance equation

The system under analysis considers an infinitely deep soil column and use an upward oriented vertical axis, z, with $z = 0$ at the ground surface (Figure 4.1). Another important hypothesis is that soil properties such as effective porosity, n, grain size distribution, and water retention curves, are assumed uniform in space and constant in time. The horizontal area of interest is the plot scale (e.g., 1–100 m^2) and is supposed to be reasonably flat. Local heterogeneities in soil and vegetation, topographic gradients and regional groundwater dynamics are neglected.

The water content existing at any point of the soil column is expressed in terms of soil moisture, s ($0 \leq s \leq 1$). The soil matric potential, ψ (negative), and unsaturated hydraulic conductivity, k, can be expressed as functions of the soil moisture s through the *Brooks and Corey* (1964) model, truncated at small values of hydraulic conductivity:

$$\psi_s(s) = \psi_s \cdot s^{-1/m} \tag{4.1}$$

$$k(s)=\begin{cases} k_s \cdot s^{(2+3m)/m} & if \quad s_{fc} < s \le 1 \\ 0 & if \quad s \le s_{fc} \end{cases} \tag{4.2}$$

where ψ_s is the (negative) air entry pressure head or saturated soil matric potential, m is the pore size index, s_{fc} is the soil moisture at field capacity, and k_s is the saturated hydraulic conductivity. Field capacity, s_{fc}, is operationally defined as the soil water content at which the unsaturated hydraulic conductivity becomes negligible if compared to other fluxes into the soil (see also *Laio et al.*, 2001b; *Laio*, 2006). In particular, the potential evapotranspiration rate, T_p is taken as a reference flux and then s_{fc} is defined considering the relation $k(s_{fc})=0.05T_p$, and then using the following relation:

$$s_{fc}=\left(\frac{0.05 \cdot T_p}{k_s}\right)^{\frac{m}{2+3m}} \tag{4.3}$$

According to the local water content, it is possible to identify three zones in the soil column: (1) the *saturated zone* (C in Figure 4.1), where all the soil pores are filled with water (i.e., $s = 1$); (2) the *unsaturated zone with high soil moisture* (HM zone - B in Figure 4.1)), where the water content is larger than field capacity (i.e., $s_{fc} \le s < 1$); and (3) the *unsaturated zone with low soil moisture* (LM zone - A in Figure 4.1)), where the water content is smaller than field capacity (i.e., $s < s_{fc}$).

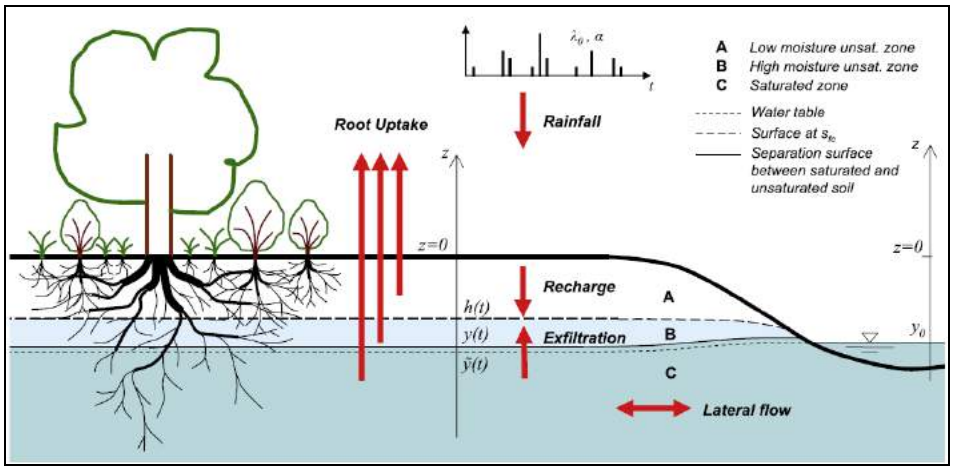

Figure 4.1: Scheme of the water fluxes in the soil column (from *Laio et al.*, 2009)

The HM zone is characterized by large values of the hydraulic conductivity, while in the LM zone, the hydraulic conductivity is assumed to be negligible, as in Eq.(4.2). The boundary between these zones is the layer at field capacity, found at a depth $h(t)$ from the soil surface (where t is time).

The water table, defined as the saturated soil surface at zero pressure, lays at depth $\tilde{y}(t)$ from the soil surface, variable in time t. The saturated capillary fringe is assumed to occupy a constant portion of soil above the water table, extending up to a distance from $\tilde{y}(t)$ equal to $|\psi_s|$. Thus the surface separating saturated and unsaturated soil lies at a depth $y(t)$ defined as:

$$y(t) = \tilde{y}(t) - \psi_s \tag{4.4}$$

where ψ_s is the (negative) bubbling pressure head, or saturated matric potential. Since the model does not account for soil submergence and it is limited at $y \leq 0$, the shallowest water table position which can be captured by the model lies at a depth $|\psi_s|$ from the soil surface.

The separation surface between saturated and unsaturated soil is of particular interest for the modeling scheme adopted (see Figure 4.1). In fact, according to *Laio et al.* (2009), it is mathematically convenient to model the dynamics of the water table by means of the variable $y(t)$ rather than by means of $\tilde{y}(t)$. The results corresponding to the water table position, $\tilde{y}(t)$, can then be obtained with the simple Eq.(4.4).

The water balance equation, relating the variations in time of the water table position to the incoming and outgoing fluxes, reads:

$$\beta \cdot \frac{d\tilde{y}(t)}{dt} = \beta \cdot \frac{dy(t)}{dt} = Re \pm f_l - U_s - Ex \tag{4.5}$$

where β, Re , f_l, U_s and Ex are the specific yield, the recharge rate, the lateral flow from/to an external water body, the root uptake from the saturated zone and the exfiltration from the water table due to the capillary flux, respectively (see Figure 4.1).

The variations in time of the water table position, and correspondingly of $y(t)$, are modulated by the specific yield, β, which is the ratio between the volume of water released from storage (per unit cross-sectional area of the aquifer) and the corresponding drop in water table elevation.

The effect of evaporation, which is small compared to transpiration when a dense vegetation cover is present, can be neglected and for this reason is not present in the water balance equation [Eq.(4.5)].

The model considers two different regimes: *shallow water table* (SWT) and *deep water table* (DWT), according to the position of y with respect to a critical depth, y_c. The regime SWT is characterized by the absence of the LM unsaturated zone and occurs when y is above y_c; otherwise the regime is that of DWT. The critical depth y_c, that will be discussed subsequently, marks then the transition between SWT conditions and DWT conditions.

In Figure 4.2 it is shown an example to better understand the role played by the various terms of the water balance equation in the dynamics of $y(t)$, and the factors contributing to the partitioning of the soil column into the saturated and unsaturated (HM and LM) zones. In particular it is shown the case of a soil column that reaches complete saturation (i.e., $y = 0$) during a rainfall event. At the initial time, $t = t_0$, when $y(t_0) = 0$, the rain stops and the soil starts to dry out. At this point the recharge rate tends to zero while root uptake, lateral flow, and exfiltration induce a water loss from the soil column; the upper soil layers start drying out, y decreases, and a nonuniform profile of soil moisture establishes. The shape of this profile is dictated by the balance between the capillary flux from the saturated zone, and root uptake from the high moisture zone, as detailed in next section. At a certain time $t = t_1$ soil moisture is still larger than s_{fc} in all layers. Thus, at this time there is no low moisture zone. At a subsequent time t_2 soil moisture is at field capacity at the ground surface [i.e., $s(0) = s_{fc}$] and $h(t_2) = 0$. Then, the critical depth, y_c at which $h(t) = 0$ marks the transition from the shallow water table (SWT) regime, for $y > y_c$, to the deep water table (DWT) regime, for $y \leq y_c$. If soil drying continues for $t > t_2$ the soil water content in the upper portion of the soil column achieves soil moisture values below field capacity and y is deeper than y_c. As a consequence, a low moisture zone is present in the soil column only under DWT conditions, that is only when $y > y_c$.

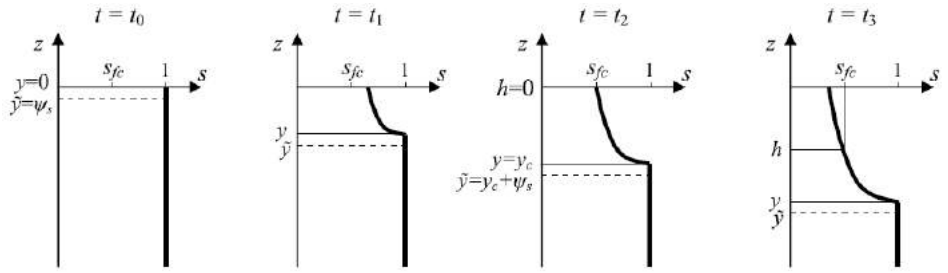

Figure 4.2: Schematic representation of the coupled water table and soil moisture dynamics in a soil drying phase (from *Laio et al.*, 2009)

4.4.1.2 Shallow Water Table regime

In this section the model specifications under SWT conditions are discussed, expressing the various terms of the water balance equation. Under shallow water table conditions, the water balance equation with respect to the (saturated/unsaturated zone) separation surface, y, can be written as:

$$\beta(y)\cdot\frac{dy(t)}{dt} = Re(t) \pm f_l(y) - U_s(y) - Ex(y) \tag{4.6}$$

where the specific yield, $\beta(y)$, depends on the water table position, and then on the depth y; $Re(t)$ is the recharge rate as a function of the time; while $f_l(y)$, $U_s(y)$ and $Ex(y)$ are the lateral flow (to or from an external water body), the plant water uptake from the saturated zone and the exfiltration flux due to capillary rise, respectively, and all are dependent on the water table position and then on the depth y.

The first component on the r.h.s. of the balance equation [Eq.(4.6)] is the *recharge rate* $Re(t)$. Groundwater recharge is the result of the processes of precipitation, infiltration and redistribution through the soil column. Rainfall is the main input of water into the soil column and it is here taken as a stochastic forcing and represented, at the daily timescale, as a marked Poisson process, $P(\lambda, \alpha)$, with rate λ and exponentially distributed rainfall depths with mean α [in the same manner of WCEs ecohydrological modelling discussed in the previous chapter, e.g., *Rodriguez-Iturbe et al.* (1999a); *Laio et al.* (2001b)]. Precipitation lost before infiltration includes canopy interception, which acts on rainfall as a threshold filter preserving the Poissonian nature of the forcing but reducing the frequency of the wetting events. The net rate is thus $\lambda_0 = \lambda e^{-\delta/\alpha}$, where δ is the threshold for canopy interception (*Rodriguez-Iturbe et al.*, 1999a).

Following *Laio* (2006) and *Botter et al.* (2007), the processes of infiltration and redistribution in the HM zone are modeled as a soil moisture wave propagating downward as a piston flow and are considered to occur instantaneously (at the daily timescale). In fact, according to the definition of SWT conditions, all soil layers are characterized by soil moisture values larger than s_{fc}. The high values of the unsaturated hydraulic conductivity [that can be found through Eq.(4.2)] characterizing most soils, together with the assumption of a daily timescale, allow one to assume that water redistribution within the HM zone occurs instantaneously and then all the rainfall events contribute to groundwater recharge. The same is also valid for fine-grained soil with a smaller hydraulic conductivity, where the instantaneous redistribution is

enabled by a field capacity close to saturation, which leads to small moisture gradients and quick redistribution within the HM zone (*Laio et al.*, 2009).

Under SWT conditions, groundwater recharge occurs then as a sequence of events that matches that of rainfall occurrences and it can be modeled as a Poisson process with rate λ_0 and exponential probability distribution of the recharge depths (with mean α):

$$Re(t) = P(\lambda_0, \alpha) \tag{4.7}$$

The second component on the r.h.s. of Eq.(4.6) is the *lateral flow* term that takes into account the presence of a nearby water body or a regional groundwater of fixed depth which may have a not negligible effect on the water table dynamics. Lateral flow depends on the relative position of the local water table, $\tilde{y}$, and the free surface of the external water body. Considering an external water body with level y_0 (Figure 4.1), relative to the soil surface elevation at the site under consideration, constant in time and at a distance large enough to assume for the water table to be horizontal at the same site, the lateral flow can be described as a linear relationship, similar to the Darcy's law:

$$f_l(y) = k_l \cdot (y_0 - y + \psi_s) \tag{4.8}$$

The lateral flow term then requires two parameters to be estimated: y_0 and k_l. The model parameter y_0 corresponds to the position of the free surface in the nearest water body, measured with respect to the soil surface, while k_l is the proportionality constant for the saturated lateral flow.

The scheme in Figure 4.3 shows the lateral flow that occurs from/to an external water body having a free water surface at depth y_0 and a distance d_0 from the area under analysis. The average lateral flow per unit width, Q_L, can be approximated by:

$$Q_L = \frac{k_s}{d_0}(y_0 - \tilde{y}) \cdot \left[h_0 - \frac{(y_0 - \tilde{y})}{2} \right] \tag{4.9}$$

where k_s is the saturated hydraulic conductivity, equal in all directions, and h_0 is the bedrock depth relative to the water body surface.

The corresponding rate of variation of the water table depth for the entire area can be obtained dividing Eq.(4.9) by the horizontal dimension D of that area. If the distance $(y_0 - \tilde{y})$ is negligible with respect to h_0, the lateral flow reads as in Eq.(4.8), with the parameter k_l defined as:

$$k_l = \frac{k_s \cdot h_0}{d_0 \cdot D} \tag{4.10}$$

The third term on the r.h.s. of the water balance equation [Eq.(4.6)] is the *plant water uptake* from the saturated and HM unsaturated zone, U_s. The mechanism of plant water uptake is a crucial point in the evaluation of groundwater-vegetation interactions. On the one hand, the vertical distribution of roots is influenced by water table dynamics, and on the other hand, root uptake decreases the soil water content and contributes to lower the water table position. Root growth strategies (*Naumburg et al.*, 2005) and plant resources allocation (e.g., *Ho et al.*, 2004) are strongly affected by the frequency and duration of flooding. For all these reasons, root functioning plays a key role on the ecohydrological dynamics of wetlands, and on the complex feedbacks between abiotic and biotic factors of such ecosystems.

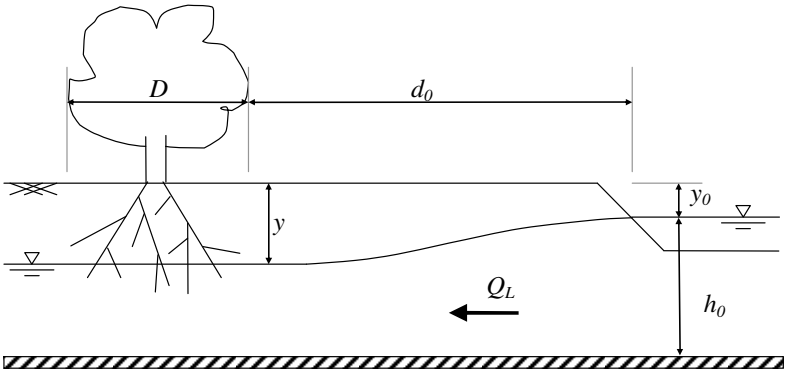

Figure 4.3: Schematic representation of the variables involved in the evaluation of the lateral flow term

The daily fluctuations of the water table positions can be partially be explained by the different use of water by the plants between the day and the night. During the day the water uptake driven by photosynthetic and physiological demand is more relevant than during the night and a significant local drop in water table position may occur. A partial recovery occurs at night due to groundwater redistribution, thereby inducing regular day-night water table fluctuations. Nevertheless, the model under consideration works at a daily timescale and then oscillations occurring at subdaily timescales are not resolved.

A general characteristic of humid land ecosystems is that prolonged flooded conditions may lead to plant water stress and anoxia, which can

ultimately result in the death of submerged roots. However, the plant species established in frequently submerged sites and wetlands may be well adapted to soil anoxic conditions and able to face long period with soil saturated by adopting different strategies to survive water-logging. For example they may have anaerobic metabolisms and may be able to increase oxygen provision to the roots (e.g., *Naumburg et al.*, 2005; *Vartapetian and Jackson*, 1997). The different strategies of water uptake and the different responses to anoxic conditions by vegetation depend on the plant species. For example, the non-specialized mesophytes, terrestrial plants usually present under moderate to hot and humid climatic regions that are adapted to neither a particularly dry nor particularly wet environment, take up water mostly from the shallower soil and then suffer water stress conditions if rainfall is highly intermittent. Phreatophytes typically consume groundwater and are more resistant to drought stress. Hydrophytes are typical in submerged wetlands and have roots well adapted to constantly flooded soils.

Despite, at the field scale, different species with different root allocation strategies cohabits, the model has been developed to work at a plot-scale to investigate the overall behavior of groundwater dependent ecosystems. As a consequence, *Laio et al.* (2009) made the following simplifying assumptions on the functioning of root uptake:

- the uptake flux is unaffected by anoxic (saturated) conditions in the soil and then no uptake-reduction function is applied for large values of soil moisture;
- roots in each soil layer is assumed to take up water independently of the others and do not compensate for limitations in transpiration and uptake, which may occur somewhere along the soil profile, then a non-cooperative root functioning is considered, which neglects any compensation mechanisms (see, e.g., *Guswa*, 2005, 2008);
- the plot-scale averaged root distribution can be represented through a simple function $r(z)$: in particular, following other authors (e.g., *Schenk and Jackson*, 2002; *Schenk*, 2005; *Laio*, 2006), an exponential distribution of the root biomass is considered in the model here discussed, and then

$$r(z) = \frac{1}{b} \cdot \exp\left(\frac{z}{b}\right) \tag{4.11}$$

where b is the average rooting depth.

Under these assumptions, plant water uptake from a soil layer at a depth, z, in the saturated or unsaturated high moisture zone is equal to the product of the maximum potential evapotranspiration, T_p, and $r(z)$. It is worth to note that, being the soil at (or very close to) saturated conditions, the maximum potential

evapotranspiration is controlled by atmospheric conditions, such as net solar irradiance, wind speed, air temperature, and humidity. As a consequence, the term of the water balance equation [Eq.(4.6)] denoting the total root uptake from the saturated zone under SWT condition, can be obtained as

$$U_s(y) = T_p \int_{-\infty}^{y} r(z)dz = T_p \cdot \exp\left(\frac{y}{b}\right) \tag{4.12}$$

The last term on the r.h.s of Eq.(4.6) is the *exfiltration*, which denotes the upward vertical flux of water from saturated to partially saturated soil layers due to capillary rise mechanisms. In the particular case of bare soil (i.e. absence of root uptake), the capillary flux is driven by differences in soil matric potential induced by evaporation (*Ridolfi et al.*, 2008). In the case of vegetated soils and then in the presence of root uptake the capillary flux is still driven by differences in soil matric potential in the soil layers, but now these differences are mainly induced by uptake rather than evaporation. Plant root apparatus take up water at different depths in the soil, depending on where roots are allocated, while evaporation acts only at the soil surface.

When a dense vegetation is present, evaporation can be neglected, because very low in respect to transpiration. The capillary flux, $\nu(z)$, varies as a function of z, due to water withdrawal by roots. To model the functional dependence of v on z, the water balance equation for an horizontal infinitesimal soil layer, dz, at a depth z, in the high moisture unsaturated zone, is here considered:

$$n \cdot \frac{\partial s_y(z,t)}{\partial t} = \frac{\partial \nu(z,t)}{\partial z} - T_p \cdot r(z) \tag{4.13}$$

where n is the soil porosity, $s_y(z, t)$ is the (y-dependent) soil water content in the HM unsaturated zone at time t, and $\partial \nu(z,t)/\partial z$ represents the difference between the capillary flux entering the layer at a depth z and exiting at the depth $z + dz$, at time t.

Under the assumption that, at the daily timescale, $s_y(z, t)$ varies slowly in time, responding to variations in y, it is possible to represent the dynamics of $s_y(z)$ and $\nu(z)$ as a sequence of stationary states, obtaining

$$\frac{\partial \nu(z)}{\partial z} - T_p \cdot r(z) = \frac{T_p}{b} \cdot \exp\left(\frac{z}{b}\right) \tag{4.14}$$

The assumption of negligible evaporation allows us to assume the boundary condition $\nu(0) = 0$. Then, after integrating between 0 and z, Eq.(4.14) reads $\nu(z) = T_p[1 - \exp(z/b)]$.

The exfiltration flux leaving the saturated zone, $Ex(y)$, is the capillary flux at depth y; then the term $Ex(y)$ in the water balance equation [Eq.(4.6)] and under SWT condition, can be obtained as

$$Ex(y) = T_p\left[1 - \exp\left(\frac{y}{b}\right)\right] \tag{4.15}$$

The last term of the water balance equation [Eq.(4.6)] to be discussed is the *specific yield*, β. The specific yield converts the volumetric variations of water in the aquifer into corresponding variations of the water table position and it is given by the ratio between the volume of water, V_w, an aquifer releases or takes into storage, per unit aquifer area, and the corresponding change in water table depth, Δ (*Freeze and Cherry*, 1979). The specific yield depends on soil properties and water table depth. In particular, with the aim to model the water table dynamics, it is convenient to consider the limit of the specific yield for infinitesimal variations of the water table depth:

$$\beta(y) = \lim_{\Delta \to 0} \frac{V_w}{\Delta} \tag{4.16}$$

In the evaluation of the specific yield, *Laio et al.* (2009) assumed that the profile evolves, at the daily scale, as a succession of instantaneous steady states neglecting the continuous time dependence in the dynamics of the soil moisture profile.

The volume V_w, released by an increase of water table depth, can be determined from the soil moisture profiles using the relation

$$V_w = n \cdot \left[\int_{s_{y+\Delta}(0)}^{1} z_{y+\Delta}(s)ds - \int_{s_y(0)}^{1} z_y(s)ds \right] \tag{4.17}$$

where $s_y(0)$ is the soil moisture content at the soil surface when the separation surface between saturated and unsaturated soil lays at depth y, and $z_y(s)$ is the soil moisture profile, expressed using the soil moisture content s as the independent variable, and z as the dependent variable. A Taylor expansion of $z_{y+\Delta}(s)$ around $\Delta = 0$, truncated to the first order, provides

$$z_{y+\Delta}(s) = z_y(s) + \frac{\partial z_y(s)}{\partial y}\Delta \tag{4.18}$$

Setting Eq.(4.18) in Eq.(4.17) and for $\Delta \to 0$, Eq.(4.16) becomes (*Laio et al.*, 2009):

$$\beta(y) = \lim_{\Delta \to 0} \frac{V_w}{\Delta} = n \cdot \int_{s_y(0)}^{1} \frac{\partial z_y(s)}{\partial y} ds \tag{4.19}$$

In order to obtain a suitable approximation of the soil moisture profile [i.e. $s(z)$ as a function of y], essential for the evaluation of the specific yield, it is possible to consider a steady state approximation of Richard's equation, with an additional sink term $T_p\, r(z)$ due to root uptake, that is:

$$\frac{\partial}{\partial z}\left[k(\psi)\left(\frac{\partial \psi}{\partial z} + 1 \right)\right] = T_p \cdot r(z) \tag{4.20}$$

Considering the exponential form of the root profile [Eq.(4.11)] and Eqs.(4.1) and (4.2), after integration between z and 0, Eq.(4.20) becomes:

$$-k_s s^{(2+3m)/m}\left(1 - \frac{ds}{dz}\frac{\psi_s}{m} s^{-(1+m)/m} \right) = T_p\left[1 - \exp\left(\frac{z}{b} \right)\right] \tag{4.21}$$

where the last term is the steady state, z-dependent, capillary flux, $v(z)$ and s = $s_y(z)$, i.e., the depth-dependent soil moisture in the HM unsaturated zone.

This equation cannot be solved analytically. In the model, *Laio et al.* (2009) used an approximated relation between s, z and y through the expression

$$s_y(z) = \left[1 + \left(s_{fc}^{-1/2m} - 1 \right)\left(\frac{y - z}{y_c} \right)\right]^{-2m} \tag{4.22}$$

In the paper by *Tamea et al.* (2009), that will be discussed later (Section 4.4.2), the suitability of this expression to represent the actual soil moisture profile is investigated. In particular, inverting Eq.(4.22), one can obtain z as a function of s for a given depth of water table position y:

$$z_y(s) = y - y_c\left(\frac{s^{-1/2m} - 1}{s_{fc}^{-1/2m} - 1}\right) \tag{4.23}$$

The specific yield as a function of the depth y, under SWT condition, can be then obtained through the following expression derived from Eq.(4.19), and considering that, in virtue of Eq.(4.23), $\partial z_y(s)/\partial y = 1$:

$$\beta(y) = n \cdot [1 - s_y(0)] = n - n \cdot \left[1 + \left(s_{fc}^{-1/2m} - 1\right)\left(\frac{y}{y_c}\right)\right]^{-2m} \tag{4.24}$$

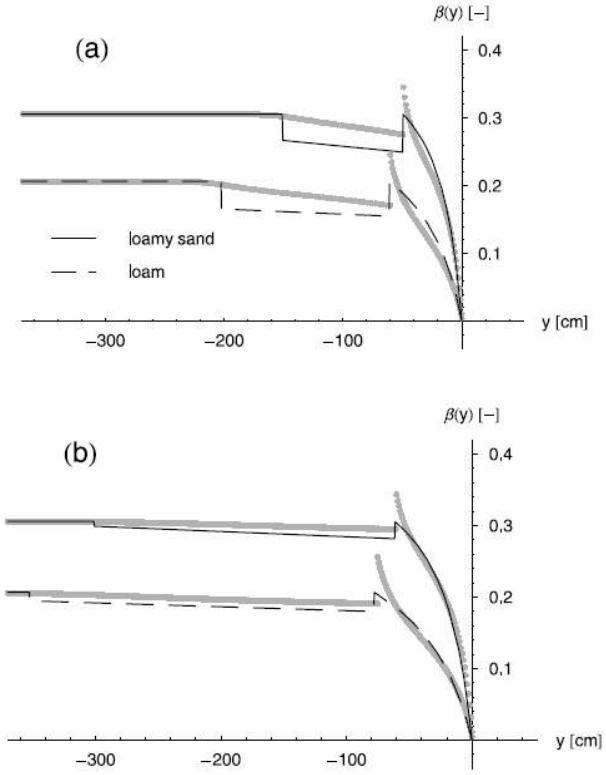

Figure 4.4: Specific yield, β, as a function of y in a loamy sand and a loam, for two mean root depths: (a) b = 10 cm and (b) b = 40 cm. Comparison between the numerical results (gray dots) and the approximations (continuous and dashed lines) presented in *Laio et al.* (2009)

Figure 4.4, from *Laio et al.* (2009), shows a representation of the specific yield, $\beta(y)$. In particular the part of the curves at the right of the critical depth ($y > y_c$) denote $\beta(y)$ obtained by Eq.(4.24). For $y \to 0$, the specific yield tends to zero because of the small storage capacity and high soil water content in the unsaturated zone when y approaches the soil surface.

4.4.1.3 Critical depth (y_c)

As already mentioned in previous sections, the critical depth, y_c, denotes that particular position of the separation surface between the saturated and unsaturated zones, marking the transition from shallow to deep water table conditions. The exact value of y_c should be obtained by integrating Eq.(4.21) and imposing the boundary condition $s(0) = s_{fc}$. Since no analytical solutions can be found, *Laio et al*. (2009) obtained a valid approximation, using in Eq.(4.21) a suitable z-independent rate of capillary flux, that is

$$\nu^* = \frac{T_p}{1 + c_0 b} = \frac{T_p}{1 + (0.35 - 0.65n)b} \tag{4.25}$$

Considering $\nu(z) = \nu^*$ (*Ridolfi et al.*, 2008), the solution of equation (4.21) gives the following expression

$$\begin{aligned} y_c = {} & \psi_s F_1\left[\frac{1}{2+3m}, 1, 1+\frac{1}{2+3m}, -\frac{\nu^*}{k_s} s_{fc}^{-(2+3m)/m}\right] \\ & - \psi_s F_1\left[\frac{1}{2+3m}, 1, 1+\frac{1}{2+3m}, -\frac{\nu^*}{k_s}\right] \end{aligned} \tag{4.26}$$

where F_1[a, b, c, x] is the hypergeometric function (*Abramowitz and Stegun*, 1965). Figure 4.5, from *Laio et al.* (2009), shows a comparison between the approximate solution and the numerical solution of equation (4.21), for different soil types and different values of the average rooting depth b. From this comparison it is possible to note that the approximate solution, given by Eq.(4.26), provides a very good approximation of the critical depth.

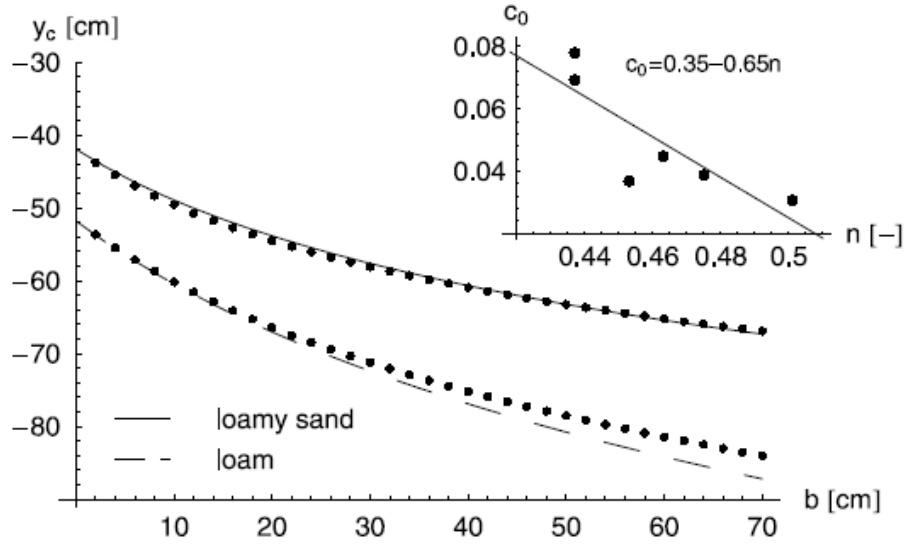

Figure 4.5: Comparison between the numerical solution (black dots) and the approximated solution (gray lines) given by Eq.(4.26). Critical depth, y_{cc} as a function of the mean root depth, b for a loamy sand and a loam. The functional dependence of ν^* on b is given by Eq.(4.25), where the parameter c_0 is correlated to the soil porosity n (after *Laio et al.*, 2009)

Figure 4.6, again taken from *Laio et al.* (2009), shows the variability of the critical depth y_c across different soils, represented in the USDA soil texture triangle (*Soil Conservation Service*, 1975). The figure shows that the critical depth tends to be larger in silty soils compared to sandy and clayey soils. Notice that in clayey soils, the pedotransfer functions between soil composition and hydraulic parameters are not valid (*Rawls and Brakensiek*, 1989) and, since these relationships have been used to create the plot shown in Figure 4.6b, the top part of the USGS triangle shows results of uncertain reliability, due to the extrapolation of hydraulic parameter values.

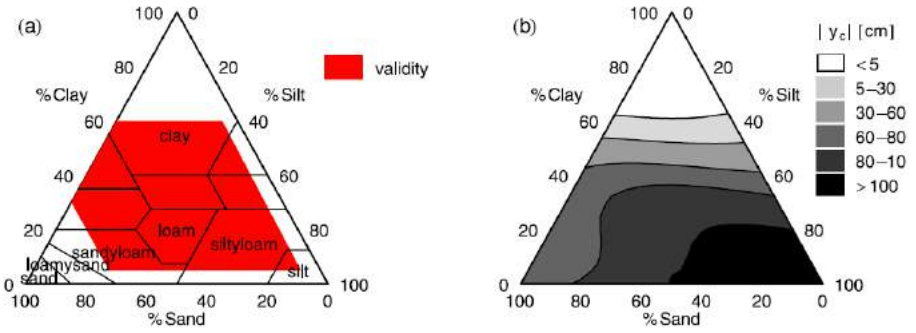

Figure 4.6: USDA soil texture triangle: (a) validity zone for the empirical pedotransfer functions relating soil hydraulic parameters and soil composition (see *Rawls and Brakensiek*, 1989), and (b) the critical depth, y_c, computed across different soils, for a mean root depth b of 30 cm (after *Laio et al.*, 2009)

4.4.1.4 Deep Water Table regime

Some of the terms of the water balance equation are different according on the regime under consideration. Under deep water table (DWT) conditions the water balance equation (4.5) can be expressed through the following relation

$$\beta(h,y)\cdot\frac{dy(t)}{dt}=Re(h,\bar{s}'_m,t)\pm f_l(y)-U_s(y)-Ex(h,y) \tag{4.27}$$

For the lateral flux and uptake terms evaluation, equations found in SWT conditions [Eqs.(4.8) and (4.12), respectively] are still valid, while the rates of recharge, exfiltration and the specific yield need to be expressed differently.

In the case of DWT not all rain events are actually able to reach the high moisture zone. Under the hypothesis of instantaneous redistribution in the low moisture zone, supported by numerical simulations (*Laio*, 2006), each rain event generates a wetting front which separates soil layers whose water content, s, is supposed (at the daily timescale) to instantaneously reach field capacity from layers which remain unaffected. The wetting front reaches a depth that depends on the rain depth and on the soil moisture content before the event. Only the rain events generating a wetting front that reaches the top of the HM zone, contribute to recharge the groundwater. In the HM unsaturated zone $s \geq s_{fc}$, and then the incoming water is instantaneously drained toward deeper layers. The sequence of these recharge events is stochastic due to the random nature of rainfall. Although in general this sequence is non-Poissonian, *Laio* (2006)

showed that if one assumes that all rainfall events find the same average soil moisture content, $\bar{s}'_m(h)$, in the LM zone, the recharge process retains the Poissonian properties of rainfall occurrences. Under this assumption, the recharge rate does not depend on the fluctuations of $s(z)$ but only on the local long-term average values.

Denoting with $\bar{s}'(z)$ the long-term average of the soil moisture content in the layer at a depth z, conditional upon $s < s_{fc}$ (because the occurrence of recharge events depends only on the soil water content above $z = h$), the local long-term average content in LM unsaturated zone, $\bar{s}'_m(h)$, can be found as

$$\bar{s}'_m(h) = -\frac{1}{h}\int_h^0 \bar{s}'(z)dz \tag{4.28}$$

In this case the water storage capacity in the soil column above h depends on h but not on $s(z)$ and it is equal to $-nh\left[s_{fc} - \bar{s}'_m(h)\right]$.

As a consequence, the sequence of recharge events remains Poissonian (*Laio*, 2006) and its rate can be determined as in the case of canopy interception:

$$\lambda\left[h, \bar{s}'_m(h)\right] = \lambda_0 \exp\left[\frac{nh\left(s_{fc} - \bar{s}'_m(h)\right)}{\alpha}\right] \tag{4.29}$$

where the recharge depths is exponentially distributed with mean α. The recharge rate is then

$$Re\left(h, \bar{s}'_m(h), t\right) = P\left(\lambda\left[h, \bar{s}'_m(h)\right], \alpha\right) \tag{4.30}$$

Under DWT conditions, the water table dynamics depend on the soil water content in the low moisture zone through the long-term average soil moisture $\bar{s}'_m(h)$. The water table dynamics are then also related to the soil moisture dynamics in the overlying layers. The vertical profile of average soil moisture in the LM zone is, in turn, related to the local climate (precipitation and potential evapotranspiration) and to the vertical distribution of roots (e.g., *Laio et al.*, 2006). All these soil moisture dynamics are investigated in *Tamea et al.*, (2009), where it is also provided a suitable representation of $\bar{s}'_m(h)$ for the case of vegetation with an exponential distribution of the root biomass.

It is also important to point out that, while $\bar{s}'_m(h)$ affects y through the recharge rate, y does not affect the dynamics of soil moisture in the LM zone. An important model assumption is, in fact, that the capillary flux through the surface at depth $z = h$ is negligible compared to the other fluxes occurring where $s \leq s_{fc}$, and for this reason the surface separating the LM and HM unsaturated zones at depth h is called *zero-flux surface*. With this assumption, the LM zone can be considered as a stand-alone system, not related to the HM zone below it. Thus, soil moisture dynamics in the LM zone can be studied as in the case of water-limited ecosystems (e.g., *Laio et al.*, 2001b; *Laio*, 2006), without considering the presence of the water table.

In order to determine the exfiltration in DWT conditions an approach similar to that used in the case of SWT conditions is considered, taking into account the water balance equation for an infinitesimal soil layer in the HM unsaturated zone. The capillary flux at the generic depth z in the HM zone can be obtained by integrating equation (4.14) from h to z:

$$\nu(z) = T_p \cdot \left[\exp\left(\frac{h}{b}\right) - \exp\left(\frac{z}{b}\right) \right] \tag{4.31}$$

Assuming that the hydraulic conductivity for $s < s_{fc}$ (i.e. above h) is null [see Eq.(4.2) and Sect. 4.4.1.1], it is possible to impose the boundary condition $\nu(h) = 0$. The overall exfiltration flux out of the saturated zone is then given by

$$Ex(h, y) = \nu(y) = T_p \cdot \left[\exp\left(\frac{h}{b}\right) - \exp\left(\frac{y}{b}\right) \right] \tag{4.32}$$

The depth h represents the threshold above which the water table exerts no influence on the local soil water balance. The depths y and h represent the lower and upper boundary of the high moisture unsaturated zone, respectively. The soil moisture profile in the HM zone, $s_y(z)$, should be obtained integrating Eq.(4.21), considering Eq.(4.31) and the boundary condition $s_y(h) = s_{fc}$, while the corresponding depth of the separation surface, y, should be determined by setting $s_y(y) = 1$. However, this procedure to establish the relation between y and h, does not lend itself to analytical solutions. *Laio et al.* (2009) proposed a stepwise function to approximate the relation $h(y)$:

$$h(y)=\begin{cases} 0 & \rightarrow if \quad y \geq y_c \\ (1-A^{3/4})(y-y_c)-\dfrac{A^2(1-A^{-1/4})}{-y_c+\psi_{fc}-\psi_s}(y-y_c)^2 & \rightarrow if -5b+\psi_{fc}-\psi_s \leq y \leq y_c \\ -y_c+\psi_{fc}-\psi_s & \rightarrow if \quad y<-5b+\psi_{fc}-\psi_s \end{cases} \quad (4.33)$$

where $\psi_{fc}=\psi_s \cdot s_{fc}^{-1/m}$ and

$$A=\frac{\psi_{fc}-\psi_s-y_c}{\psi_{fc}-\psi_s-y_c-5b} \quad (4.34)$$

Note that, when the root density declines to zero and then *h* is much deeper than *b*, the distance between *h* and *y* remains constant and equal to $\psi_s-\psi_{fc}$. Figure 4.7, from *Laio et al.* (2009), shows a comparison between the approximated solution [Eq.(4.33)] and the numerical one for different soils and values of *b*. It is possible to note that for the deeper values of *h* (i.e. below the bulk of the root zone $\psi_{fc}-\psi_s-5b$), the value of (*h*–*y*) remains constant as a consequence of the fact that at such depths the soil moisture profile approaches the zero-flux profile.

Also for the evaluation of the specific yield in DWT conditions, the model approach is analogous to the one used for the case of SWT. In the case of DWT regime, the specific yield can be obtained by the following expression:

$$\beta(y,h)=\frac{n}{\Delta}\int_{s_{fc}}^{1}\left[z_{y+\Delta}(s)-z_y(s)\right]ds=n\cdot\int_{s_{fc}}^{1}\frac{\partial z_y(s)}{\partial y}ds \quad (4.35)$$

where the term on the right hand side results from the Taylor's expansion of $z_{y+\Delta}(s)$ around Δ truncated to the first order.

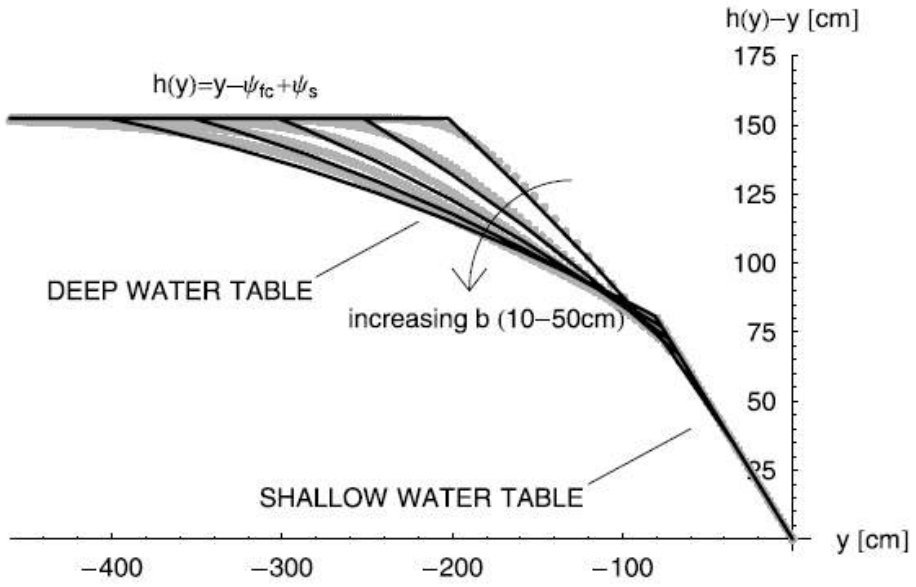

Figure 4.7: Comparison between the numerical solution of the Richard's equation for the HM unsaturated zone (gray dots), and the approximation given in Eq.(4.33) (continuous lines). Height of the HM zone, (h–y), as a function of the position of the separation surface between saturated and unsaturated zones, y, in a loamy soil and for various mean root depths: b = 10, 20, 30, 40 and 50 cm (after *Laio et al.*, 2009)

Similarly to Eq.(4.22), the soil moisture profile in the HM unsaturated zone can be represented through the following equation:

$$s_y(z) = \left[1 + \left(s_{fc}^{-1/2m} - 1\right)\left(\frac{y-z}{y-h}\right)\right]^{-2m} \tag{4.36}$$

The suitability of this expression to represent the actual soil moisture profile has been investigated in detail by *Tamea et al.* (2009). The inversion of this equation leads to

$$z_y(s) = y - (y-h)\left(\frac{s^{-1/2m} - 1}{s_{fc}^{-1/2m} - 1}\right) \tag{4.37}$$

this implies

$$\frac{\partial z_y(s)}{\partial y} = 1 - (y-h)\left(\frac{s^{-1/2m}-1}{s_{fc}^{-1/2m}-1}\right) \tag{4.38}$$

Thus, the equation representing the specific yield in DWT conditions that can be obtained by setting Eq.(4.38) in equation (4.35) reads

$$\begin{aligned}\beta(y,h) &= n(1-s_{fc}) + n\left(\frac{dh}{dy}-1\right)\cdot\int_{s_{fc}}^{1}\frac{s^{-1/2m}-1}{s_{fc}^{-1/2m}-1}ds = \\ &= n(1-s_{fc}) + n\left(\frac{dh}{dy}-1\right)\cdot B\end{aligned} \tag{4.39}$$

where the coefficient B is equal to

$$B = \frac{1}{1-2m}\left(\frac{1-s_{fc}}{1-s_{fc}^{1/2m}} + 2\cdot m\cdot s_{fc}\right) \tag{4.40}$$

The results obtained with equation (4.39), compared to those obtained with the numerical simulations of the Richard's equation, are shown in Figure 4.4 (Sect. 4.4.1.2). Note that the figure shows two discontinuities: for $-5b+\psi_{fc}-\psi_s \le y \le y_c$, the specific yield, $\beta(y, h)$, tends to slightly decrease as y tends to y_c, with a jump at $y = -5b+\psi_{fc}-\psi_s$ due to the approximation of $h(y)$ with a function with discontinuous derivative (Eq.(4.33)); at the critical depth $y = y_c$, the specific yield has another discontinuity due to the abrupt change in the derivative of $Ex(y)$ [see Eqs.(4.15) and (4.32)] at the transition from DWT to SWT regimes.

4.4.1.5 Probability distribution of the water table depth

The model proposed by *Laio et al.* (2009) and here described, provides the stationary probability density function of the position y of the surface marking the separation between saturated and unsaturated soil. It is possible to rewrite the soil water balance equation as

$$\frac{dy}{dt} = f(y) + g(y) \cdot \xi(y,t) \tag{4.41}$$

where the terms $f(y)$, $g(y)$ and $\xi(y)$ are respectively:

$$f(y) = \begin{cases} \dfrac{k_l\left(y_0 - y - \psi_s\right) - T_p}{\beta(y)} & \longrightarrow \quad SWT \\ \dfrac{k_l\left(y_0 - y - \psi_s\right) - T_p \cdot e^{h(y)/b}}{\beta(y)} & \longrightarrow \quad DWT \end{cases}$$

$$g(y) = \frac{1}{\beta(y)} \tag{4.42}$$

$$\xi(y,t) = \begin{cases} P\left(\lambda_0, \alpha\right) & \longrightarrow \quad SWT \\ P\left(\lambda_0 \cdot \exp\left[\dfrac{n \cdot h(y) \cdot \left[s_{fc} - \bar{s}_m^{'}(h(y))\right]}{\alpha}\right], \alpha\right) & \longrightarrow \quad DWT \end{cases}$$

The above stepwise continuous first-order stochastic differential equation can be solved under steady state conditions. The solution for state-dependent noise with rate $\lambda(y)$ and average $\alpha\lambda(y)$, the resulting pdf of y is given by *D'Odorico et al.* (2004) and *Porporato et al*. (2004), and reads:

$$p_Y(y) = \frac{C}{f(y)} \cdot \exp\left[-\int_0^y \frac{f(u) + \alpha \cdot \lambda(u) \cdot g(u)}{\alpha \cdot g(y) \cdot f(u)} du\right] \tag{4.43}$$

where C is a normalization constant obtained by setting $\int_{-\infty}^{0} p_y(y)dy = 1$. The probability density function of the water table depth, $\tilde{y}$, is obtained with a simple translation, and reads:

$$p_{\tilde{Y}}(\tilde{y}) = p_Y(\tilde{y} - \psi_s) \tag{4.44}$$

The *pdf* of *y* [Eq.(4.43)] ranges from the soil surface, where the probability goes to zero, to the lower bound, y_{lim}, representing the deepest position allowed by the system: this can be computed from the steady state water balance in the absence of rainfall (*Laio et al.*, 2009), i.e. $f_l(y_{\lim}) = U_s(y_{\lim}) + Ex(y_{\lim})$. As a consequence of these bounds, the *pdf* of the water table position ranges from ψ_s to $\tilde{y}_{lim}$ (equal to y_{lim} - ψ_s). It is important to point out that ponding conditions are not allowed.

Once the pdf, $p_Y(y)$, has been determined, the pdf of *h* can be obtained as a derived distribution of $p_Y(y)$ through the relation

$$p_h(h) = p_Y\left[y(h)\right] \cdot \left(\frac{dh}{dy}\right)^{-1} \tag{4.44}$$

with $y(h)$ obtained by inverting Eq.(4.33). An atom of probability, corresponding to the probability of being in SWT conditions, appears in the distribution at h= 0, with associated mass, $P_{h,0}$, i.e., $P_{h,0} = \int_{y_c}^{0} p_y(y)dy$

Figure 4.8 shows the results found by *Laio et al.* (2009) of the investigation on the dependence of the water table depth on the soil type. Soil parameters affect all the components of the water balance, which, in turn, have a strong impact on the probability density function of water table depth. In particular, the water table is closer to the soil surface in a loam than in a loamy sand. In Figure 4.8a it is also shown a comparison between the analytical curves obtained using Eq.(4.44), and the numerical solutions of the water balance equation, obtained determining the numerical profile of soil moisture in the HM unsaturated zone [through Eqs.(4.21) and (4.32)], and numerically determining the corresponding specific yield [by Eq.(4.19) under SWT conditions and Eq.(4.35) under DWT conditions], the $h(y)$ relation, and the value of the critical depth, y_c, without resorting to analytical approximations of the vertical profile of soil moisture, and without assuming a constant equivalent capillary flux, ν^*.

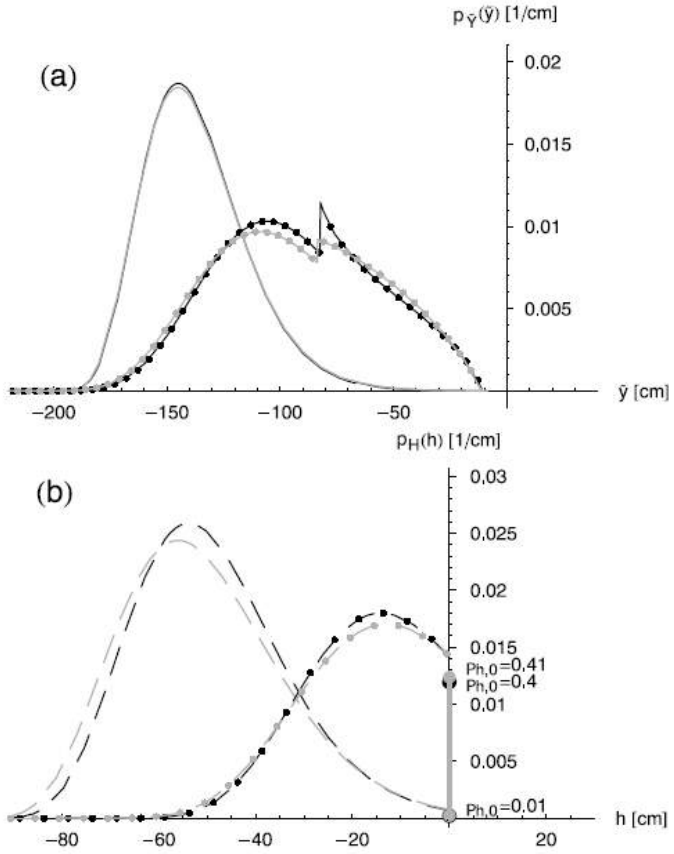

Figure 4.8: Probability density function of (a) the water table depth, $\tilde{y}$, and (b) the zero-flux surface, h, for a loamy sand (no markers) and a loam (with markers), according to *Rawls et al.* (1983) soil parameters. Other parameters are as follows: λ_0= 0.3 d^{-1}, α = 2 cm, T_p = 0.5 cm/d, b = 30 cm, y_0 = -200 cm, k_l = 3.7 10^{-3} d^{-1} (loamy sand) and k_l = 7.9 10^{-4} d^{-1} (loam). Black lines are obtained by using Eq.(4.44), and gray lines are results from numerical solutions (after *Laio et al.*, 2009)

Figure 4.8b shows clearly that the pdf of the position of zero-flux surface, h, follows a similar pattern as the pdf of the water table depth, $\tilde{y}$ (Figure 4.8a).

In Figure 4.9 are reported the results relative to another analysis of the dependence of the water table dynamics on soil texture. In particular this analysis by *Laio et al.* (2009) has been carried out by considering the mean and the coefficient of variation of $\tilde{y}$. The used soil hydraulic parameters, were calculated using the pedotransfer functions provided by *Rawls and Brakensiek* (1989), valid in the range shown in Figure 4.6a. From Figure 4.9a it is possible

to note that the mean position of the water table is deeper in sandy and clayey soils, as a consequence of the fact that sandy soils present high values of specific yield while clays present low values of hydraulic conductivity. Figure 4.9b shows the behavior of the coefficient of variation of $\tilde{y}$. It results much smaller in sands due to smaller water table fluctuations in coarse-grained soil and higher volume of water required for a unit change in depth. Notice that, analogously to the case of Figure 4.6, the top part of the triangle has an uncertain reliability, due to the extrapolation of hydraulic parameter values.

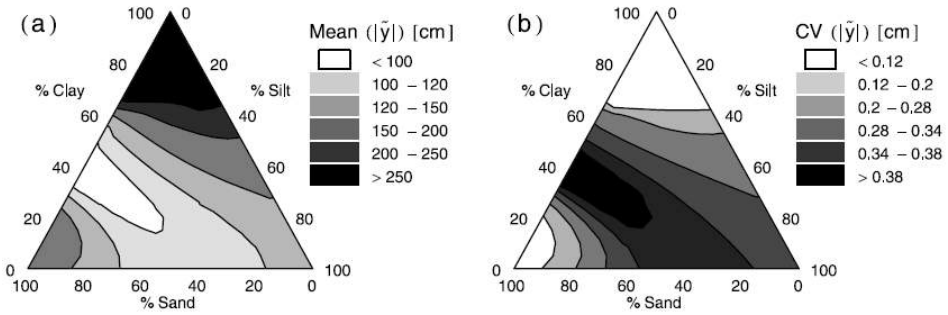

Figure 4.9: Behavior of the mean (a) and the coefficient of variation (b) of the pdf of the water table depth, $\tilde{y}$, throughout the USDA soil texture triangle. Soil parameters have been estimated with the pedotransfer function given by *Rawls and Brakensiek* (1989), while the other model parameters are as in Figure 4.8 (from *Laio et al.*, 2009)

In Figure 4.10 are reported the results of an investigation by *Laio et al.* (2009), on the effects of different climate conditions on the pdf of the water table position, $\tilde{y}$. For very dry conditions the water table depth has little variability, with values comparable to the stage of the external water body (y_0). The zero-flux surface fluctuations are very weak and plant roots remains in the LM unsaturated zone for most of the time. Then, under dry conditions, the stochastic models developed for the case of water-controlled ecosystems (e.g., *Rodriguez-Iturbe et al.*, 1999a; *Laio*, 2006) may be applied without substantial modifications. As the frequency of rainfall events, λ_0, increases, both the pdf's of the water table depth, $\tilde{y}$, and the zero-flux surface, h, results shifted toward lower depths, but they maintain a rather low dispersion around the central values (left panels in Figure 4.10). In contrast, with increasing average intensity of the rain events, α, the variability of the water table position results strongly enhanced (right panels in Figure 4.10).

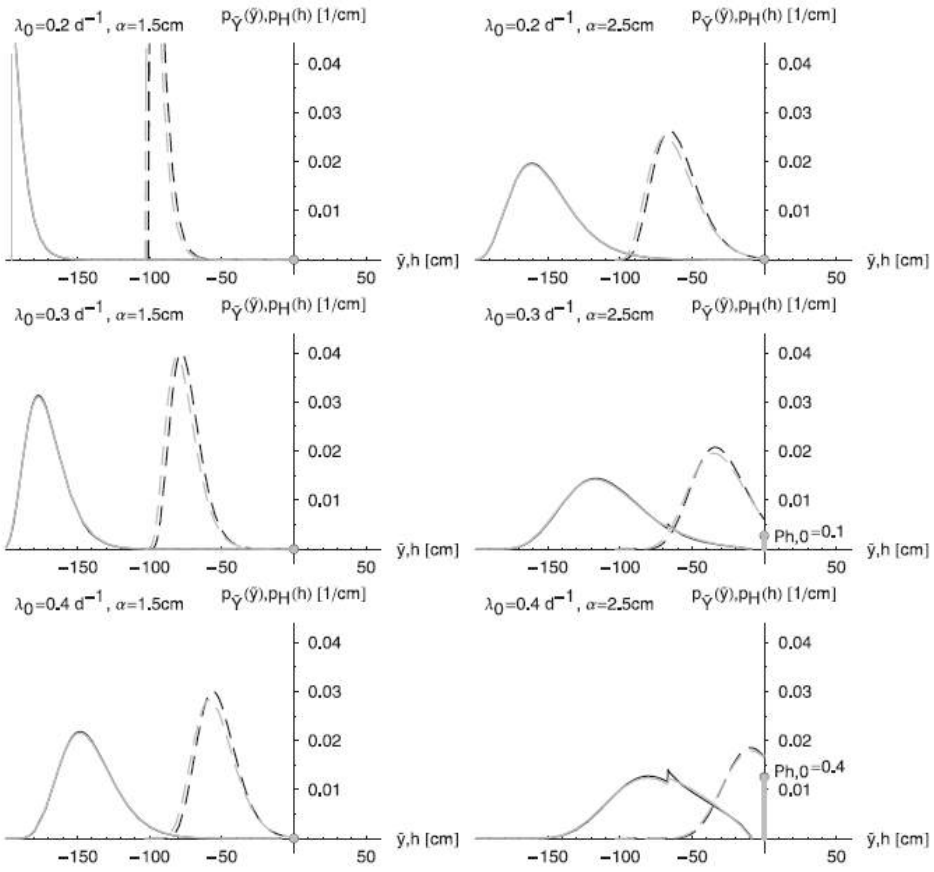

Figure 4.10: Pdf's of the water table depth, $\tilde{y}$ (solid line), and the zero-flux surface, h (dashed line), for a loamy sand under different climatic conditions: λ_0 = 0.2–0.3–0.4 d^{-1}; α = 1.5–2.5 cm. Other model parameters are as in Figure 4.8. The gray lines correspond to the exact numerical solution, while the black ones correspond to the analytical approximations (from *Laio et al.*, 2009)

Another important factor affecting the pdf of the water table depth is the plant rooting depth. Figure 4.11, from *Laio et al.* (2009), shows the results of the analysis of the impact of different mean rooting depths, b, on the pdf of $\tilde{y}$. In particular two types of vegetation are considered: herbaceous (b = 10, i.e., 95% of roots in the top 30 cm below the ground) and hardwood (b = 40, i.e., 95% of roots in the top 120 cm). Obviously deep rooted vegetation takes up more water from the saturated zone, than shallow rooted plants. Since deeper rooting systems are associated with higher fractions of transpiration contributed by the saturated zone, the resulting water table position is deeper.

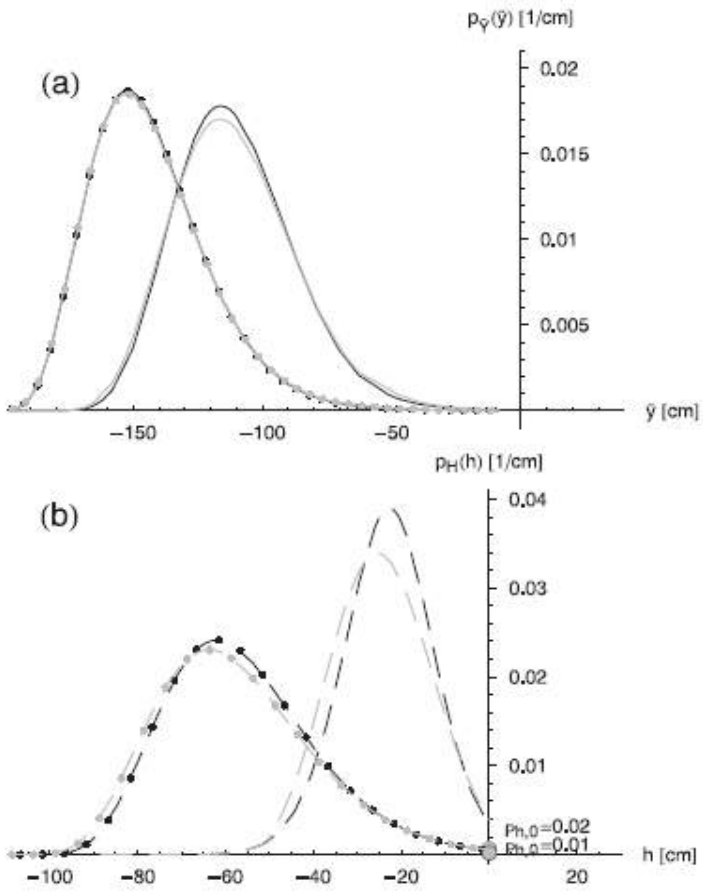

Figure 4.11: Comparison between the pdf's of the water table depth, $\tilde{y}$, (a) and the zero-flux surface, h, (b) for a shallow rooted vegetation (b = 10 cm, no markers) and a deep rooted vegetation (b = 40 cm, with markers). The soil is a loamy sand, and the other model parameters are as in Figure 4.8 (from *Laio et al.*, 2009)

4.4.2 Modelling soil moisture dynamics

The distribution of moisture along the soil column controls most of the hydrological and ecological processes occurring on the earth surface and in the shallow subsurface. In groundwater dependent ecosystems, the dynamics of soil moisture are strongly coupled to the water table fluctuations and, together, they control the overall ecosystem dynamics (*Rodriguez-Iturbe et al.*, 2007). The

coupling between water table and soil moisture dynamics is mainly due to the dependence of the processes of redistribution/percolation/groundwater recharge, and capillary flux (from the water table to the overlying soil) on the soil moisture

Tamea et al. (2009) proposed a simple process-based stochastic model for the study of soil moisture dynamics at a generic depth, to complement the stochastic model for the study of water table fluctuations, presented in the companion paper by *Laio et al.* (2009) and discussed above (Sect. 4.4.1). This model is based on a local, depth-dependent water balance driven by stochastic rainfall, modeled again as a marked Poissonian noise.

The model provides a semi-analytical formulation of the stationary probability distribution of soil water content at different depths. It focus on environments with shallow water tables (below-ground), where the groundwater plays a key role in the soil water balance of the root zone, and where strong interactions between climate, groundwater, soil moisture and vegetation exist. The model provides an important tool to investigate the dependence of soil moisture dynamics on stochastic rainfall and water table fluctuations.

In the past other different works have focused on groundwater-soil moisture interactions, associated to capillary flux and moisture redistribution (e.g., *Eagleson*, 1978; *Salvucci*, 1993) through deterministic models which do not account for the stochastic nature of rainfall nor for the role of plant root uptake. Similarly to the model for the water table depth presented before, the model by *Tamea et al.* (2009) here discussed is a consequential prosecution of the framework by *Ridolfi et al.* (2008), that proposed a stochastic model for soil moisture-water table dynamics in the case of bare soil.

4.4.2.1 Soil moisture profiles in the HM and LM unsaturated zones

The model proposed by *Tamea et al.* (2009) considers some assumptions as in the work of *Laio et al.* (2009) presented in Sect. 4.4.1: the horizontal area of interest is the plot scale, considered reasonably flat; local heterogeneities are negligible and topographic gradients are absent; at the plot scale, the overall amount of root biomass assumed exponentially distributed, with mean b; the vertical root profile is assumed constant in time and mechanism such as biomass growth and reallocation are not taken into account.

Considering again an axis z upward oriented, the system under consideration is constituted by a soil column extending from the soil surface ($z = 0$) to an indefinite (large) depth. Effective porosity, n, grain size distribution, m, saturated matric potential, ψ_s, and saturated hydraulic conductivity k_s, are supposed to be uniform in space and constant in time.

The soil water content is expressed as a function of the depth and time, $s(z,t)$, and varies from 0 to 1. Soil matric potential, ψ, and the unsaturated hydraulic conductivity, k, are related to the soil moisture through the *Brooks and Corey* (1964) model, truncated at small values of the hydraulic conductivity [Eqs.(4.1) and (4.2)].

Operationally, the soil moisture content at field capacity, s_{fc}, is defined as the value of soil moisture at which the unsaturated hydraulic conductivity becomes small (e.g., 5%) compared to the daily rate of potential evapotranspiration [Eq.(4.3)].

As in the model for the water table depths, the soil column can be seen as split into three zones according to the local degree of saturation (see Figure 4.12, left): (1) the saturated zone (i.e., s =1), (2) the high-moisture (HM) unsaturated zone, (i.e., $s_{fc} \leq s < 1$), and (3) the low-moisture (LM) unsaturated zone (i.e., $s < s_{fc}$). The surface separating saturated and unsaturated soil lays at depth $y(t)$ (where t is time) from the soil surface and has a soil matric potential equal to ψ_s. The surface at zero pressure, i.e., the water table, lays at constant distance $|\psi_s|$ from $y(t)$ [at a depth given by Eq.(4.4)].

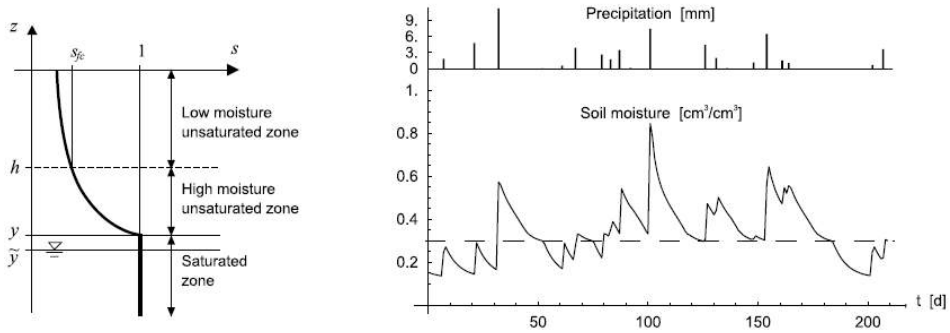

Figure 4.12: Representation of the soil moisture profile along the low-moisture, high-moisture, and saturated zones for a soil column (left). Time series of daily soil moisture dynamics (right bottom) in a fixed soil layer, with (right top) corresponding rainfall events (after *Tamea et al*., 2009)

In the HM unsaturated zone, the soil water content arises from the balance of rainfall infiltration/redistribution, plant root uptake, and capillary flux from the saturated zone. The soil moisture in the LM zone is smaller ($s < s_{fc}$) and the hydraulic conductivity may be assumed negligible. For this reason, it is possible to assume that the upward capillary flux never reaches the LM zone, but it ceases in correspondence of the zero-flux surface, at a depth $h(y, t)$, where the soil moisture is equal to s_{fc}. The zero-flux surface then marks the upper limit of groundwater influence on the soil water balance, and the soil moisture dynamics

in the LM zone can be considered independent of the presence of the water table.

As in the model described in Sect. 4.4.1, it is possible to distinguish between two different regimes: the case of shallow water table (SWT) conditions (i.e., there is no low-moisture zone and $s > s_{fc}$ in the entire soil column) and the case of deep water table (DWT) conditions [i.e., whenever all the three zones (LM/HM unsaturated and saturated) are presents]. The critical depth, y_c, marking the transition between the two regimes can be found again by Eq.(4.26). Then if the separation surface, y, is higher than the critical depth, y_c, there are SWT conditions, otherwise (i.e. $y < y_c$) DWT conditions are present. The depth of the zero-flux surface, h, is related to the position of the separation surface, y, and this relation can be again approximated according to Eq.(4.33).

The soil moisture dynamics in a given layer at depth z result from the combination of (1) low-moisture phases, with moisture dynamics, $s(z, t) = s_0(z,t)$ conditional upon $s < s_{fc}$, independent of groundwater dynamics; (2) high-moisture phases, $s(z, t) = s_y(z, t)$ conditional upon $s > s_{fc}$, with moisture dynamics deterministically related to the position of y; and (3) saturated conditions, when $s(z, t) = 1$. The decoupling of soil moisture dynamics in the LM and HM zones allows one to analyze the two zones separately.

The soil moisture gradient induced by plant root uptake establishes an upward capillary flux. Above the zero-flux surface, the capillary flux becomes negligible due to the null hydraulic conductivity in the LM zone. Exfiltration, needs thus to be balanced by root uptake in the HM unsaturated zone. From this balance, and considering that root uptake at depth z is $U(z) = T_p\, r(z)$, derives the net capillary flux, $\nu(z)$ (with $y < z < h$), that can be calculated as in Sect. 4.4.1.2 for SWT conditions and as in Eq.(4.31) for DWT conditions (see Sect. 4.4.1.4).

Working at the daily timescale and under the assumption of instantaneous redistribution (at the daily timescale) of moisture within the soil profile it is possible to model the soil moisture dynamics in the HM zone $s_y(z,t)$ as a sequence of equilibrium states, dropping the time dependence. The steady state water balance in a generic layer in the HM unsaturated zone is then described by the Darcy's law:

$$-k\left(s_y\right)\left(\frac{d\psi}{ds_y}\frac{ds_y}{dz}+1\right)=\nu\left(z\right) \tag{4.45}$$

where $s_y = s_y(z)$ is the steady state soil moisture profile for $s > s_{fc}$. Considering also Eq.(4.1), one can obtain the differential equation

$$\frac{ds_y}{dz} = \frac{m \cdot s_y^{(m+1)/m}\left[k\left(s_y\right)+\nu(z)\right]}{\psi_s \cdot k\left(s_y\right)} \tag{4.46}$$

representing the dependence of $s_y(z)$ on the water table depth y and on soil/vegetation properties. Since no analytical solutions can be found for the differential Eq.(4.46), a numerical solution is computed with a finite difference method. The imposing of two different boundary conditions, and capillary flux ν in the corresponding position, are required to solve Eq.(4.46) in SWT and DWT condition.

In the case of SWT conditions, the boundary condition considered is $s_y(y)=1$ and the first step of the numerical integration is carried out using the exfiltration rate $\nu(y)$ for SWT.

In the second case (DWT conditions) the boundary condition is $s_y(h) = s_{fc}$ at the zero-flux surface, where $n(h) = 0$. Using in the case of DWT the same boundary condition of SWT, would require a capillary flux equal to $\nu(y)= T_p(e^{h/b} - e^{y/b})$ at the first computational step of the numerical integration, with $h=h(y)$ approximated by Eq.(4.33). The different boundary condition imposed, instead, allows one to avoid the approximation error introduced by $h(y)$ and allows for an exact numerical solution for $s_y(z)$.

Tamea et al. (2009) found an explicit analytical function approximating the steady state soil moisture profile in the HM unsaturated zone, valid for a wide range of soils, root profiles, and water table depths. A good approximation was found by modelling the soil matric potential in the HM zone through a quadratic function and imposing the fixed points ψ_s and ψ_{fc} at the extremes of the HM unsaturated zone:

$$\psi(z) = \begin{cases} \psi_s\left[1+\left(s_{fc}^{-1/2m}-1\right)\cdot\left(\dfrac{y-z}{y}\right)\right]^2 & \rightarrow SWT \\ \psi_s\left[1+\left(s_{fc}^{-1/2m}-1\right)\cdot\left(\dfrac{y-z}{y-h}\right)\right]^2 & \rightarrow DWT \end{cases} \tag{4.47}$$

The soil moisture profiles for the HM zone can be obtained by setting Eq.(4.1) into Eq.(4.47), and it is equal to

$$s_y(z) = \begin{cases} \left[1 + \left(s_{fc}^{-1/2m} - 1\right) \cdot \left(\dfrac{y - z}{y}\right)\right]^{-2m} & \rightarrow SWT \\ \left[1 + \left(s_{fc}^{-1/2m} - 1\right) \cdot \left(\dfrac{y - z}{y - h}\right)\right]^{-2m} & \rightarrow DWT \end{cases} \tag{4.48}$$

which can be solved for y. Figure 4.13 shows some examples of the correct (numerical) and approximate soil moisture profiles for different depths of the separation surface.

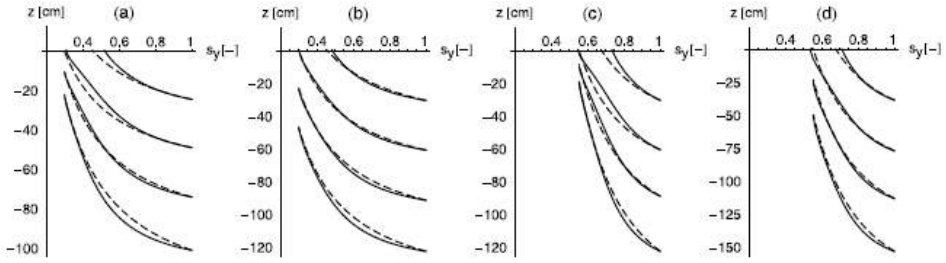

Figure 4.13: Comparison between exact (solid) numerical solution of Eq.(4.46) and approximate (dashed) equilibrium soil moisture profiles in the HM zone, for SWT and DWT conditions (y = 0.5, 1, 1.5 and 2 times the critical depth, y_c), in (a, b) loamy sand and (c, d) loam, while b = 10 cm (a, c) and b = 40 cm (b, d)

Eq.(4.48) can be used to calculate the specific yield, β. In fact Eqs.(4.19) and (4.35), expressing the specific yield in SWT and DWT conditions respectively, have been obtained from the difference between two integrated soil moisture profiles corresponding to two infinitesimally distant positions of the separation surface between saturated and unsaturated soil.

In the LM zone, instead, the soil moisture dynamics, $s(z,t) = s_0(z,t)$, is independent from the groundwater dynamics, thanks to the assumption of no capillary flux through the surface at depth h. Therefore, soil moisture dynamics in the LM zone (conditional upon $s < s_{fc}$) can be studied without considering the presence of the water table, similarly to the case of WCEs (e.g., *Laio et al.*, 2001b; *Laio*, 2006). Thus, the local water balance in the LM zone can be written as

$$n \frac{\partial s'(z,t)}{\partial t} = Q(z,t) - U_{lm}(z,s') \tag{4.49}$$

where the terms $U_{lm}(s', z)$ and $Q(z, t)$ denote the root uptake at depth z and the stochastic process of infiltrating events reaching the z layer, respectively.

The net rainfall infiltration is modeled as in the model described in Sect. 4.4.1. Every rainfall event infiltrates (at the daily timescale) as an instantaneous piston flow that initially saturates soil layers, and then drains them to field capacity, while excess water percolates down to deeper layers. The water content in soil layers not reached by the wetting front remains unmodified. Assuming that rainfall always find the same long-term average soil moisture in the soil, $\bar{s}'(z)$, the Poissonian structure of wetting events is preserved. The sequence of wetting events at generic depth $z < h$ [Eq.(4.49)] is then a state-dependent marked Poisson process with rate $\lambda[z, \bar{s}'_m(z)]$ and exponentially distributed depths with mean α:

$$Q(z,t) = P[\lambda[z, \bar{s}'_m(z)], \alpha] \tag{4.50}$$

The interarrival rate at depth z is given by

$$\lambda[h, \bar{s}'_m(z)] = \lambda_0 \exp\left[\frac{nz(s_{fc} - \bar{s}'_m(z))}{\alpha}\right] \tag{4.51}$$

where $\bar{s}'_m(z)$ is the mean above z of the long-term average soil moisture, conditional upon $z > h$.

The second term of the local water balance in the LM zone [Eq.(4.49)], denoting the root uptake in the LM zone, can be expressed as a function of depth z and depends on the root density and soil moisture at that depth:

$$U_{lm}(s', z) = T_p \cdot \rho(s') \cdot r(z) = T_p \frac{s'(z) - s_w}{s_{fc} - s_w} r(z) \tag{4.52}$$

with the water stress function, $\rho(s')$, assumed to vary linearly from 0 at the wilting point, s_w, to 1 at field capacity, s_{fc} (e.g., *Laio*, 2006).

The long-term average steady state water balance of the generic z layer of depth dz can be obtained from Eq.(4.49), taking the long-term average and setting $\partial s'(z,t)/\partial t = 0$, and it reads

$$\lambda[z, \bar{s}'_m(z)] \cdot n \cdot [s_{fc} - \bar{s}'(z)] dz = T_p \frac{\bar{s}'(z) - s_w}{s_{fc} - s_w} r(z) dz \tag{4.53}$$

Combining this equation with Eq.(4.51), one obtains

$$\lambda_0 n\left[s_{fc}-\bar{s}'(z)\right]\exp\left[\frac{nzs_{fc}}{\alpha}\right]\exp\left[\frac{n\int_z^0 \bar{s}'(u)du}{\alpha}\right]=T_p\,\frac{\bar{s}'(z)-s_w}{s_{fc}-s_w}\frac{1}{b}e^{z/b} \tag{4.54}$$

From the natural logarithm of Eq.(4.54), and its derivative with respect to z, after some mathematical passages here omitted and after integration, and imposing the boundary condition $\bar{s}'(0)=\bar{s}'_0$, one can obtain:

$$\begin{aligned} z=&\frac{b\cdot\alpha}{nb(s_{fc}-s_w)-\alpha}Log\left[\frac{\bar{s}'(z)-s_w}{\bar{s}'_0-s_w}\right]+b\cdot Log\left[\frac{s_{fc}-\bar{s}'(z)}{s_{fc}-\bar{s}'_0}\right]\\ &-\frac{nb^2(s_{fc}-s_w)}{nb(s_{fc}-s_w)-\alpha}Log\left[\frac{nb(s_{fc}-\bar{s}'(z))-\alpha}{nb(s_{fc}-\bar{s}'_0)-\alpha}\right] \end{aligned} \tag{4.55}$$

The long-term average soil moisture at the soil surface, $\bar{s}'(0)$, can be obtained from Eq.(4.54), by setting $z = 0$:

$$\bar{s}'_0=s_{fc}-\frac{T_p(s_{fc}-s_w)}{T_p+nb\lambda_0(s_{fc}-s_w)} \tag{4.56}$$

The explicit long-term average soil moisture profile, $\bar{s}'(z)$, in the LM zone can be found by solving numerically Eq.(4.55). The numerical profile, necessary to calculate the depth-dependent rate of rainfall infiltration, $\lambda[z,\bar{s}'_m(z)]$, in the case of an exponential root profile [Eq.(4.11)] can be written as

$$\lambda[z,\bar{s}'_m(z)]=\frac{T_p(\bar{s}'(z)-s_w)e^{z/b}}{nb(s_{fc}-s_w)(s_{fc}-s'(z))} \tag{4.57}$$

In the model by *Laio et al.* (2009), presented in Sect. 4.4.1, the expression for the rate of infiltration events reaching the zero-flux surface in DWT conditions [Eq.(4.29)] has been derived from Eq.(4.53) with $z = h$.

The behavior of the long-term average soil moisture profile in the LM zone can be either increasing or decreasing with depth. This type of behavior depends on the model parameters. *Tamea et al.* (2009) found that for an exponential root distribution and a consequently monotone soil moisture profile, the long-term average profile increases with depth if

$$nb\left(s_{fc} - \bar{s}'_0\right) - \alpha < 0 \tag{4.58}$$

with $\bar{s}'_0$ defined by Eq.(4.56).

This condition can be also interpreted in terms of a critical mean rooting depth, b_0. In particular, if $b < b_0$, the long-term average soil moisture profile increases with depth, if $b = b_0$, the it is uniform and $\bar{s}'(z) = const = \bar{s}'_0$, while if $b > b_0$, the profile decreases with depth and approaches s_w in the deepest soil layers. The critical mean rooting depth, b_0, can be found as

$$b_0 = \frac{T_p \cdot \alpha}{n\left(s_{fc} - s_w\right)\left(T_p - \alpha\lambda_0\right)} \tag{4.59}$$

Figure 4.14 show some examples of long-term average soil moisture profile in the LM zone having increasing or decreasing behavior with depth, under the assumption of root biomass with an exponential distribution [Eq.(4.11)].

The condition in Eq.(4.58) can also be interpreted in terms of critical rainfall parameters, for a fixed root distribution. A rainfall increase may induce a shift in the long-term average moisture content of deeper soil layers, even if the surface values do not change sensibly. In particular, the long-term average soil moisture profile in the LM zone depends only on the mean interarrival time, λ_0, of rainfall events and not on the mean rainstorm depth, α. This is due to the fact that every rainfall event reaching the soil, wets the surface, regardless of the amount of precipitation and, then, the moisture at the soil surface depends only on the average waiting time between two rainfall events. This type of dependence of the long-term average soil moisture profile in the LM zone on the rainfall parameters is shown in Figure 4.15.

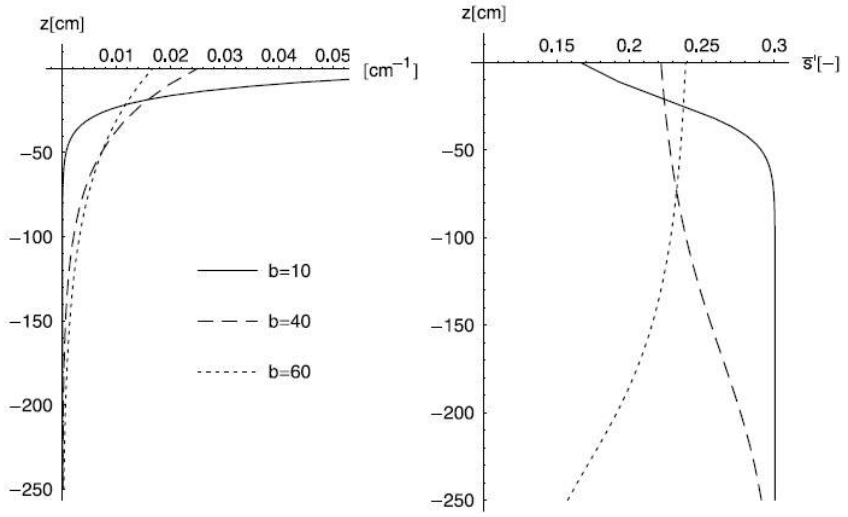

Figure 4.14: Examples of (left) different vertical root distributions, $r(z)$ [all are exponential, see Eq.(4.11)], and (right) the corresponding long-term average soil moisture profiles in the LM zone (conditional upon $s_0 < s_{fc}$). In the right panel, the soil is a loamy sand and rainfall parameters are $\lambda_0 = 0.2$ d^{-1} and $\alpha = 1.5$ cm. The critical mean rooting depth, b_0, is 49 cm (from *Tamea et al.*, 2009)

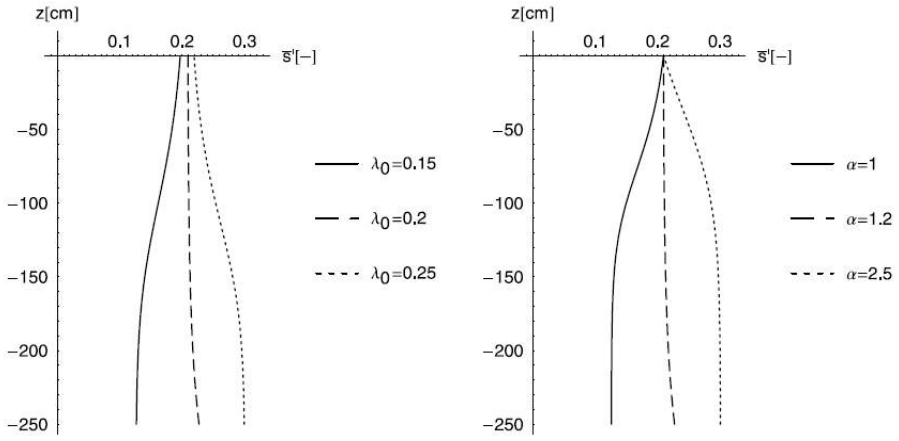

Figure 4.15: Impact of rainfall parameters on the long-term average soil moisture profile in the LM zone (conditional upon $s_0 < s_{fc}$). Soil and vegetation are the same as in Figure 4.14, while rainfall parameters are $\alpha = 1.2$ cm and (left panel) and $\lambda_0 = 0.2$ d^{-1} (right panel). From *Tamea et al.* (2009)

4.4.2.2 Probability density functions of soil moisture

The steady state soil moisture profiles in the HM zone and the long-term average soil moisture profiles in the LM zone presented in the previous section, together with the pdf's of the position, y, of the separation surface and the zero-flux surface, h, discussed in Sect. 4.4.1.5, allow us to determine the steady state pdf of soil moisture at generic depth.

The pdf of soil moisture at a given depth z results from the combination of three different contributions that correspond to the three states that may occur at depth z: LM conditions, HM conditions, and saturated conditions. That is, a different weight may be associated to each contribution on the basis of the probability to be in the correspondent condition of that contribution. The three weights can be obtained from the cumulative density functions of y and h, as sketched in Figure 4.16.

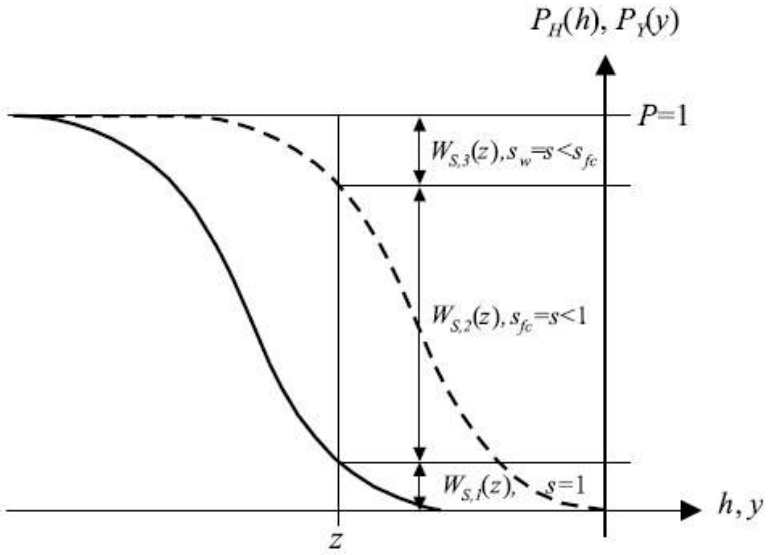

Figure 4.16: Scheme of the derivation of weighting constants, $W_1(z)$, $W_2(z)$ and $W_3(z)$, from the cumulative probability functions of the separation surface and zero-flux surface (from *Tamea et al.*, 2009)

The first weight is given by the probability for a soil layer at depth z to be saturated and it equals the probability that $y \geq z$, i.e.,

$$W_{S,1}(z) = \int_{z}^{0} p_Y(u)du \tag{4.60}$$

where p_Y can be obtained by Eq.(4.43).

The second weight is given by the probability for the same layer to be in the HM unsaturated zone and it depends on the probability distributions of both y and h, i.e.,

$$W_{S,2}(z) = \int_{z}^{0} p_H(h)dh - W_{S,1}(z) \tag{4.61}$$

where $p_H(h)$ can be obtained from Eq.(4.44).

Finally, the last weight to be determined corresponds to the probability associated with LM unsaturated conditions and it can be obtained in order to have a total weight equal to one, i.e.,

$$W_{S,3}(z) = 1 - \int_{z}^{0} p_H(u)du = 1 - W_{S,1}(z) - W_{S,2}(z) \tag{4.62}$$

The three portions of the overall probability distribution of s at the generic depth z are calculated separately. The probability for the z layer to be saturated is an atom of probability centered at the value s=1, whose associated probability mass is $W_{S,1}(z)$.

The pdf of soil moisture in a layer of the HM zone is obtained as a derived distribution of y. The relation between the separating surface, y, and the soil moisture profile in the HM zone, $s_y(z)$ can be obtained setting Eq.(4.33) in Eq.(4.48). Considering the same position for the term A [Eq.(4.34)] given in Sect. 4.4.1.4 and the following positions:

$$D = \frac{\left(A^{1/4} - 1\right)A^{3/4}\left(1 - s_y^{-1/2m}\right)}{5b + y_c - \psi_{fc} + \psi_s} \tag{4.63}$$

and

$$\begin{aligned} a_0 &= D \cdot y_c^2 - \left(A^{3/4} - 1\right)\left(s_y^{-1/2m} - 1\right)y_c + \left(s_{fc}^{-1/2m} - 1\right)z \\ a_1 &= -2D \cdot y_c + A^{3/4}\left(s_{fc}^{-1/2m} - 1\right) - s_{fc}^{-1/2m} + 1 \\ a_2 &= D \end{aligned} \tag{4.64}$$

and, finally, solving the relation of the soil moisture profile in the HM zone for y, it can be obtained:

$$y(s_y, z) = \begin{cases} z - y_c\left(\dfrac{s_y^{-1/2m}+1}{s_y^{-1/2m}-1}\right) & \rightarrow if \quad y \geq y_c \\ \left(a_1 - \sqrt{a_1^2 - 4a_0a_2}\right)/(2a_2) & \rightarrow if \quad -5b + \psi_{fc} - \psi_s \leq y \leq y_c \\ z + (\psi_{fc} - \psi_s)\left(\dfrac{s_y^{-1/2m}-1}{s_y^{-1/2m}-1}\right) & \rightarrow if \quad y < -5b + \psi_{fc} - \psi_s \end{cases} \tag{4.65}$$

The derived pdf of soil moisture, conditional upon the HM state of layer at depth z, can be obtained from Eq.(4.65), i.e.,

$$p_{S,2}(s_y \mid z) = \frac{p_Y[y(s_y, z)]}{W_{S,2}(z)} \frac{dy(s_Y, z)}{ds_y} \tag{4.66}$$

with $W_{S,2}(z)$ used as the normalizing constant for a unitary area in the soil moisture interval from s_{fc} to 1.

With regard to the LM zone, the pdf of soil moisture (conditional upon $s < s_{fc}$), being independent from the water table position (see the previous section), can be calculated in the same manner of *Laio* (2006), and it reads

$$p_{S,3}(s' \mid z) = \frac{n\lambda[z, \bar{s}'_m(z)]}{r(z) \cdot T_p} \left(\frac{s'(z) - s_w}{s_{fc} - s_w}\right)^{\frac{n\lambda[z, \bar{s}'_m(z)](s_{fc} - s_w)}{r(z) T_p} - 1} \tag{4.67}$$

where $r(z)$ is the exponential vertical root distribution.

The overall piecewise probability density function of $s(z^*)$ found by *Tamea et al.* (2009), is then

$$p_S(s \mid z^*) = \begin{cases} W_{S,1}(z^*) & \rightarrow if \quad s = 1 \\ W_{S,2}(z^*) \cdot p_{S,2}(s \mid z^*) & \rightarrow if \quad s_{fc} < s(z^*) < 1 \\ W_{S,3}(z^*) \cdot p_{S,3}(s \mid z^*) & \rightarrow if \quad s_w < s(z^*) < s_{fc} \end{cases} \tag{4.68}$$

Figure 4.17 shows the results of an analysis concerning the case of a deep water table with small fluctuations. In particular the pdf's of y and h are shown in the upper part while the bottom part show the pdf's of soil moisture at different depths. Figure 4.17 shows the case of a loamy sand soil where the water table and the zero-flux surface spend most of the time below the bulk of the root zone, and the soil moisture dynamics are not affected by the groundwater. From the comparison between the pdf's of soil moisture at different depth, it is possible to note that in shallower soil layers (z_1 and z_2) the pdf's of soil moisture are similar to that obtained by *Laio* (2006) for WCEs, while deeper layers exhibits higher soil water contents, reflecting the intermittent presence of the HM zone. For $z = z_4$ the probability that $y > z$ is no zero and the pdf of soil moisture exhibits an atom of probability corresponding to saturation.

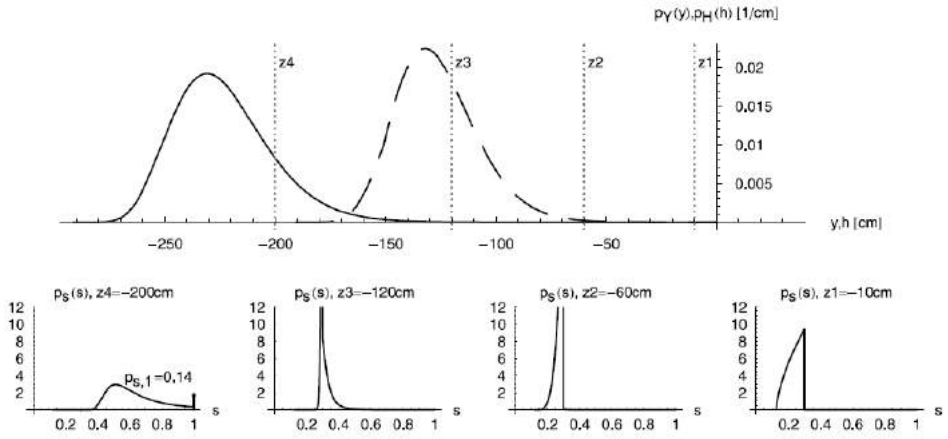

Figure 4.17: On the top the pdf's of (top) the positions of the separation surface, y (continuous line), and the zero-flux surface, h (dashed line), and at the bottom the pdf's of soil moisture at different depths. The soil is a loamy sand (parameters as in the work of *Rawls et al.,* 1983); rainfall parameters are $\lambda_0 = 0.3$ d^{-1} and $\alpha = 2$ cm, vegetation parameters are $T_p = 0.5$ cm/d and $b = 30$ cm; while $k_l = 3.7\ 10^{-3}$ d^{-1} and $y_0 = -3$ m (from *Tamea et al.*, 2009)

In presence of more abundant rainfall and shallower external water bodies, the water table is shallower and exhibits stronger fluctuation. If part of the pdf of water table depths lies above the critical depth y_c, an atom of probability appears in the pdf of h (corresponding to the probability that soil belongs to the HM zone) and the groundwater, through capillary flux, intermittently affects the long-term soil moisture content in all soil layers up to the soil surface. *Tamea et al.* (2009), considering an external water table depth equal to -2 m and the other parameters as in Figure 4.17, found that although for shallow soil layers the condition of LM soil still prevails, the relative importance of the HM zone increases with depth.

Figure 4.18 shows the case of a loamy soil (i.e., a fine-grained soil with shallower water table and higher soil moisture contents), where it is possible to note that a discontinuity appears in correspondence of y_c. This discontinuity derives from the discontinuity in the specific yield β and also affects the derived pdf of soil moisture in the HM zone. It is important to point out that jumps and discontinuities do not reflect reality, but depend on the reasonable and consistent approximations introduced by the numerous assumption and simplifications necessary for the models computation.

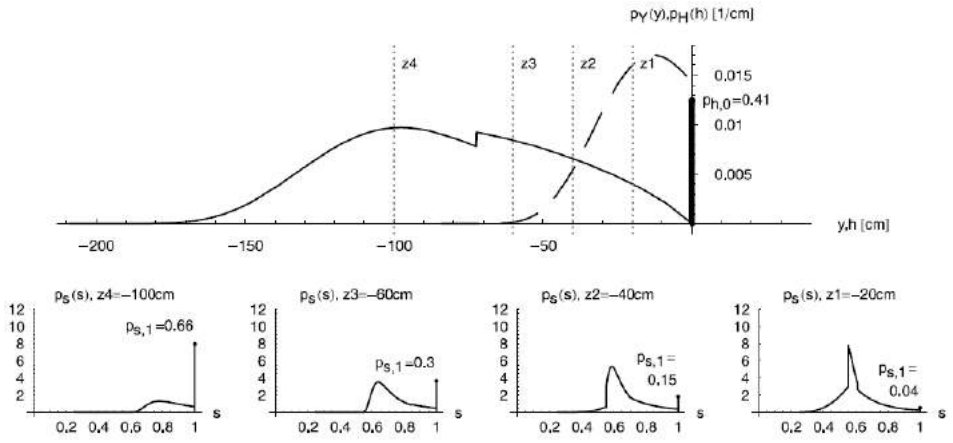

Figure 4.18: On the top the pdf's of (top) the positions of the separation surface, y (continuous line), and the zero-flux surface, h (dashed line), and at the bottom the pdf's of soil moisture at different depths. The soil is a loam (parameters as in the work of *Rawls et al.,* 1983); k_l= 7.9 10^{-4} d^{-1} and y_0= -2 m. Other parameters are as in Figure 4.17 (from *Tamea et al.*, 2009)

4.5 Application of the model for the study of water table fluctuations to the Everglades

In this section an application to the Everglades (Florida, USA) of the model discussed in Sect. 4.4.1 is presented. The model, accounting for hydrologic mechanisms such as infiltration, root water uptake, water flow from/to an external water body and capillary fluxes, is able to simulate the complex interactions among rainfall, groundwater and vegetation in areas with a relatively shallow water table. In particular, the water table dynamics are considered as a random process stochastically driven by a marked Poisson noise representing rainfall events, and the model provides a probabilistic description of the water table fluctuations below the soil surface.

The water table model is validated using field data of groundwater levels recorded in three different sites located in southeast Florida (USA), within the Everglades National Park. Model parameters are estimated from the characteristics of vegetation, soil and from time series of precipitation and evapotranspiration available at the same sites; the analysis is carried out using two different parametric aggregation schemes: annual and seasonal. In particular, the steady-state probability distribution functions and cumulative distribution functions of water table levels predicted by the model are compared with the empirical ones obtained using field data of groundwater levels recorded in the three sites.

4.5.1 Description of the sites

The model by *Laio et al.* (2009), discussed in Sect. 4.4.1, has been applied to three different sites, where measurements of groundwater depths were available, as well as data of precipitation, evapotranspiration, soil and vegetation. Since the model does not account for standing water, the sites have been chosen after an extensive search in order to have water level fluctuations within the shallow soil and to warrant that submergence of the sites is limited or not occurring.

All the sites are located in southeast Florida (USA), Dade County, within the Everglades National Park (Figure 4.19). Each site lies in proximity of a groundwater well, having historical data series available. The landscape of the Florida Everglades includes extended and prolonged flooding areas, especially during the wet season (from June to November). Thus the three sites are only partially representative of the general conditions of water level fluctuations in the Everglades. The sites have been chosen in this specific area in virtue of the abundance of public datasets availability (e.g. water table depths, rainfall, evapotranspiration, soil and vegetation properties, etc.). Some of the most

important agencies monitoring the Florida Everglades together with their web-based archives, frequently referred in this application, are:

- *USGS - U.S. Geological Survey* (www.usgs.gov);
- *EDEN - Everglades Depth Estimation Network* (www.sofia.usgs.gov/eden);
- *FCE-LTER - Florida Coastal Everglades-Long Term Ecological Research* (www.fcelter.fiu.edu);
- *SFWMD - South Florida Water Management District* (www.sfwmd.gov).

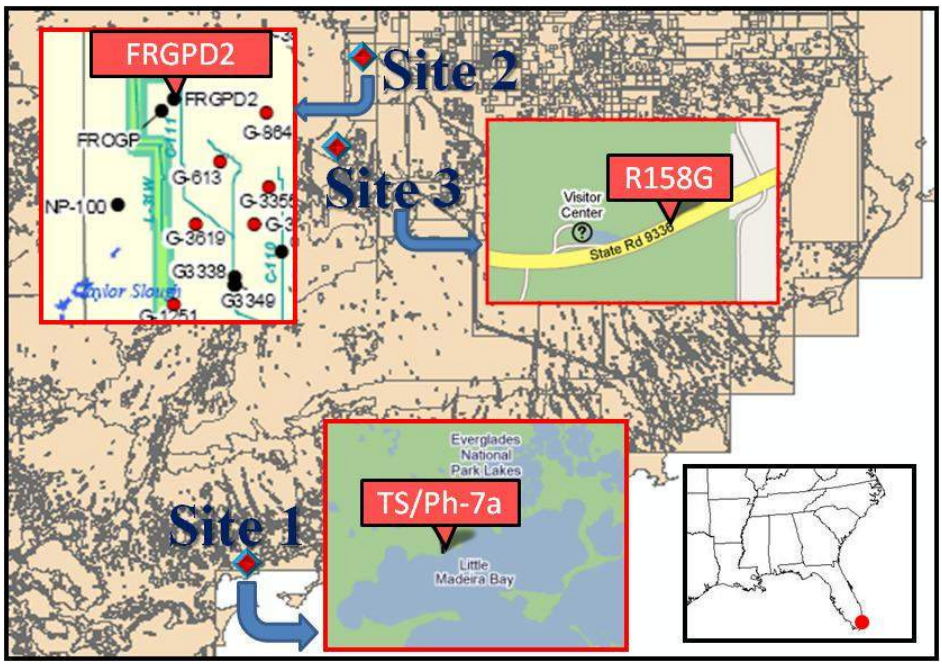

Figure 4.19: Schematic map of the three sites used for the model application (Dade County, Florida, USA)

Site 1 is located in the Florida Bay, very close to the ocean. The gauging station is named *Taylor River at Mouth* (alias TS/Ph-7a), and the operating agency is the USGS. The data of groundwater levels, rainfall and potential evapotranspiration are available at the EDEN, USGS and FCE-LTER web sites. The site, located within the *Taylor Slough* watershed, presents flat topography, with a tidal creek and limestone bedrock. The shallowest portion of soil is made up of wetland peat (>1 m thick) while the vegetation is essentially constituted by mangrove.

Site 2 is located within the so-called *Frog Pond Area*, between the canal C111 and the levee L31W. The groundwater well, identified by the code FRGPD2, is operated by SFWMD, and the data are available at their web site. For precipitation and evapotranspiration data, the station considered is the L31W (alias TS/Ph-1b), managed by ENP (*Everglades National Park*), with data available at the EDEN web site. This weather station is almost 2 km from the groundwater well FRGPD2. This site is also located within the *Taylor Slough* watershed, and is characterized by flat topography and limestone bedrock. The shallower soil is wetland marl and the vegetation is mainly sparse sawgrass.

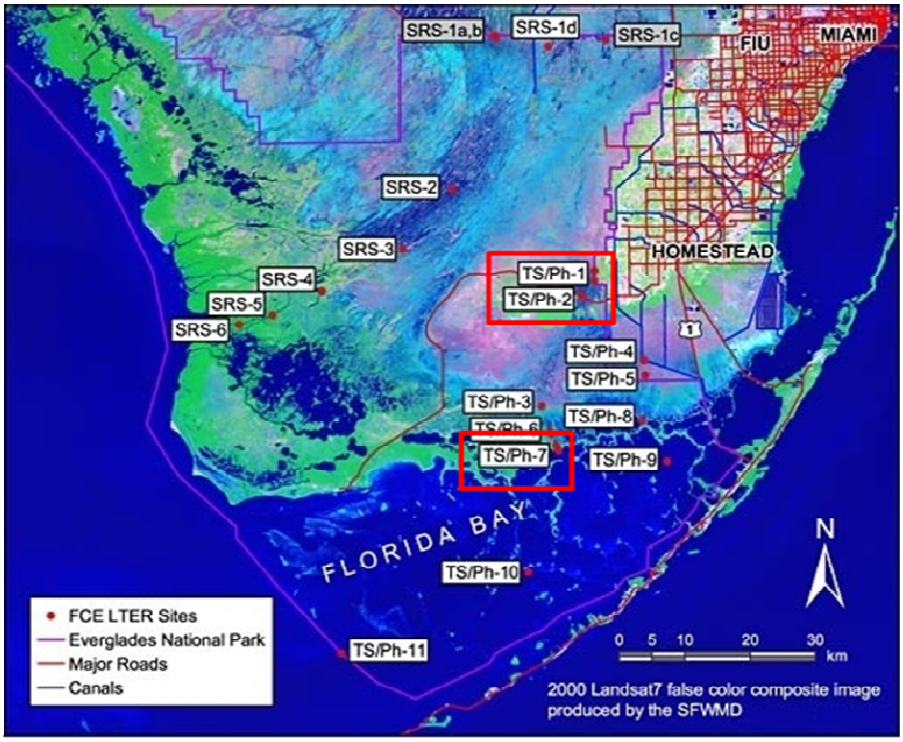

Figure 4.20: Map of the sites monitored by FCE-LTER (Landsat map). Notice the location of stations TS/Ph-7 (groundwater and weather station for Site 1), TS/Ph-1 (weather station for Site 2) and TS/Ph-2 (weather station for Site 3)

Site 3 is located within the *Everglades National Park*, near the levee L31W, close to the northern area of the *Taylor Slough*. The groundwater well name is R158G and the operating agency is the ENP. Groundwater data are available at the SFWMD web site. For precipitation and evapotranspiration

data, the station considered is TS2 (alias TS/Ph-2), managed by ENP, with data available at the EDEN web site; this station is located about 2 km from the station R158G. The topography of the area is flat and the geology is characterized by limestone bedrock. The soil presents a layer of wetland marly peat (about 1 m thick) and the vegetation cover is sparse sawgrass.

Figure 4.21: Some photos of Site 1 from FCE-LTER website. An example of the root apparatus of mangrove (right) and aerial photo of Site 1(left)

Figure 4.22: Part of the SFWMD monitoring locations map (active groundwater well sites). Notice the location of the groundwater well FRGPD2, relative to Site 2

It is important to point out that for the first site, the closest water body is the ocean, while for the other two sites the closer water bodies are large canals (C111 and L31W), where daily records of water levels are available. These canals are part of the water management system developed in the South Florida during the 19th and throughout most of the 20th century. The canals were initially conceived as drainage canals, with small success for their original purpose. The initial impact of the canal network on the Everglades groundwater was that of lowering the water table thus creating a hydraulic gradient between the Everglades and the Atlantic Ocean that caused an unexpected increase of marine intrusion. For this reason, the most recent constructions have been addressed towards the re-establishment of the natural conditions of the water levels within the Everglades. After a first development of the water system, the Central and Southern Florida Flood Control Project and District (predecessor of the SFWMD), initiated a major construction project known as the "Comprehensive Plan" (Figure 4.23). Canal and levee construction expanded greatly during the 1950s and 1960s (Figure 4.24), reaching its final phase in the 1980s (Figure 4.24), with completion of the Everglades-South Dade conveyance system (*Renken et al.*, 2005). In Figure 4.25 an example of South Florida levee is shown.

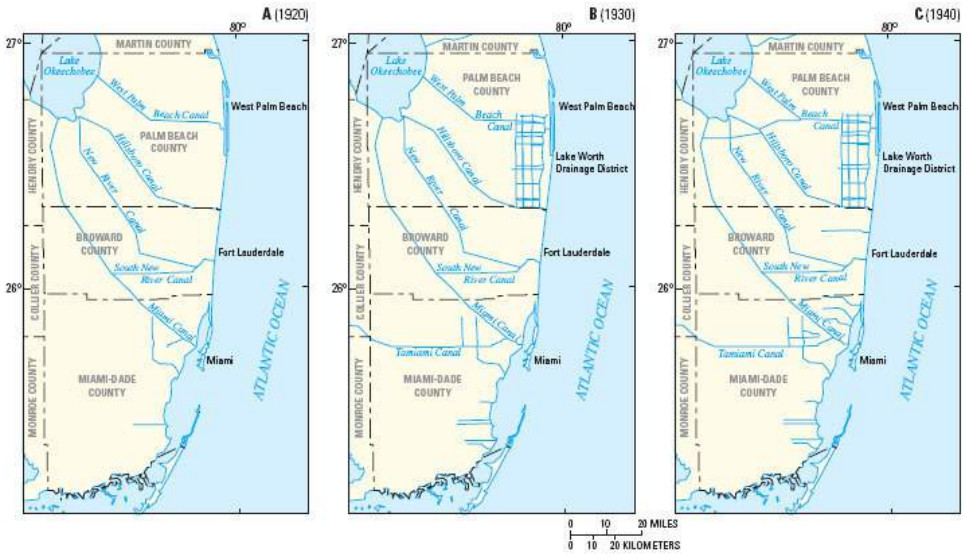

Figure 4.23: Development of Water-Management System of southeastern Florida (USA). Surface-water conveyance features in Miami-Dade, Broward and Palm Beach Counties in 1920 (A), 1930 (B) and 1940 (C). From *Renken et al.*, 2005

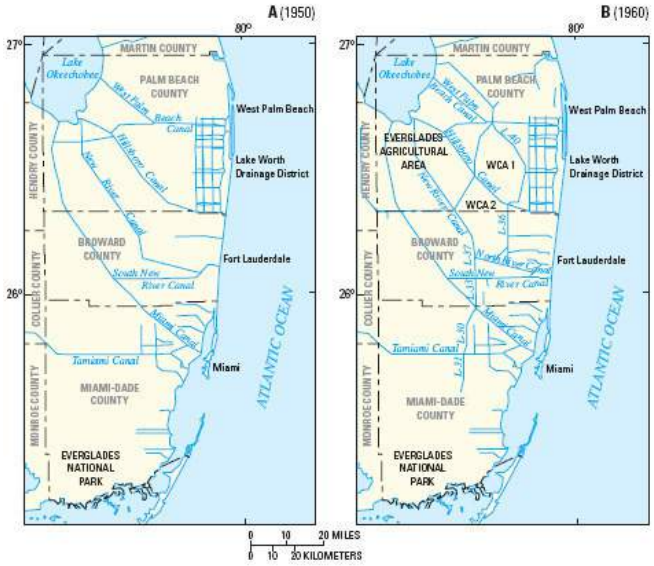

Figure 4.24: Development of Water-Management System of southeastern Florida (USA). Surface-water conveyance features in Miami-Dade, Broward and Palm Beach Counties in 1950 (A) and 1960 (B). From *Renken et al.*, 2005

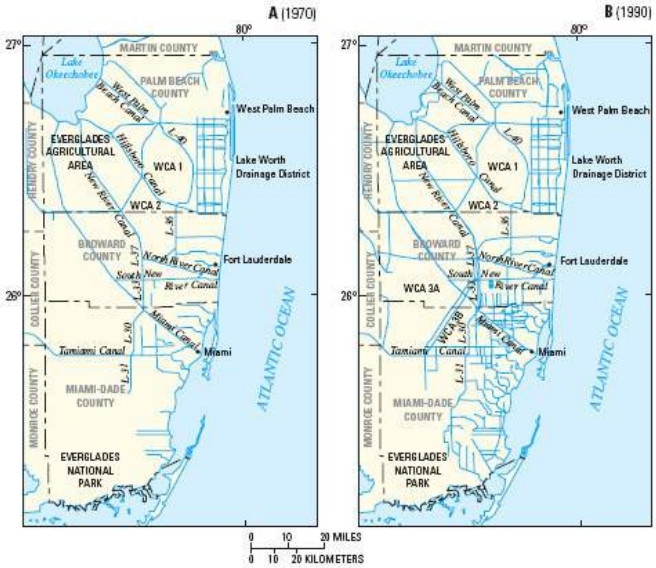

Figure 4.25: Development of Water-Management System of southeastern Florida (USA). Surface-water conveyance features in Miami-Dade, Broward and Palm Beach Counties in 1970 (A) and 1990 (B). From *Renken et al.*, 2005

Figure 4.26: Example of levee in the Frog Pond Area (where Site 2 is located). North to south photo of S332 and levee removal on eastern boundary of levee L31 (from FCE-LTER website)

4.5.2 Analysis of the historical data series of water table

The ground elevation for each site has been derived from *The National Map* - Seamless Server (provided by USGS), having a resolution of approximately 30 m. The horizontal datum is the NAD83 (*North American Datum* of 1983) while the vertical datum is the NAVD88 (*North American Vertical Datum* of 1988). The elevations found from this map are also consistent with those coming from another map, the *High Accuracy Elevation Data Map* by USGS-Sofia (*South Florida Information Access*), available in the web site of *Global Change Master Directory*, *Goddard Space Flight Center-NASA* (resolution 400 m, vertical datum NAVD88, horizontal datum NAD83, vertical accuracy 15 cm). The ground elevations found at the three sites are shown in Table 4.1.

As mentioned above, the water table levels have been recorded by the following stations: TS/Ph-7a (Site 1); FRGPD2 (Site 2); R158G (Site 3). All these information are reported in Table 4.1.

		Site 1	Site 2	Site 3
Water Table Measurement Station		*TS/Ph7a*	*FRGPD2*	*R158G*
Operating Agency		*USGS*	*SFWMD*	*ENP*
Ground Elevation - *m a.s.l. (NAVD88)*		0.10	1.09	0.83
Vegetation		*Mangrove*	*Sawgrass*	*Sawgrass*
Soil		*Peat*	*Marl*	*Marly Peat*

Table 4.1: General information about the three sites

For each site the observation period, the mean annual groundwater depths below the soil surface and the mean seasonal water table positions during the wet and dry season, as well as the standard deviations are listed in Table 4.2. In the same table there are also the total number of hydroperiods (i.e. periods with water levels above the soil surface) and the mean duration for each series.

Figure 4.27 shows the time series of water table depth for Site 1 measured in cm and referred to the NAVD88; the original data for Sites 2 (Figure 4.28) and 3 (Figure 4.29) were referred to the NGVD29 (*National Geodetic Vertical Datum* of 1929), thus they have been converted to the NAVD88 with the vertical conversion factors provided by the EDEN web site for the nearby station L31W (Site 2) and TS2 (Site 3). The three time series show clearly strong seasonality, mainly driven by rainfall: the water table is shallower during the wet season (from June to November) when most of the precipitation occurs, while it lies in deeper layers during the rest of the year. The behavior of the groundwater fluctuations shown in Figures 4.27, 4.28 and 4.29 also manifests the presence of some hydroperiods, but they are relatively short and not very numerous (see Table 4.2), and thus not very crucial for the purposes of this application.

Figures 4.30a, 4.31a and 4.32a show the autocorrelation functions (ACF) of the historical water table data relative to Site 1, Site 2 and Site 3, respectively. The ACF's highlight the strong seasonality in the water level time series, showing peaks of autocorrelation values at multiples of 365, with a regular periodic fluctuation. In order to analyze the influence of seasonality on the groundwater dynamics, the seasonality has been removed from each series, by subtracting to each daily value, the average groundwater level relative to that day throughout the years. This procedure allows one to obtain the time series of water table fluctuations around the mean value (that will be here referred as *detrended series*), whose ACF's (Figure 4.30b, 4.31b and 4.32b) show less relevant peaks without strong periodicity.

It is also possible to note that the detrended ACF for Site 1 (Figure 4.30b) is rather different from those of the other sites (Figures 4.31b and 4.32c); Sites 2 and 3, in fact, maintain higher correlation values also in the detrended series. This could be due to the different nature of the influence of the external water bodies on the dynamics of the water levels; as mentioned above, in the case of Site 1 the closest water body is the ocean while the other two sites are controlled by canals. The seasonal component of the ocean influence is more regular and thus more effectively removed after detrending procedure. The presence of high correlation values in the detrended series for Sites 2 and 3 could be due to human activities; in fact, the two nearby canals are often used to supply water during the driest periods.

The Power Spectra Functions (PSF) of the original data in the three case studies are shown in Figure 4.33, which also shows their slopes (m), in double

logarithmic graphs, evaluated via least squares applied for the highest frequencies. The slopes corresponding to the detrended series are also given and, as expected, are very similar to the original ones. One can note that the main signal for the PSF's relative to the original series occurs at frequency of $10^{-2.56}$, correspondent to a frequency of 1/365 days^{-1} (annual cycle). For all the three sites the slope *m* decreases (in absolute value) passing from the original series to the detrended series.

		Site 1	Site 2	Site 3
Water Table Observation Period	*from*	*10/2/1995*	*10/11/1996*	*10/1/1983*
	to	*1/26/2009*	*1/14/2009*	*11/3/2003*
Mean Annual Water Table Position	*cm*	-28.4	-43.6	-46.8
Standard Deviation (Annual)	*cm*	*10.7*	*19.2*	*23.8*
Mean Water Table Position - Dry Seas.	*cm*	-34.4	-54.8	-60.6
Standard Deviation (Dry Seas.)	*cm*	*8.1*	*16.2*	*19.1*
Mean Water Table Position - Wet Seas.	*cm*	-22.6	-32.6	-33.4
Standard Deviation (Wet Seas.)	*cm*	*9.8*	*15.1*	*20.0*
Total Number of Hydroperiods		22	10	21
Mean Duration of Hydroperiods	*day*	2.1	3.0	8.0

Table 4.2: Observed mean water table positions (annual and seasonal: *Dry Season* from December to May; *Wet Season* from June to November) in cm below the soil surface, standard deviations and information about the hydroperiods for the three sites

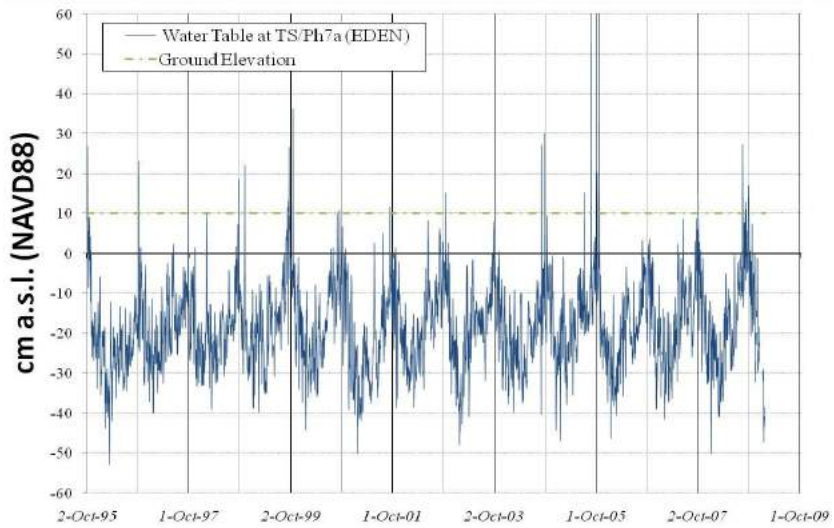

Figure 4.27: Time series of water table levels and ground elevation for Site 1. Elevations in cm above the North America Vertical Datum 1988

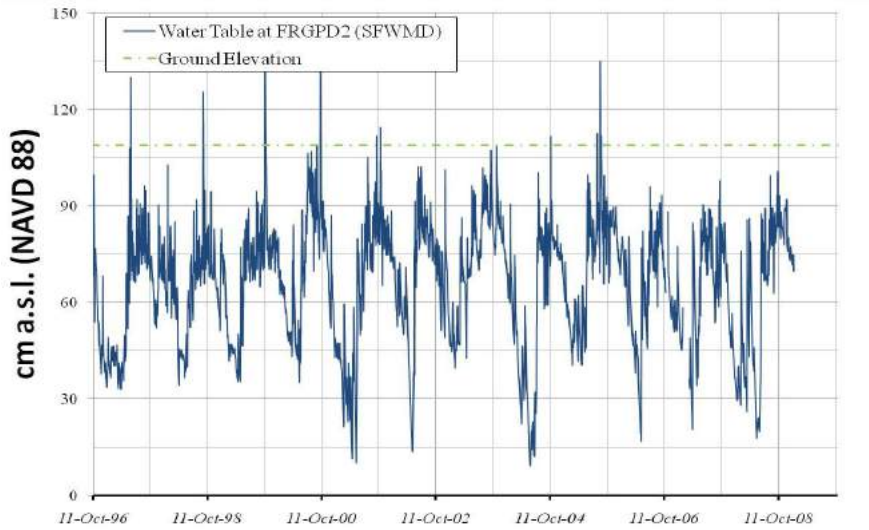

Figure 4.28: Time series of water table levels and ground elevation for Site 2. Elevations in cm above the North America Vertical Datum 1988

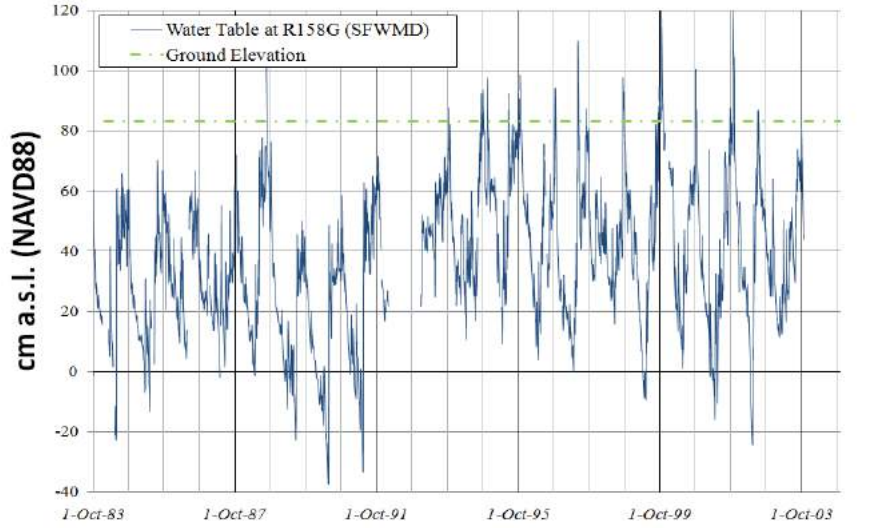

Figure 4.29: Time series of water table levels and ground elevation for Site 3. Elevations in cm above the North America Vertical Datum 1988

(a)

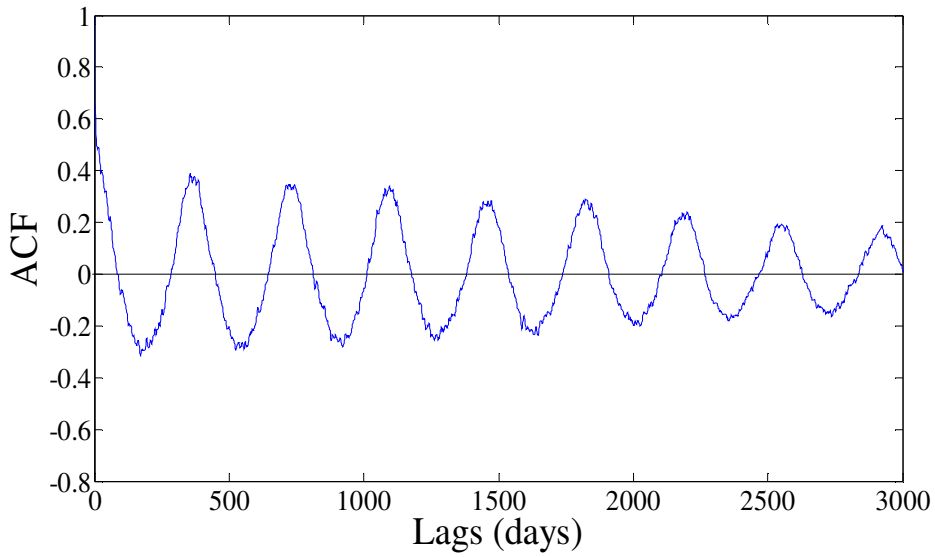

(b)

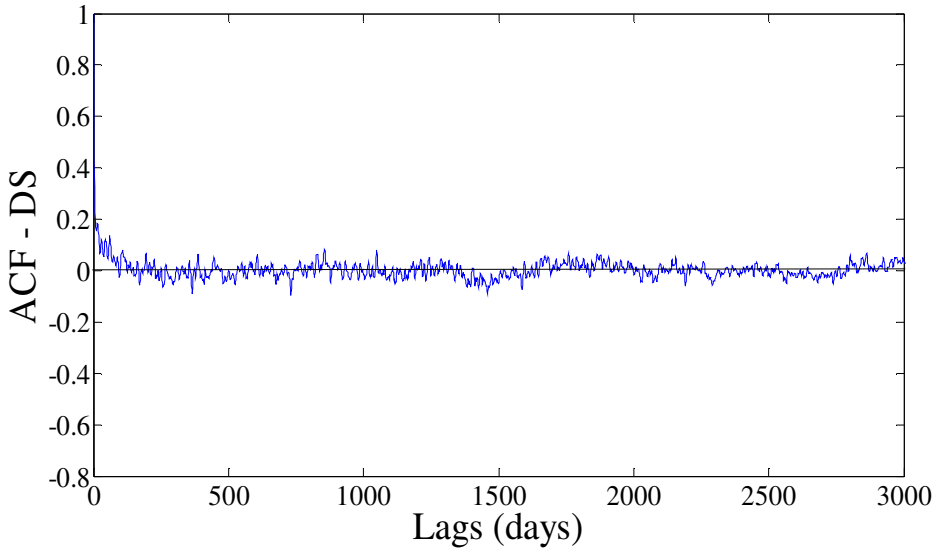

Figure 4.30: Site 1. Autocorrelation Function (ACF) for the original water table series (a) and for the detrended series after the removal of the seasonal cycle (ACF – DS, b)

(a)

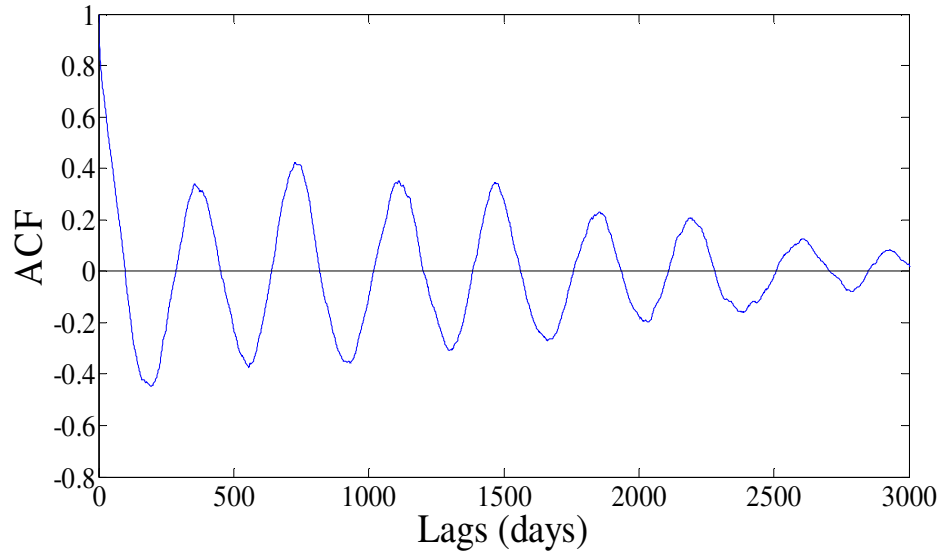

(b)

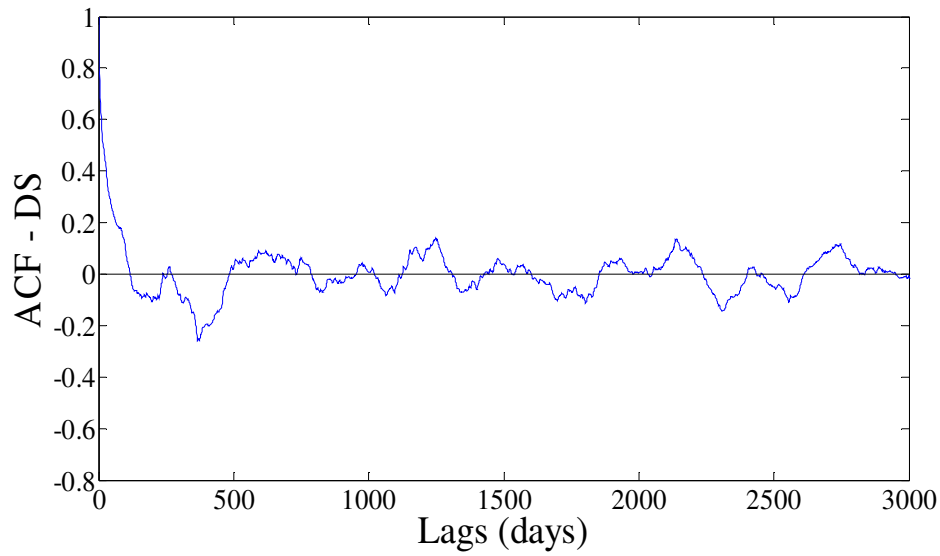

Figure 4.31: Site 2. Autocorrelation Function (ACF) for the original water table series (a) and for the detrended series after the removal of the seasonal cycle (ACF – DS, b)

(a)

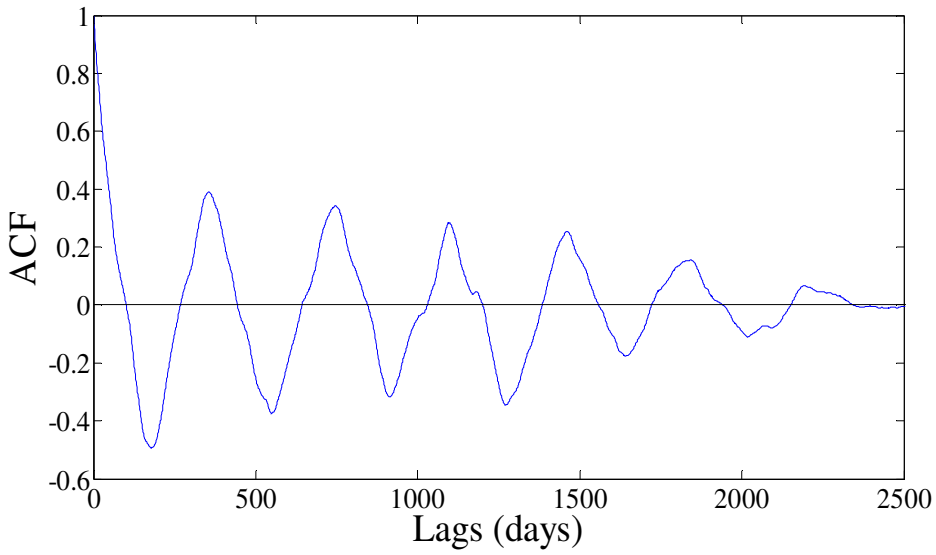

(b)

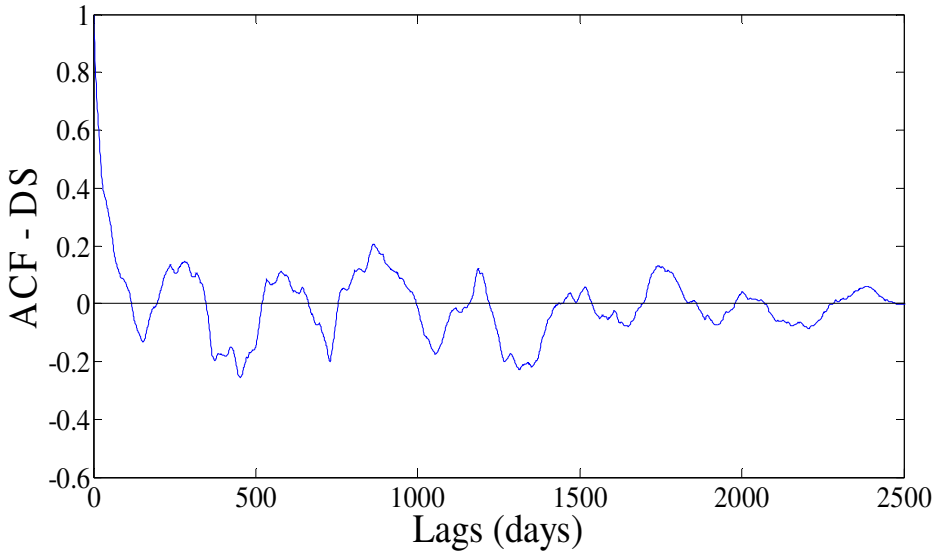

Figure 4.32: Site 3. Autocorrelation Function (ACF) for the original water table series (a) and for the detrended series after the removal of the seasonal cycle (ACF – DS, b)

(a)

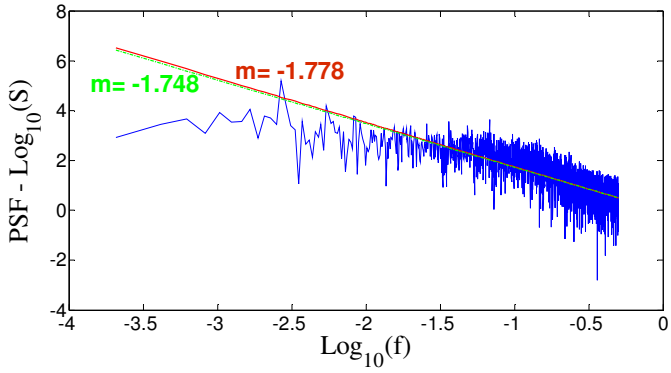

(b)

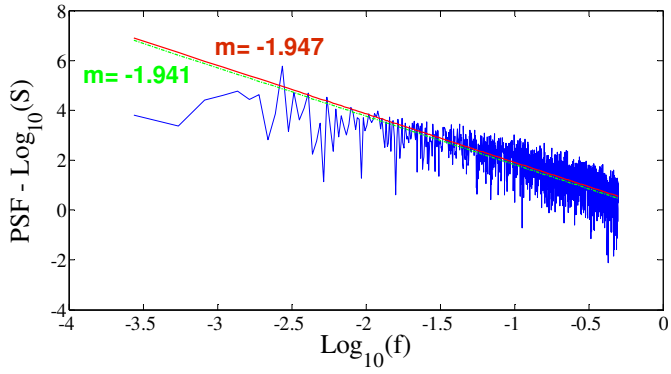

(c)

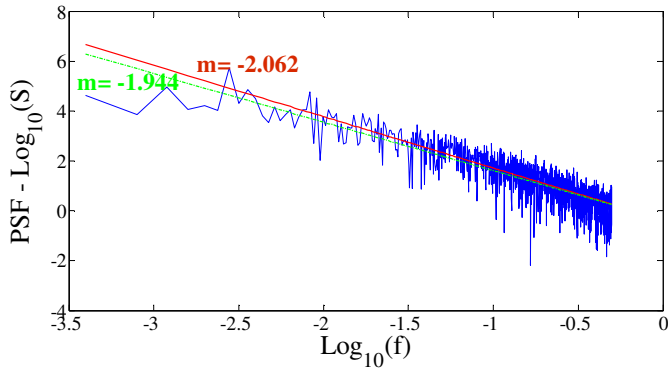

Figure 4.33: Power Spectra Functions (PSF) for the original series, with the slopes marked in red, while the slopes in green refer to the detrended series. Figures 4.33a, 4.33b and 4.33c refer to Site 1, Site 2 and Site 3, respectively

4.5.3 Estimation of the model input parameters

The estimation of the input parameters needed to apply the model to the sites described before is discussed in this section. Two different parametric aggregation schemes have been investigated: annual and seasonal. In the annual analysis the model uses as input parameters the average annual values for the potential evapotranspiration, for the rainfall parameters (mean depth and frequency) and for the elevation of the water surface in the nearest water body. In the seasonal analysis, the model considers two hydrological seasons, each one having its own set of input parameters: dry season (from December to May) and wet season (from June to November).

4.5.3.1 Vegetation parameters

The dominant vegetation within the Everglades is constituted by sawgrass, specifically called Jamaica swamp sawgrass, although many other marsh plants are also present in the Everglades (*Lodge*, 2004). In the examined sites, the vegetation is mainly constituted by mangrove at Site 1 and by sparse sawgrass at Site 2 and Site 3. Sawgrass vegetation in the Florida Everglades (Figure 4.34) includes species such as *Claudium jamaicense*, *Eleocharis cellulose, E. elongata*, *E. interstincta* and *Panicum hemitomon*. Sawgrass is a coarse, rhizomatous, perennial sedge. Often it grows in dense, nearly monospecific stands which result from an extensive network of rhizomes. Apical meristems arise from the top of the rhizomes. In the Everglades, *Yates et al.* (1974) found that rhizomes were generally within the top 10 cm in marly soil, and within the top 15-20 cm in peat.

Mangrove vegetation in South Florida (Figure 4.35) includes species such as *Rhizophora mangle*, *Avicenna germinas*, *Laguncularia racemosa* and *Conocarpus erectus*. Some of the main features and botanical characteristics of this species are provided by *Little* (1983) and the US Forest Service web site (www.fs.fed.us). Mangrove is usually an evergreen shrub 1.5 to 4 m height but sometimes can be present as a tree (for some species such as *Avicenna germinas* and *Lagunaria racemosa*) up to 12 m tall (vegetation at Site 1 is classified as mangrove with low stature). The root system consists mainly of laterals and fine roots that are dark brown, weak and brittle, and have a corky bark (*Conocarpus erectus*).

The model by *Laio et al*. (2009) assumes an exponential distribution of the root biomass into the soil. Using the information available on the vegetation cover of the three sites, the parameter *b* [average rooting depth, Eq.(4.11)] has been set equal to 12 cm for the mangrove vegetation (Site 1) and 10 cm for the sawgrass (Site 2 and Site 3). In this way the model considers the root biomass concentrated mainly in the first 10-25 cm of the soil (almost 80% of the total

root biomass), while only 5% of the total biomass is deeper than 30-45 cm (with the lower values referring to sawgrass while the higher ones to mangrove). Input parameters regarding vegetation at the three sites are listed in Table 4.3.

Figure 4.34: Examples of sawgrass in South Florida wetlands. Left photo: site TS/Ph-1 near Site 2 (photo by G. Rubio and D. Rondeau). Right photo: Claudium jamaicense – Jamaica swamp sawgrass – Florida (photo by Larry Allain)

Figure 4.35: Examples of mangroves in South Florida wetlands. Left photo: Florida Everglades Shark River Slough mangrove forest (photo by AmeriFlux website). Right photo: mangroves in Florida Bay (photo by USGS)

4.5.3.2 Soil parameters

Two soil types are usually present in the Florida Everglades: marl and peat. Marl is the main soil of the short-hydroperiod wet prairies near the edges of the southern Everglades while peat is more common in Everglades marshes (*Everglades peat* and *Loxahatchee peat*). In particular, Everglades peat is composed almost entirely of the remains of sawgrass (*Lodge*, 2004).

The existing body of knowledge concerning peat soil is not as large as that concerning mineral soil. However, in recent years, there has been increasing interest about wetlands (*Hoag et al.*, 1995) which encouraged an increasing number of analysis focused on the hydraulic properties of peat (*Boelter*, 1965; *Ingram*, 1967; *Hoag et al.*, 1995; *Holden et al.*, 2003; *Rizzuti et al.*, 2004; *Rosa et al.*, 2007). Almost all the studies agree in the fact that the characteristics of peat strongly depend on the nature of peat, in terms of organic matter fraction and botanical composition.

Peat must contain no more than a certain maximum inorganic content (20% is a typical value, see *Myers*, 1999). The ash content (or mineral content) for the Everglades peat usually ranges from about 25% to 90%; however, despite this high percentage of mineral content, it behaves hydrologically as peat (*Myers*, 1999). Porosity in pure peat is high if compared to that of mineral soils. As the percentage of peat in a mixture peat-mineral soil increases from zero to 100%, the porosity increases from 40% to 90% (*Boggie*, 1970; *Myers*, 1999; *Walczak et al.*, 2002).

A generic classification of soil at the three sites under analysis is given by the FCE-LTER web site. The soil at Site 1 is classified as wetland peat, at Site 2 the soil is wetland marl, and at Site 3 is wetland marly peat. The FCE-LTER web site provides also the fraction of organic matter in the three sites: 22% (Site 1); 14% (Site 2); 25% (Site 3). Starting from this information, the porosity in the three sites has been derived from the relation porosity-peat fraction (Figure 4.36) presented by *Myers* (1999), obtaining the following values: 0.48 (Site 1); 0.45 (Site 2); 0.49 (Site 3).

These values of porosity are very similar to those typical of silty clay (Site 1 and Site 3) and clayey loam (Site 2). Some literature confirms the analogy between peat and clayey soils; for example, *Myers* (1999), investigating peat characteristics within the Florida Everglades, states that organic matter in soils, as well as clayey soils, is known to interact with water at microscopic level through chemical and electrostatic forces; moreover, as in clays, shrinking and swelling behavior in organic soils may show a hysteretic behavior. Therefore, recurring to such analogy, the parameters m, demarking the pore size distribution index [Eqs.(4.1) and (4.2)], for the three sites considered have been set equal to those given by *Rawls et al.* (1989), relative to a silty clay soil (Site 1, Site 3) and a clayey loam soil (Site 2). For all the three sites, the values of

bubbling pressure head ψ_s have been fixed in -9.19 cm, in agreement with *Naasz et al.* (2005), who analyzed a peat by means of laboratory experiments (using the *Instantaneous Profile Method*) during a wetting-drying cycle. The same authors provide two pairs of parameters for the *van Genuchten* (1980) retention model; one is relative to the wetting values while the other refers to the drying ones. Assuming an average behavior, and then considering mean parameter values between the two different pairs, the value of ψ_s has been obtained, following *Morel-Seytoux et al.* (1996), to convert *van Genuchten* (1980) parameters to *Brooks and Corey* (1964) model parameters.

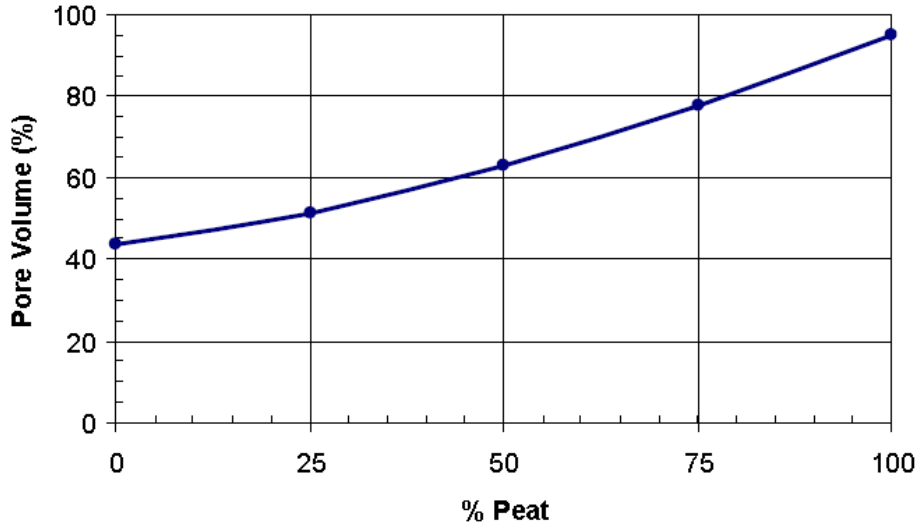

Figure 4.36: Effect of peat fraction in a peat-sand mixture on the total porosity of the mixture (from *Myers*, 1999 and based on *Boggie*, 1970)

The saturated hydraulic conductivity has been assumed equal to 7 cm/day for peat (Site 1), 16 cm/day for marl (Site 2) and 14 cm/day for marly peat soil (Site 3). These values fall within the range found in peat samples taken from isolated wetlands in southern Florida (that is 0.63÷25.92 cm/day; *Myers*, 1999) and are very close to those obtained by other authors from laboratory analysis (*Naazs et al.*, 2005; *Katimon et al.*, 2007). All the soil characteristics here adopted are summarized in Table 4.3, together with the vegetation parameters.

It is important to point out that the model developed by *Laio et al.* (2009) assumes the soil column homogeneous and isotropic. Actually, the pure peat porosity decreases as the depth increases, assuming an almost constant value in the *catotelm zone* (deeper layer with a well-decomposed peat) while the hydraulic conductivity of the *acrotelm* (shallower layer commonly between 0-20 cm and made up of undecomposed dead plant material) has been found to be

up to five orders of magnitude greater than that of the catotelm (*Boelter*, 1965). Moreover, pure peat presents a strong anisotropy in hydraulic conductivity with horizontal conductivity usually greater than the vertical one (*Weaver and Speir*, 1960; *Boelter*, 1965). This anisotropy can be observed also in the vertical direction: when the flux of water is upward the peat can present a slightly higher saturated conductivity than when it is downward oriented (*Myers*, 1999). Although the two assumptions of homogeneity and isotropy may appear too severe if applied to a pure peat, they seem reasonable if the ash content is as elevated as in the sites under consideration.

		Site 1	Site 2	Site 3
Vegetation		*Mangrove*	*Sawgrass*	*Sawgrass*
Average rooting depth (b)	*cm*	12	10	10
Soil		*Peat*	*Marl*	*Marly Peat*
Pore size distribution (m)		0.127	0.194	0.127
Saturated Hydraulic Conductivity (k_s)	*cm/day*	7.0	16.0	14.0
Porosity (n)		0.48	0.46	0.49
Bubbling pressure head (ψ_s)	*cm*	-9.19	-9.19	-9.19

Table 4.3: Vegetation and soil parameters at the three sites

4.5.3.3 Parameters for the lateral flow evaluation

The estimation of the lateral flow term [Eq.(4.8)] requires to evaluate two parameters: y_0 and k_l. The model parameter y_0 corresponds to the position of the free surface in the nearest water body, measured with respect to the soil surface (ground elevation at the site examined) and it is supposed to be constant in time, while k_l is the proportionally constant for the saturated lateral flow [Eq.(4.10)].

When the external water body is the ocean (Site 1), y_0 is simply the opposite of the ground elevation, measured with respect to the mean sea level. For Sites 2 and 3, the nearest water bodies are two different water canals, with available measurements of daily water levels. In a generic site, the difference in elevation between the water table position and the water surface in the nearest canal, can generate two different conditions: the water body provides water to the site (Figure 4.37a) or the site loses water towards the water body (Figure 4.37b).

The reference elevations y_0, are taken as constant and equal to the mean annual value for the annual analysis, and to the mean seasonal value for the seasonal analysis. At Site 2, the nearest water body is the canal C111, whose historical daily series of water levels recorded at station S176H has been used.

For Site 3 the nearest canal is the levee L31W, which has a gauging station (S175H) about 2 km from the groundwater well. The observation periods, the mean annual and seasonal values of the water levels in the canals, the ground elevations and the resulting annual and seasonal values of y_0 for both sites are summarized in Table 4.4.

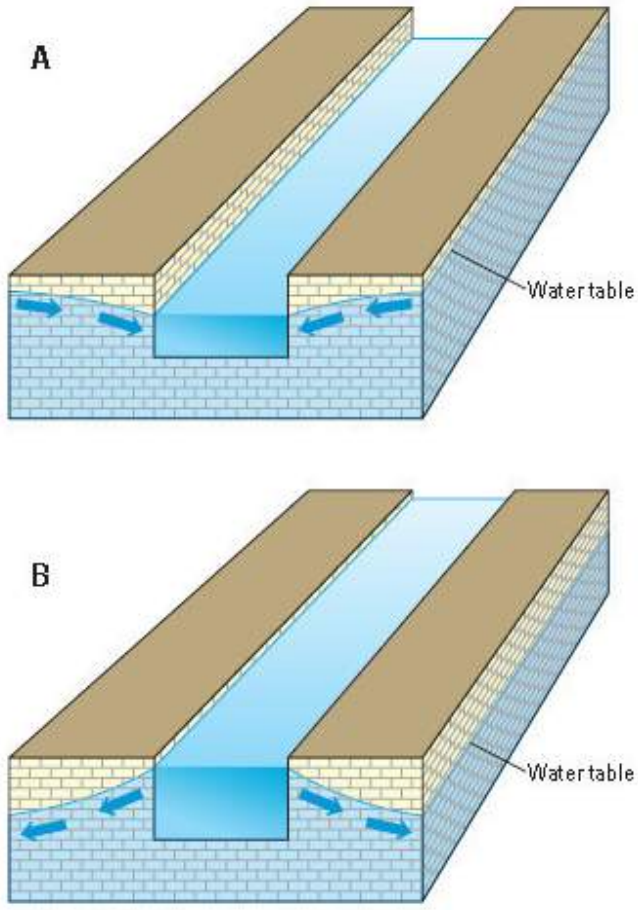

Figure 4.37: Schematic representation of the canals of southern Florida. The lateral flow can be oriented towards the canals (A) or can be outgoing from the canals (B) according to the relative position of the water surface into the canals and the water table (from *Renken et al.*, 2005)

Site		Site 2	Site 3
Water Canal		*C111*	*L31W*
Water Levels Measurament Station		*S176H*	*S175H*
Operating agency		*SFWMD*	*SFWMD*
Water Level Observation Period	*from*	*1/1/1978*	*6/17/1970*
	to	*6/30/2007*	*7/8/1997*
Water Levels (*m a.s.l. - NAVD88*)	**Annual**	0.83	0.56
	Wet Season	0.91	0.73
	Dry Season	0.75	0.37
y_0 (*m*)	**Annual**	-0.26	-0.27
	Wet Season	-0.18	-0.08
	Dry Season	-0.36	-0.46

Table 4.4: Mean annual and seasonal water levels into the canals C111 and L31W (in m a.s.l. - NAVD88) and annual and seasonal values of the model parameter y_0 for Sites 2 and 3 (in m below the soil surface for each site). For Site 1, the nearest water body is the ocean, and y_0 is simply the opposite of the ground elevation (-0.10 m). *Dry Season* from December to May; *Wet Season* from June to November

The model constant k_l, for each site, has been evaluated taking into account the distance d_0 from the water table station to the nearest water body, the horizontal dimension of the considered area (D) and the bedrock depth referred to the free surface of the external water body (h_0).

Although the model works at a plot scale (1-100 m^2), considering that the external water bodies are rather close to the sites, it seems opportune to consider a dimension D not too high to assure the horizontality of the water table in the areas under consideration and the applicability of the Eq.(4.8). For this reason, a dimension D has been fixed equal to 7.5 m for all the three sites after a calibration procedure.

The bedrock depths in the three sites have been obtained from a map (Figure 4.38) showing the configuration of the base of the superficial aquifer system in Dade County (*Fish et al.*, 1991). In the cases of canals (Site 2 and Site 3), the values of h_0 have been referred to the mean annual levels of the free surface in the nearest water body, also in the seasonal analysis (k_l invariant in time).

The values of k_l obtained for each site, as well as all the other parameters required for their estimation, are shown in Table 4.5. It is worth noting that Site 1, being much closer to the external water body than the other two sites,

presents a lateral flow coefficient almost three times higher than the other two sites.

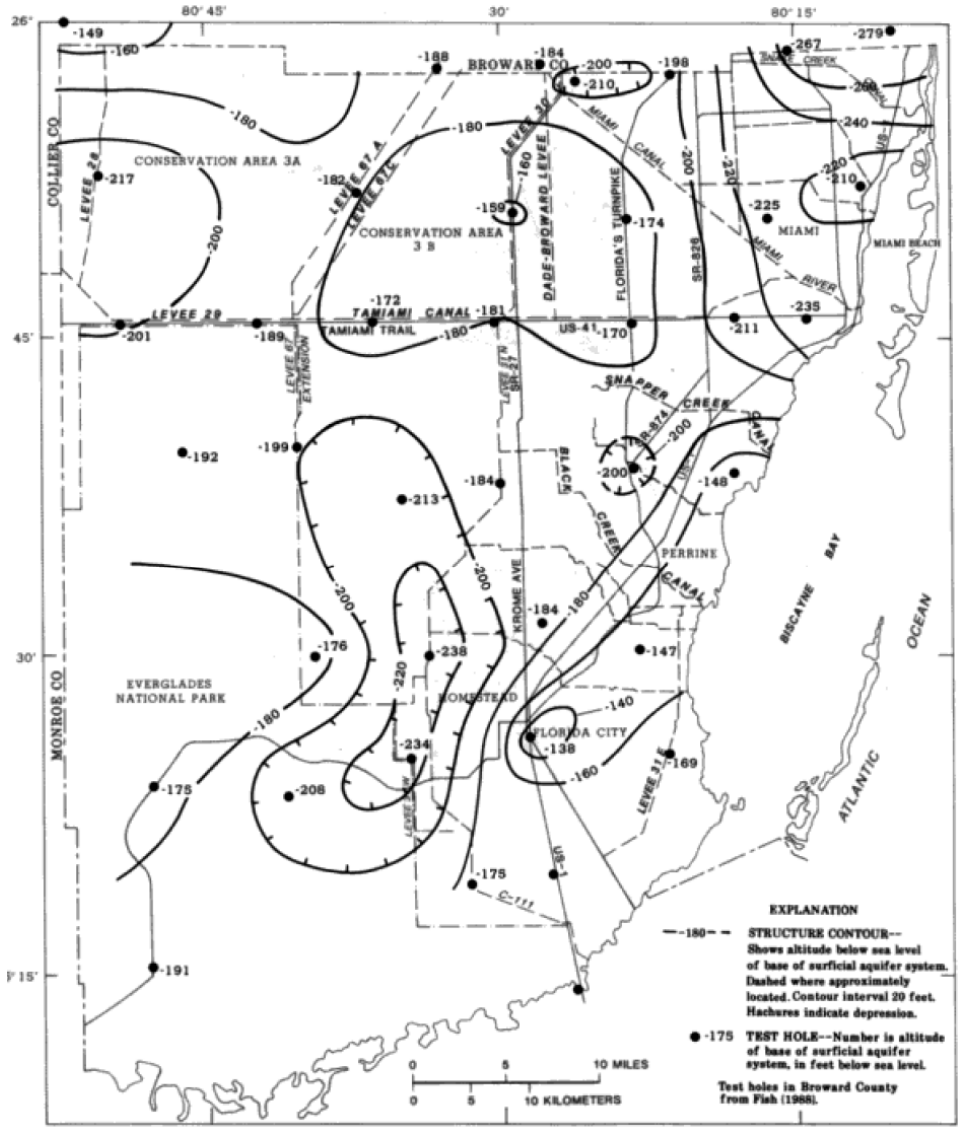

Figure 4.38: Configuration of the base of the superficial aquifer system in Dade County, Florida, USA; isolines in feet (from *Fish et al.*, 1991)

Site	nearest water body	h_0	D	d_0	k_1
		m	*m*	*m*	*1/d*
Site 1	*ocean*	77.3	7.5	69	0.01051
Site 2	*canal C111*	73.5	7.5	411	0.00381
Site 3	*levee L31W*	64.1	7.5	366	0.00327

Table 4.5: Parameters for the estimation of the coefficient k_1 for each site. h_0 is the bedrock depth respect to the water body surface in m; D is the horizontal dimension of the considered area in m; d_0 is the distance of each site from the nearest water body (see Figure 4.3)

4.5.3.4 Rainfall and evapotranspiration

The climatic forcings required by the water balance model are the daily potential evapotranspiration rates and two rainfall parameters: daily mean depth α and interarrival rate λ. The EDEN web site provides historical series of rainfall and potential evapotranspiration useful for the generation of such climatic parameters.

Rainfall data based on *Next Generation Radar* (NEXRAD) provides a complete spatial coverage of rainfall amounts for the State of Florida. The NEXRAD coverage for the South Florida Water Management District area includes rainfall amounts at 15-minute resolution intervals for the period January 1st, 2002 to present with a spatial resolution of 2 km (EDEN web site). The daily rainfall series considered for the three sites are referred to the period from 01/01/2002 to 09/30/2008 (Figure 4.39). The annual and seasonal values of α and λ obtained from the series in the three different sites are summarized in Table 4.6 (annual) and Table 4.7 (seasonal).

Daily potential evapotranspiration (PET) estimates on a 2 km-resolution grid have been produced by EDEN for the State of Florida by means of a model that uses solar radiation obtained from *Geostationary Operational Environmental Satellites* (GOES) and climate data coming from the *Florida Automated Weather Network*, the *State of Florida Water Management Districts* and the *National Oceanographic and Atmospheric Administration* (NOAA). Daily PET values (in millimeters) are then extrapolated by location for each of the EDEN stations and published at the EDEN web site. The daily series of potential evapotranspiration considered in this application for the three sites are relative to the period from 06/01/1995 to 12/30/2007 (Figure 4.40). Table 4.6 and Table 4.7 show, for each site, the mean daily values of potential evapotranspiration during the year and during the two seasons, respectively.

Site	Weather Station associated (EDEN)	Annual Parameters			
		Rainfall			PET
		α	λ	Θ	
		cm	*1/d*	*cm/year*	*cm/day*
Site 1	*Taylor River at Mouth*	0.79	0.347	99	0.42
Site 2	*L31W*	0.82	0.431	130	0.38
Site 3	*TS2*	0.79	0.414	119	0.39

Table 4.6: Mean annual values of the rainfall parameters (mean depth α, mean frequency λ and total precipitation amount Θ) and potential evapotranspiration (*PET*). The weather stations associated are managed by SFWMD and the data are available at the EDEN web site

Site	Weather Station associated (EDEN)	Dry Season Parameters				Wet Season Parameters			
		Rainfall			PET	Rainfall			PET
		α	λ	Θ		α	λ	Θ	
		cm	*1/d*	*cm/seas*	*cm/day*	*cm*	*1/d*	*cm/seas*	*cm/day*
Site 1	*Taylor River at Mouth*	0.62	0.206	23	0.37	0.86	0.491	77	0.46
Site 2	*L31W*	0.71	0.245	32	0.34	0.87	0.621	99	0.42
Site 3	*TS2*	0.70	0.244	31	0.35	0.83	0.588	89	0.43

Table 4.7: Mean seasonal values of the rainfall parameters (mean depth α, mean frequency λ and total precipitation amount Θ) and potential evapotranspiration (*PET*). *Dry Season* from December to May; *Wet Season* from June to November. The weather stations associated are managed by SFWMD and the data are available at the EDEN web site

(a)

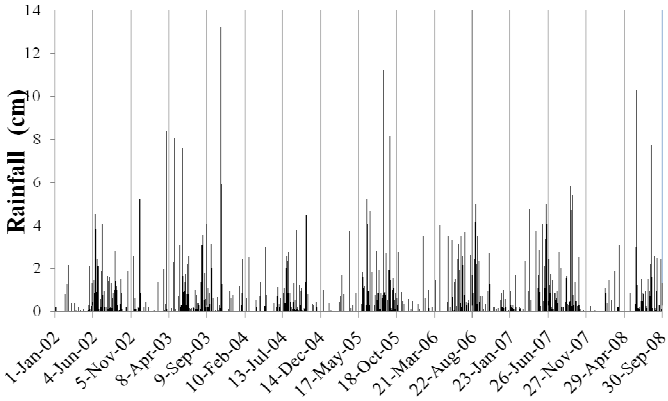

(b)

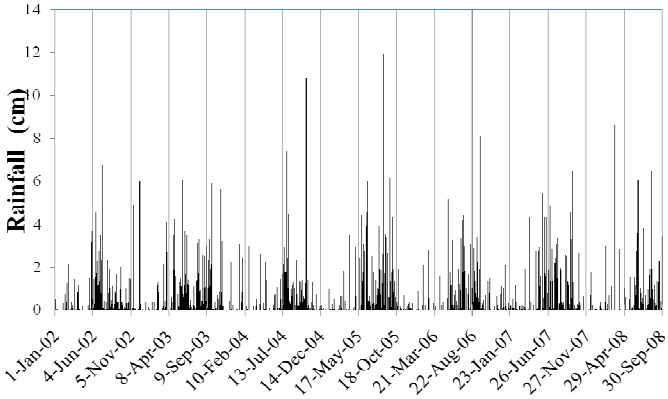

(c)

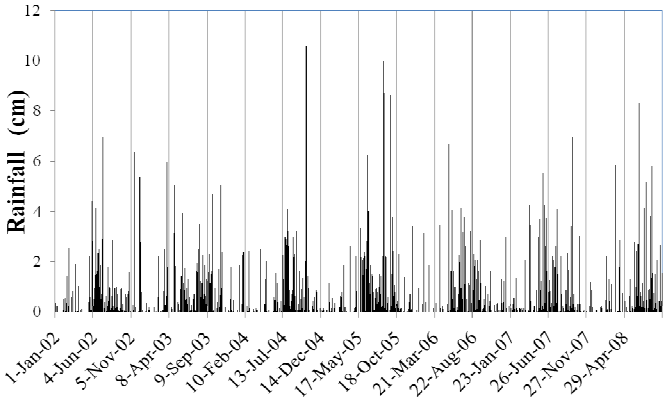

Figure 4.39: Daily rainfall time series (from EDEN web-archives): a) Site 1 (station Taylor River at Mouth); b) Site 2 (station L31W); c) Site 3 (station TS2)

(a)

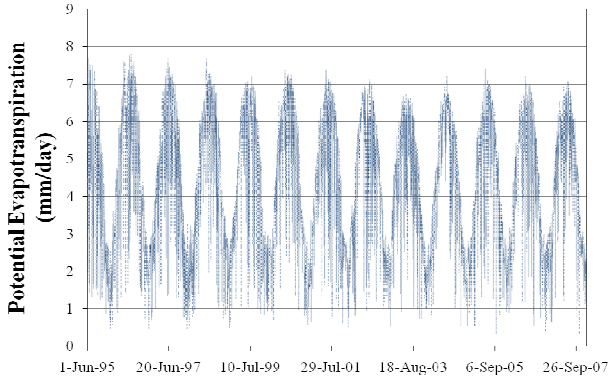

(b)

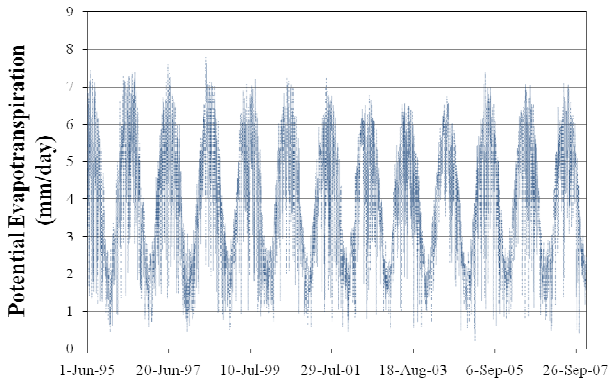

(c)

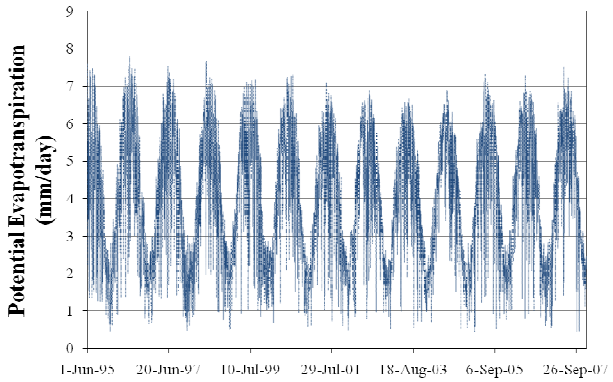

Figure 4.40: Daily Potential Evapotranspiration time series (from EDEN web-archives): a) Site 1 (station Taylor River at Mouth); b) Site 2 (station L31W); c) Site 3 (station TS2)

4.5.4 Results and analysis

The comparison between the model results and the observed water table levels has been carried out in terms of pdf's and cdf's. In particular the analytical results are compared to the empirical relative frequency distribution, a relative frequency histogram obtained from the data.

As previously mentioned, the model does not take into account water levels above the soil surface, and describes fluctuations of the saturated zone up to the soil surface, which corresponds to finding the water table at a depth $\tilde{y}=\psi_s$; this position is taken as the upper threshold value for data to be used (see Sect. 4.4.1.5). The rare and short periods of submergence occurring at some sites are limited to a few days per year, and have been ignored in this analysis. Only the water table positions below the depth ψ_s have been then considered in the computation of the empirical distribution functions. The Markovianity of the dynamic system allows for such simplification and guarantees that the analytical probability distribution function correctly describes the conditional probability of $y \leq \psi_s$.

4.5.4.1 Annual Analysis

The annual analysis has been carried out with a set of model input variables (rainfall parameters, potential evapotranspiration, water levels into the canals) evaluated as annual average values from the daily time series. The measured time series are simultaneous only for a relatively short period of time (Table 4.8) and do not cover the whole time span of the water level measurements; however, since the aim of this work is to characterize the long-term hydrological behaviour of groundwater at each site, it has been chosen to keep the entire series of water level data and extend the validity of the parameters evaluated from shorter time series.

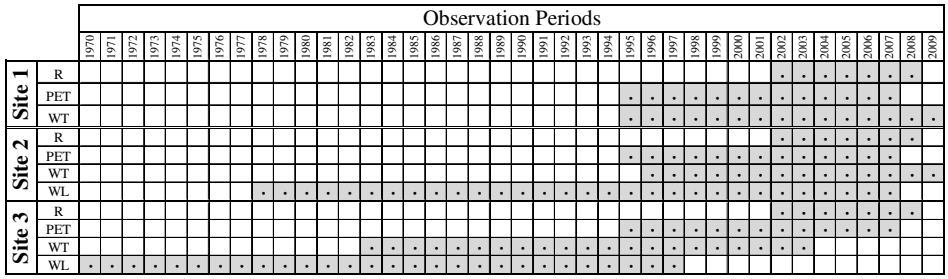

Table 4.8: Observation periods for the different time series: R= Rainfall; PET= Potential Evapotranspiration; WT= Water table depth; WL= Water levels into the canal

Figures 4.41a, 4.42a and 4.43a show the pdf's of water table position for the three different sites (Site 1, 2 and 3 respectively) using the annual parameterization. The water table positions (cm) are reported with respect to the ground surface at each site. Figures 4.41b, 4.42b and 4.43b show the comparison between the empirical cdf's of water table and the cdf's obtained from the model for the three sites under analysis. The values of the critical water table position y_c marking the transition between SWT and DWT conditions are respectively -34 cm (Site 1), -45 cm (Site 2) and -47 cm (Site 3); consequently, the pdf's show a discontinuity at water table positions equal to $y_c + \psi_s$ (-43 cm, -54 cm and -56 cm respectively).

The pdf's and cdf's of water table depth obtained by the model for the three sites match accurately those obtained from the empirical data, demonstrating how the model, using annual parameters, is capable of representing the physical reality in each site. In Table 4.9, a comparison between some statistics relative to the entire observed series and those arising from the model pdf's, is shown. The mean positions of the water table observed and those obtained by the model are very similar, with differences on the order of 2 cm. Also the values of standard deviation found by the model are rather similar to that observed, with difference on the order of 3-8 cm, even if an underestimation of the standard deviations from the model can be observed and, thus, the model underestimates the variability of the observed process in all the considered sites.

	Annual			
	Observed		***Model***	
	Mean WT	**SD**	**Mean WT**	**SD**
Site	*cm*	*cm*	*cm*	*cm*
Site 1	-28.4	10.7	-30.1	7.6
Site 2	-43.6	19.2	-41.5	13.2
Site 3	-46.8	23.8	-49.2	15.1

Table 4.9: Comparison between model results and empirical data for the mean annual values of water table position (Mean WT). Standard deviations (SD) are also reported

As mentioned above (see Sect. 4.4.1.5), the analytical pdf has a lower bound, $\tilde{y}_{lim}$, equal to -46 cm, -75 cm, and -83 cm for the sites 1, 2 and 3 respectively. In the historical time series one can find that the minimum water table positions recorded are -63 cm (Site 1), -100 cm (Site 2) and -120 cm (Site

3). These different values are probably due to an overestimation of the lateral flow or an underestimation of the exfiltration occurring at large depths.

The empirical pdf of Site 2, shown in Figure 4.42a, presents bimodal features. Site 2, in fact, displays a range of variation of water table depths between the wet and the dry season consistently different from that observed in the Site 1. From Table 4.2 one can note that the difference between the mean seasonal depths of the water table during the dry and the wet season for Site 2 is almost two times that relative to Site 1. Also the difference between the standard deviations during the dry and the wet seasons for Site 2 is almost two time that relative to Site 1.

The wide range of variation of water table depths for Site 2 could be physically explained by the presence of a nearby canal, where the water levels during the wet and the dry seasons are maintained at consistently different positions (see Table 4.4) for agricultural scopes. One of the main aims of the canals is, in fact, to supply water during the drier periods. This fact leads to different lateral flow contributions during the two seasons that, obviously, affect the water table positions at the seasonal scale, and, as a consequence, also at the annual scale. From the analysis of the historical data of water table for Site 2 (Sect. 4.5.2), one can note that, after the procedure for removing the seasonality from the original series, the "detrended" series of water table still presents a strong signal in the ACF (Figure 4.31b) due to the influence of the nearby canal on the water table dynamics. The fact that the empirical pdf of Site 2 shows a bimodal shape could be also due, in a minor way, to the different soil properties (overall the hydraulic conductivity) in respect to those relative to the soil in Site 1. Marly soils (as in Site 2) are usually characterized by a hydraulic conductivity higher than peat (as in Site 1) and this could makes the water table dynamics faster, thus emphasizing the effects of the seasonal climatic variability on the water table fluctuations.

Analogues considerations could be applied for Site 3, whose nearest water body is again constituted by a canal and where the soil is classified as marly peat. In fact, the empirical pdf of Site 3 (Figure 4.43a) also shows a weak impact of seasonality, with a bimodal shape even if this behaviour is less marked than in the case of Site 2.

The model, working at the annual scale, considers a water level into the external canals constant and equals to the mean annual position. For this reason, it is not able to take into account the different seasonal contributions of the lateral flow. On the other hand, the use of smoothed climatic parameters at the annual scale allows the model to reduce the effect of the seasonal climatic variability. The results obtained for the three sites suggest that the model, at the annual scale, is likely to underestimate the lower tail of the distribution of water table levels, but provides a probabilistic description very close to the empirical one, especially for the Site 1.

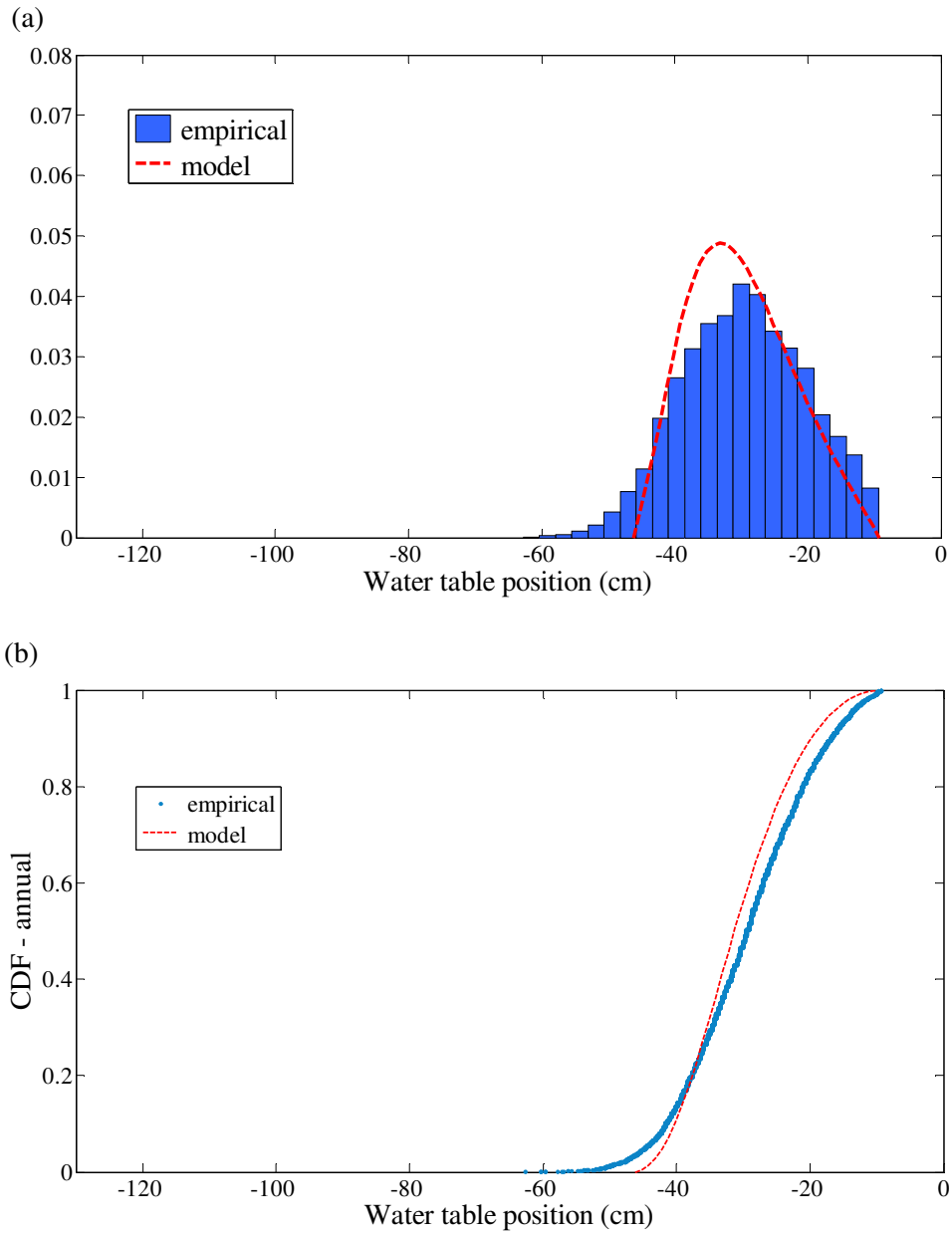

Figure 4.41: Site 1, Annual Analysis. a) pdf of the water table position obtained from the model compared to the empirical pdf of the water table. b) Comparison between the cdf's obtained from the observed series of water table and from the model

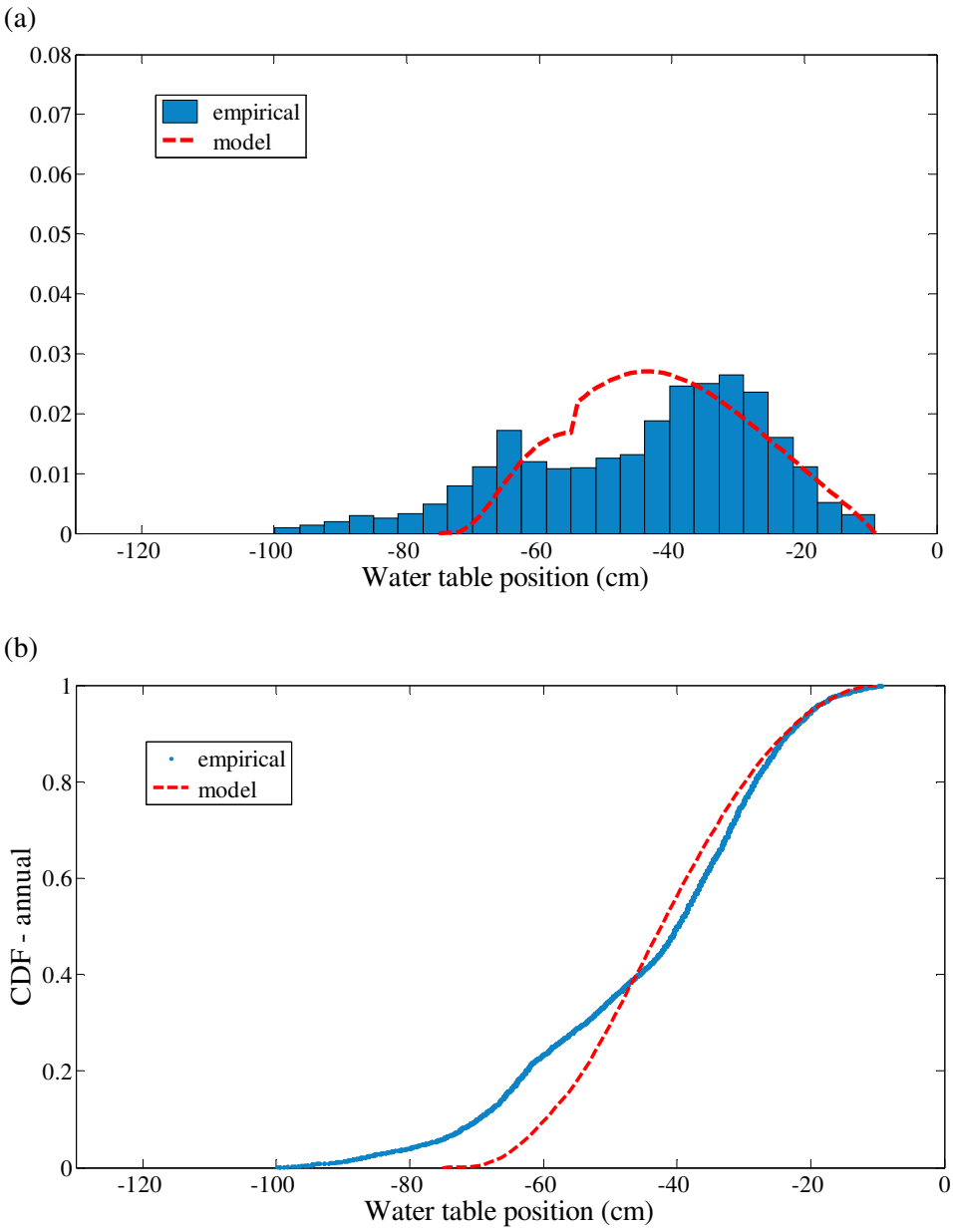

Figure 4.42: Site 2, Annual Analysis. a) pdf of the water table position obtained from the model compared to the empirical pdf of the water table. b) Comparison between the cdf's obtained from the observed series of water table and from the model

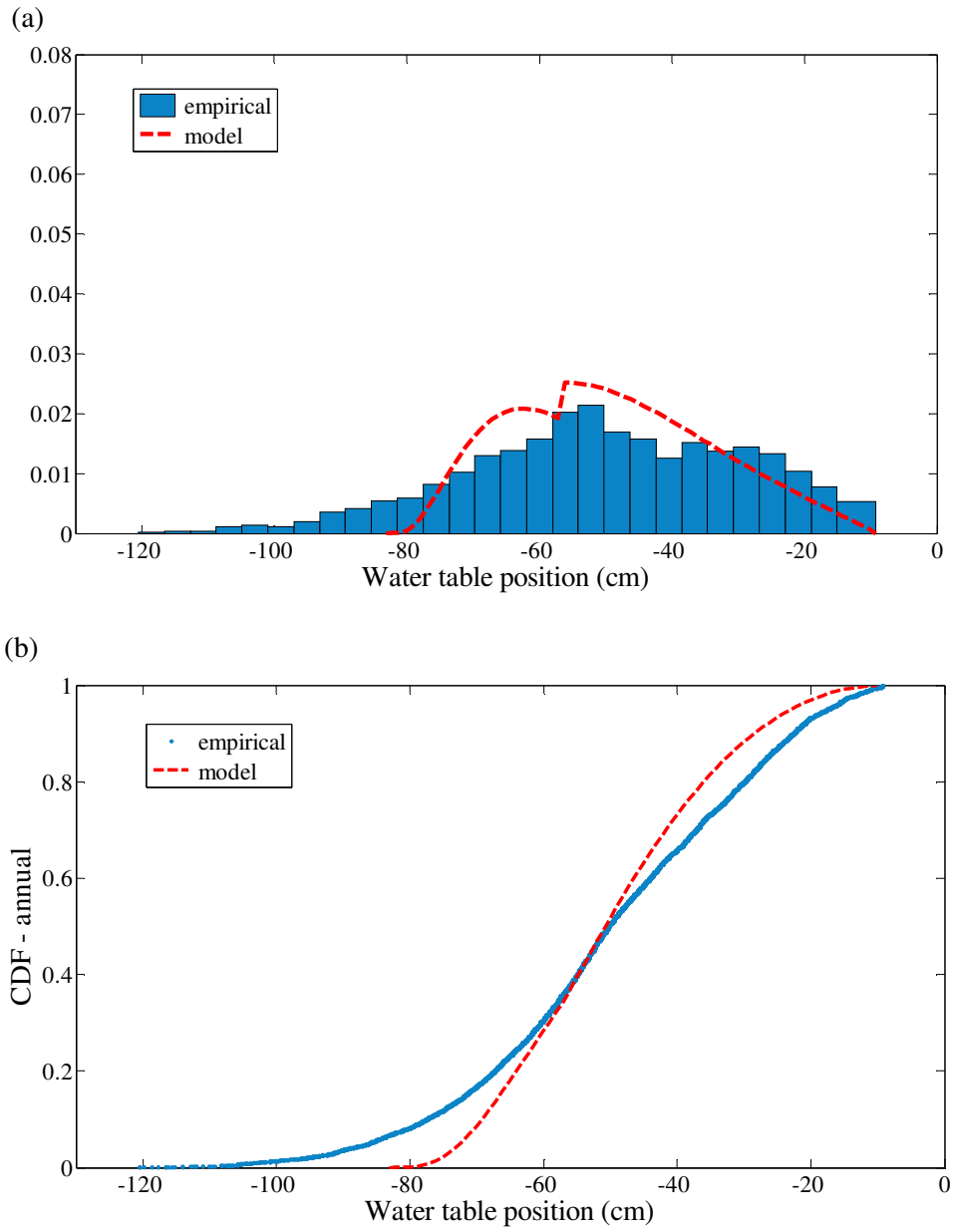

Figure 4.43: Site 3, Annual Analysis. a) pdf of the water table position obtained from the model compared to the empirical pdf of the water table. b) Comparison between the cdf's obtained from the observed series of water table and from the model

4.5.4.2 Seasonal Analysis

The seasonal analysis has been carried out by splitting the annual time series into two seasons (i.e. computing the average seasonal values for the daily depth of rainy days and rate of occurrence, for the potential evapotranspiration and for the water surface position of the external water bodies) and comparing the resulting model pdf's and cdf's with the seasonal empirical ones. The wet season ranges from June to November and the dry season from December to May.

As shown in Table 4.7, the wet season is characterized by more intensive and frequent rainfall events, with a total amount of precipitation about three times the values of the dry season. Thus, a higher amount of water achieves the soil but, at the same time, there is a higher rate of evapotranspiration. The resulting water table is shallower during the wet season and all the observed hydroperiods occur during this season. Moreover, during the dry season, the water table position fluctuates in a wider range of depths than that occurring during the wet season because of the prolonged period with fewer rainfall events from December to May. Another cause of this wide range is that, in Sites 2 and 3, the external water bodies are constituted by two different canals, that, as mentioned before, are often used to supply water to that places during the dry season, altering the natural dynamics of the water table.

The effects on water table fluctuations due to the differences in the climatic variables between the wet and the dry season, are more pronounced when the hydraulic conductivity of the soil is higher, because the water table dynamics becomes faster. For this reason, in the cases of more permeable soils, the differences in the seasonal water table position are expected to be more noticeable. In fact, this is the case observed in the data for Site 2 and 3, where the soil types present are marl and marly peat, respectively, whose hydraulic conductivities are higher than that relative to a peat (soil present at Site 1).

Figures 4.44, 4.45 and 4.46 show the seasonal comparison between the pdf's resulting from the model and the empirical data, while Table 4.10 summarizes the mean seasonal values, together with the standard deviations, predicted by the model and those observed at each site. The comparison in terms of mean values is indeed positive, and the differences during the wet season are only about 1.5÷5 cm, while during the dry season they are larger and in the order of 10÷14 cm (except for the case of Site 1, whose difference is negligible). As in the case of the annual analysis, the model gives lower values of standard deviation than those observed in both the seasons, showing again a model underestimation of the variability of the observed process.

The analysis shows that the model results at seasonal level are not as accurate as at the annual level. This is evident mainly at Sites 2 and 3 (Figure 4.45 and 4.46), while the model seems to have a better performance at Site 1

(Figure 4.44). For the other two sites, the model pdf's of water table shift towards shallower values during the wet season and towards deeper values during the dry season. This behaviour is probably due to the dependency of the water table position to the initial condition at the beginning of each season, rather than to the model parameter for the season itself; this effect is expected to play an important role, especially when the differences between the two seasons are marked, and it cannot be accounted by the model, which represents only a steady state statistical condition.

The persistence of a shallow water table at the end of the wet season and the relatively slow dynamics of the water table, influence the water table depth over almost the entire dry season. Similarly, the initial condition at the beginning of the wet season influences the water table positions during the period from June to November but being the rainfall events more frequent and intense, it is likely that a steady condition is reached earlier during the wet season. This could explain the fact that the model provides performances during the wet season better than those during the dry season. Another reason that, in a minor way, could affect the accuracy in the seasonal modelling of the water table dynamics during the dry season is that, when the water flow is upwards oriented, the soil at the three sites is characterized by an upwards hydraulic conductivity higher than the downwards one (*Myers*, 1999). Such behavior is not captured by the analytical model, which assumes an isotropic soil, but it may enhance the ability of wetlands to maintain shallow water table even in absence of precipitation.

Despite the above considerations, the model seems to capture adequately the general shape of the water table pdf's during the wet season, giving a reasonable representation of the mode and dispersion of the empirical pfd's.

Although in the seasonal analysis the model takes into account the different seasonal contributions of the lateral flow, by considering two different water levels into the canals (one for each season, that is equal to the mean seasonal position), however, as in the case of the annual analysis, the presence of canals as external water bodies could be responsible of discrepancy between the model and the empirical pdf's of water table. The external water surface has been considered constant in time for the each season, while the water levels into the canals are also subjected to daily fluctuations which may increase the variability of water table positions, and that the model is not able to consider. This could explain the fact that the model performances relative to Site 1, close to the ocean, are better than those relative to Sites 2 and 3.

Site	Dry Season				Wet Season			
	Observed		*Model*		*Observed*		*Model*	
	Mean WT	*SD*	Mean WT	*SD*	Mean WT	*SD*	Mean WT	*SD*
	cm	*cm*	*cm*	*cm*	*cm*	*cm*	*cm*	*cm*
Site 1	-34.4	*8.1*	-34.2	*6.5*	-22.6	*9.8*	-27.5	*7.7*
Site 2	-54.8	*16.2*	-64.4	*9.3*	-32.6	*15.1*	-29.3	*10.4*
Site 3	-60.6	*19.1*	-74.5	*10.7*	-33.4	*20*	-33.4	*12.0*

Table 4.10: Comparison between model results and empirical data for the mean seasonal values of water table position (Mean WT). Standard deviations (SD) are also reported. *Dry Season* from December to May; *Wet Season* from June to November

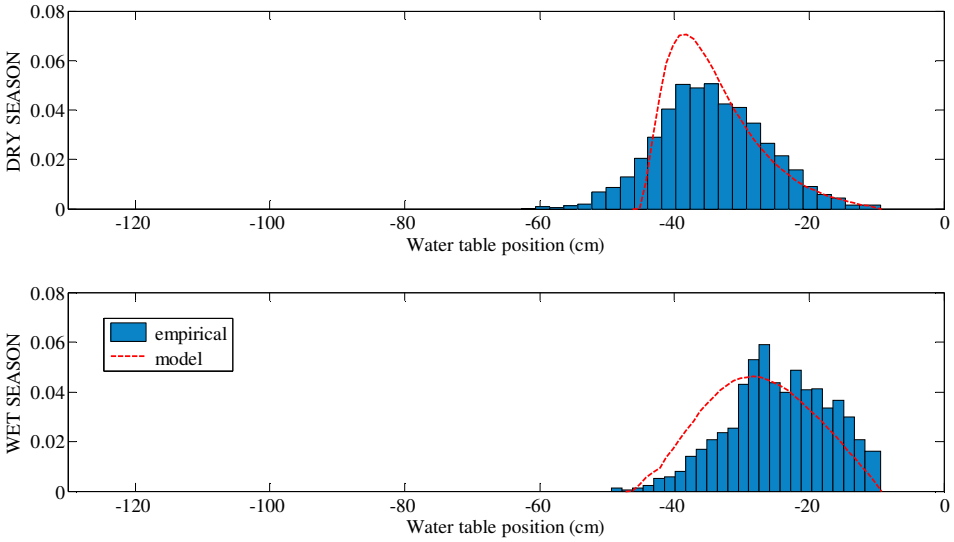

Figure 4.44: Site 1 - Seasonal Analysis. Probability density functions of water table position obtained from the model compared to the empirical data. On the top the results relative to the dry season (from December to May); at the bottom those relative to the wet season (from June to November)

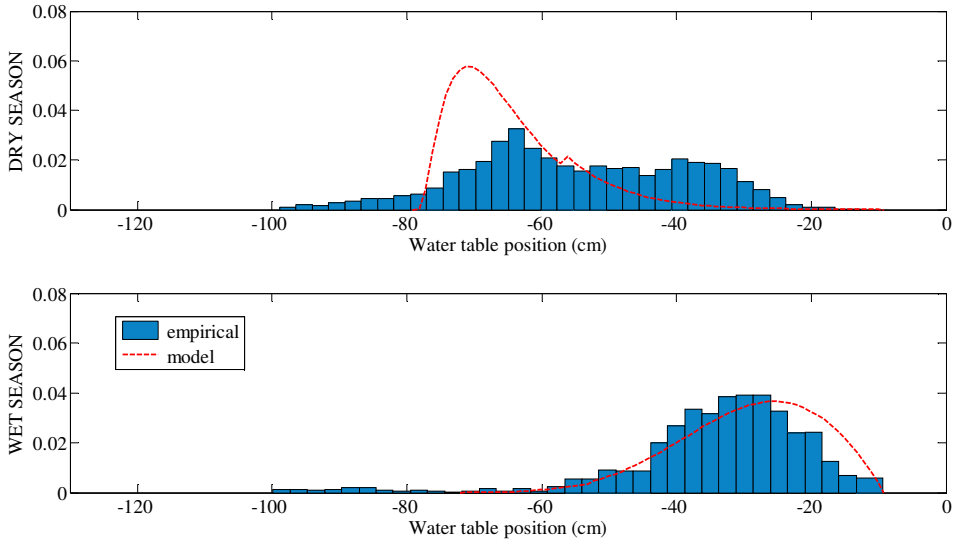

Figure 4.45: Site 2 - Seasonal Analysis. Probability density functions of water table position obtained from the model compared to the empirical data. On the top the results relative to the dry season (from December to May); at the bottom those relative to the wet season (from June to November)

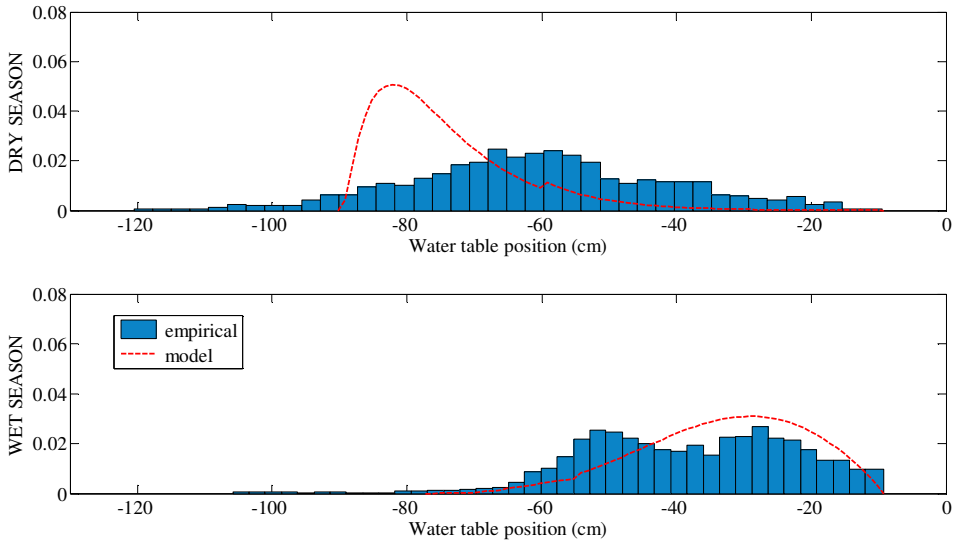

Figure 4.46: Site 3 - Seasonal Analysis. Probability density functions of water table position obtained from the model compared to the empirical data. On the top the results relative to the dry season (from December to May); at the bottom those relative to the wet season (from June to November)

4.6 Concluding Remarks

Considering the increasing attention devoted in recent years to wetlands and groundwater-dependent ecosystems, it is becoming increasingly relevant to develop and test quantitative models for the analysis of such ecosystems. With this aim, *Rodriguez-Iturbe et al.* (2007) highlighted the need of an analytic approach to the dynamics of interactions between climate, soil and vegetation in such humid ecosystems. In groundwater dependent ecosystems the water table has a crucial role in supplying water to plants, interacting directly with the root zone. For this reason it is fundamental to consider the strong coupling between water table and soil moisture dynamics. A recent ecohydrological framework, derived from a work by *Ridolfi et al.* (2008) and proposed by *Laio et al.* (2009) and *Tamea et al.* (2009), provides a probabilistic description of the water table fluctuations and the soil moisture dynamics in groundwater-dependent ecosystems. In particular the authors proposed two analytical models, which have been discussed in Sect. 4.4.1 and 4.4.2 respectively.

Since a validation of this model on real cases is still missing, an application to different sites has been carried out and presented in Sect. 4.5.

In particular, the model by *Laio et al.* (2009) for the study of the stochastic water table depth has been applied to three sites in the Florida Everglades using both annual and seasonal parameterizations. The resulting pdf's and cdf's of water table depths have been compared to those resulting from daily historical series recorded at each site.

The annual analysis has shown the capability of the model to reproduce the observed distribution, using mean annual values of rainfall depth and frequency, evapotranspiration and water surface position of the nearest water body as input parameters. In particular, the model seems to be more accurate in the case of Site 1, where the water table dynamics during the wet and the dry season equally depend on lateral flow from an external water body. Since the other two case studies (Sites 2 and 3) are characterized by the presence of a nearby canal, where, for agricultural practices, the water levels during the dry season are maintained at consistently different position from those during the wet season, the empirical pdf's of water table present a shape almost bimodal that the model, working at the annual scale, is unable to reproduce.

Using the seasonal parameterization, the model still reproduces the observed pdf in Site 1 quite well. For the other two sites, the seasonal pdf's are strongly affected by the initial position of the water table at the beginning of each season and the model reproduces the data distribution less accurately. In particular, during the dry season, the model pdf's are shifted towards deeper values, while the pdf's of the wet season are shifted towards shallower water table values. This effect is much more evident during the dry season, when

reaching a steady state condition requires more time than that required during the wet season.

The model results, in both the annual and seasonal analysis, are then affected by the fact that the external water surface has been considered constant in time, while both the ocean and the water level in the canals are subjected to daily/seasonal fluctuations which may increase the variability of water table positions.

The discrepancies in the annual and seasonal analysis between the observed values and the model results may be also justified by soil parameters, which have been evaluated on the basis of the available information, e.g. mineral and organic content, rather than field or laboratory analysis. Furthermore, the model assumes the homogeneity and isotropy of soil, while peat is known to have an anisotropic and hysteretic behavior. Considering the extreme variability in the hydraulic characteristics of soils, and in particular of peat, the real parameter values could be different than those assumed in the application.

In addition to this, the rainfall and evapotranspiration parameters have been estimated with time series shorter than those of water table position, and might be not fully representative of the climatic conditions occurring throughout all the time.

The model tested, using annual parameters, has shown an ability to reproduce the probabilistic description of the water table dynamics for groundwater dependent ecosystems, having limited, or no, hydroperiods. Although the application of the model has provided outstanding and important results for the specific sites considered, the study of Florida Everglades and in general of frequently submerged sites would require taking into account also water levels above the soil surface, which is the aim of ongoing and future researches.

Conclusions

This study focused on the science known as *ecohydrology*, a discipline that seeks to study the mutual interaction between the hydrologic cycle and the ecosystems. In particular, this thesis investigated the ecohydrological modelling in Mediterranean water-controlled ecosystems and in some groundwater dependent ecosystems such as the wetlands. Despite several ecohydrological studies have already dealt with Mediterranean ecosystems, often characterized by the presence of transient conditions in the soil moisture dynamics, the modelling in such areas still results rather complex and needs to find new approaches able to simplify the study of the interactions among soil, climate and vegetation. On the contrary, the applications of ecohydrological principles to the wetlands represent an extremely new field of research and, considering the increasing attention on the importance of such ecosystems, it could provide an important step toward a better understanding of these areas.

Through this thesis, after a brief general introduction to ecohydrology, where some of the most important and consolidated notions and definitions were discussed, the state of the art and the major references texts were revisited. The peculiar aspects of water-controlled ecosystems and wetlands were also highlighted. In the introductive chapter, the basis concept of a probabilistic steady-state model, conceived by *Rodriguez-Iturbe et al.* (1999a) for arid and semiarid water-controlled ecosystems in absence of transient conditions, was discussed in detail with the aim to facilitate the comprehension of the numerical model, specific for Mediterranean water-controlled ecosystems, which was proposed and discussed in the successive chapter.

The first part of this study investigated a numerical approach to the study of the soil moisture dynamics and the consequent response of vegetation, that allows to overcome the limitations connected to the adoption of an analytical approach in areas characterized by Mediterranean climatic regimes. The most important of such limitations is certainly constituted by the impossibility to hypothesize a steady-state condition to solve mathematically the soil water balance equation. In Mediterranean areas the growing season and the wet

season are markedly out of phase and this implies the insurgence of transient conditions that make the steady-state hypothesis inapplicable.

In particular, this thesis presented an innovative non steady numerical ecohydrological model for Mediterranean areas, able to reproduce the soil moisture probability density functions obtained analytically, in previous studies, for different climates and in steady-state conditions. Taking into account the seasonality of rainfall and evapotranspiration demand, the model is able to reproduce the winter process of water recharge into the soil, responsible for the soil moisture condition at the beginning of the growing season, which, in turn, could lead to transient conditions.

The peculiar aspect of the proposed model is that it solves the soil water balance through a finite difference method, working with a certain temporal step. An analysis on the importance of a correct choice of the temporal step was also carried out, showing that, in order to give a satisfactory approximation of the water losses, it should be sub-daily (in the order of 4-8 hours in Mediterranean water-controlled ecosystems). The model, working on synthetic series of rainfall, allows to compute the soil moisture time profiles, from which is then possible to derive the pdf's of soil moisture during the growing season.

To quantify the response of the vegetation in terms of water stress, an index known as *dynamic water stress* and introduced by *Porporato et al.* (2001), is used in the model. The estimate of this index requires the computation of another stress index, that is the *mean static water stress modified*, and the evaluation of two crossing properties, that are the mean number and duration of the water stress periods. Differently from the analytical computation of the dynamic water stress, the proposed model assesses the crossing properties year by year from the static water stress time profiles, which, in turn, are obtained from the soil moisture time profiles. The evaluation of the mean static water stress modified is also different, since it is not obtained analytically from the pdf of the static stress, but it is evaluated starting from the water stress time-profile, averaging year by year the static water stress only on the periods in which it is different from zero, and then evaluating the mean value using the entire simulated series. In order to obtain representative results is then opportune that the synthetic rainfall series used are sufficiently long (e.g., 100 years).

The proposed model was applied to the case study of the *Eleuterio at Lupo* river basin (Italy), a Sicilian watershed presenting a typical Mediterranean climate. In particular, two different applications were carried out. The basin is characterized by three types of soil (i.e., loamy sand, sandy loam and clay) and three types of vegetation (trees, shrubs and grasses).

In the first application, all the three soil types present within the basin were taken into account, while only the woody component of the vegetation, that is

also the most present in the basin, was investigated because it is the most critical with regard to the effects on soil moisture dynamics due to a transient period. Through this application, the influence of the modelling description of the annual climate variability on the soil moisture pdf was analyzed, by using two different annual discretizations of the model climatic parameters (i.e., mean frequency, λ, and depth, α, of rainfall and the daily potential evapotranspiration, E_{max}). In the first (named SCHEME A), the year was divided into two seasons, growing season (GS) and dormant season (DS), each one with its set of parameters (α, λ and E_{max}), time-invariant quantities representative of the season. In the second one (SCHEME B), the sets of parameters are assumed to be time-invariant quantities at monthly time-scale, so twelve sets of these parameters were considered.

The numerical pdf's of soil moisture obtained by the model were compared with those analytically obtained, showing important differences. The numerical pdf's showed a symmetry much lower than that relative to the analytical pdf's and it spread over a wider range of soil moisture, from the field capacity, which is a likely value at the beginning of the growing season, to the stomata closure point, which is the most likely value during the growing season. From this comparison, and in particular under the hypothesis of SCHEME A, the values of the mean soil moisture during the growing season obtained by the numerical model resulted higher than the values obtained using the analytical model. This is due to the fact that the numerical approach allows to take into account the transient effects and consequently, during the first part of the season the values of the soil water contents in the moisture profiles are affected by the initial soil moisture condition established at the end of the previous dormant season. This high initial value of soil moisture, often warrants the survival of woody species and theirs presence in Mediterranean areas, otherwise impossible to explain by the analytical approach, that, in fact, would lead to very high water stress indexes.

Another relevant conclusion arising from the results of the first application is that, considering a monthly climatic parameterization (SCHEME B), the numerical approach leads to a bimodal pdf of soil moisture. The behavior of the pdf arising from this type of schematization shows as in a Mediterranean area, two different periods during the growing season can be identified: the former is characterized by high values of soil moisture due to both the winter water recharge into the soil and the persistence of high precipitations and low water losses from the soil, while the latter, characterized by lower values of precipitations and higher water losses, is not dependent on soil moisture state at the beginning of the growing season and it could be considered as a steady period. The shape of the soil moisture pdf relative to SCHEME B appears hence as the result of an overlap of a typical analytical pdf in steady state condition and a more disperse non-steady pdf relative to the transient period.

The results of this application also showed that using a greater temporal discretization, as in the case of SCHEME B, the model provides higher values of all the vegetation water stress indexes, and in particular of the static water stress modified. The substantial difference between the two considered schematizations is that the SCHEME B simulates shorter stress periods with more intensive static water stress.

The latest report of the *Intergovernmental Panel on Climate Change* (*IPCC*, 2007) affirms that the climate is changing in all the world. According to such projections, Mediterranean ecosystems will face, in the next future, a radical modification of the climatic conditions, with an increase in atmospheric CO_2 concentration, whose main effects can be summarized in a rainfall reduction and a temperatures increase. In the second application of the proposed model to the *Eleuterio at Lupo* river basin, the effects of such climatic changes on vegetation water stress was investigated.

The application was carried out considering two different vegetation covers (trees and grasses), and all the three types of soils present within the basin, with the purpose to evaluate the vegetations response as function of vegetation and soil characteristics. The model was performed considering a bi-seasonal annual discretization of the model climatic parameters, using then the same parameterization considered in SCHEME B of the previous application.

Different future scenarios were hypothesized, investigating three temporal horizons (i.e., previsions at 25, 50 and 100 years), and applying, first at all, only the predicted temperatures trend (i.e., temperatures increase), successively, only the predicted rainfall trend (i.e., rainfall reduction), and finally, applying simultaneously both the climatic trends. These two climatic trends were supposed linear and were derived from the projection at 100 years predicted by *Christensen et al.* (2007).

In order to overcome the uncertainties due to the lack of information about potential future variations in the frequency and intensity of rainfall events and in the seasonal distribution of precipitation, a parametric study on rainfall frequency was carried out, modeling the future rainfall distribution over the year with two different schemes (named Case *A* and Case *B*). The first is the case of rainfall reduction equally distributed during the whole year, obtained by maintaining the same ratio between the total precipitation during the growing and the dormant seasons, for all the three temporal horizons under analysis. The second is the case of rainfall reduction concentrated only during the dormant season, a case supported by some analysis of historical rainfall data trends (e.g., *Cannarozzo et al.*, 2006).

For each temporal horizon, eight possible combinations of the mean frequency and depth of rainfall events that provide the same annual amount of rainfall, were considered. In this way, 76 different future scenarios (25 for each

investigated temporal horizon) in total were simulated, including also the current scenario and the scenarios relative to the application of only the temperature trend (three different scenarios having rainfall parameters equal to those current).

The model results relative to the application of only the temperature trend showed that the temperatures increase, and the consequent increment in the evapotranspiration rates, would lead toward an increase of the vegetation water stress. Moreover, a relevant conclusion arising from the comparison between the results relative to the two different vegetation types under analysis, is that, following the evapotranspiration demand, the increase in water stress for woody vegetation is consistently higher than that relative to grasses.

A comparison between the results relative to the only application of the temperatures trend and those relative to the only application of the rainfall trend (under the assumptions relative to Case *A*) showed that rainfall reduction increases the vegetation water stress much more than temperatures increase. Comparing then the dynamic water stress indexes obtained with the eight different combinations relative to each scenario, one can note that intense and rare rainfall events, as they are expected to be in the future, could attenuate the effects of rainfall reduction because of the less interception correlated to them.

Also the comparison between the results relative to Case *A* and those relative to Case *B* showed relevant aspects. If the current ratio between the growing season and the dormant season rainfall is maintained (Case *A*), trees and grasses could be subjected to an increase of water stress, which seems more severe for trees than for grasses. Otherwise, if the rainfall reduction is concentrated during the dormant season (Case *B*), as emerges from literature, grasses would have some advantages over the trees species. In this conditions grasses would keep the water stress similar to the nowadays value, while trees would suffer for the lack of the winter recharge, increasing their water stress.

The second application carried out also an analysis on the role of the model parameter q (an exponent that figures in the relation linking soil moisture and vegetation water stress) in the evaluation of the woody vegetation response. From this analysis it was possible to observe that the use of a linear (q=1), or almost linear (q=2), relation between the soil moisture condition and the consequent plant response, could further exacerbate the future water stress values in respect to the results predicted by the model by using a relation strongly nonlinear (q=3).

The two application to the *Eleuterio at Lupo* river basin have demonstrated that the numerical model proposed, differentially from the steady-state analytical models for arid and semi-arid ecosystems where no transient condition in the soil moisture profiles is present, can be easily used also in Mediterranean water-controlled ecosystems, where the steady-state hypothesis is inapplicable, maintaining the same simplicity and accuracy. The model

represents an important tool for the investigation of future climate changes in Mediterranean areas, and, in fact, the second application, providing a quantitative response of the vegetation water stress increment consequent to the predicted climatic trends, have highlighted that, in the coming years, such changes (if confirmed) could cause a significant modification in the vegetation pattern of the *Eleuterio at Lupo* river basin, with herbaceous vegetation that should be favorite in respect to the woody vegetation.

Finally, in the last part of the thesis, the peculiarities of groundwater dependent ecosystems and the state of the art related to the ecohydrological modelling for such environments were deeply described and discussed.

Considering the increasing attention devoted in recent years to the wetlands and groundwater-dependent ecosystems, it is becoming increasingly relevant to develop and test quantitative models for the analysis of such ecosystems. With this aim, *Rodriguez-Iturbe et al.* (2007) highlighted the lack of an analytic approach to the dynamics of interactions between climate, soil and vegetation in humid ecosystems. In groundwater dependent ecosystems the water table has a crucial role in supplying water to plants, interacting directly with the root zone. For this reason it is fundamental to consider the strong coupling between water table and soil moisture dynamics.

Following other studies [e.g., *Ridolfi et al.* (2008); *Laio et al.* (2009); *Tamea et al.* (2009)], in this study, an ecohydrological analytical approach to the study of the coupled water table and soil moisture dynamics in vegetated soils was investigated and applied to a real case study. In particular, two extremely new probabilistic models (*Laio et al*., 2009 and *Tamea et al.*, 2009) were discussed in detail. The former, for the investigation of the water table dynamics, is based on a soil water balance equation where the unknown quantity is the water table depth. The second, for the study of the soil moisture dynamics in the unsaturated zone, is based on a local, depth-dependent water balance equation where the unknown quantity is the soil moisture. Both the water balance equations are forced by stochastic precipitation, accounting for mechanisms such as rainfall infiltration and water table recharge, plant water uptake, capillary rise, groundwater lateral flow due to the presence of a nearby external water body. Solving such water balance equations, the two models are able to provide the probability distribution functions of the water table depth and of soil water content at different depths.

Since a validation of these models on real cases is still missing, an application of the first model, for the study of the water table fluctuations (*Laio et al.*, 2009), to three sites, located in southeast Florida (USA), within the Everglades National Park, was also carried out.

The water table model was validated using field data of groundwater levels recorded at the three sites. Model parameters and forcings were estimated from the characteristics of vegetation, soil and from time series of precipitation and evapotranspiration available at the same sites; the analysis was carried out using two different parametric aggregation schemes: annual and seasonal. In particular, the steady-state probability distribution functions and cumulative distribution functions of water table levels predicted by the model were compared with the empirical ones obtained using historical field data.

Two of the three considered sites are located near artificial water canals while, in the other site, the nearest external water body is the ocean. The two canals are used for agricultural practices and the water levels recorded show consistently different values during the dry and the wet seasons. The two canals, as well as in a minor way the ocean, show relevant daily/seasonal fluctuations of the water level around the mean annual and season values, that were used by the model to compute the lateral flow. This fact could be considered as the major cause of discrepancy between the field observations and the model results for both the annual and the seasonal analysis. In addition to this, the rainfall and evapotranspiration model parameters have been estimated with time series shorter than those of water table position, and might be not fully representative of the climatic conditions occurring throughout all the time.

Despite the above consideration, the annual analysis showed a good ability of the model to reproduce the observed distribution, using mean annual values of rainfall depth and frequency, evapotranspiration and water surface position of the nearest water body as input parameters. In particular, the model performances in the site near the ocean (Site 1) were more accurate than those relative to the other two sites (Sites 2 and 3), probably because of the presence in these lasts of the canals as closest external water bodies. The model, working at the annual scale, is unable to take into account the different seasonal contributions of the external water body, especially if this difference is due to human activities. On the other hand, this fact could have played an important role in determining the real water table depths, from which the empirical pdf's derive.

The results relative to the seasonal analysis showed that, with the seasonal parameterization, the model still reproduced the observed pdf in Site 1, while, for the other two sites, the seasonal pdf's are strongly affected by the initial position of the water table at the beginning of each season and, for this reason, the model performances were less accurate. In particular, during the dry season, the model pdf's were shifted towards deeper values, while the pdf's of the wet season were shifted toward shallower water table values. This effect was much more evident during the dry season, when reaching a steady state condition requires more time than that required during the wet season. For this reason, the comparison between the model pdf's of water table depths and the empirical

ones during the wet season gave better results than the same comparison during the dry season.

Other two factors that could have played an important role in the discrepancies between the observed values and the model results, are the choice of the soil parameters and the fact that the considered model assumes the homogeneity and isotropy of soil. The soil parameters were evaluated on the basis of the available information (e.g., soil types, mineral and organic content, etc.) and using several values from literature, while, considering their importance in the modelling, it would be more appropriate to use field or laboratory analysis. Moreover, the three sites chosen are characterized by soils types, such as peat and marly soils, which usually show an anisotropic and hysteretic behavior; for these reasons, the real soil parameter values could be different than those assumed in the application.

It is important to point out that the model tested in this study showed a good ability to describe the water table dynamics for groundwater dependent ecosystems, having limited, or no, hydroperiods. Although the application of the model provided outstanding and important results for the specific sites considered, especially working at the annual scale, the study of Florida Everglades and in general of frequently submerged sites would require taking into account also water levels above the soil surface, which is the aim of ongoing and future researches.

References

Abramowitz, M., and Stegun, I. A., 1965. *Handbook of Mathematical Functions*, Dover, New York

Adeoye, K. B., Rawlins, S. L., 1981. *A split-root technique for measuring root water potential*. Plant Physiology, 68, 44-47

Amanatidis, G.T., Paliatsos, A.G., Repapis, C.C. and Bartzis, J.G., 1993. *Decreasing Precipitation Trend in the Marathon Area, Greece*. International Journal of Climatology, 13(2): 191-201

Augi, S., 2003. *Deduzione di serie temporali di contenuto e di stress idrico da un modello stocastico di bilancio idrologico*, Università degli Studi di Palermo (Dottorato di Ricerca in Idronomia Ambientale, XV ciclo, Tesi per il conseguimento del titolo)

Baird, A. J., Wilby, R. L. (eds), 1999. *Ecohydrology: Plants and Water in Terrestrial and Aquatic Environments,* Routledge, London, UK

Baldocchi, D. D., Xu, L., Kiang, N., 2004. *How plant functional-type, weather, seasonal drought, and soil physical properties alter water and energy fluxes of an oak-grass savanna and an annual grassland*, Agricultural and Forest Meteorology, 123, 13-39

Berendrecht, W. L., Heemink, A. W., van Geer, F. C., and Gehrels, J. C., 2004. *State-space modeling of water table fluctuations in switching regimes*, J. Hydrol., 292(1–4), 249– 261

Beven, K., 2004. *Robert E. Horton's perceptual model of infiltration processes.* Hydrological Processes, 18, 3447-3460

Bierkens, M. F. P., 1998. *Modeling water table fluctuations by means of a stochastic differential equation*, Water Resour. Res., 34(10), 2485–2499

Boetler, D.H., 1965. *Hydraulic conductivity of peats*. Soil Science, Vol.100, No.4, pp 227-231

Boelter, D.H. 1969. *Physical properties of peats as related to degree of decomposition*. Proceedings of the Soil Science Society of America, Vol. 33, pp. 606-609

Boggie, R. 1970. *Moisture characteristics of some peat-sand mixtures*. Scientific Horticulture, Vol. 22, pp. 87-91

Bolle, H.J., 2003. *Mediterranean Climate,* Regional Climate Studies Springer, Berlin, 320 pp

Botter, G., Porporato, A., Rodriguez-Iturbe, I., and Rinaldo, A., 2007. *Basin-scale soil moisture dynamics and the probabilistic characterization of carrier hydrologic flows: slow, leaching-prone components of the hydrologic response*, Water Resources Research, 43, W02417, doi:10.1029/2006WR005043

Bradford, K. J., and Hsiao, T. C., 1982. *Physiological responses to moderate water stress*, in *Physiological Plant Ecology II, Water Relations and Carbon Assimilation*, Lange O.L., Nobel P.S.,Osmaond C.B. and Ziegler H., 279-286, New York, Springer-Verlag

Brady, N. C., and Weil, R. R., 1996. *The Nature and Property of Soils*, 11th ed., Prentice-Hall, Upper Saddle River, N. J.

Brinson, M.M., 1993. *A hydrogeomorphic classification for wetlands*. Wetlands Research Program, Technical Report WRP-DE-4, August 1993. Prepared for US Army Corps of Engineers

Brolsma, R. J., and Bierkens, M. F. P., 2007. *Groundwater - soil water - vegetation dynamics in a temperate forest ecosystem along a slope*, Water Resources Research, 43, W01414, doi:10.1029/2005WR004696

Brooks, R. H., and Corey, A. T., 1964. *Hydraulic properties of porous media*. Hydrol. 386 Pap.(3), Colorado State Univ., Fort Collins, CO, USA

Caylor, K.K., Manfreda, S., Rodriguez-Iturbe, I., 2005. *On the coupled geomorphological and ecohydrological organization of river basins*, Advanced in Water Resources, n.28, pages 69-89

Cannarozzo, M., Noto, L.V. and Viola, F., 2006. *Spatial distribution of rainfall trends in Sicily (1921-2000)*. Physics and Chemistry of the Earth, 31(18): 1201-1211

Chambers, J. C., and Linnerooth A. R., 2001. *Restoring riparian meadows currently dominated by Artemisia using alternative state concepts - The establishment component*, Appl. Veg. Sci., 4, 157–166

Chartzoulakis, K. and Psarras, G., 2005. *Global change effects on crop photosynthesis and production in Mediterranean: the case of Crete, Greece*. Agriculture Ecosystems and Environment, 106(2-3): 147-157

Christensen, J.H, Hewitson, B., Busuioc, A., Chen, A., Gao, X., Held, I., Jones, R., Kolli, R.K., Kwon, W.T., Laprise, R., Magaña Rueda, V., Means, L., Menéndez, C.G., Räisänen, J., Rinke, A., Sarr, A., Whetton, P., 2007. *Regional Climate Projections. In: Climate Change 2007: The Physical Science Basis*. Contribution of Working Group I to the Fourth Assessment Report of the Intergovernmental Panel on Climate Change, Cambridge, United Kingdom and New York, NY, USA

Cislaghi, M., De Michele, C., Ghezzi, A., Rosso, R., 2005. *Statistical assessment of trends and oscillations in rainfall dynamics: Analysis of long daily Italian series*, Atmospheric Research, 77 (1-4), 188-202

Clapp, R.B. and Hornberger, G.M., 1978. *Empirical Equations for Some Soil Hydraulic-Properties*. Water Resources Research, 14(4): 601-604

Cowan, I. R., 1965. *Transport of water in the soil-plant-atmosphere system*. Journal of Applied Ecology, 2(1)

Cox, D. R., Miller, H. D., 1965. *The Theory of Stochastic Processes*. London, Methuen

Cox, D. R., and Isham, V., 1986. *The virtual waiting-time and related processes*. Advances in Applied Probability, 18, 558-573

Dacey, J. W. H., and Howes B. H., 1984. *Water uptake by roots controls water table movement and sediment oxidation in short spartina marsh*, Science, 224, 487–489

Davidson, J. M., Nielsen, D. R. and Biggar, J. W., 1963. *The measurement and description of water flow through Columbia silt loam and Hisperia silt loam.* Hilgardia, 34, 601-616

De Luis, M., Raventos, J., Gonzalez-Hidalgo, J.C., Sanchez, J.R. and Cortina, J., 2000. *Spatial analysis of rainfall trends in the region of Valencia (East Spain)*. International Journal of Climatology, 20(12): 1451-1469

D'Odorico, P., and Porporato, A., 2004. *Preferential states in soil moisture and climate dynamics*, PNAS, 101 (24), 8848-8851

D'Odorico, P., and Porporato, A., 2006. *Dryland Ecohydrology*, Springer-Verlag New York Inc.

Dowty, P., Frost, P., Lasolle, P., Midgley, G., Mukrlabai, M., Otter, L., Privette, J., Ramontsho, J., Ringrose, S., Scholes, R.J., Wang, Y., 2001. *Summary of the SAFARI 2000 wet season field campaign along the Kalahari transect.* The Earth Observer, 12(3), 29-34

Dube´, S., Plamondon, A. P. and Rothwell, R. L., 1995. *Watering up after clear-cutting on forested wetlands of the St. Lawrence lowland*, Water Resour. Res., 31(7), 1741–1750

Dunne, T., 1978. *Field studies of hillslope flow processes*. Hillslope Hydrology, M.J.

Kirkby, Chichester, John Wiley & Sons, pp. 227-293

Eagleson, P. S., 1978. *Climate, soil, and vegetation (parts 1-7).* Wat. Resour. Res. 14, 705-776

Eagleson, P. S., 2002. *Ecohydrology – Darwinian Expression of Vegetation Form and Function*. Cambridge, U.K., Cambridge University Press

Eamus, D., Hatton, T., Cook, P., Colvin, C., 2006. *Ecohydrology: Vegetation Function, Water and Resource Management*. Csiro Publishing

Eamus, D., 2009. *Identifying groundwater dependent ecosystems*. University of Technology, Sidney. Land and Water Australia

Esteban-Parra, M.J., Rodrigo, F.S. and Castro-Diez, Y., 1998. *Spatial and temporal patterns of precipitation in Spain for the period 1880-1992*. International Journal of Climatology, 18(14): 1557-1574

Feddes, R. A., Kabat, P., Vanbakel, P. J. T., Broswijk, J. J. B., and Albertsma J., 1988. *Modeling soil-water dynamics in the unsaturated zone - State of the art*, J. Hydrol., 100(1–3), 69–111

Fish, J.E. and Stewart, M., 1991. *Hydrogeology of the Superficial Aquifer System, Dade County, Florida* – U.S. Geological Survey – Water Resources Investigations Report 90-4108

Freeze, R., and Cherry J., 1979. *Groundwater*. Prentice-Hall, Old Tappan (NJ)

Garritsen, A. C.,1993. *Linking hydrological and ecological models. In: The Use of Hydro-ecological Models in the Netherlands* (ed. by J.C. Hooghart & C.W.S. Posthumus), 67-79. Proceedings and Information no. 47, TNO Committee on Hydrological Research, Delft, The Netherlands

Gilvear, D. J., Tellam, J. H., Lloyd, J. W., and Lerner, D. N., 1989. *The hydrodynamics of East Anglian fen systems*, Hydrogeology Research Group, School of Earth Sciences, The University of Birmingham, Edgbaston, U.K

Grootjans, A.P., Van Wirdum, G., Kemmers, R.H., Van Diggelen, R., 1996. *Ecohydrology in the Netherlands: principles of an application-driven interdisciplin.* Acta Botanica Neerlandica (45), 491-516

Giuffrida, A. and Conte, M., 1989. *Long term evolution of the Italian climate outlined by using the standardized anomaly index (SAI)*, Conference on Climate and Water (I), Helsinki, Finland, pp. 197

Guswa, A. J., Celia M. A., and Rodriguez-Iturbe I., 2002. *Models of soil moisture dynamics in ecohydrology: A comparative study*, Water Resources Research, 38 (9), 1166

Guswa, A. J., 2005. *Soil-moisture limits on plant uptake: An upscaled relationship for water-limited ecosystems*, Advances in Water Resources, 28, 543-552

Hale, M. G., and Orcutt, D.M., 1987. *The Phisiology of Plants Under Stress*. New York, J. Wiley & Sons

Hino, M., 1977. *Eco-hydraulics, an attempt*. Tech. Report no. 22, Department of Civil Engineering, Tokyo Institute of Hydrology, 29-59. (also presented at the XVII Congress of the International Association for Hydraulic Research, held in Baden-Baden in August 1977)

Ho, M., Mc Cannon, B., and Lynch, J., 2004. *Optimization modeling of plant root architecture for water and phosphorus acquisition*, J. Theor. Biol., 226(3), 331– 340

Hoag, R.S. and Price, J.S., 1995. *A field-scale, natural gradient solute transport experiment in peat at a Newfoundland blanket bog.* Journal of Hydrology, 172, pp.171-184 – Elsevier

Holden, J., and Burt, T.P., 2003. *Hydrological studies on blanket peat: the significance of the acrotelm-catotelm model.* Journal of Ecology, 91, pp.86-102 – British Ecological Society

Horton, R. E., 1933. *The role of infiltration in the hydrological cycle*. Trans. American Geophys. Union, 14: 446-460

Hsiao, T. C., 1973. *Plant responses to water stress*. Annual Review of Plant Physiology, 24, 519-570

Hubbell, S., 2001. *The Unified Neutral Theory of Biodiversity and Biogeography*, Monographs in Population Biology, Princeton and Oxford, Princeton University Press

Ingram, H.A.P., 1967. *Problems of Hydrology and Plant Distribution in Mires.* Journal of Ecology, Vol.55, No.3, pp.711-724 – British Ecological Society

Ingram, J., and Bartels, D., 1996. *The molecular basis of dehydration tolerance in plants*. Annual Review of Plant Physiology and Plant Molecular Biology, 47

IPCC, 2007. *Climate Change 2007: The Physical Science Basis*. Contribution of Working Group I to the Fourth Assessment Report of the Intergovernmental Panel on Climate Change [Solomon, S., D. Qin, M. Manning, Z. Chen, M. Marquis, K.B. Averyt, M. Tignor and H.L. Miller (eds.)]. Cambridge University Press, Cambridge, United Kingdom and New York, NY, USA, 996 pp.

Katimon, A., Melling, L., 2007. *Moisture retention curve of tropical sapric and hemic peat*. Malaysian Journal of Civil Engineering, 19 (1): 84-90

Kiang, N., 2002. *Savannas and seasonal drought: the landscape-leaf connection through optimal stomatal control*, Ph.D. thesis, University of California, Berkley

Kozlowski, T. T., 1984. *Responses of woody plants to flooding*, in Flooding and Plant Growth, edited by T. T. Kozlowski, pp. 129– 163, Elsevier, New York

Kundzewics, Z. W., 2002. *Ecohydrology – seeking consensus on interpretation of the notion.* Hydrological Sciences – Journal des Sciences Hydrologiques, 47(5) October 2002

Kutiel, H., Maheras, P. and Guika, S., 1996. *Circulation and extreme rainfall conditions in the eastern Mediterranean during the last century*. International Journal of Climatology, 16(1): 73-92

Laio, F., Porporato A., Ridolfi, L., Rodriguez-Iturbe, I., 2001a. *Plants in water-controlled ecosystems: active role in hydrologic processes and response to water stress - IV.* Discussion of real cases, Adv. Water Resour., 24, 745-762

Laio, F., Porporato A., Ridolfi, L., Rodriguez-Iturbe, I., 2001b. *Plants in water-controlled ecosystems: active role in hydrologic processes and response to water stress - II.* Probabilistic soil moisture dynamics, Adv. Water Resour., 24, 707-723

Laio, F., Ridolfi, L., Rodriguez-Iturbe, I., and Porporato, A. , 2001c. *Intensive or extensive use of soil moisture: plant strategies to cope with stochastic water availability*, Geophisical Research Letters, Vol. 28, NO. 23

Laio, F., 2006. *A vertically extended stochastic model of soil moisture in the root zone*. Water Resour. Res., 42, W02406, doi:10.1029/ 2005WR004502

Laio, F., D'Odorico, P.,, Ridolfi, L., 2006. *An analytical model to relate the vertical root distribution to climate and soil proprieties*, Geophys. Res. Lett., 33(18), L18401, doi:10.1029/2006GL027331

Laio, F., Tamea, S., Ridolfi, L., D'Odorico, P. and Rodriguez-Iturbe, I., 2009. *Ecohydrology of groundwater-dependent ecosystems: 1. Stochastic water table dynamics.* Water Resour. Re., Vol. 45, WO5419, doi:10.1029/2008WR007292

Lange, O. L., Kappen, L., Schuzle, E.D., 1976. *Water and Plant Life: Problems and Modern Approaches*. Berlin, Springer-Verlag

Larcher, W., 1995. *Physiological Plant Ecology*. New York, Springer-Verlag

Lauenroth, W. K., Dodd, J. L., Sims, P. L., 1978. *The effects of water and nitrogen induced stresses on plant community structure in a semi-arid grassland*. Oecologia, 36

Levitt, J., 1980. *Responses of Plants to Environmental Stresses*. Vol. I, 2nd edn., New York, Academic Press

Liguori, V., Raimondi, S., Dazzi, C., Cirrito, V. , 1983. *Modello di studio integrato del territorio (Ficuzza-Palermo)*, Estratto da Quaderni di Agronomia, n.10, Istituto di Agronomia Generale e Coltivazioni Erbacee dell'Università degli Studi di Palermo

Linn, D. M., and Doran, J. W., 1984. *Effect of water-filled pore space on carbon dioxide and nitrous oxide production in tilled and nontilled soils*, Soil Sci. Soc. Am. J., 48, 1267– 1272

Little, E.L. Jr., 1983. *Common fuelwood crops: a handbook for their identification*. McClain Printing Co., Parsons, WV

Liuzzo, L., Noto, L.V., Cannarozzo, M., Viola, F. and La Loggia, G., 2008. *Analisi dei trend climatici in Sicilia*, 31° Convegno Nazionale di Idraulica e Costruzioni Idrauliche, Perugia

Lodge, T.E., 2004. *The Everglades handbook: Understanding the Ecosystem*. Second Edition. CRC Press

Manfreda, S., Fiorentino, M., Iacobellis, V., 2005. *DREAM: a distributed model for runoff, evapotranspiration, and antecedent soil moisture simulation*, Advances in Geosciences, 2, 31-39

McKnight, J. S., Hook, D. D., Langdon, O. G., and Johnson, R. L., 1981. *Flood tolerance and related characteristics of trees of the bottomland forests of the southern United States*, in Wetlands of the Bottomland Hardwood Forests, edited by J. R. Clark and J. Benforado, pp. 29–69, Elsevier, Amsterdam

Meixner, F. X., and Eugster, W. , 1999. *Effects of landscape pattern and topography on the emissions and transport, in Integrating Hydrology, Ecosystem Dynamics and Biogeochemistry in Complex Landscapes*, edited by J. D. Tenhunen and P. Kabat, John Wiley, New York

Mitsch, W.J., Gosselink, J.G., 2007. *Wetlands* (fourth edition). John Wiley and Sons. Hoboken, NJ

Mitsch, W.J., Gosselink, J.G., Zhang, L., Andesrson, C.J., 2009. *Wetlands Ecosystems*, John Wiley and Sons, New York

Myers, R.D., 1999. *Hydraulic proprieties of South Florida wetland peats*. Thesis presented to the Graduate School of the University of Florida in partial fulfillment of the requirements for the Degree of Master of Engineering

Morel-Seytoux, H.J., Meyer, P.D., Nachabe, M., Touma, J., van Genuchten, M.T., Lenhard, R.J., 1996. *Parameter equivalence for the Brooks-Corey and van Genuchten soil characteristics: Preserving the effective capillary drive*. Water Resources Research, Vol. 32, NO.5, 1251-1258

Naasz, R., Michel, J.C., Charpentier, S., 2005. *Measuring Hysteretic Hydraulic Properties of Peat and Pine Bark using a Transient Method.* Soil Sci. Soc. Am. J. 69: 13-22

Naiman, R. J., Decamps, H., and McClain, M. E., 2005. *Riparia*, Elsevier, New York

Naumburg, E., Mata-Gonzalez, R., Hunter, R. G., McLendon, T., and Martin, D. W., 2005. *Phreatophytic vegetation and groundwater fluctuations: A review of current research and application of ecosystem response modeling with an emphasis on great basin vegetation*, Environ. Manage., 35(6), 726–740

Nemani R. R., Keeling, C. D., Hashimoto, H., Jolly, W. M., Piper, S. C., Tucker, C. J., Myneni R. B., Running S. W., 2003. *Climate-driven increases in Global Terrestrial Net Primary Production from 1982 to 1999*. Science vol. 300. 1560-1563

Nilsen, E. T. and Orcutt, D. M., 1998. *Phisiology of Plants under Stress: Abiotic Factors*. New York, John Wiley

Noto L.V., Bono E, La Loggia G. and Liuzzo L., 2007. *Trend analysis of climatic indexes in Sicily*, IUGG XXIV General Assembly, Perugia

Novitzki, R. P., 1979. *Hydrologic characteristics of Wisconsin's wetlands and their influence on floods, stream flow, and sediment*. Wetland functions and values: The state of our understanding. P. E. Greeson, J. R. Clark, and J. E. Clark, ed., American Water Resources Association, Minneapolis, MN, 377-388

Nuttle, W.K., 2002. *Eco-hydrology's Past and Future in Focus*. American Geophysical Union, Eos 83:205, 211, and 212

Palutikof, J.P., Goodess, C.M. and Guo, X., 1994. *Climate-Change, Potential Evapotranspiration and Moisture Availability in the Mediterranean Basin*. International Journal of Climatology, 14(8): 853-869

Piervitali, E., Colacino, M. and Conte, M., 1997. *Signals of climatic change in the central-western Mediterranean basin*. Theoretical and Applied Climatology, 58(3-4): 211-219

Porporato, A., Laio, F., Ridolfi, L., Rodriguez-Iturbe, I., 2001. *Plants in water-controlled ecosystems: active role in hydrologic processes and response to water stress III.* Vegetation water stress, Adv. Water Resour., 24 (7), 725-744

Porporato, A., and Rodriguez-Iturbe, I., 2002. *Ecohydrology – a challenging multidisciplinary research perspective*, Hydrological Sciences – Journal des Sciences Hydrologiques, 47(5)

Porporato, A., and D'Odorico, P., 2004a. *Phase transitions driven by state-dependent poisson noise*, Phys. Rev. Lett., 92 (11), 110,601, doi:10.1103/PhysRevLett.92.110601

Porporato, A., Daly, E. and Rodriguez-Iturbe, I., 2004b. *Soil water balance and ecosystem response to climate change*. American Naturalist, 164(5): 625-632

Pumo D., Viola, F., Noto, L.V., 2008. *Ecohydrology in Mediterranean areas: a numerical model to describe growing Seasons out of phase with precipitations*. Hydrol. Earth Syst. Sci., 12, 303-316

Ramsar Convention Bureau, 1996. *Wetlands and biological diversity: cooperation between theconvention of wetlands of international importance especially as waterflowl habitat (Ramsar, Iran, 1971) and the convention on biological diversity*. Document UNEP/CBD/COP/3/Inf.21

Rawls, W. J., Brakensiek, D. L., and Saxton, K. E., 1983. *Estimation of soil water properties*, Trans. ASAE, 25(5), 1316– 1320

Rawls, W.J. and Brakensiek, D.L., 1989. *Estimation of soil water retention and hydraulic proprieties*, Unsaturated flow in hydrological modeling, edited by H.J. Morel-Seytoux, pp.275-300, Kluwer Academic Publisher, Dordrecht, The Netherlands

Renken, R.A., Dixon, J., Koehmstedt, J., Ishman, S., Lietz, A.C., Marella, R. L., Telis, P., Rogers, J., Memberg, S., 2005. *Impact of Anthropogenic Development on Coastal Ground-Water Hydrology in Southeastern Florida, 1900-2000.* Prepared as part of the U.S. Geological Survey Greater Everglades Priority Ecosystems Science Program. Circular 1275. U.S. Department of Interior and U.S. Geological Survey

Ridolfi, L., D'Odorico, P., and Laio, F., 2006. *The effect of vegetation–water table feedbacks on the stability and resilience of plant ecosystems*, Water Resour. Res., 42, W01201, doi:10.1029/2005WR004444

Ridolfi, L., Laio, F., and D'Odorico, P., 2007. *Vegetation dynamics induced by phreatophyte-aquifer interactions*, J. Theor. Biol., 248(2), 301–310

Ridolfi, L., D'Odorico, P., Laio, F., Tamea, S., Rodriguez-Iturbe, I., 2008. *Coupled stochastic dynamics of water table and soil moisture in bare soil condition*, Water Resour. Res., 44, W01435, doi:10.1029/2007WR006707

Rizzuti, A.M., Cohen, A.D., Stack, E.M, 2004. *Using hydraulic conductivity and micropetrography to asses water flow through peat-containing wetlands.* Intenational Journal of Coal Geology 60, 1-16

Rodriguez-Iturbe, I., Porporato, A., Ridolfi, L., Isham, V., Cox, D.R., 1999a. *Probabilistic modelling of water balance at a point: the role of climate, soil and vegetation*. Proceedings of the Royal Society of London Series a-Mathematical Physical and Engineering Sciences, 455(1990): 3789-3809

Rodriguez-Iturbe, I., Porporato, A., Ridolfi, L., Isham, V., Cox, D.R., 1999b. *Tree-grass coexistence in savannas: the role of spatial dynamics and climate fluctuation*. Geophysical Research Letters, 26 (2)

Rodriguez-Iturbe, I., D'Odorico, P., Porporato, A., and Ridolfi, L., 1999c. *On the spatial and temporal links between vegetation, climate, and soil moisture*, Water Resources Research, n.12 (vol.35), 3709-3723

Rodriguez-Iturbe, I., 2000. *Ecohydrology: a hydrologic perspective of climate-soli-vegetation dynamics.* Wat. Resour. Res. 36(1), 3-9

Rodriguez-Iturbe, I., Porporato, A., Laio, F. and Ridolfi, L., 2001a. *Intensive or extensive use of soil moisture: plant strategies to cope with stochastic water availability*. Geophysical Research Letters, 28(23): 4495-4497

Rodriguez-Iturbe, I., Porporato, A., Laio, F., Ridolfi, L., 2001b. *Plants in water-controlled ecosystems: active role in hydrological processes and responses to water stress - I. Scope and general outline.* Advances in Water Resources, 24(7), 697-705

Rodriguez-Iturbe, I. and Porporato, A., 2004. *Ecohydrology of water-controlled ecosystem: soil moisture and plant dynamics*. Cambridge University Press, Cambridge, United Kingdom

Rodriguez-Iturbe, I., D'Odorico, P., Laio, F., Ridolfi, L. and Tamea, S., 2007. *Challenges in humidland ecohydrology: Interactions of water table and unsaturated zone with climate, soil, and vegetation*, Water Resour. Res., 43, W09301, doi:10.1029/2007WR006073

Rosa, E. and Larocque, M., 2008. *Investigating peat hydrological proprieties using field and laboratory methods: application to the Lanoraie peatland complex*. Hydrol. Process. 22, 1866-1875

Roy, V., Ruel, J.-C., and Plamondon, A. P., 2000. *Establishment, growth and survival of natural regeneration after clearcutting and drainage on forested wetlands*, For. Ecol. Manage., 129, 253– 267

Salvucci, G. D., 1993. *An approximate solution for steady vertical flux of moisture through an unsaturated homogeneous media*, Water Resour. Res., 29 (11), 3749-3753

Salvucci, G. D., and Entekhabi, D., 1994. *Equivalent steady soil moisture profile and the time compression approximation in water balance modeling*, Water Resour. Res., 30, 2737– 2749

Salvucci, G. D., and Entekhabi, D., 1995. *Hillslope and climatic controls on hydrologic fluxes*, Water Resour. Res., 31(7), 1725– 1739

Scholes, R. J., 1997. Savanna, in Vegetation of Southern Africa, R.M. Cowling, D. M. Richardson, S. M. Pierce, (ed.), Cambridge, Cambridge University Press

Schulze, E.D., 1986. *Carbon dioxide and water vapor exchange in response to drought in the atmosphere and in the soil.* Annual Review of Plant Phisiology, 37, 247-274

Sisson, J. B., Klittich, W.M., and Salem, S.B., 1988. *Comparison of two methods for summarizing hydraulic conductivities of layered soil.* Water Resources Research, 24 (8)

Skopp, J., Jawson, M. D., and Doran, J. W., 1990. *Steady-state aerobic microbial activity as a function of soil water content*, Soil Sci. Soc. Am. J., 54, 1619– 1625

Smith, J. A. C., and Griffith, H., 1993. *Water Deficits: Plant Responses from Cell to Community*. Oxford, UK, Bios Scientific Publishers

Tamea, S., Laio, F., Ridolfi, L., D'Odorico, P. and Rodríguez-Iturbe, I., 2009. *Ecohydrology of groundwater-dependent ecosystems: 2. Stochastic soil moisture dynamics*. Water Resources Research, Vol. 45, W05420, doi:10.1029/2008 WR007293

Thornthwaite, C. W., 1948. An Approach toward a Rational Classification of Climate, The Geographical Review, Vol. 38, pp. 55-94

Turner, N. C., Schulze, E. D., Gollan, T., 1985. *The response of stomata and leaf gas exchange to vapour pressure deficits and soil water content. II. In the mesophytic herbaceous species*. Helianthus annuus, Oecologia, 65, 348-355

Yates, Susan A. 1974. *An autecological study of sawgrass, Cladium jamaicense, in southern Florida*. Coral Gables, FL: University of Miami. 117 p. Thesis. [17794]

Yeh, P. J. F., and Eltahir, E. A. B., 2005. *Representation of water table dynamics in a land surface scheme. part I: Model development*, J. Clim., 18(12), 1861– 1880

van Den Broeck, C. , 1983. *On the relation between white shot noise, Gaussian white noise, and the dichotomic Markov process*, J. Stat. Phys., 31 (3), 467-483

van Genuchten, M. T., 1980. *A closed-form equation for predicting the hydraulic conductivity of unsaturated soils.* Soil Sci. Soc. Am., 44, 892-898

Viola, F., Daly, E., Vico, G., Cannarozzo, M. and Porporato, A., 2008. *Transient Soil Moisture Dynamics and Climate Change in Mediterranean Ecosystems*. Water Resources Research, 44, W11412, doi:10.1029/2007WR006371

Walczak, R., Rovdan, E., Witkowska-Walczak, B., 2002. *Water retention characteristics of peat and sand mixtures*. International Agrophysics, 16, 161-165

Wassen, M.J., Grootjans A.P., 1996. *Ecohydrology: an interdisciplinary approach for wetland management and restoration.* Vegetatio (126),1-4

Weaver, H.A. and Speir , W.H., 1960. *Applying basic soil water data to water control problems in Everglades peaty muck*. U.S. Agricultural Research Service 41-40, 15 pp

Wilde, S. A., Steinbrenner, E. C., Pierce, R. S., Dosen, R. C., and Pronin, D. T., 1953. *Influence of forest cover on the state of the ground water table*, Soil Sci. Soc. Proc., 17, 65– 67

Wolansky, E., 2007. *Estuarine Ecohydrology*. Elsevier

Wood, P.J., Hannah, D.M., Sadler, J.P., 2008. *Hydroecology and Ecohydrology: Past, Present and Future*. Wiley, John & Sons

Wright, J. M., and Chambers, J. C., 2002. *Restoring riparian meadows currently dominated by Artemisia using alternative state concepts - Above-ground response*, Appl. Veg. Sci., 5, 237– 246

Zalewski, M., Janauer, G. A., Jolankai, G., 1997. *Ecohydrology, a new paradigm for the sustainable use of aquatic resources.* IHP-V. Tech. Documents in Hydrology no. 7. UNESCO, Paris, France

Biographical sketch

Dario Pumo was born in Palermo (Italy), in 1978. In 2005, he graduated in civil engineering at the University of Palermo (*Università degli Studi di Palermo*, Italy) with full marks and honour. In 2006, he won a six months research scholarship (title: *"An ecohydrological approach to the analysis of desertification dynamics at catchment scale"*) at the department DIIAA (*Dipartimento di Ingegneria Idraulica ed Applicazioni Ambientali*) of the University of Palermo. In the following year, he entered graduate school for the degree of Doctor of Philosophy at the same department. He spent the last year of the triennial graduate school at Princeton (New Jersey, USA), collaborating as visiting assistant professional specialist at the department CEE (Civil and Environmental Engineering) of Princeton University. He specializes in hydraulic and environmental engineering (*Dottorato in Ingegneria Idraulica ed Ambientale – XXI ciclo*).